

**THE DRYING OF FOODS USING SUPERCRITICAL
CARBON DIOXIDE**

ZOË KATHERINE BROWN

A Thesis Submitted to The University of Birmingham for the
Degree of Doctor of Engineering

Department of Chemical Engineering
The University of Birmingham
October 200

UNIVERSITY OF
BIRMINGHAM

University of Birmingham Research Archive

e-theses repository

This unpublished thesis/dissertation is copyright of the author and/or third parties. The intellectual property rights of the author or third parties in respect of this work are as defined by The Copyright Designs and Patents Act 1988 or as modified by any successor legislation.

Any use made of information contained in this thesis/dissertation must be in accordance with that legislation and must be properly acknowledged. Further distribution or reproduction in any format is prohibited without the permission of the copyright holder.

SUMMARY

Food drying techniques such as air and freeze drying are not ideal: high temperatures used during air drying result in degradation of nutrients and sensorial properties, while freeze drying is expensive and therefore only applicable to high value foods. As an alternative to such drying techniques, drying with supercritical carbon dioxide was investigated here.

Initially, carrot was dried using this technique. Addition of a co-solvent (ethanol) to the supercritical fluid was used as a method to increase the water solubility in the supercritical fluid and therefore aid drying. Analysis of the dried and rehydrated product structure, rehydration properties and mechanical properties was carried out which gave an indication of product quality.

Drying of agar, containing varying concentrations of sugar was carried out on a laboratory and pilot plant scale. Gel structure and gel properties were studied. Addition of sugar to agar gel pieces improved structural retention considerably during drying. Fourier transform infrared analysis was used to investigate interactions that may be responsible for structural differences seen during supercritical drying. Changes in experimental parameters such as flow rate and depressurisation rate did not appear to have a significant effect on the dried gel structure.

The supercritical drying technique investigated allowed food products to be dried and unique structures to be created with different rehydration and textural properties to the equivalent food products dried by air or freeze drying.

ACKNOWLEDGEMENTS

This thesis owes its existence to the help, support and inspiration of many people. In the first place, I wish to acknowledge the EPSRC, Unilever and the University of Birmingham for financial support during the four years of study and the use of laboratory facilities which enabled this work to be carried out.

I would especially like to thank my primary supervisor Dr Rachel Bridson for her continued support, guidance and invaluable input. I am also grateful to my associate supervisors, Professor Peter Fryer and Professor Ian Norton, without whose knowledge and assistance this study would not have been successful. I would like to thank Dr Richard Greenwood for his assistance with all EngD matters. Thanks also to colleagues at Unilever, Vlaardingen for assisting me in the work that I carried out at their research facilities, in particular I would like to thank Stephan Schumm.

Many thanks are extended to my friends and colleagues at the University of Birmingham for their encouragement and advice on technical matters. In particular, I would like to thank Dr Teijun Lu, Dr Serafim Bakalis, Dr Phil Robbins and Dr Gary Leeke. I would also like to acknowledge all those in the workshop within the school of engineering for their endless assistance and support.

Finally, I extend my gratitude to my friends and family for their continued support, encouragement, motivation and understanding throughout the duration of my studies.

CONTENTS

	Page
Summary.....	I
Acknowledgements.....	II
Contents.....	III
List of figures.....	VIII
List of tables.....	XIV
Abbreviations.....	XV
1.0 Literature Review	1
1.1 Introduction to supercritical fluids.....	2
1.1.1 Properties and characterisation of supercritical fluids.....	3
1.1.2 Carbon dioxide as a solvent	4
1.1.3 Addition of co-solvents to supercritical systems	5
1.2 Uses and applications of supercritical fluids	6
1.2.1 Supercritical extraction	6
1.2.2 Supercritical drying.....	8
1.2.3 Polymer processing using supercritical fluids	11
1.2.3.1 Fourier transform infrared analysis to study the interactions of supercritical carbon dioxide with polymers.....	14
1.3 Introduction to drying of foods	16
1.3.1 Advantages and disadvantages of conventional methods for drying of foods.....	18
1.3.2 Drying kinetics.....	21
1.3.3 Water content measurement.....	23
1.3.4 Drying of fruit and vegetables	25
1.3.4.1 Drying of carrots.....	26
1.3.5 Gels in the food industry.....	27
1.3.5.1 Introduction to agar.....	28
1.3.5.2 Drying of gels	31
1.3.5.3 Addition of sugar to biopolymer gels and their effect on microstructure and physical properties	32

1.4 Importance of food structure resulting from drying	34
1.5 Analysis of internal microstructure.....	37
1.5.1 Microscopy	38
1.5.2 X-ray micro-computed tomography	38
1.6 Macrostructural measures of quality.....	40
1.6.1 Texture analysis	40
1.6.2 Colour analysis techniques	42
1.6.3 Rehydration.....	43
1.7 Aims of this work.....	45
2.0 Drying of carrots using supercritical carbon dioxide.....	46
2.1 Introduction.....	47
2.1.1 Solvent systems and the use of ethanol as a co-solvent.....	48
2.2 Materials	49
2.2.1 Rig components	49
2.2.2 Carrot preparation and storage.....	49
2.2.3 Carbon dioxide and ethanol	49
2.3 Apparatus and methodology	49
2.3.1 High pressure equipment and supercritical drying method	49
2.3.2 Initial sample characterisation and preparation of carrots	53
2.3.3 Method for supercritical drying of carrot pieces using supercritical carbon dioxide .	55
2.3.3.1 Addition of ethanol as a co-solvent	57
2.3.4 The use of liquid carbon dioxide for drying experiments.....	60
2.3.5 Method for air drying of carrot pieces	61
2.3.6 X-ray micro-computed tomography for the analysis of microstructure	61
2.3.7 Method for rehydration of carrot pieces	61
2.3.8 Light microscopy for microstructural studies	62
2.3.9 Cryo-scanning electron microscopy for microstructural analysis	62
2.3.10 A texture analysis method to measure the hardness of carrot pieces.....	62
2.3.11 A method for colour measurement of carrot pieces.....	63
2.3.12 Statistical analysis techniques.....	64

2.4 Results and discussion	65
2.4.1 Drying profile for air and supercritically dried carrot pieces	65
2.4.1.1 Addition of ethanol as a co-solvent during supercritical drying.....	66
2.4.1.2 Comparison of supercritical drying with air drying.....	67
2.4.1.3 Drying with liquid carbon dioxide.....	71
2.4.1.4 The effect of temperature on drying rate	74
2.4.1.5 The effect of cooking on drying rate.....	76
2.4.1.6 The effect of flow rate on supercritical drying	80
2.4.1.7 The effect of increased surface area on drying rate	82
2.4.1.8 A proposed mechanism for supercritical drying.....	85
2.4.2 Structural analysis.....	89
2.4.2.1 Microscopy: light microscopy and cryo-scanning electron microscopy for analysis of wet carrot microstructure following rehydration.....	89
2.4.2.2 X-ray micro-computed tomography for analysis of the dried carrot structure	95
2.4.2.3 Rehydration properties of dried carrot pieces.....	99
2.4.2.4 Texture analysis of rehydrated carrot pieces to measure hardness.....	108
2.4.2.5 Colour analysis of carrot pieces.....	114
2.5 Conclusion	118
3.0 Drying of biopolymer gels using supercritical carbon dioxide.....	120
3.1 Introduction.....	121
3.2 Materials	122
3.2.1 Rig components	122
3.2.2 Gel preparation.....	122
3.2.3 Carbon dioxide and ethanol	123
3.3 Apparatus and methodology	123
3.3.1 High pressure drying equipment.....	123
3.3.2 Method for supercritical drying of gel pieces using supercritical carbon dioxide....	123
3.3.3 High pressure windowed pressure vessel	124
3.3.4 Method for air drying of gel pieces.....	126
3.3.5 Method for freeze drying of gel pieces	126

3.3.6 X-ray micro-computed tomography for the analysis of gel microstructure	126
3.3.7 Method for rehydration of gel pieces.....	127
3.3.8 A texture analysis method to measure the hardness of gel pieces	127
3.3.9 Fourier transform infrared analysis of gel pieces in the presence of supercritical carbon dioxide.....	127
3.4 Results and discussion	129
3.4.1 Drying protocols: drying times and normalised moisture contents achieved	129
3.4.2 Visual appearance of dried gels and the effect of sucrose addition.....	132
3.4.3 X-ray micro-computed tomography analysis.....	134
3.4.4 Effect of supercritical process conditions on gel structure	137
3.4.5 Fourier transform infrared spectroscopy to investigate molecular interactions.....	145
3.4.6 Rehydration properties of dried gel pieces	158
3.4.7 Texture analysis of rehydrated gel pieces to measure hardness	165
3.5 Conclusion	168
4.0 Drying of agar gel on pilot plant scale equipment using supercritical carbon dioxide.....	170
4.1 Introduction.....	171
4.2 Materials	171
4.2.1 Rig components	171
4.2.2 Gel preparation.....	172
4.2.3 Solvents.....	172
4.3 Apparatus methodology	173
4.3.1 Equipment	173
4.3.2 Method for supercritical drying	174
4.3.3 Air drying method.....	176
4.3.4 Freeze drying method	176
4.3.5 X-ray micro-computed tomography for the analysis of gel microstructure	176
4.3.6 Method for rehydration of gel pieces.....	176
4.3.7 A texture analysis method to measure the hardness of gel pieces	176
4.4 Results and discussion	177

4.4.1 The effect of sucrose addition on the drying and rehydration of agar gel pieces, dried using air, freeze and supercritical drying techniques.....	177
4.4.2 The effect of Glucidex 21D addition (and comparison with sucrose addition) on the drying and rehydration of agar gel pieces, dried using air, freeze and supercritical drying techniques	181
4.4.3 Texture analysis of rehydrated gel pieces, containing sucrose and Glucidex 21D, to measure hardness	187
4.4.4 X-ray micro-computed tomography for analysis of the structure of gels containing sucrose and Glucidex 21D	190
4.4.5 Effect of supercritical process conditions on gel structure	195
4.4.5.1 Drying and rehydration of agar gels containing sucrose	195
4.4.5.2 Texture analysis of dried and rehydrated agar gel to measure hardness.....	198
4.4.5.3 X-ray micro-computed tomography and photographic images of cylindrical gels, dried using unmodified supercritical carbon dioxide at varying flow rates.....	201
4.5 Conclusion	206
5.0. Overall conclusion and suggestions for future work	208
5.1 Overall conclusion	208
5.2 Suggestions for future work.....	211
6.0. References.....	215

LIST OF FIGURES

Figure 1.1 Generic pressure-temperature phase diagram of a pure substance.....	2
Figure 1.2 Figure illustrating the formation of a supercritical, homogeneous phase as the critical point is reached.....	3
Figure 1.3 A food stability map, illustrating the relationship of food deterioration rate as a function of water activity.....	18
Figure 1.4 A drying rate curve.....	22
Figure 1.5 The molecular structure of agarose.	28
Figure 1.6 A schematic showing the gelling mechanism of agar.	29
Figure 2.1 Schematic representation of the experimental apparatus used for supercritical drying.	50
Figure 2.2 Photograph of the experimental apparatus	53
Figure 2.3 A photograph of a horizontal cross section through a carrot.....	55
Figure 2.4 A photograph of the purpose built sample holder.	56
Figure 2.5 Plots showing the moisture content of carrot pieces, dried for 5400 seconds using $\text{scCO}_2(\text{EtOH})$ over a range of EtOH concentrations.	58
Figure 2.6 An illustration of the ‘L*a*b*’ colour model (CIELAB)	63
Figure 2.7 Drying profiles for raw carrot pieces dried in air, $\text{scCO}_2(\text{pure})$ and $\text{scCO}_2(\text{EtOH})$	66
Figure 2.8 Moisture content plotted against time for raw carrot pieces dried in air and $\text{scCO}_2(\text{pure})$	68
Figure 2.9 A plot of $\ln(X_d)$ versus time for carrot pieces, air dried at 40°C, 50°C and 60°C	70

Figure 2.10 Drying experiments carried out using liquid CO _{2(pure)} , liquid CO _{2(EtOH)} , scCO _{2(pure)} and scCO _{2(EtOH)}	73
Figure 2.11 Comparison of carrot drying profiles at 40°C, 50°C and 60°C using air drying or drying with scCO _{2(pure)}	75
Figure 2.12 Comparison of carrot drying profiles for cooked and raw samples dried using air drying, and cooked and raw samples dried with scCO _{2(pure)}	77
Figure 2.13 Moisture content plotted against time for cooked and raw carrot pieces dried using air drying, in the initial stages of drying.....	78
Figure 2.14 Comparison of carrot drying profiles for cooked and raw samples, dried using scCO _{2(EtOH)}	80
Figure 2.15 Drying profiles for carrot pieces dried with scCO _{2(pure)} , using flow rates of 0.5 l/minute, 1 l/minute, 2 l/minute and 3 l/minute.....	81
Figure 2.16 Graph showing the rate of water removal for pieces of carrot and grated carrot, dried in scCO _{2(pure)} at varying flow rates.....	83
Figure 2.17 Plot showing the actual water loss against the possible water loss for pieces of carrot, at various flow rates, and grated carrot, at various flow rates.....	84
Figure 2.18 An illustration of the phase boundaries crossed for air, freeze and supercritical drying.....	88
Figure 2.19 Light microscopy images	90
Figure 2.20 The internal microstructure of carrot pieces, imaged using cryo-SEM.....	94
Figure 2.21 Reconstructed 2D cross-sectional x-ray images.....	96
Figure 2.22 A rehydration curve of samples that were air dried at 50°C and dried with scCO _{2(pure)} at 50°C, followed by rehydration at 50°C.....	102

Figure 2.23 NMC, during rehydration at 50°C, plotted against initial NMC, before rehydration at 300 seconds and 2400 seconds for samples dried at 50°C..	103
Figure 2.24 NMC, during rehydration at 50°C, plotted against initial NMC, before rehydration at 300 seconds and 2400 seconds for samples dried at 50°C and 60°C.....	105
Figure 2.25 NMC, during rehydration at 80°C, plotted against initial NMC, before rehydration at 300 seconds and 2400 seconds for samples dried at 50°C..	106
Figure 2.26 TA-XT2i, texture analyser from Stable Micro System, UK.	109
Figure 2.27 Graph showing the force required to puncture cylindrical raw carrot pieces that had been cooked (in water at 100°C) for different amounts of time.	110
Figure 2.28 Puncture testing of carrot samples, dried using different techniques	111
Figure 2.29 Puncture testing of carrot samples, dried using air and scCO ₂ (pure) (both at 60°C) and rehydrated at 50°C or 80°C.....	114
Figure 2.30 An example of scanned dried carrot pieces (air dried, 80°C) used to obtain L*a*b* values in Adobe Photoshop.	115
Figure 2.31 Comparison of the total colour change (ΔC), following drying and rehydration at 50°C and 80°C, for samples dried using various techniques	116
Figure 3.1 Schematic representation of the experimental set up used to view gels during exposure to supercritical conditions and on subsequent depressurisation.....	125
Figure 3.2 Schematic representation of the experimental set up used for FT-IR analysis of agar gels, during exposure to scCO ₂ and scCO ₂ (EtOH).	128
Figure 3.3 Photographs comparing the visual appearance of 2% agar gels before drying, and 2% agar gels dried using different techniques..	134
Figure 3.4 A schematic representation of the agarose gel network, in comparison with a network formed from random polymer chains at a similar polymer concentration	143

Figure 3.5 FT-IR spectra of dried 2% agar gel, containing 10% sucrose, exposed to $\text{scCO}_2(\text{pure})$	147
Figure 3.6 FT-IR spectrum of $\text{scCO}_2(\text{pure})$ and $\text{scCO}_2(\text{EtOH})$ at 20 MPa/50°C.....	148
Figure 3.7 FT-IR spectrum of $\text{scCO}_2(\text{EtOH})$, during depressurisation.	149
Figure 3.8 FT-IR spectra of partially dried 2% agar gel, containing 10% sucrose, exposed to $\text{scCO}_2(\text{pure})$, compared with $\text{scCO}_2(\text{pure})$ alone and the agar gel before exposure to $\text{scCO}_2(\text{pure})$	150
Figure 3.9 FT-IR spectra of partially dried 2% agar gel, containing 10% sucrose, exposed to scCO_2 , after EtOH addition for 60 seconds, 420 seconds and 1500 seconds.....	152
Figure 3.10 FT-IR spectra of supercritically dried 2% agar gel, containing 10% sucrose at 0.1 MPa/21°C with (green line) and without EtOH present (blue line).	153
Figure 3.11 An illustration of the proposed interactions that may occur during exposure of (dried and partially wet) agar gel to scCO_2 and $\text{scCO}_2(\text{EtOH})$	155
Figure 3.12 An illustration of the proposed interactions that may occur between the agar helices during exposure of agar gel to $\text{scCO}_2(\text{EtOH})$	157
Figure 3.13 Graphs showing the rehydration (25°C) of dried gels containing 0% sucrose and 10% sucrose, which were dried with $\text{scCO}_2(\text{pure})$, $\text{scCO}_2(\text{EtOH})$, air and freeze dried	161
Figure 3.14 Graphs showing the rehydration (25°C) of supercritically dried gels, containing 10% sucrose, dried using $\text{scCO}_2(\text{pure})$ and $\text{scCO}_2(\text{EtOH})$	164
Figure 3.15 Chart illustrating the force required to puncture agar gel pieces measured in Newtons (N).	167
Figure 3.16 Texture analysis traces, illustrating the force, in Newtons (N), required to puncture gel pieces dried with $\text{scCO}_2(\text{pure})$ and freeze dried gel pieces.....	168

Figure 4.1 Schematic representation of the experimental apparatus used for supercritical drying.	174
Figure 4.2 Photographs comparing the visual appearance of air dried, freeze dried and supercritically dried 2% agar gel pieces, before and after rehydration (84000 seconds, 21°C), made up with different concentrations of sucrose (5%, 10%, 20% or 30%).	178
Figure 4.3 Rehydration (at 21°C) of air dried, freeze dried and supercritically dried sucrose-infused agar gels.....	180
Figure 4.4 (a) Photographs comparing the visual appearance of air dried 2% agar gel pieces, before and after rehydration (84000 seconds, 21°C), made up with different concentrations of Glucidex 21D (0%, 1%, 2%, 5%, 10% or 20%).	182
Figure 4.4 (b) Photographs comparing the visual appearance of freeze dried 2% agar gel pieces, before and after rehydration (84000 seconds, 21°C), made up with different concentrations of Glucidex 21D (0%, 1%, 2%, 5%, 10% or 20%).	183
Figure 4.4 (c) Photographs comparing the visual appearance of supercritically dried 2% agar gel pieces, before and after rehydration (84000 seconds, 21°C), made up with different concentrations of Glucidex 21D (0%, 1%, 2%, 5%, 10% or 20%).	184
Figure 4.5 Rehydration (at 21°C) of air dried, freeze dried and supercritically dried Glucidex 21-D-infused agar gels	185
Figure 4.6 Comparison of the force required to puncture 2% agar gel pieces before drying, and after air, supercritical and freeze drying, all followed by rehydration..	189
Figure 4.7 (a) 2-D x-ray micro-CT images (taken horizontally through the gel) of air dried agar gels, containing (0, 20 or 30%) sucrose or (0 or 20%) Glucidex 21D.	190
Figure 4.7 (b) 2-D x-ray micro-CT images (taken horizontally through the gel) of freeze dried agar gels, containing (0, 20 or 30%) sucrose or (0 or 20%) Glucidex 21D.	191

Figure 4.7 (c) 2-D x-ray micro-CT images (taken horizontally through the gel) of supercritically dried agar gels, containing (0, 20 or 30%) sucrose or (0 or 20%) Glucidex 21D. 192

Figure 4.8 Rehydration of sucrose-infused agar gel cylindrical pieces, dried using a scCO₂ flow rate of 900 l/hour, 200 l/hour or 200 l/hour for 7200 seconds, followed by a flow rate of 900 l/hour for 10800-14400 seconds..... 197

Figure 4.9 (a) & (b) Charts illustrating the force (measured in Newtons (N)) required to puncture agar gel pieces, containing 10% sucrose.. 199

Figure 4.9 (c) & (d) Charts illustrating the force (measured in Newtons (N)) required to puncture agar gel pieces, containing 20% sucrose.. 200

Figure 4.10 (a) Photographic images of supercritically dried agar gels and subsequently rehydrated gels, containing varying concentrations of sucrose (0-20%), dried at a flow rate of 900 l/hour. 202

Figure 4.10 (b) Photographic images of supercritically dried agar gels and subsequently rehydrated gels, containing varying concentrations of sucrose (0-20%), dried at a flow rate of 200 l/hour. 203

Figure 4.10 (c) Photographic images of supercritically dried agar gels and subsequently rehydrated gels, containing varying concentrations of sucrose (0-20%), dried at a flow rate of 200 l/hour followed by a flow rate of 900 l/hour. 204

Figure 4.11 X-ray micro-CT images of supercritically dried agar gel pieces, containing varying concentrations of sucrose (0-20%) and also dried at different flow rates. 205

LIST OF TABLES

Table 1.1 Characteristic ranges of gas, liquid and SCF physical properties.....	3
Table 1.2 Critical temperatures and pressures of a range of common SCF solvents.....	4
Table 2.1 The critical temperature and pressure of CO ₂ -EtOH mixtures	48
Table 2.2 Examples of average CO ₂ and EtOH flow rates required to reach 6 mol% EtOH at STP.	58
Table 2.3 Drying rates for supercritical and air drying.....	69
Table 2.4 Experimental conditions used to achieve CO ₂ liquid and supercritical phases for drying, while maintaining the same density.	72
Table 2.5 Photographs illustrating the appearance of dried carrot pieces using various drying techniques, followed by rehydration	100
Table 3.1 X-ray micro-CT, 2-D images of gels dried using scCO ₂ (EtOH), which were dried further to remove the final traces of moisture	132
Table 3.2 X-ray micro-CT 2-D images of air, freeze and supercritically dried gels.	137
Table 3.3 X-ray micro-CT 2-D images of supercritically dried gels (all containing 10% sucrose), dried using various processing conditions.....	140
Table 3.4 Images taken inside a pressure vessel of wet agar gel (containing 10% sucrose), exposed to scCO ₂ (pure) and scCO ₂ (EtOH).	144
Table 3.5 A table summarising the results of FT-IR experiments	146

ABBREVIATIONS

ABPR	automated back pressure regulator
ANOVA	analysis of variance
AFM	atomic force microscopy
ATR-IR	attenuated total reflection infrared
a_w	water activity
BPR	back pressure regulator
CIELAB	L*a*b* colour model
CLSM	confocal laser scanning electron microscopy
CO ₂	carbon dioxide
cryo-SEM	cryo-scanning electron microscopy
d	diameter
d.b.	dry basis
DSC	differential scanning calorimetry
EDA	electron donor-acceptor (complex)
EMC	equilibrium moisture content
EtOH	ethanol
ESEM	environmental scanning electron microscopy
FT-IR	Fourier transform infrared
GRAS	generally regarded as safe
HPLC	high performance liquid chromatography
IR	infrared (spectroscopy)
k	rate constant
KF	Karl Fischer
L	length
ln	natural log
MeOH	methanol
m	mass of sample
m_s	mass of dry solids
MV	micrometering valve

n	number of moles
N	newtons
n.d.	no date
NMC	normalised moisture content
NRV	non-return valve
O.D.	outside diameter
P_c	critical pressure
PET	poly(ethylene terephthalate)
PGSS	particles from gas saturated solutions
P_{lab}	local (laboratory) atmospheric pressure
R_0	rehydration ratio
RESS	rapid expansion of supercritical solutions
RH	relative humidity
ROI	region of interest
$scCO_{2(pure)}$	supercritical carbon dioxide that has not been modified with a co-solvent
$scCO_{2(EtOH)}$	supercritical carbon dioxide that has been modified with ethanol
SCF	supercritical fluid
SEM	scanning electron microscopy
STP	standard temperature and pressure
T_c	critical temperature
T_g	glass transition temperature
T_{lab}	local (laboratory) temperature
T_m	melting temperature
V	volume of gas
VOI	volume of interest
MVD	vacuum microwave drying
W_d	weight of dried sample
W_r	weight of rehydrated sample
WTM	wet test meter
X	moisture content at time, t
X_0	initial moisture content

X_d	moisture content following drying
X_r	moisture content following rehydration
x-ray micro-CT	x-ray micro-computed tomography
2-D	two dimensional
3-D	three dimensional
ΔC	total colour change
Δt	time difference

1.0 Literature Review

ABSTRACT

Drying of food is important for the preservation of the product, by inhibiting the growth of micro-organisms, and also for reducing the weight and bulk of food for cheaper transport and storage. Here, current drying techniques such as air and freeze drying are discussed and compared. However, these are not ideal: high temperatures used during air drying result in degradation of nutrients and sensorial properties, while freeze drying is expensive and therefore only applicable to high value foods.

Supercritical fluids (SCFs) are commonly used in food processing, mainly for extraction purposes. However, SCFs have also been used previously to dry substances such as inorganic gel systems, and it is proposed that this method may be extended to foods and biopolymer gels that are used in food products. The possibility that this alternative drying technique may allow creation of different microstructures to those achieved through conventional drying methods is of particular interest.

The first part of this chapter discusses the properties and uses of SCFs, in particular supercritical carbon dioxide (scCO₂), highlighting why SCFs may be expected to be suitable solvents for drying and furthermore, creation of unusual microstructures. The second part describes and compares the current methods for removal of water from foods. Finally, methods to measure the quality of food products, on both a microstructural and macrostructural level, have been considered and discussed.

1.1 Introduction to supercritical fluids

A substance that exists as a gas at ambient conditions can undergo sufficient compression to allow it to solidify, liquefy or become supercritical. The temperature of the fluid and the pressure achieved as a result of compression will determine its final state (Figure 1.1).

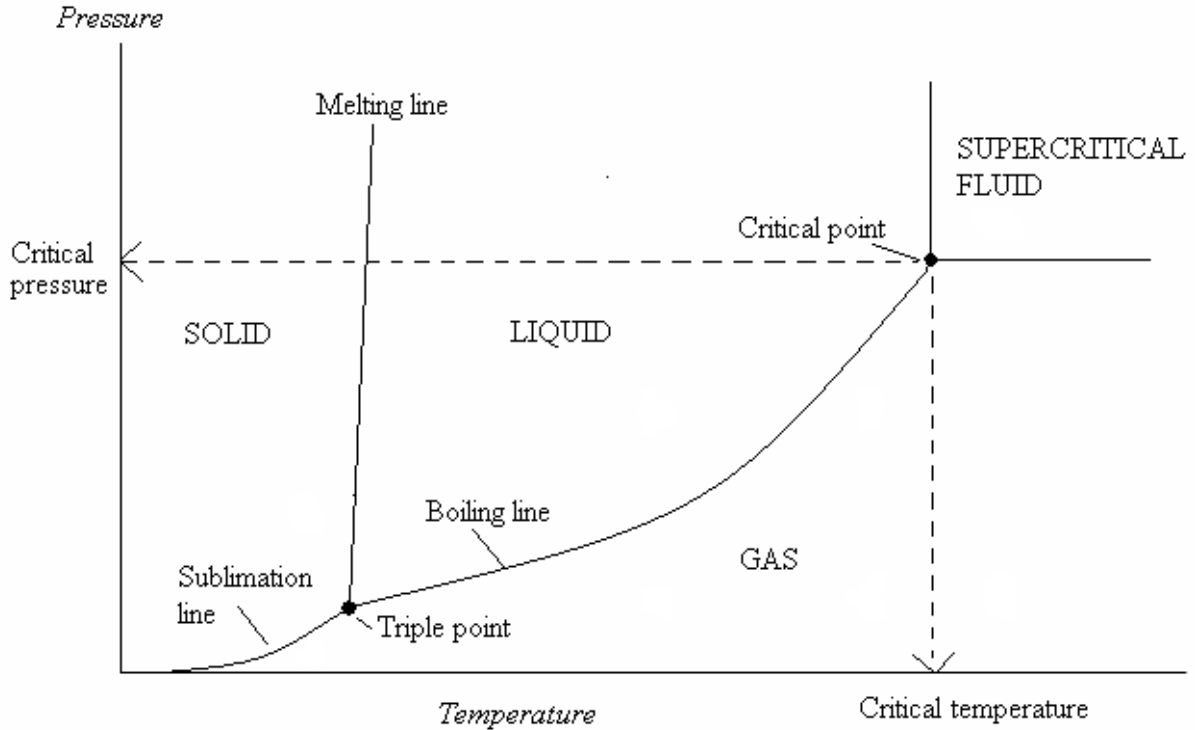


Figure 1.1 Generic pressure-temperature phase diagram of a pure substance.

The supercritical region is reached when a gas is taken beyond its critical temperature (T_c) and pressure (P_c) (the critical point). Above the critical point the substance exists as a single phase. Figure 1.2 ((i)-(vi)) illustrates the formation of a homogeneous phase as the supercritical region is reached (vi).

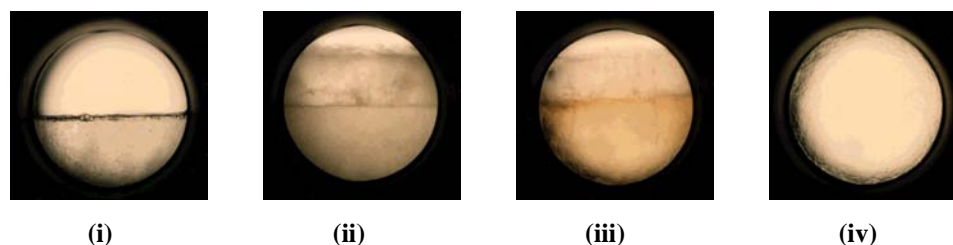


Figure 1.2 Figure illustrating the formation of a supercritical, homogeneous phase as the critical point is reached: (i) The gas liquid interface is clearly visible below the critical point; (ii-iii) the densities of the two phases become more similar as the temperature and pressure approach the critical point; (iv) the critical point is reached and a homogeneous phase exists. (Rayner n.d.).

1.1.1 Properties and characterisation of supercritical fluids

SCFs are of specific interest due to them possessing advantageous characteristics of both liquids and gases. The liquid like densities, gas like viscosities, diffusivities higher than liquids, and gas-like compressibility properties (Table 1.1) make SCFs desirable for use as solvents, while additionally facilitating mass transfer and reaction rates. Furthermore, these properties can be varied by simply adjusting the pressure and/or temperature, allowing for a very tuneable process. The selectivity and solvating power of any SCF is a function of its density, which can be adjusted between that of a liquid or a gas without having to undergo a phase change.

CO₂ (carbon dioxide) in particular has received much interest in this area due to several advantages over other solvents which are discussed in section 1.1.2.

Table 1.1 Characteristic ranges of gas, liquid and SCF physical properties, adapted from Brunner (2005).

Phase of substance	Density (kg/dm ³)	Diffusivity (m ² /s)	Viscosity (Pa s)
Gas	(0.6-2.0) x 10 ⁻³	(0.1-0.4) x 10 ⁻⁴	(0.6-2.0) x 10 ⁻⁵
Liquid	0.6-1.6	(0.2-2.0) x 10 ⁻⁹	(0.2-3.0) x 10 ⁻³
SCF	0.2-0.9	(0.2-0.7) x 10 ⁻⁷	(0.1-0.9) x 10 ⁻⁴

The critical temperatures (T_c) and pressures (P_c) for a range of substances are shown in Table 1.2 (Knox 2005).

Table 1.2 Critical temperatures and pressures of a range of common SCF solvents, adapted from Knox (2005).

Fluid	T_c ($^{\circ}\text{C}$)	P_c (MPa)
Ammonia	132.4	11.3
Carbon dioxide	31.1	7.4
Ethane	32.5	4.9
Ethanol	243.1	6.4
Nitrous Oxide	36.6	7.2
Propane	96.8	4.3
Trifluoromethane	26.0	4.7
Water	374.1	22.1

1.1.2 Carbon dioxide as a solvent

CO_2 is the most commonly used SCF due to it being inexpensive, inert, environmentally benign, non-flammable, and possessing a GRAS (generally regarded as safe) status. Additionally, supercritical conditions are easily reached at $T_c = 31.1^{\circ}\text{C}$ K and $P_c = 7.38$ MPa, so scCO_2 may be used in the treatment of thermally sensitive substances, and additionally has the benefit of being a gas at ambient pressure so all solvent traces can be expelled, upon returning to atmospheric conditions.

CO_2 used for processing is a recycled by-product of other industrial processes therefore it is readily available and does not add to global warming. It also reduces the use of ozone-depleting solvents that it may be used in place of.

One drawback is that scCO_2 will only dissolve non-polar or slightly polar substances but this can be adjusted by using binary and multi-component processing fluids. For example, a widely-used strategy, employed to increase the solubility of polar substrates in scCO_2 , is to add small quantities of co-solvent to the system so that the CO_2 is then said to be “modified”. Co-solvents are usually organic solvents, for example ethanol (EtOH), acetone and ethyl acetate and can be used to increase the solubility of many compounds in scCO_2 (Kopcak and Mohamed 2005; Tanaka and Nakanishi 1994), as well as manipulating the critical temperature of the new mixture. Binary mixtures have critical temperatures between those of the two components, while the critical pressures are often higher than the critical pressures of the pure components (Kiran and Brennecke 1993). Solubility measurements are used to determine the enhanced solubility as a result of adding a co-solvent. EtOH is an ideal co-solvent for use in the food industry as it has a GRAS status.

1.1.3 Addition of co-solvents to supercritical systems

As mentioned in section 1.1.2, EtOH is commonly employed as a co-solvent for supercritical processing and more specifically for increasing the solubility of polar solutes in scCO_2 (Ekart *et al.* 1993; Ke *et al.* 1997). The supercritical solvent is then said to be “modified” with EtOH ($\text{scCO}_{2(\text{EtOH})}$). The increased solubility is a consequence of interactions occurring between the co-solvent and the scCO_2 . These interactions have been studied by Lalanne *et al.* (2004) with the use of vibrational spectroscopy. Presence of hydrogen bonding and also a Lewis acid-base type interaction between the carbon atom of CO_2 , which acts as an electron acceptor, and the oxygen atom of EtOH, acting as the electron donor, has been suggested as possible interactions. Vibrational spectroscopy carried out by Lalanne *et al.* (2004) confirmed the presence of a relatively strong specific OH- CO_2 interaction. Studies carried out using liquid CO_2 and methanol (MeOH) provided evidence of a Lewis acid-base interaction, but no evidence of hydrogen bonding was reported (Reilly *et al.* 1995).

The enhanced solubility of solutes in $\text{scCO}_{2(\text{EtOH})}$ is also thought to be due to chemical and physical interactions occurring between the co-solvent and solute. The presence of hydrogen bonding between co-solvents (EtOH and acetone) and the solute has been reported as a reason for the enhanced solubility of disperse dyes in scCO_2 (Muthukumaran *et al.* 1999). Increased

hydrogen bonding between the co-solvent and water may also explain the enhanced solubility of water in $\text{scCO}_2(\text{EtOH})$, which was observed by Brown *et al.* (2008). Physical interactions such as dipole-dipole, dipole-induced dipole, or induced dipole-induced dipole may also occur (Foster *et al.* 2002).

Finally, the addition of the co-solvent increases the density of the SCF, and solute solubility increases with increasing density (Güçlü-Üstündag and Temelli 2005).

1.2 Uses and applications of supercritical fluids

Many applications of SCFs exist (Brunner 2005; King and Williams 2003). The most widely used are listed below:

- In chromatography for separation and analysis
- In extractions, to isolate a desired compound or remove undesirable components
- As a reaction media for polymerisation and oxidation
- Particle formation
- Cleaning
- For coal and petroleum processing
- In environmental remediation

The most developed area for the use of SCFs is in extraction processes and is discussed further in the following section (1.2.1).

1.2.1 Supercritical extraction

Traditionally organic solvents are used for extractions but they introduce the disadvantage of residual solvent in the final product and also generate solvent waste. Therefore, the use of SCFs, particularly CO_2 is a promising alternative. Common examples of where supercritical extraction is used include the decaffeination of coffee and tea (McHugh and Krukonis 1986), and the extraction of flavours, fragrances and essential oils from natural sources (Brunner 2005).

Reverchon (1997) has reviewed the extraction and fractionation of essential oils using scCO_2 . Solubility is an important factor in extraction techniques and it has therefore been discussed in

relation to various pressure and temperature process conditions. By varying the temperature and pressure, selective solubility of specific compounds may be achieved.

The effect of temperature on solubility is an effect of two mechanisms: the increase in vapour pressure with temperature results in a solubility increase, and at the same time the decrease in solvent density (or solvent power) with increasing temperature causes a decrease in solubility (Güçlü-Üstündag and Temelli 2004). These opposing factors result in the crossover of solubility isotherms and have been discussed in relation to the solubility of dyes in supercritical systems by Haarhaus *et al.* (1995). The dominant mechanism is dictated by pressure: at pressures lower than the crossover value (where the density is the dominating factor), the solubility decreases with increasing temperature; at pressures above the crossover value the solubility increases with increasing temperature. Therefore the possibility exists to tune the solvent solubility through small changes in temperature or pressure. However, it should be noted that SCFs are generally only sensitive to changes around the critical point of the fluid.

Essential oil extraction is largely controlled by solubility but may also be controlled by mass transfer mechanisms within the solid phase (Reverchon 1997). For example, waxes are known to exist on a leaf's surface and also for vegetable matter, and despite having very low solubilities in scCO₂ they have no affinity with other parts of the leaf's surface, therefore they may be extracted with limited mass transfer resistances. In contrast, essential oils have very high solubilities in scCO₂ but exhibit large mass transfer resistances in the solid phase, therefore their extraction is controlled by mass transfer mechanisms. If co-extraction of such products occurs, further fractionation may be required to separate the desired essential oil afterwards. The addition of co-solvents to aid both solvent power and selectivity is also discussed in this review (Reverchon 1997). However, care should be taken when using co-solvents to extract complex mixtures of compounds such as essential oils, since modification of compounds may occur. Co-solvents are most useful in extraction techniques for selective extraction of particular compounds. For extraction of essential oils, Reverchon (1997) recommends the use of low density scCO₂ (0.25-0.50 g/cm⁻³), while higher densities are useful for extraction of non-essential oil compounds.

The extraction rate of capsicum oleoresin and capsaicinoids from pre-pelletized peppers with scCO₂ was investigated by del Valle *et al.* (2003), and was shown to depend on solubility of the components of interest, at the conditions used in the study. However, localisation of the solutes in the plant matrix, solute-matrix-solvent interactions, and co-solvent effects of other solutes present will also contribute to the actual extraction rate, when the process is controlled by phase equilibria factors at different conditions. Increasing the superficial solvent velocity was also shown to have a favourable effect on extraction rates, near the critical point. This was thought to be due to improved transport properties at near-critical conditions, since mass transfer coefficients are higher.

The effect of operating conditions on the solubility of components in scCO₂ has been discussed in detail by Güçlü-Üstündag and Temelli (2004). However, the authors also pointed out the importance of the location, in the solid matrix of the natural materials, of the components being extracted. As in all extraction process, supercritical extraction kinetics are made up of three periods: solubility controlled or constant extraction rate period; transition period; and diffusion controlled period or falling rate period.

The solubility of β -carotene in scCO₂ is also of interest here since chapter 2 investigates the drying of carrots using scCO₂ which contain large amounts of β -carotene (Cygnarowicz *et al.* 1990). Removal of β -carotene during supercritical processing is anticipated to have an undesirable effect on the final product quality, since it provides colour to the food and also nutritional benefits - β -carotene is a precursor to vitamin A in human metabolism. Solubility behaviour of β -carotene has been widely investigated, for example Cygnarowicz *et al.* (1990) and Sovova *et al.* (2001) measured the solubility of β -carotene at various temperatures and pressures, with the highest solubility being measured at higher temperatures and higher pressures. Solubility was increased further by addition of 1 wt. % EtOH co-solvent.

1.2.2 Supercritical drying

It could be argued that supercritical drying is similar to an extraction process, where the water is the solute being extracted and the SCF is the extraction solvent. The supercritical solvent may enter the sample being dried, in the same way that a solvent may enter a product during extraction of a particular substance. Supercritical drying however differs from air drying, since

air drying relies on the one-way diffusion of water out of the sample to the sample surface where it is removed by the air.

Drying techniques using scCO_2 , although not previously reported for food drying, have attracted interest in other industries e.g. for drying gels composed of silica (Rangarajan and Lira 1991; Takishima *et al.* 1997); chromia (Abecassiss-Wolfovich *et al.* 2003); and carbon (Job *et al.* 2005). Supercritical drying by a sol-gel process has been widely used to dry inorganic gel systems to create aerogels (Estella *et al.* 2007; Namatsu *et al.* 1999; Novak *et al.* 2004; Rangarajan and Lira 1991; Takishima *et al.* 1997) and some work has been carried out where organic gel systems are dried to produce organic aerogels, including resorcinol-formaldehyde and melamine-formaldehyde (Schaefer *et al.* 1995; Tamon *et al.* 1997). Supercritical drying for preparation of catalysts has also been reported (Milburn *et al.* 1996; Novak *et al.* 2004; Ratti 2001; Wang *et al.* 2003). Aerogels possess several remarkable properties: they are the lightest and lowest-density solid known to exist; the energy absorbing properties has led to their use for protection in motor vehicles and protection of sensitive equipment; they are also effective thermal insulators; and act as strong desiccants.

A particular advantage of supercritical drying is that vapour-liquid interfaces can be avoided by working in a homogeneous phase. As such, capillary-induced tensile stresses seen during air drying are not experienced by the product, thus helping to preserve structure. Cracking and collapse of gels, experienced during drying has been reported to be preventable by using supercritical drying (Namatsu *et al.* 1999). Additionally, as CO_2 has a low critical temperature (31.1°C), it is possible to exploit this advantage at relatively low temperatures (considerably lower than those used during conventional drying), preventing thermal damage.

SCFs also have high diffusivities: diffusivity of gases and liquids is one of the main factors affecting transport properties in a material, therefore transport properties during supercritical drying would be expected to be respectable.

During air drying, diffusivity is highly dependent on air temperature, air velocity and air humidity - air temperature being considered as the most important factor (Krokida *et al.* 2003). However, higher temperatures required to promote moisture diffusivity during air drying have a detrimental impact on the dried product structure.

Supercritical drying has been compared to air drying for the removal of water from porous silicon nanostructures (von Behren *et al.* 1997). For supercritical drying, it was shown that the outcome of the desired porous structure depended exclusively on the supercritical conditions maintained throughout the drying process. Air drying in comparison, always resulted in collapse of the pore texture, thought to be a consequence of liquid-vapour interfaces present during evaporation which produce capillary-induced tensile stresses. Hence, the use of SCFs for drying allowed shrinking and cracking to be avoided. However, it was also found that damage in silica gels could be caused in all stages of the supercritical drying process, due to rapid changes in composition, pressure and temperature (Takishima *et al.* 1997). In some cases of supercritical drying a small amount of shrinkage (~15%) may still be observed, most of which occurs during the depressurisation step (Rangarajan and Lira 1991). However, Rangarajan and Lira (1991) assigned this shrinkage to the redistribution of condensed phases within the gel by desorption from one pore and readsorption to another, concluding that the removal of EtOH, water or CO₂ was not responsible for the shrinkage.

The sol-gel process of drying of gels has been well documented (Estella *et al.* 2007; Laudise and Johnson 1986). Inorganic alcogels are created by hydrolysis and polycondensation reactions of metal alkoxides or metal chlorides in an alcohol, namely MeOH or EtOH. The alcohol is then removed by the SCF, followed by venting of the SCF-alcohol mixture, resulting in production of an aerogel. SCFs have been used in this way to dry polyethylene glycol/tetramethoxysilicate hybrid gels, resulting in larger pore sizes when compared with gels dried via evaporative drying (Higginbotham *et al.* 2003).

Alternative supercritical drying techniques involve the displacement of the water with a solvent prior to the 'supercritical drying' step: either by filling the vessel with EtOH prior to pressurisation, or by soaking the gel in an excess of EtOH before placing in the high pressure vessel (Rangarajan and Lira 1991). EtOH serves as a good intermediate solvent since it is miscible with both water and CO₂, whereas water alone has only modest solubility in non-polar scCO₂. From the work of Sabirzyanov *et al.* (2002), water solubility in scCO₂ can be estimated to be approximately 4 mg/g at 50°C and 20 MPa, and 2.5 mg/g at 40°C and 20 MPa (Sabirzyanov *et al.* 2002; King *et al.* 1992).

Consequently, limited work has been carried out on direct removal of the water with scCO₂. In the work reported in this thesis, the initial water displacement method, prior to supercritical drying (to create an alcogel) was not used due to concerns over the impact of immersing food material in EtOH, prior to drying. Instead, addition of small quantities of co-solvent (EtOH) directly to the scCO₂ stream was used as a method of increasing the solubility of water in scCO₂, to remove the water directly from the material being dried. This method is discussed further in chapters 2 and 3, and was used for drying experiments reported in these chapters and in the literature (Brown *et al.* 2008; Brown *et al.* 2010).

Other authors have also reported the use of modifiers (surfactants) to improve water solubility in scCO₂ and aid the removal of water from photoresists, preventing pattern collapse (Lee *et al.* 2007; Zhang *et al.* 2004). Surfactants aided the drying by emulsifying the water present on the resist and therefore effectively increasing the solubility of water in the scCO₂.

This aim of this work was to apply the supercritical drying methods discussed here to the drying of foods and biopolymer gels, used in food products.

1.2.3 Polymer processing using supercritical fluids

Biopolymer gels such as agar are commonly used in food products, for example as additives for gelling and thickening. There is limited research on the processing of biopolymers with SCFs, however numerous studies examining supercritical processing of polymers in general do exist. Therefore, research carried out in this area is outlined here, and is discussed further in relation to the processing of biopolymer gels, the subject of chapters 3 and 4 of this thesis

SCFs (CO₂ in particular) are currently used for polymer processing and are favourable over organic solvents, as there is no interface between the organic and aqueous phases and low temperatures may be used. Furthermore, organic solvents are not environmentally friendly and in some cases are toxic.

High molecular weight polymers generally have a low solubility in scCO₂ under mild conditions (<100°C and <35 MPa), although exceptions exist, including amorphous fluoropolymers and silicones (Davies *et al.* 2008). Interactions of the CO₂ with the C-F bond and the flexibility of the

Si-O-Si moieties are responsible for the increased solubilities seen in fluoropolymers and silicones, respectively. However, scCO₂ is soluble in several polymers and the solubility and diffusivity of scCO₂ may be influenced by the molecular structure (the interaction between CO₂ and molecular chains) and/or the morphology (crystalline or amorphous) of the polymer (Davies *et al.* 2008). Sorption and swelling of polymers is a common phenomenon seen and has been related to specific interactions between the CO₂ and polymers. These interactions have been observed with the use of Fourier transform infrared (FT-IR) and attenuated total reflection infrared (ATR-IR) spectroscopy, which is discussed further in section 1.2.3.1. Chain flexibility of polymers has been reported to aid dissolution of the scCO₂ while groups such as carbonyl and ether groups that are accessible in the backbone or on side chains may interact specifically with the scCO₂ (Kazarian *et al.* 1996; Nalawade *et al.* 2006; Shieh and Liu 2003).

The swelling and plasticisation of glassy polymers leads to a depression in the T_g (glass transition temperature). The plasticisation effect also increases the mobility of the polymer chains, reducing the energy barrier for crystallisation and therefore crystallisation can be bought about in some polymers under moderate conditions (Wentao *et al.* 2007). Plasticisation at high temperatures is not desirable, as degradation of the polymer may occur (Smith and Malone 1997).

The addition of small amounts of polar co-solvent to the SCF is well known to aid the solubility of low molar mass polar solutes by increasing the interaction between the SCF and the solute, which has been discussed earlier in section 1.2.3 and has been reported by Muthukumar *et al.* (1999). This method may also aid plasticisation by increasing the interaction of the SCF with the high molar mass polymer in the same way (Hirogaki *et al.* 2005). The partitioning of solutes between scCO₂ (with added co-solvent) and polymers was investigated by Brantley *et al.* (1999) and Kazarian *et al.* (1998), and specific interactions were discussed. Evidence of hydrogen bonding to the basic sites on the polymer, and also dispersion forces between methyl groups on the co-solvent and methyl groups on the polymer were reported. Furthermore, the use of water as a co-solvent has been investigated and successfully found to enhance the plasticising effect of scCO₂ on the semi-crystalline polymer, polycarbonate (Wentao *et al.* 2007).

Several applications of SCFs for polymer processing exist, particularly for the pharmaceutical industry, including the production of drug delivery systems and for the formation of highly porous tissue engineering scaffolds (Davies *et al.* 2008). Polymerisation reactions, polymer impregnation and dyeing of polymers may also be aided by using SCFs.

A number of methods exist for the production of drug delivery systems from polymers using scCO₂, including rapid expansion of supercritical solutions (RESS), anti-solvent techniques, and the production of particles from gas saturated solutions (PGSS). Anti-solvent applications are mainly used for polymers with low solubility in scCO₂ and are widely used for the encapsulation of pharmaceuticals into biodegradable polyesters. In contrast, the RESS process relies on the solute solubilising in the scCO₂. PGSS is used to form particles from polymers that are plasticised by a SCF (through the lowering of their T_g, thus reducing the polymer melt viscosity). These processes are discussed in detail by Davies *et al.* (2008).

Porous polymer scaffolds for tissue engineering may be produced by gas foaming methods which involves rapid depressurisation of plasticised polymers. As pressure is released, pockets of gas nucleate and grow in the polymer. Additionally, as the SCF is released from the polymer, the T_g increases until some point when the T_g is higher than the processing temperature, and the porous structure is set. Addition of small amounts of EtOH to the scCO₂ during foaming was seen to alter the polymer's foamed structure, resulting in a more homogeneous porous structure, with larger pore sizes than those foamed using scCO₂ without EtOH present (Tsivintzelis *et al.* 2007b). It was suggested that this effect was a result of the sorption of the CO₂ and EtOH into the polymer matrix, causing a reduction in the melting temperature (T_m) and viscosity. Growth and nucleation of pores may occur more readily in an amorphous plasticised matrix, which would explain the observation of larger and more homogeneous pores when scCO₂(EtOH) was used (Tsivintzelis *et al.* 2007b).

An alternative to the SCF gas foaming technique is emulsion templating, where an emulsion is created and removal of the internal phase is carried out using supercritical processing, leaving behind a porous template. SCF extrusion has also been reported as a new method to successfully foam biodegradable, pre-gelatinised starch for insulation applications (Mariam *et al.* 2008).

1.2.3.1 Fourier transform infrared analysis to study the interactions of supercritical carbon dioxide with polymers

Infrared (IR) spectroscopy is a chemical analytical technique, which measures the IR intensity of transmitted or reflected light versus the wavelength (wavenumber) of light. IR spectroscopy detects the vibration characteristics of chemical functional groups in a sample, since the molecule absorbs light at a specific frequency relating to that vibration. The absorption spectrum therefore gives information about which bonds groups and functional groups exist within the molecule, and provides information about the specific type of bond deformations within the molecular microstructure, such as bending, wagging or stretching (Furer 1990).

Materials are commonly analysed at ambient conditions. Recently however, high pressure accessories have allowed visualisation of polymers under supercritical conditions and therefore the interaction of polymers with high pressure CO₂ may be investigated using FT-IR analysis. Traditional IR instruments were of the dispersive type which separated the individual frequencies of energy emitted from the IR source, accomplished using a prism or grating. A detector would then measure the amount of energy at each frequency that has passed through the sample, resulting in a plot of intensity versus frequency. FT-IR is preferable over dispersive or filter methods of IR spectral analysis, as it allows measurement of all the IR frequencies simultaneously using an interferometer, and therefore has several advantages over previous methods, for example increased speed, sensitivity and a greater optical throughput (Thermo Nicolet n.d.).

ATR-IR allows analysis of the surface of materials through IR and is particularly useful for materials that may be too thick or too strongly absorbing to be analysed by transmission spectroscopy (Bart 2006). The IR radiation is passed through an IR transmitting crystal with a high refractive index, allowing the radiation to reflect within the ATR element several times. The ATR system has also been adapted to allow its use at high temperatures and pressure and therefore may be used in addition to FT-IR to study polymers under supercritical conditions (Fleming *et al.* 2006; Pasquali *et al.* 2008).

Sorption and swelling of polymers in a scCO₂ environment was thought to be a purely physical phenomenon, until FT-IR and ATR-IR spectroscopy were used to study intermolecular interactions between CO₂ and polymers (Nalawade *et al.* 2006b).

Interactions of CO₂ with polymers may be an indication of polymer plasticisation which occurs due to sorption of CO₂ into the polymer. This induces swelling and plasticisation which is evidenced by a reduction in the T_g or T_m of the polymer. A reduction in the viscosity may also be observed, resulting from a transition of the polymer from a glassy to a rubbery state, where the polymer chains can move more freely. The polymer interdiffusion and dissolution of CO₂ which is responsible for increased polymer mobility and the plasticisation phenomenon has also been studied using this technique (Fleming *et al.* 2006). Increased polymer chain flexibility can aid dissolution of CO₂, leading to plasticisation. Information on enhancing or accelerating the interdiffusion process is anticipated to be useful for polymer processing methods with high pressure CO₂.

Interactions have been reported to occur between CO₂ and specific chemical groups existing within the polymer (that are accessible via a back bone or side chains): carbonyl groups, ether groups, and ester groups (Kazarian *et al.* 1996; Nalawade *et al.* 2006a; Nalawade *et al.* 2006b; Shieh and Liu 2003). The carbonyl stretching vibrations on polymers have been investigated in the past for evidence of polymer-CO₂ interactions (Fried and Li 1990). More recently, the bending mode of CO₂ (ν_2) at $\sim 660\text{cm}^{-1}$, has been studied as evidence of these interactions since it is more sensitive to such interactions

The interaction is expected to be of a Lewis acid-base nature where the carbonyl group acts as an electron donor and the CO₂ acts as an electron acceptor (Nalawade *et al.* 2006b). However, it is important to note that band shifts are not only dependent on the structure of the chemical group, but also the thermal property of the polymer (T_g or T_m) and polymer free volume, such that the same chemicals groups in different polymers may give different shifts. Changes in the polymer absorption band have been reported to provide evidence of a depression in the T_m of the polymer, under the action of scCO₂ and also provide a similar measure of the T_g (Nalawade *et al.* 2006a).

The antisymmetric (ν_3) stretching mode of CO₂ at $\sim 2340\text{cm}^{-1}$ was also used by Shieh and Liu (2003), and Pasquali *et al.* (2008) to prove the occurrence of interactions between the CO₂ and polymer. Additionally, the width of the band was reported to give information about the number of sites available in the polymer matrix for the CO₂ and a rough estimate of the solubility, while observation of the bands over time (CO₂ desorption) may give an indication of the strength of the interaction. The width of the CO₂ bending (ν_2) mode could also be used to estimate the solubility of the CO₂ in the polymer and was shown to be influenced by both temperature and pressure (Pasquali *et al.* 2008).

In addition to observation of polymer-CO₂ interactions, FT-IR analysis has enabled confirmation of Lewis acid-base type interactions occurring between the CO₂ and EtOH in a scCO₂-EtOH system which have previously been discussed in section 1.1.3 (Lalanne *et al.* 2001).

In summary, FT-IR imaging equipment may be modified to enable measurements under supercritical conditions and subsequently FT-IR has proven to be a very useful tool to study specific interactions between polymers and CO₂ at high pressures and temperatures. Quantitative and qualitative analysis has been carried out on CO₂ dissolution, CO₂ solubility and CO₂ interactions with polymers, in addition to measurement of physical properties, such as polymer swelling, T_m and T_g .

FT-IR with the use of ATR as a sampling technique has been extended to study the interactions during the supercritical drying of biopolymer gels, for the use in food product's and is reported in chapter 3 (section 3.4.5).

1.3 Introduction to drying of foods

The main aim of this thesis is to study the supercritical drying of food products and the effect of the drying technique on the products structure and final quality, compared with conventional techniques. Therefore, this section outlines the conventional drying methods used for foods, and discusses their advantages and disadvantages. The drying of specific foods and food materials (e.g. fruits, vegetables and biopolymer gels) are also mentioned, summarising some of the challenges involved.

Food dehydration is still one of the most significant and challenging processes in food processing despite being developed many centuries ago. Optimization of the process in terms of food quality and economics is an ongoing widely researched area (Vega-Mercado *et al.* 2001; Sun 2008).

The main purpose of drying foods is to lower the moisture content in order to reduce water activity and prevent spoilage. Water activity (a_w) is a critical factor that determines shelf life, with most bacteria unable to grow below a value of 0.91 and moulds generally cease growing below 0.80 (Beuchat 1981). At a_w values of 0.70 spoilage is greatly delayed and may not occur during prolonged storage, therefore investigators have suggested that foods be dried to 0.7 a_w , if wanting to be kept for a few years. However, some molds are known to grow very slowly at water activities ranging between 0.60 and 0.62 (Jay *et al.* 2005). Water activity also plays a significant role in determining the activity of enzymes and vitamins in foods and can have a major impact on their colour, taste and aroma. For example, in foods containing reducing sugars, browning may occur due to the Maillard reaction. Other chemical changes that take place in the drying of foods include loss of vitamin C in vegetables, discolouration, structural changes and toughness in the rehydrated product. Methods however exist to minimise chemical changes, such as keeping the moisture content as low as possible, reducing the levels of reducing sugars, blanching and pre-treatment with sulphur dioxide.

A product with the same water content, can achieve several different water activity values by changing the composition of that product. A practical relationship between water activity values and water content is given by a food stability map (Figure 1.3) and although water activity may be easily measured using commercially available instruments, moisture content analysis remains the most practical criterion in food drying technology (Hui 2005). As a guide, the water activity of fresh vegetables falls into the range 0.97-0.99, while dried vegetables with a water content of 14-24% have water activity values of 0.70-0.77 (Hui 2005).

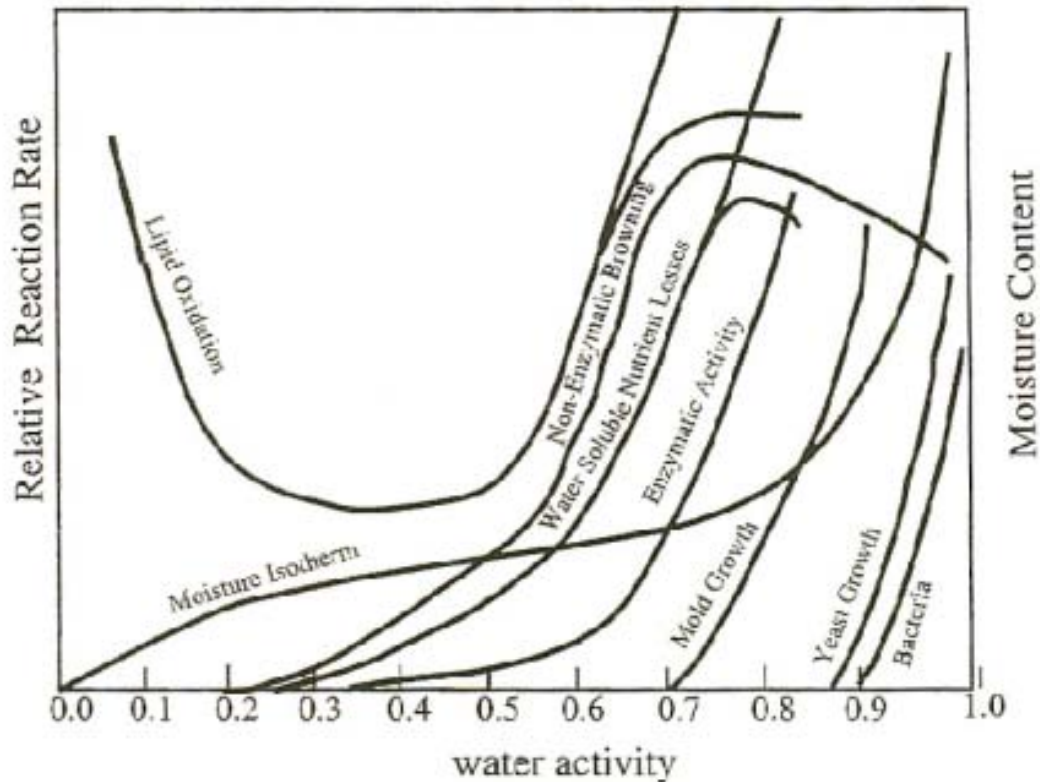


Figure 1.3 A food stability map, illustrating the relationship of food deterioration rate as a function of water activity (Shimek n.d.).

Extending the shelf life of foods is the most important reason for drying foods, however moisture removal also reduces the weight and the bulk of food products to facilitate transport and storage. While imparting these benefits, the combination of mass and heat transfer during drying may also inflict undesirable effects on the product's microstructure. This is unfortunate given that food structure influences nutritional availability, chemical and microbiological stability, texture and physical properties and transport properties (Aguilera *et al.* 2000; Aguilera 2005; Aguilera *et al.* 2003; De Roos 2003). In drying technology, a trade-off between increased stability at low moisture and the associated structural changes often has to be made.

1.3.1 Advantages and disadvantages of conventional methods for drying of foods

Air drying is the most commonly used dehydration process in the food and chemical industry, producing products that are characterised by low porosity and high apparent density (Krokida and Maroulis 1997). The high temperatures commonly used during industrial air drying

(typically 65-85°C) cause damage to the microstructure (e.g. case hardening and shrinkage) and may also have a negative influence on the colour, texture, taste, aroma and nutritional value of the product, thereby influencing the quality of both the dried and subsequently rehydrated product (Ratti 2001). These changes in structure during drying are defined, and discussed in more detail in section 1.4. Other parameters that are controlled during industrial air drying are relative humidity (20-40%) and air velocity (1.5-2.5 m/s), in order to control the drying rate (Krokida *et al.* 2003).

In addition to high temperatures, another disadvantage of air drying is the low energy efficiency. Low thermal conductivity of foods limits heat transfer to the inside of foods resulting in a lengthened drying process. As the product dries from the outside, the heat must be transferred through a moisture-resistant dry layer to evaporate the water held inside, causing a drop in the drying rate known as the falling rate period. This is discussed in section 1.3.2.

Although there are several alternatives to air drying: microwave, freeze, osmotic, and vacuum drying, none is ideal in every respect (Nijhuis *et al.* 1998; Vega-Mercado *et al.* 2001; Wang and Xi 2005). For example, while microwave drying promotes quick drying, difficulties in controlling the rapid mass transport may cause uneven heating and damage in the form of 'puffing', resulting in a poor quality product. Additionally, this technique is associated with high start-up costs and ongoing costs relating to the replacement of expensive magnetrons (Nijhuis *et al.* 1998). However, this technique is particularly applicable to foods with high water content, for example fruits and vegetables, since the dielectric water absorbs the microwave energy quickly and efficiently. The energy absorption is proportional to the moisture content remaining, as other food components such as lipids and proteins do not absorb microwave energy as readily.

In contrast, freeze drying is known to produce products of excellent quality, allowing significant structural preservation (Sinesio *et al.* 1995). Freeze drying removes water by sublimation of a frozen product. Due to the absence of liquid water and the low temperatures required for the process, any deterioration and microbiological reactions that may have occurred in air drying are prevented which results in a higher quality product (Ratti 2001). Furthermore, the solid state of the water during freeze drying protects the primary structure and shape of the product, with

minimal reduction in volume (5-15% compared with ~80% seen with air drying) and excellent structural retention. The subsequent products have a sponge like texture, and rapidly reabsorb liquid when reconstituted. Indeed, it has been reported that the products of freeze drying are of higher porosity than those of air drying (Karathanos *et al.* 1996; Marabi and Saguy 2004; Rahman *et al.* 2002) and other drying methods such as microwave (Tsami *et al.* 1999), and vacuum drying (Rahman *et al.* 2002). However, the technique may result in losses of flavour volatiles resulting in a tasteless product (Lin *et al.* 1998), and is generally considered to be expensive (costs are 4-8 times higher than air drying) and energy-consuming (Ratti 2001; Lombraña and Díaz 1987). Therefore, the technique is in general only considered for high value foods, or if the process gives added value to the product, for example: (a) seasonal and perishable commodities, due to their limited availability; (b) baby foods, since it is desirable to feed them with maximum quality and nutritional foods; (c) nutraceutical foods; (d) distinguished organoleptic foods such as aromatic herbs or coffee; and (e) special end use foods, as those used for outdoor activities, military rations or instant meals (Ratti 2001). Generally freeze drying results in excellent structure retention, however collapse (loss of structure, reduction in pore size, and volumetric shrinkage) has been seen in freeze dried products which exceed their T_g (Levi and Karel 1995).

Combinations of conventional drying technologies have also been investigated. Wang and Xi (2005) reported a two-stage drying process that increased the quality of the final product, in this case carrot. This method involves a forced-air convective drying, followed by microwave drying, resulting in the combination of a higher quality product with the saving of energy and time.

Vacuum microwave drying (MVD) is a variation on normal microwave drying. The vacuum allows a low temperature to be used and fast mass transfer occurs due to the heat being generated from within the food, resulting in fast drying. This, coupled with the rapid energy transfer from the microwave heating, generates fast, low temperature drying. Other advantages of using a vacuum include the exclusion of air which inhibits oxidation, preserving the colour and nutrient content, and the ability to modify the texture of the sample by manipulating the power and pressure of the vacuum. For example, the high internal vapour pressure produced within the food by microwave heating combined with the low chamber pressure from the

vacuum cause samples to expand and puff. A detailed comparison of MVD, air drying and freeze drying applied to the drying of carrot slices is reported by Lin *et al.* (1998), summarising the usefulness of each technique. Krokida and Maroulis (1999) also reported the usefulness of MVD for the improved quality of dried fruit and vegetables, in terms of increased porosity and prevention of colour damage.

Several variations on freeze drying have been researched in an effort to reduce costs while maintaining the same quality, but none are currently used in industry. Microwave assisted freeze drying can increase the product quality even further than freeze drying alone, but there are technical problems associated with this process (e.g. corona discharges, melting and overheating, non-uniform heating) and costs are not always lower. Adsorption freeze drying uses a desiccant which creates a high vapour drive at low temperatures. This method has many advantages over traditional freeze drying but results in a lower quality product. Atmospheric freeze drying in a fluidised bed (containing adsorbent particles, fluidised with cold air) allows the simplification of drying apparatus and a reduction in energy costs due to the absence of the vacuum chamber (Di Matteo *et al.* 2003). Operation in a fluidized bed improves external heat and mass transfer rates, and since the process is at atmospheric pressure the internal heat transfer process by conduction becomes more efficient. The main drawback of this technique is the increase in drying time due to the latter stages of drying being controlled by internal vapour diffusion, and also the quality of the product may be reduced due to risk of the product collapsing at atmospheric pressure.

Consequently an opportunity exists for new drying techniques that could be used in the food industry. The future development of drying technology will be focused on optimization of the drying process, with respect to both product quality and process economics. In this work the possibility of drying with scCO₂ has been examined and the outcomes compared primarily with a conventional air drying technique.

1.3.2 Drying kinetics

Drying kinetics of various foods has been widely reported (Krokida *et al.* 2003; Mwithiga and Olwal 2005; Sereno and Medeiros 1990). Drying rate plotted versus the moisture content gives, what is known as the drying rate curve (Figure 1.4).

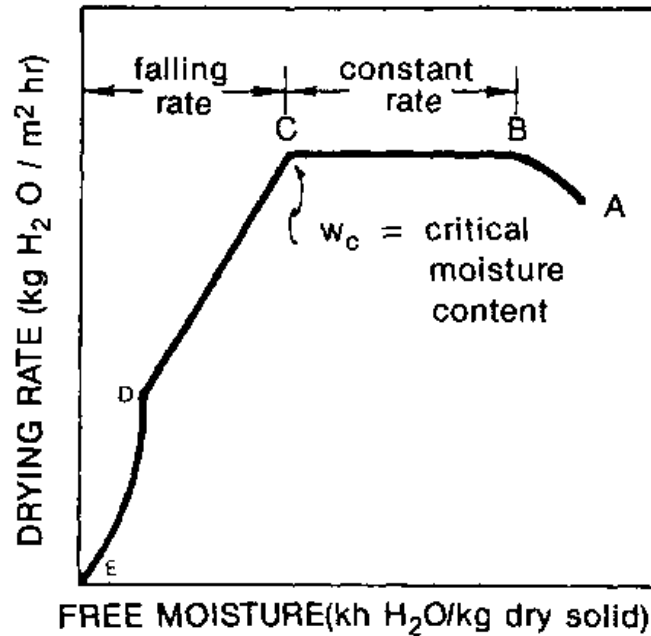


Figure 1.4 A drying rate curve illustrating the heating period (A-B), the constant drying rate (B-C), the falling drying rate (C-E) and the critical moisture content (w_c) at which the rate changes from one to the other (Naewbanij and Thepent n.d.).

A typical drying curve exhibits a heating period (Figure 1.4 (A-B)) directly followed by an initial constant drying rate period (Figure 1.4 (B-C)) which is governed fully by the rates of external heat and mass transfer. This occurs during the evaporation of water at the surface of the material being dried and the rate is nearly independent of the material being dried. Many foods (e.g. grains) do not exhibit this constant drying rate period, since no surface water is available, and internal heat and mass transfer rates determine the rate at which water becomes available at the exposed evaporating surface (Arévalo-Pinedo and Murr 2006). At a specific moisture content known as the critical moisture content (Figure 1.4 (w_c)) (which may be determined experimentally), the drying rate begins to fall, as the water cannot diffuse to the surface of the material as quickly as it is being evaporated due to internal resistances. The transport within the material depends on both the material and the drying conditions. This period is known as the falling drying rate period (Figure 1.4 (C-E)). This is discussed by Mujumdar and Devahastin (2000) in relation to both food and other materials.

The effect of temperature on drying rate and effective diffusivity is discussed by Mwithiga and Olwal (2005). The authors reported that as the temperature was increased, the drying rate and

the effective diffusivity also increase. Material thickness caused a decrease in the drying rate, which would be expected due to the longer distance that the water has to migrate before reaching the material surface.

The drying kinetics of pumpkin (containing 90-93% water) was investigated by Arévalo-Pinedo and Murr (2006). Vacuum drying enabled lower temperatures to be used during drying, offering production of a higher quality dried product. Drying occurred in the falling rate period; no constant drying rate was seen.

Shrinkage of material being dried plays an important part in calculation of the drying kinetics and is particularly significant in high water content foods, such as fruit and vegetables. There is however, limited information on the relationship between shrinkage and mass diffusivities reported in the literature. Some work was carried out by Arévalo-Pinedo and Murr (2006), where shrinkage was used to estimate the effective moisture diffusivity more accurately than if shrinkage had not been considered. A linear equation was used to relate linear dimensions of the material (length, width and thickness) to changes in moisture content.

Pre-treatment methods may be used to improve product quality but may also be used to modify the structure with the intention of improving mass transfer coefficients during drying (Arévalo-Pinedo and Murr 2006). It was shown that pre-frozen samples and blanched samples both increased the moisture transport rate during pumpkin drying.

1.3.3 Water content measurement

Water content is an important quality parameter as can influence the taste, shelf life and appearance of a product. Water determination is the most frequent analysis carried out on food, and because water is present in practically every food it can be widely applied. Water exists in several different forms: free water, adsorbed water and bound water. Free water is the easiest to remove and exists in cavities or in the pores of the food; adsorbed water and bound water are more tightly bound (especially bound water which involves strong hydrogen bonds) therefore more energy is required to remove these forms of water. There are several different techniques for determining the water content. However, some methods do not remove all the forms of water

present. Therefore, the level of accuracy required, and the specific form of water that is to be measured should be considered before choosing a water determination method.

Water measurement techniques may be sub-divided into direct and indirect techniques (Isengard 2001). Direct measurements aim at a quantitative determination of the water itself. Common direct techniques include the physical separation of water from the product (through heating, desiccation or distillation) and methods based on a chemical reaction of the water molecules, for example the Karl Fischer (KF) titration method. Indirect methods measure a property of the sample that depends on the water content, or measure the response of the water molecules to a physical influence. The use of nuclear magnetic resonance, near IR spectroscopy and microwave for water content measurement methods are all examples of indirect techniques.

Gravimetric analysis, despite being a direct technique, does not measure the water content as such but a mass loss under the conditions applied. The direct heating used in this method may be problematic due to the possible loss of volatile matter present, and the higher temperatures that are required to remove more tightly bound water can result in decomposition and production of more volatiles. Gravimetric drying has good repeatability but may exhibit limited reproducibility (the reproducibility depends on how well the climatic conditions of the laboratory, and the temperature and relative humidity of the oven can be controlled). However, this method is commonly used in the literature and is recommended as an official method of analysis for moisture content measurement in several foods (AOAC 1980; AOAC 1995; Tedjo *et al.* 2002).

A comparison of the different methods of water content determination in powdered milk concluded that the KF titration method was the best choice as a basic reference method (Reh *et al.* 2004). It is particularly useful because it identifies and quantifies the total water content present in all forms. The standard air drying oven method and a desiccation method were found to remove less water than the KF method, leading to the assumption that some water remained in the samples that were oven dried or desiccated. However, the KF technique is also not ideal as reactions may occur with the KF reagent and other ingredients in the sample. For example, vitamin C is known to react with KF reagents.

When deciding which method of water determination yields the correct or most accurate result, the bonding state of the water of interest should be considered, for example only 'available'

water contributes to microbiological instability. Therefore, quantification of the water contributing to microbiological instability may be measured accurately by gravimetric analysis. Distinguishing between different forms of water however, is problematic.

1.3.4 Drying of fruit and vegetables

Dried fruit and vegetables are important ingredients for many products, and are becoming increasingly more important due to the growing demand for convenience and healthier foods from consumers. Additionally, there is demand for processed products to retain more of their original characteristic (Torrington *et al.* 2001). Unfortunately drying often leads to chemical and physical changes which can affect sensory properties such as colour, taste, aroma, nutritional value, texture and swelling capacity, especially as most conventional methods use elevated temperatures. For example, the quality of red pepper (measured by colour characteristics and the antioxidant quantity) could be increased by air drying at lower temperatures (Simal *et al.* 2005).

Fruit and vegetables have high water contents so undesirable changes are often associated with dehydration, particularly shrinkage (Major and Sereno 2004). Heat treatment may alter the amount of volatiles present, either by loss of original volatiles or creation of new ones, and therefore will subsequently influence the flavour of the product (Nijhuis *et al.* 1998).

Current drying methods have been discussed in section 1.3.1 and constant improvements are being made to existing methods to increase final product quality. For example, pre-treatment of fruit and vegetables before drying has been accepted as a method to increase final product quality, and modification of the products structure may also improve mass transfer coefficients during drying (Arévalo-Pinedo and Murr 2006; Lewicki *et al.* 2002; Lewicki and Porzecka-Pawlak 2005; Tedjo *et al.* 2002).

Blanching is a commonly used pre-treatment as it inactivates enzymes which may cause loss of colour and flavour during drying and storage, but the process uses heat which may also have a detrimental impact on the product quality. Tedjo *et al.* (2002) investigated several pre-treatment methods which do not require high temperatures, including the use of scCO₂ prior to osmotic dehydration of mangoes, and studied their effect on mass transfer properties during osmotic dehydration. It was hoped that permeabilisation of the cell membranes during the pre-treatment

would enhance the mass transfer of solutes during osmotic dehydration. The application of scCO₂ however minimized water loss during osmotic dehydration (compared with standard untreated samples) but variation of the process parameters enabled manipulation of cell membrane permeabilisation: increasing temperature and pressure resulted in increased membrane permeabilisation. Such changes may be of significance during drying, as are expected to cause an increase in the mass transfer properties, despite showing no benefits during osmotic dehydration (Tedjo *et al.* 2002).

A post drying method, involving sudden decompression has also been investigated as a method to expand air dried products and provide more favourable organoleptic (e.g. taste, colour, odour and feel) characteristics (Louka and Allaf 2004). CO₂ may be used for this process and has been reported to cause the ‘puffing’ of vegetables.

Therefore, conventional drying techniques in general are not ideal but pre- and post-drying treatments may offer assistance in production of a better quality processed product.

1.3.4.1 Drying of carrots

Drying of carrots is the focus of chapter 2 of this thesis and therefore they have been discussed here with reference to previous research.

Carrots are one of the most commonly used vegetables for human nutrition due to high vitamin and fibre content (Doymaz 2004). However, drying of delicate plant materials such as carrot commonly results in a decrease in product quality, therefore it is important to consider the effect of the drying method on quality attributes such as shrinkage, texture, rehydration, colour, and nutrition.

The effect of air drying on carrots has been previously investigated at various air temperatures, ranging between 50°C and 75°C (Doymaz 2004). Typical falling drying rate periods were observed, but temperature gradients produced in carrot during air drying affected the predicted moisture loss of carrot pieces (calculated from moisture diffusivity information). Therefore a new model was proposed by Srikiatden and Roberts (2006) to account for these temperature gradients. Alternative drying methods, for drying of carrots have also been reported by Lin *et al.*

(1998). Vacuum microwave was shown to be rapid compared to air drying and also improved the texture, rehydration properties, nutritional value and colour of the dried product.

The effect of carrot structure (affected by blanching) on texture and rehydration was observed by Sanjuán *et al.* (2005). This reported work showed that carrot cell wall structure and contact between cell walls was important for both texture and rehydration properties.

Marabi *et al.* (2006) used a sensory panel to observe rehydrated carrot particulates that had been air dried and vacuum-puffed dried. Differences in flavour and texture were observed between carrot particulates dried via the two techniques. Furthermore, rehydration times (60–150 seconds) were shown to only have a marginal effect on the flavour profile, but had a marked effect on the texture profile.

1.3.5 Gels in the food industry

Gelling agents are of great importance in the food industry enabling manufacturers to meet convenience and indulgence trends as well as cut costs. A gel structure may be related to sensory texture and perception, and many processed foods such as meat, cheese, yogurt and confectionary depend on a gel network to provide the desired texture (Renard *et al.* 2006).

Agar, pectin, sodium alginate and other polysaccharide gels are commonly added to liquid foods to be dried and may also be used as thickeners or gel formers. Polysaccharide gels have also been used for biomedical and biotechnological applications such as drug delivery (Coviello *et al.* 2005). Biopolymer gels are divided into two main classes of gels: protein and polysaccharide based gels. The main differences are discussed by Renard *et al.* (2006). The work reported in chapters 3 and 4 has focused on the drying of a particular polysaccharide gel, agar. In contrast to protein gels, most polysaccharide gels are cold setting gels and the process of gelation is reversible. Gelation mechanisms and the consequent microstructure of specific biopolymer gels are discussed by Renard *et al.* (2006). The gel microstructure is important when considering the transport of small molecules in the gel, as the transport properties are expected to vary depending on the gel type and microstructure. Furthermore, microstructure is important for texture and flavour perception. The mechanism of gelation and structure of agar, is discussed in section 1.3.5.1

1.3.5.1 Introduction to agar

Agar is a colloid extracted from seaweed currently used as an additive for gelling, thickening and stabilising. Food uses of agars fall mainly within the following areas: bakery products, confectionary, desserts, meat, fish and poultry products, dairy products and beverages (Stephen *et al.* 2006).

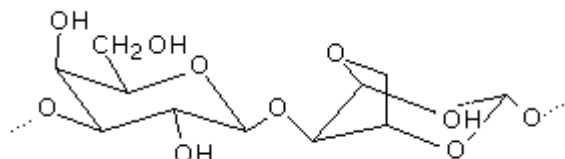


Figure 1.5 The molecular structure of agarose which is made up of this individual unit repeated.

The main structure of agar is Agar consists of two groups of polysaccharides: agarose and agarpectin. Agarose is the gelling component of agar and is chemically characterised by repeating galactose units (Figure 1.5). Agarpectin is a heterogeneous mixture of smaller molecules that occur in lesser amounts and gel poorly. Agarose may be prepared by fractionation of whole agar, but is too costly for food applications. Unfractionated agar is less expensive and provides the gelling function adequately. Typically, just 1% agar is enough to make a strong gel, making it a popular choice within the food industry. Agar must be heated above 85°C to melt the biopolymer and upon cooling to 30-40°C (dependent on gell type and concentration) the sol sets to form a gel. Functionality of agars in food products depends almost exclusively on their ability to bind water and to form thermoreversible gels which in theory may be melted and set an infinite amount of times.

The physical properties (gel strength, viscosity and melting point) of agar gels of different apparent molecular weight, extracted from different kinds of seaweed were compared by Suzuki *et al.* (2001). Gel forming power is governed by the existence of helices, and an increasing degree of regularity stabilises the helices. Different types of agarose exist, containing different substituents on the oxygen of the galactose residues which make up the polymer. These may alter the stability of the tertiary structure especially when the aggregation of the helices exists.

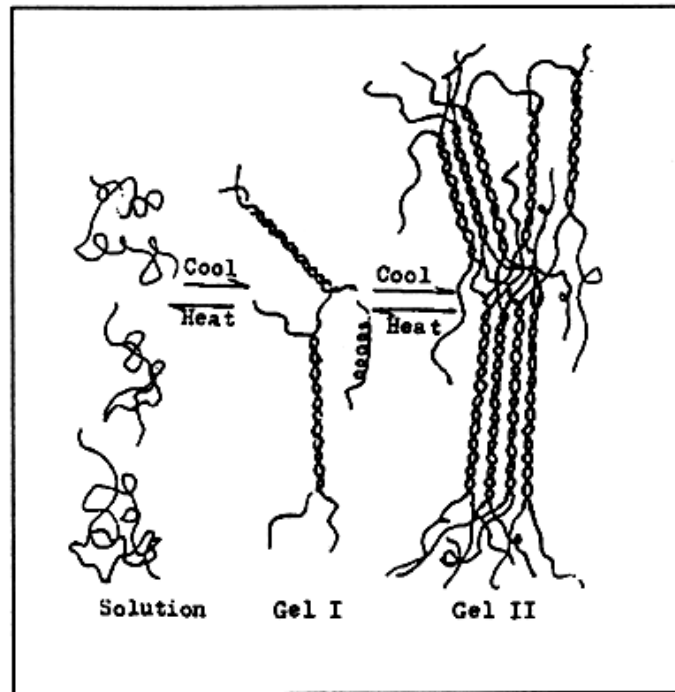


Figure 1.6 A schematic showing the gelling mechanism of agar. Above 60°C the gel exists in solution and upon cooling double helices are formed (Gel I) which then aggregate at junction points with other double helices to form a three dimensional network (Gel II) (Department of Aquatic Products 1990)

The gelling mechanism is illustrated in Figure 1.6: at temperatures above the melting point of the gel (60°C), thermal agitation overcomes the tendency to form helices and the polymer exists in solution as a ‘random coil’. Below this temperature intermolecular hydrogen bonding occurs which stabilizes formation of an ordered double helix (Figure 1.6 (Gel I)). The relationship between agarose gel properties and the double helix has been discussed in detail by Arnott *et al.* (1974). Thermoreversible gels, such as agar, also contain junction zones that are points at which the helices interact with themselves through secondary bonding, such as hydrogen bonding, and this formation makes up the gel’s tertiary structure (Figure 1.6 (Gel II)). This three dimensional rigid network is then capable of immobilising water molecules.

Much research has been carried out to investigate the mechanism of the gelation of biopolymer-water systems. Manno *et al.* (1999) has summarised this work to involve the interplay of three processes, including molecular conformational changes, spinodal demixing of the solution and molecular crosslinking. The first process (more commonly occurring at low concentrations of

polymer) involves the formation of low and high polymer concentration domains in the solution, due to phase separation. This occurs when the solution is in a thermodynamically unstable region (spinodal demixing) or in a metastable region (nucleated demixing). Spinodal demixing occurs when interactions within one molecular species prevail upon those among different species and upon the entropy of mixing, self sustained fluctuations generate the so-called “spinodal demixing”, that is the formation and growth of solvent-rich and solute-rich regions. The second process is that of molecular crosslinking when solute molecules exhibit multiple sites for linking. This process generally occurs at high polymer concentrations. Such crosslinking can also be nucleated but should not be confused with nucleated demixing. The third process is molecular conformational change which like demixing is thermodynamically driven. The favourable configurations of which involve solute-solvent interactions. The three mechanisms can be multiply interconnected.

Competition between the three processes has been reported to be affected by the addition of cosolute (Bulone *et al.* 1999). By appropriate choice of solvent and quenching temperature Bulone *et al.* (1999) showed that it was possible to modulate the kinetic competition between demixing and gelation, and therefore alter gel structural properties. Addition of ethanol to the polymer system has also been shown to inhibit a long range ordering process (San Biagio *et al.* 1989). Quenching temperatures were shown to have an effect on the rate of growth during the gelation process (Manno *et al.* 1999), while cooling at different temperatures and rates were reported to affect the strength of the gel due to the demixing process – demixing during curing caused a reduction in the elastic modulus and failure strain and stress (Aymard *et al.* 2001).

Competition between the gelation process and phase separation was reported to be controlled by the rate of ordering, with fast ordering favouring homogeneous gelation and slow ordering and/or aggregation giving rise to demixing in the gel state (Aymard *et al.* 2001). At high concentrations of polymer (2% agarose) direct gelation was seen without any spinodal demixing however spinodal demixing is commonly seen in solutions of lower polymer concentration (San Biagio *et al.* 1986). In low polymer concentration solutions, gelation may occur locally in regions of high polymer concentration, resulting from spinodal demixing (San Biagio *et al.* 1996; Bulone *et al.* 1997; Bulone and San Biagio 1991).

At low polymer concentrations, the introduction of a physical disruption (shear) during the gelation process has been used to create gelled particles (nuclei) which form a fluid or paste like gel (Norton *et al.* 1999). The nuclei grow to a size dictated by the shear environment and the gel concentration. Here it is suggested that the mechanism of gelation is one of nucleation and growth rather than spinodal decomposition (Norton *et al.* 1999).

Further discussion on the secondary (double helix) structure and tertiary structure of agarose is reported by Rees and Welsh (1977). The number of junction zones may affect the gel formation and also the chemical and physical properties of the consequent gel. The mechanism of gel formation and final gel microstructure has been reported by Renard *et al.* (2006) to influence texture and flavour perception. This is of particular importance in the food industry, as these attributes contribute to consumer acceptance. The importance of structure in food has been discussed further in section 1.4.

1.3.5.2 Drying of gels

This section discusses the drying of gels in general, incorporating some discussion on the drying of non-food gels. This research may then be related and applied to the drying of biopolymer food gels.

A gel consists of space filling networks of cross linked polymers, formed through various interactions between polymer chains, in which water is entrapped. The network formation is responsible for the mechanical properties of the gel but also for the behaviour and mobility of the incorporated water.

During drying of high water content gels under atmospheric conditions, pore fluid which maintains the liquid-vapour interface at the gel surface is lost, followed by the liquid-vapour meniscus receding into the gel interior, at the final stage of drying. This leads to extensive shrinkage, therefore if retention of the structure is important, current air drying techniques are unsuitable. Freeze drying, while offering good structural and volume retention produces brittle, fragile structures which do not store or transport well (Nussinovitch *et al.* 1993; Nussinovitch *et al.* 2000). Cracks may also occur in larger specimens due to slow freezing and therefore the formation of large ice crystals (Carrington *et al.* 1999).

Kalichevsky-Dong *et al.* (1999) investigated the effect of pressure shift freezing on the structure of frozen agar gel since it offers the potential to cause less damage to food materials than conventional methods of freezing because the rapid freezing allows ice nucleation to occur uniformly throughout the sample with the generation of smaller, more uniform ice crystals. However, agar gels were reported to have a reduced strength as a result of mechanical damage to the gel microstructure cause by ice crystal formation, independent of their size. Other gels such as starch and ovalbumin were reported to exhibit enhanced gel strength as a results of molecular structural changes that take place in the frozen state. This research may become important for the improvement of gel structure during freeze drying.

Fillers such as alumina, activated carbon, starch, pectin or silica may be used to strengthen mechanical properties and maintain structure in gels during drying. They may be inert, structure reinforcing, or chemically active. Addition of fillers (bentonite, cornstarch and rice-starch) to alginate gels were seen to help reduce shrinkage and also influenced the textural properties of the gel upon drying (Rassis *et al.* 2002).

Different drying techniques (evaporative drying and supercritical drying) were shown to have an effect on polyethylene glycol/tetramethoxysilicate hybrid gel surface area and pore size (Higginbotham *et al.* 2003). Microstructural measurements such as these are important for gel systems as they may be linked to physical properties of the dried gel, such as rehydration properties and texture. Further discussion on the supercritical drying of non-food gels can be found in section 1.2.2.

Conventional drying techniques generally result in extreme shrinkage of gels with high water contents, and may even cause degradation of biopolymer gels if high temperatures are used during drying (Freile-Pelegrín *et al.* 2007). Therefore other methods have been investigated here in order to preserve structure through drying.

1.3.5.3 Addition of sugar to biopolymer gels and their effect on microstructure and physical properties

The inclusion of sugar into gels has been shown to have a favourable effect on gel structure. The addition of sucrose to agarose biopolymer gels has been shown to change the gel network

structure, increasing the number of cross links (created by hydrogen bonds between the hydroxyl groups in sugar and agarose) and decreasing the size of the junction zones (Suzuki *et al.* 2001). This consequently influences the mechanical properties of the gel (Normand *et al.* 2003). Normand *et al.* (2003) suggested that the sucrose may increase the affinity of the polymer helix for the binary solvent and therefore limit the drive towards helix aggregation. An increase in sugar content was reported to make the gels harder but with a less cohesive texture. Normand *et al.* (2003) also reported that with increasing sucrose concentration, the resulting gel network appeared to be more uniform with smaller pore size. A pure agarose-water network forms an inhomogeneous microstructure through aggregation of the chains in polymer-poor and polymer-rich areas. Higher quantities of sucrose also contributed to a more elastic and deformable, but less brittle agarose gel network. This may be due to an increased internal flexibility of the fibres which were seen to be thinner and less coarse than comparable agarose fibres, produced without sucrose present. The addition of sucrose may cause an increase in the affinity of the helix for the solvent therefore limiting the drive to helix aggregation.

The physical properties of Indian and standard Oxoid agars were also seen to alter with the addition of sugars: addition of 50% sucrose to the agar caused the gel strength to double (Meena *et al.* 2006). The FT-IR spectra of these different agar types were also reported by Meena *et al.* (2006) which illustrated some differences in the chemical structural of the different agar types.

Addition of sucrose has also been used to assist freezing of biopolymer gels, leading to favourable effects on the microstructure (Fuchigami and Teramoto 2003). Sucrose addition was shown to decrease the freezing temperature of gels and 5% sucrose was effective in preventing the formation of ice crystals. Structure was observed by cryo-scanning electron microscopy (cryo-SEM) and an improvement in the structure of frozen gels was seen in those samples containing more than 5% sucrose. However, above 10% no change in the structure was seen – the same coarse network existed.

Addition of sucrose to alginate aqueous solutions (>0.5% w/w) was shown to increase the elastic nature of the system. This was thought to be due to the decreased availability of water through sucrose hydration and therefore the alginate is concentrated locally, increasing the probability of overlapping and entanglement of alginate chains (Pongsawatmanit *et al.* 1999). In contrast,

sucrose addition was reported to prevent packing of agar in centrifuged gels due to sucrose solvation, suggesting that less overlapping of the chains was occurring (Shin *et al.* 2002). Water was reported to be less mobile in gels containing sucrose due to interactions with the sucrose and a competitive effect on water binding between sucrose and agar.

In summary, it appears that the addition of sucrose enables more cross linking and entanglement of polymer chains, while less aggregation and close packing of the polymer chains occurs due to sucrose solvation. Consequently, this results in changes to the mechanical properties of the gel. Sucrose and other sugars may therefore provide a useful tool to allow maintenance and manipulation of gel structure through drying.

The addition of sucrose to gels during drying, and the effect of different concentrations of sucrose addition on the structure, texture and rehydration properties has been investigated in chapters 3 and 4.

1.4 Importance of food structure resulting from drying

In addition to preservation, dehydration can be used as a means to add convenience and control release in the mouth. For example, dehydrated foods may be eaten without rehydrating first, providing a ready to eat convenience food. Alternatively, they may require instant rehydration enabling a food to be prepared and ready to eat in a short space of time. Therefore the properties of both the dried and rehydrated structure and also the rehydration properties themselves are important for dried convenience foods. Secondly, the consumption and breakdown of a food product in the mouth takes place in three stages: an initial ingestion phase, a repetitive chewing phase, and swallowing. The internal structure of the food becomes most important during the chewing phase, when breakdown of the product takes place and physical parameters such as melting, viscosity, sound and firmness of foods are realised (Aguilera and Stanley 1999).

Typically it is desired to preserve the well-known structure and sensorial characteristics of the starting material although sometimes a new structure may be required that serves a different functional purpose. The structure obtained after dehydration depends on the product being dried and the method of drying. Air drying for example, can result in major structural changes in some foods, while other foods experience little structural variation. Following dehydration, grains and

legumes retain their structure, remaining viable as seeds, whereas foods such as meat and fish experience large structural and organoleptic changes. In spite of this, both are still widely consumed. Fruit and vegetables also experience severe structural changes (as well as discolouration and loss of valuable nutrients) during air drying and their structure currently can only be retained by freeze drying. Drying of fruit and vegetables, in particular, is discussed in section 1.3.4.

The change in microstructure (typically below 100 μm) during drying is important when it comes to relating these changes to those at the macrostructural level, such as density, mechanical behaviour, rehydration kinetics, and water location (Aguilera *et al.* 2003). Food structure is also related to nutrition and chemical/microbiological stability (Aguilera 2005). The ultimate intention is to develop relationships between the microstructure and quality parameters that influence sensorial perception and consumer preference.

One of the most important structural changes that food suffers during drying is the reduction of its external volume. Loss of water and heating cause stress in the cellular structure of the food, leading to change in the shape and decrease in dimension. Shrinkage may have a negative effect on the quality of the dehydrated product and therefore gives a negative impression to the consumer. However, some dried products such as raisins, dried plums, dates or peaches are accepted in their traditionally shrunken appearance.

Solid and semi-solid food systems consist of a heterogeneous three-dimensional (3-D) solid network or matrix holding large quantities of a liquid (in most cases aqueous) phase. Biopolymers are the common structural elements of the solid matrix. When water is removed from these systems, a pressure imbalance is produced between the inner and outer pressure, leading to shrinkage, collapse, changes in shape, and occasionally cracking (Achanta *et al.* 2004). The lack of shrinkage seen in freeze drying is owed to the process occurring under vacuum. However, collapse (which sums up loss of structure, reduction of pore size and volumetric shrinking) has been observed by Levi and Karel (1995) in highly porous materials, produced by freeze drying. Collapse occurred when the temperature of the dried portion increased above the T_g of the material.

T_g can be defined as the temperature at which an amorphous system changes from the glassy to the rubbery state, and it can be determined experimentally (Ratti 2001). It is thought that the T_g may be responsible for the deterioration mechanisms during processing, and is an indicator of food stability, but more importantly the quality of foodstuffs has been reported to be seriously altered if a process exceeds the T_g (Peleg 1996). This characteristic may not be so significant in drying methods that use lower temperatures, as it is unlikely that the T_g will be reached in these cases.

Collapse may adversely affect the properties of the dried material and cause poor rehydration capabilities. For example, collapse may cause sealing of capillaries which in turn leads to poor rehydration and reduced volume gain. Furthermore, surface cracking occurs when shrinkage is not uniform during the drying process, resulting in unbalanced stresses (Mayor and Sereno 2004). Browning is also an undesirable result of structure collapse, caused by the subsequent release of encapsulated lipids or oils from the matrix (Ratti 2001). Oxidation of these substances leads to the development of the brown pigment, associated with the Maillard reaction.

A comparison of the effect of microwave and convective drying methods on the structure and quality of potatoes has been studied recently, with particular emphasis on shrinkage (Khraisheh *et al.* 2004). In the case of air drying, temperature is the main parameter affecting shrinkage. In low temperature processing, diffusion of water from the inner to the outer zone of the material happens at the same rate as evaporation from the surface therefore there are no sharp moisture gradients. In this case, a more uniform moisture distribution exists, reducing the internal stresses and allowing the sample to shrink until the latter stages of drying, when the shape becomes fixed. At higher temperatures (rapid drying rates), intense moisture gradients are present throughout the material, causing case hardening to occur and the volume becomes fixed at an earlier stage. Case hardening is associated with systems where water removal from the surface is faster than the rate at which water migrates from the interior. The surface therefore dries to form a hard layer, and the volume becomes fixed before the product is fully dried. In this case less shrinkage is observed but due to stresses in the dried material, cracking and breakage may occur. In addition, hot air dried products are often difficult to rehydrate because of case hardening and shrinkage that has taken place (Khraisheh *et al.* 2004).

In microwave drying, mass transfer of moisture through the product is accelerated which results in improved drying rates compared with air drying and also lower energy consumption. Potato samples dried in a microwave generally exhibited less shrinkage than air dried samples and their rehydration properties were improved due to their 'puffed structure' (Khraisheh *et al.* 2004). Similarly, 'puffing' brought about by a sudden decompression technique has been shown to favourably increase the volume of partially dried vegetables, potentially providing a method for controlling quality of dried vegetables (Louka *et al.* 2004). Nevertheless, damage to the structure may also be caused by 'puffing' and furthermore, microwave drying can bring about complex chemical conversions and reactions which may cause degradation of vitamins, lipid oxidation and browning.

Texture, nutrition and chemical/microbiological activity are additionally affected by a product's microstructure (Aguilera 2005). In the case of nutrition, the presence of cell walls can be a controlling factor in the proportion of ingested nutrients made available for absorption in the gut. Mashing carrot for example releases more of the cellular content, making micronutrients more available. Additionally, disruption of cell microstructure influences formation of flavours, off-flavours and browning reactions. High pressure drying processes may cause severe texture loss, due to structure breakdown, especially in fruits and vegetables.

In summary, food quality is a difficult parameter to measure, combining factors such as rehydration potential, colour, volume/shrinkage, density, nutritional value, and textural properties. Food quality is often inferred by measurement of parameters such as the appearance, texture and taste. These changes on a macrostructural level are directly affected by the product's microstructure, hence making measurements on a much smaller scale increasingly important.

1.5 Analysis of internal microstructure

Several methods for the analysis of internal microstructure of food products exist. Microscopy is the most common method employed and is discussed in section 1.5.1. However, some microscopy methods require the sample to be cut or fractured, thereby destroying the sample. X-ray micro-computed tomography (x-ray micro-CT) is a non-destructive technique, enabling viewing of a product's internal structure without the need to destroy it. Further, advantages and disadvantages of both techniques are discussed in sections 1.5.1 and 1.5.2.

1.5.1 Microscopy

Recent advances in microstructural studies (measurements below 100 μm) have transformed our knowledge of foods as materials. Food structure may be studied at almost any dimensional level, in real time and with minimal intrusion. Structure formation throughout the drying process can be followed, whether from a tissue, a liquid dispersion or a dry powder.

Microscopy has progressed beyond simple light and electron microscopy, to newer forms available for food study at the microstructural level (Aguilera *et al.* 2000; Kalab *et al.* 1995). Atomic force microscopy (AFM) can be used to study the surface topography of food materials, while confocal laser scanning electron microscopy (CLSM) is most advantageous in its ability to provide thin, high resolution optical sections through a thick specimen. Environmental scanning electron microscopy (ESEM) allows samples to be studied in a hydrated state, without having to undergo any of the usual sample preparation steps for SEM, namely drying and coating. Additionally, the usual high vacuum pressure required in SEM is not needed. Finally, cryo-SEM allows delicate cellular structures such as plant tissue to be frozen quickly, preserving their natural state. Subsequent fracturing allows visualisation of the materials internal structure (Sanjuán *et al.* 2005). The application of SEM for studying the microstructure of wet samples has been discussed by James (2009) in more detail.

The visualisation of true food structure is extremely difficult, as most analytical techniques, with the exception of x-ray micro-CT and ESEM, require some kind of sample preparation which will inevitably alter the food product in some way. Several imaging techniques may therefore be used alongside each other, for comparison and/or confirmation of results.

1.5.2 X-ray micro-computed tomography

X-ray micro-CT is particularly useful as it allows information to be gained on the product's internal microstructure without invasive investigation, and also allows delicate cellular materials to be examined. It has several advantages over microscopy methods, such as light microscopy and electron microscopy: (i) the ability to investigate samples in their natural state at atmospheric pressure and temperature, free from artefacts; (ii) greater spatial resolution than some other microscopy methods; (iii) the ability of x-rays to penetrate through any material and,

in most cases, capture 3-D details of the inner microstructure; (iv) the ability to obtain reliable, quantitative, two dimensional (2-D) and 3-D information (Lim and Barigou 2004).

This technique however, is not suitable for the viewing of wet samples, since the image is dependent on the attenuation (absorption and scattering) of x-rays, arising principally from differences in density within the specimen (Lim and Barigou 2004). When high water content is present the x-rays are strongly absorbed therefore making it difficult to observe the wet microstructure of the sample, independent of the water and no contrast exists in the image. However, providing the specimen is dry, x-ray micro-CT can yield an image that displays differences in density throughout the sample. Bubbles and voids in foods have also been imaged by Lim and Barigou (2004), and the voids left by ice crystals have also been observed by Mousavi *et al.* (2007). Many other features in food products, for example connective tissue in freeze dried meat and different types of tissue in carrot (phloem and xylem) have also successfully been observed (Mousavi *et al.* 2007).

Perhaps the most useful feature of x-ray micro-CT is the ability to carry out quantitative analysis on x-ray micro-CT images, in addition to qualitative analysis. 2-D quantitative information can be gathered from horizontal images collected, including air cell count, number-mean cell size, total cell area and relative cell area. Analysis software also allows a 3-D model to be produced. Subsequent structural analysis of this 3-D model allows parameters such as air cell volume fraction, cell surface-to-volume ratio, cell wall thickness distribution, index of connectivity, and degree of anisotropy (a measure of 3-D structural symmetry) to be collected. The degree of connectivity and degree of anisotropy are both important factors in determining the mechanical strength of a cellular structure, which consequently affects the final product quality. The spatial cell size distribution may also be reconstructed from the x-ray micro-CT images using a stereological technique. Stereological methods are used to obtain quantitative 3D structural information (number, length, surface or volume) from measurements made on 2D sections.

Several aerated food products (solid and semi-liquid) have been quantitatively analysed using x-ray micro-CT (Lim and Barigou 2004). Information such as voidage, cell wall-thickness distribution, air cell connectivity and degree of microstructure anisotropy were obtained. The technique has also been applied to the imaging and quantifying of ice crystal structures, formed

during freezing of food (Mousavi *et al.* 2007). The parameters of voids (left by ice crystals), including size, area and width were quantified using this technique. Léonard *et al.* 2001 also used x-ray micro-CT to observe the shrinkage of (non-food) soft material (waste water sludge) during drying. Image analysis on the samples allowed shrinkage curves to be plotted. This may also prove a useful technique for the analysis of food shrinkage during drying.

This reported research, albeit limited, illustrates that x-ray micro-CT has advantages over other techniques for microstructural analysis of dried food structures.

1.6 Macrostructural measures of quality

During food processing, microstructural changes are inevitable. However, it is the effect of these microstructural changes on the macrostructural properties, such as rehydration and texture that will influence the final product quality. Therefore macrostructural properties are hugely important when considering product quality and how it may be perceived by the consumer. Texture, colour and rehydration, in particular, are discussed in the following sections.

1.6.1 Texture analysis

Textural attributes of food are often derived from the product's structure, and are perceived by the consumer through mastication - when a food product is eaten. Texture plays an important part in the sensorial perception of food therefore measurement of texture is of particular importance during food processing. Texture is discussed in relation to perception of foods by Renard *et al.* (2006). Commonly, mechanical properties of a food are measured which may then be related to specific textural attributes in the material.

Microstructure changes such as cellular turgor and cell wall integrity are the main contributing factors to textural property changes in fruit and vegetable tissue. Tissue softening is common in fruit and vegetables that are blanched prior to processing, although some pre-treatments, such as addition of calcium, are available to minimise this effect (Ahrné *et al.* 2003). Calcium acts by strengthening the cell walls which are usually firm in pre-processed fruit and vegetable tissues. Heat and high pressure processing may also result in the breakdown or separation of cell walls, resulting in a product with a softer texture. For example, texture loss in carrots during high

pressure processing (where vacuum packed carrots were held in a mixture of propylene and glycol transmitting 100-550 MPa of pressure, for 120-1800 seconds) was reported to be due to disruption and/or rupturing of cellular membranes and therefore a reduction in the cell turgor pressure, due to rapid changes in pressure (Aguilera 2005; Trejo Araya *et al.* 2007). In contrast, high pressure (200-400 MPa) treatment during freezing of gels has been reported to improve the texture of gels and gelled systems such as tofu (Fuchigami *et al.* 2002; Fuchigami *et al.* 2006). This effect is due to fast freezing which occurs during pressure release, resulting in formation of smaller crystals than those produced through freezing at atmospheric pressure.

Texture analysis can be done using a trained sensory panel, however instrumental methods can save time, reduce costs and provide more consistent, objective results. The results of which may then be correlated with those from sensory panels. Texture analysis equipment provides a repeatable method for collecting comparable results quickly. Typically the material of interest is placed into a test area and force is applied using a probe or fixture. The deformation and force applied to compress, bend or puncture for example, is recorded which can give measure of a material's hardness, firmness or ability to fracture. A puncture test which measures the force required to penetrate or puncture the sample under analysis is commonly used and gives a measure of sample hardness. Different methods exist for different types of food products, for example a three point test support 'punch' test was developed for the texture analysis of potato chips. Texture of potato chips was found to be dependent on the moisture content which is expected for a dried product such as this (Segini *et al.* 1999).

Textural properties of a dried product may also be measured during rehydration of the product, as a function of time and temperature (Cunningham *et al.* 2008). Quantification of textural properties during rehydration allows maximisation of product quality and prediction of textural attributes that a consumer might experience upon eating a dried-rehydrated product. The rehydrated texture may also be compared with that of the pre-dried product, giving a measure of the influence of the process on texture.

As discussed above, texture is commonly related to physical properties such as firmness, hardness and viscosity measurements. However, recent research has also begun to study textural attributes that are not directly related to physical properties of food, for example creamy,

crumbly and watery characteristics (van Vilet *et al.* 2009). Therefore, other material properties must be considered, such as the structural elements of the material forming the food structure and giving it its breakdown pattern; the structural elements that form the food bolus; and finally those elements that form the coatings on the oral surfaces during processing in the mouth. Hence, there is emphasis on the interplay between product properties, oral processing and sensory perception, as well as chemical processes that take place during mastication.

Textural analysis therefore provides a useful analytical tool for providing a link between physical properties, textural attributes and sensorial perception of a material. Analysis can be quick, easy and provide repeatable results. One disadvantage of the technique however, is that the sample being tested is usually destroyed upon analysis.

1.6.2 Colour analysis techniques

Colour is an important quality measure of food products and its measurement is particularly important following processing such as drying, where colour changes are likely to occur. Qualitative analysis is possible by visual inspection but quantitative analysis provides a more comparable, repeatable method.

Several commercially used methods exist for the quantitative measurement of colour, such as colourimetry and spectrophotometry. These techniques however, require a minimum sized sample piece (2cm²) with a uniform colour, and a flat surface on which to measure colour is also desirable. These disadvantages are avoidable by homogenizing the food sample using a blender or grinder to achieve uniform colour, but this destroys the sample and renders it unusable for other quality measurements.

A method for the measurement of the colour of food surfaces without the need to destroy the sample was reported by Yam and Papadakis (2004). The technique uses a combination of a digital camera, computer and graphics software. Quantitative information of the colour in terms of the L*a*b* colour model (CIELAB) was obtained. The L*a*b* model is an international standard for colour measurements and is extensively used in many industries for providing exact colour specs for paint, dyes, ink and paper. It is described in more detail in section 2.3.11.

This method is advantageous as it is both versatile and affordable. Since the colour of a food sample depends on the part of the spectrum which is reflected from it, a proper light source when capturing the images is of huge importance. The angle between the camera lens and the lighting source is important and should stay constant between measurements. Finally, the resolution of the camera is also important.

Alternatively, a scanner may be used as the image capturing method. The light source and image capturing method is then kept constant which is especially useful when recording measurements several days apart, allowing for accurate comparison of results (Kiliç *et al.* 2007). Results reported by Kiliç *et al.* (2007) agreed with those obtained from a spectrophotometer, proving the accuracy of this technique.

Both methods used a computer and colour analysis software to obtain $L^*a^*b^*$ values which could then be converted to a total colour change (ΔC) compared with a standard coloured sample:

$$\Delta C = \sqrt{(\Delta L^*)^2 + (\Delta a^*)^2 + (\Delta b^*)^2} \quad (1.1)$$

This simple and low cost method provides an attractive alternative to commercially used colour analysis instruments that have drawbacks, such as high cost and requirement of specific sample size and uniformity.

1.6.3 Rehydration

Most food structures are expected to perform in the dry state as well as the rehydrated one. No dried product that is eventually intended to be rehydrated can be of good quality if its rehydratability is low. Dried vegetables are used in many industrial food products, especially in instant foods which require a very short preparation time. It is therefore important that dried products have short rehydration times, while maintaining the characteristics of the fresh food product. The degree of rehydration is dependent on the processing conditions, sample composition and extent of structural and chemical disruption induced during drying (Marabi *et al.* 2006).

The rehydration ratio, calculated at particular time points gives a quantitative measure of how easily a dried product can be rehydrated:

$$\text{Rehydration ratio } (R_0) = W_r/W_d \quad (1.2)$$

Where W_d = weight of dried sample (kg) and W_r = weight of rehydrated sample (kg).

The moisture content and kinetics of moisture uptake may also be used as a method to monitor rehydration (Krokida and Marinos-Kouris 2003). For example, rehydration rate gives information about the speed of the rehydration process which may be influenced by the structure of the dried product; while equilibrium moisture content (EMC) gives information about how much total water the rehydrated product can hold. EMC can be compared with the initial water content of the pre-dried product and is often dependent on the extent of structural damage that has occurred through processing.

Rehydration of dehydrated food has been shown to be affected by bulk and open porosity. For example, the effective moisture diffusivity during dehydration was seen to increase with increased bulk and open porosity in dried carrots (Marabi and Saguy 2004). When considering rehydration of food particulates it may be important to consider capillary imbibition as well as the standard diffusion process that is expected for water movement into the product (Saguy *et al.* 2005). Water transport in foods is typically described as following molecular diffusion, but vapour diffusion, surface diffusion, Knusden diffusion, capillary flow, and hydrodynamic flow, can also contribute (Saguy *et al.* 2005).

Reported work on the rehydration kinetics of various fruit and vegetables showed that rehydration temperature appeared to have an effect on the rate of rehydration and the EMC of the rehydrated products (Krokida and Marinos-Kouris 2003).

Therefore several factors may affect the rehydration properties of dried food material, including rehydration temperature and dried structure. Structural differences such as porosity are influenced by the drying technique and therefore drying technique will also affect the rehydration properties (Rahman *et al.* 2002). The drying method should therefore be considered when rehydration properties of the dried product are important.

1.7 Aims of this work

Although many techniques for drying food products exist, none are currently ideal. Therefore a need exists to explore alternative food drying techniques. Given that SCFs have been successfully employed in other fields for drying, the overall objective of this work was to explore whether similar methods could be applied to food drying.

More specifically, the main aims of this work were to:

- Design, construct and optimise process equipment for supercritical drying, using CO₂ as the fluid of choice, and additionally investigate co-solvent addition and changes in experimental process parameters.
- Investigate supercritical drying as a method for removal of water from foodstuffs, including delicate vegetable structures and biopolymer gels.
- Investigate the potential to manipulate gel microstructure during supercritical drying, examine the effect of sugar addition to the formulation prior to drying and link any microstructural changes observed to the material's macrostructural properties such as rehydration, colour and texture.
- Compare this novel process with conventional methods of food drying, including air and freeze drying, with particular emphasis on final product quality.
- Finally, investigate the supercritical drying process on pilot plant scale equipment, to assess the industrial application of this technique.

A key requirement of an engineering doctorate is that it focuses on research with direct industrial importance. As discussed throughout this chapter, drying of foods is a key operation in the food industry which impacts on product quality, performance and economic viability. Customer satisfaction will be directly influenced by all of these. In this way, getting drying right is crucial and exploring alternative methods may improve outcomes and support product innovation.

2.0 Drying of carrots using supercritical carbon dioxide

ABSTRACT

The use of supercritical carbon dioxide (scCO₂) for the removal of moisture from cylindrical pieces of carrot (length = 25 mm and diameter = 4 mm) was investigated. All experiments were carried out at 20 MPa pressure. The effects of temperature, co-solvent (ethanol) addition and flow rate on moisture removal were examined. Additionally, the effects of sample internal structure and surface area on the rate of moisture removal were investigated. Comparison of these results with those obtained through air drying enabled a mechanism for water removal during supercritical drying to be suggested.

A range of conditions could then be chosen to dry carrot pieces for microstructural studies (using light microscopy, cryo-scanning electron microscopy and x-ray micro-computed tomography) and further analysis of sample properties, including rehydration, colour and texture. All samples were compared with carrot pieces that had been air dried.

Carrot pieces dried in the supercritical fluid environment were seen to retain their shape much better than air dried carrot pieces which underwent shrinkage. Samples dried with scCO₂ containing co-solvent (scCO₂(EtOH)) possessed more porous, less dense structures and consequently displayed more favourable rehydration and textural properties than the air dried equivalents. Some colour loss was observed when drying with scCO₂(EtOH). However, this was largely reversible upon rehydration of the samples.

2.1 Introduction

There is increasing demand from consumers for convenience from foods, but they are also opting for healthier and fresh-like produce. Hence, there is an opportunity for dried foods, in particular fruit and vegetables. However, fruit and vegetables contain high moisture contents and removing this water may subsequently damage the product. The challenge therefore exists to produce a higher quality product, following the processing stages.

The potential use of scCO₂ for drying foods was investigated as an alternative to conventional methods. Carrots were first used as a test material for supercritical drying because they contain ~90% water making them a suitable material for water removal studies. Their structure is also well-characterised in previous studies (Ng *et al.* 1998; Lin *et al.* 1998; Sila *et al.* 2006; Sanjuán *et al.* 2005) and additionally carrot is commonly employed as a dried ingredient. Various drying techniques have been applied to carrots, including vacuum drying, microwave drying freeze drying and conventional air drying (Lin *et al.* 1998; Doymaz 2004; Litvin *et al.* 1998; Wang and Xi 2005). Improvements on the colour, flavour and rehydration ability of carrot pieces dried using new techniques when compared with those dried using conventional methods have been reported by Lin *et al.* (1998).

Carrot is desirable as a dried ingredient in instant soups or meals as it has a high carotene, vitamin and fibre content. This makes it a desirable healthy food and a commonly used vegetable for human nutrition, while drying enhances the keeping ability of the food. This is of course dependant on the preservation of the nutritional value throughout the drying process.

Carrot pieces discussed in this thesis were dried to moisture contents that were low enough (<10%) to significantly delay spoilage. Discussion of the water activity and moisture content in relation to product shelf life can be found in section 1.3. Hui (2005) reported that dried vegetables with a water content of 14-24% have water activity values of 0.70-0.77 which is low enough to delay spoilage (Jay *et al.* 2005).

Once desirable moisture contents had been reached through supercritical and air drying, the properties and microstructure of the carrot pieces were studied in detail. This was the main area of research in this chapter: internal structure (dried and rehydrated) of carrot pieces was

investigated, as well as texture, colour and rehydration properties. Supercritically dried structures showed some benefits over those that had been air dried at the same temperature.

2.1.1 Solvent systems and the use of ethanol as a co-solvent

Drying using both pure scCO_2 ($\text{scCO}_{2(\text{pure})}$) and scCO_2 modified with EtOH ($\text{scCO}_{2(\text{EtOH})}$) was studied in this chapter. The critical point of $\text{CO}_{2(\text{pure})}$ has been well documented as 31.1°C and 7.38 MPa (Reid *et al.* 1987). This however changes for mixtures of solvents. When a co-solvent is added to scCO_2 , a binary solvent system is produced and the critical point of this mixture determines whether the system exists as a single phase or a two-phase vapour-liquid equilibrium, at the chosen experimental conditions. To ensure this work was carried out in the supercritical, single phase region, phase diagrams were consulted and Table 2.1 shows the critical points of different CO_2 -EtOH mixtures.

Table 2.1 The critical temperature and pressure of CO_2 -EtOH mixtures. Critical temperatures and pressures increase as the concentration of EtOH increases. Adapted from Reid *et al.* (1987). Mol % (as a measure of EtOH concentration) is defined in equation 2.5.

Mol % EtOH	T_c ($^\circ\text{C}$)	P_c (MPa)
0	31.1	7.38
0.95	32.7	7.65
2.14	35.3	7.83
2.78	37.2	8.07
3.66	39	8.25
4.64	42.1	8.61
6.38	47	9.19
7.32	52	9.74

2.2 Materials

2.2.1 Rig components

The high pressure rig was constructed from seamless 1/4" or 1/8" O.D. (outside diameter) 316 stainless steel rated to 75 MPa, connected by stainless steel Swagelok fittings (Swagelok, Manchester, UK). Details of further rig components and the experimental set up is described in section 2.3.1.

2.2.2 Carrot preparation and storage

Fresh carrots were purchased from a local supermarket. To determine the best storage conditions the weight loss of carrots stored at different conditions was measured over a week and compared. The percentage weight loss for each condition was recorded: refrigerator at 4°C (17%); ambient at 25°C (19%); humidity cabinet at 70% RH (relative humidity) and 20°C (41%); humidity cabinet at 40% RH and 20°C (45%). Storing the carrots in the refrigerator proved to be the most favourable conditions for retaining the most moisture therefore prior to their use in the drying experiments, they were stored in a refrigerator at 4°C within moisture-resistant packaging.

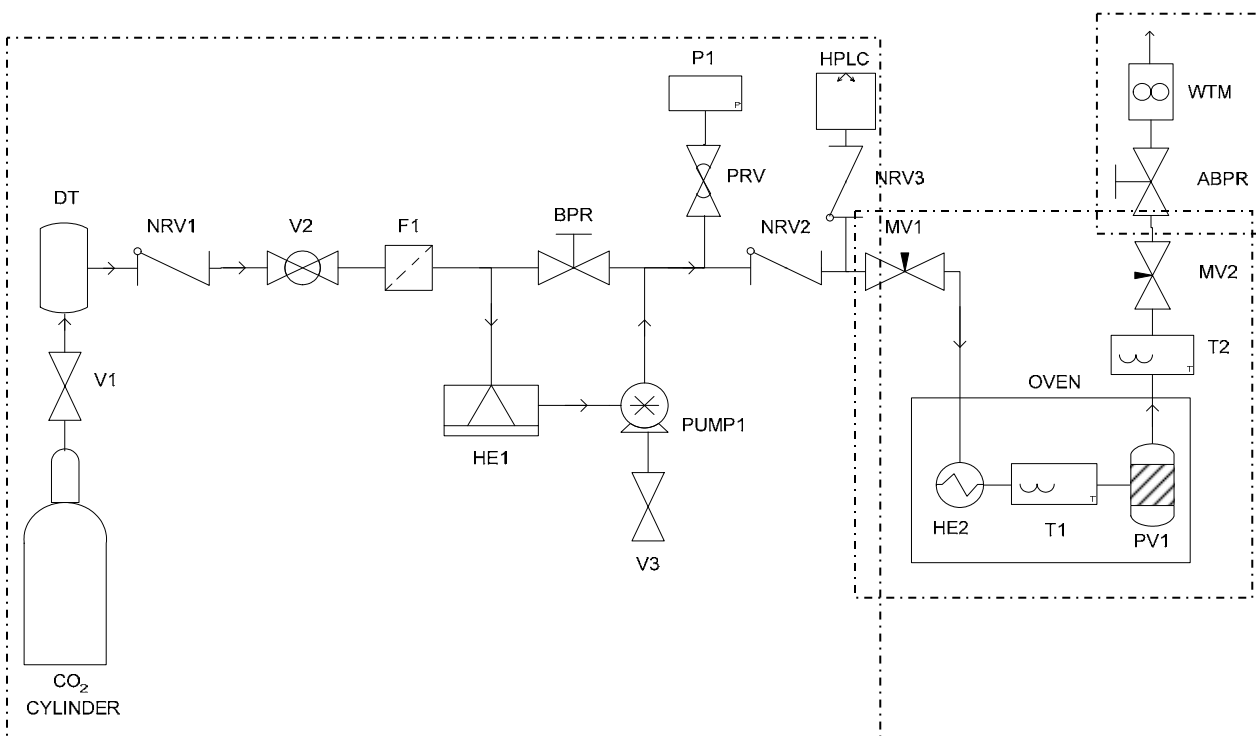
2.2.3 Carbon dioxide and ethanol

CO₂ (liquid withdrawal) was supplied by BOC (Guildford, UK). Absolute EtOH (99.9% pure) was supplied by Fisher Scientific (Loughborough, UK) and was of Analar grade.

2.3 Apparatus and methodology

2.3.1 High pressure equipment and supercritical drying method

The experimental rig, constructed by the author, for carrying out the supercritical drying experiments is shown in Figure 2.1. Notation used in the diagram is referred to throughout the following sections.



Key:

V1 = CO ₂ inlet valve	DT = desiccator tube
NRV1, 2, 3 = non-return valves	V2 = ball valve
F1 = in-line filter	BPR = back pressure relief valve
HE1 = refrigerated heat exchanger (cooling)	V3 = pneumatic pump air valve
PUMP1 = pneumatic liquid CO ₂ pump	PRV = safety pressure relief valve
P1 = pressure gauge	HPLC = HPLC co-solvent pump
MV1, 2 = micrometering valves	HE2 = heat exchanger (heating)
T1, 2 = thermocouples	PV1 = reaction pressure vessel
ABPR = automated back pressure regulator	WTM = wet test flow meter

Figure 2.1 Schematic representation of the experimental apparatus used for supercritical drying.

As indicated in figure 2.1 the rig can be described in three parts: 1) supercritical fluid delivery section, 2) drying section and 3) depressurisation section (each section is enclosed with dotted lines in figure 2.1 for clarity).

Supercritical fluid delivery section

This section delivered CO₂ at the correct pressure to the drying section. The apparatus forming this part of the rig is represented by all components upstream of the first micrometering valve (MV1) in Figure 2.1. Although not part of this section, the valve incorporated into the automated back pressure regulator (ABPR, Thar Technologies Inc., Pittsburgh, PA, USA) would always be closed during filling of the rig, until the required pressure was obtained.

Liquid CO₂ was supplied from a 25kg cylinder and passed through a desiccator tube to remove any residual moisture, and was then passed through a 2 µm filter (F1, Swagelok SS-2TF-2) to remove particulate contaminants. A non-return valve (NRV1, Swagelok SS-CH2-10 with ethylene propylene seals) was situated on the gas inlet to ensure no CO₂ could return to the supply cylinders. The CO₂ was cooled by a jacketed refrigerated heat exchanger coil (HE1) to a liquid state (to allow efficient pumping and avoid cavitation effects in the pump) and was compressed to the desired pressure using an air-driven liquid pump (PUMP1, Powerstar 4 Liquid pump 4F-64). The pressure was monitored with a pressure transducer (P1, Druck PTX-521-00) coupled to an associated digital indicator (Druck, DEI 260).

The stroke rate of this pump was controlled by an air regulation valve (V3, Wilkerson CB6-C4-F00). The heat exchanger coil was chilled by a continuous flow of coolant fluid from a recirculation bath (Grant W14), maintained below 5°C by a refrigeration unit (Grant FC15 Flow Cooler). All piping from HE1 to PUMP1 was lagged with insulating material in order to retain the CO₂ in its liquid state.

CO₂ leaving PUMP1 passed through a back pressure relief valve (BPR, Haskel 15670-2), employed for the fine adjustment and maintenance of the system pressure. Excess CO₂, beyond that required for maintaining the system pressure was recycled back via a loop.

An HPLC (high performance liquid chromatography) pump (HPLC, Gilson 308) with in-built flow rate control was used to add EtOH (when required) to the system. The EtOH was delivered by the pump from a graduated 25 ml burette that was used to accurately quantify the amount added. A non-return valve (NRV3) was situated on the EtOH inlet line to prevent pressurised CO₂ flow to the HPLC pump. The micrometering valve at the exit (MV2) remained open during

this stage. The desired pressure was maintained by keeping another micrometering valve closed which was a component of the ABPR and was computer controlled.

Drying section

This part of the rig is represented in Figure 2.1 by components downstream of, and including MV1 through to MV2. The CO₂ was delivered at a controlled pressure and was heated in this section to the desired temperature, before passing over the material which was being dried.

After the MV1, the compressed CO₂ was passed through a heat exchanger coil (HE2) and into a 50 ml pressure vessel (PV1, Baskerville), held within an oven which was pre-heated to the desired experimental temperature. Calibration of the oven was carried out using an average reading from three thermocouples. The temperature of the CO₂ was monitored directly before entering the pressure vessel and also at the exit, by K-type thermocouples encased in a stainless steel sheath (T1 and T2, RS Components). Measured temperatures were displayed on a digital 12-point readout (RS Components). Once the desired temperature (50°C or 60°C) and pressure (20 MPa) had been reached, the heated ABPR micrometering valve was opened and a constant flow rate of ~2 l/minute at standard, temperature (0°C) and pressure (0.1 MPa) (STP) was achieved. The flow was monitored throughout the experiments using a wet test flow-meter (WTM, Allied Instruments Ltd., A120) (part of the depressurisation equipment section) and adjusted when necessary using the ABPR micrometering valve. The WTM was calibrated by the displacement of air into the WTM from a container of known volume, using water.

Depressurisation section

Following the required drying period of the experiment, the ABPR micrometering valve was closed so that a depressurisation program could be set, using the associated computer. A constant depressurisation rate (0.4 MPa/minute) was used for these experiments and was controlled by the ABPR. The ABPR micrometering valve was heated to 85°C which prevented blocking of the valve due to ice formation when the CO₂ was vented to atmospheric pressure. The flow of CO₂ routed to a WTM via tubing, enabling monitoring of the flow rate during depressurisation and also the total volume of CO₂ passing through the rig. A photograph of the drying and depressurisation section of the rig is shown in Figure 2.2.

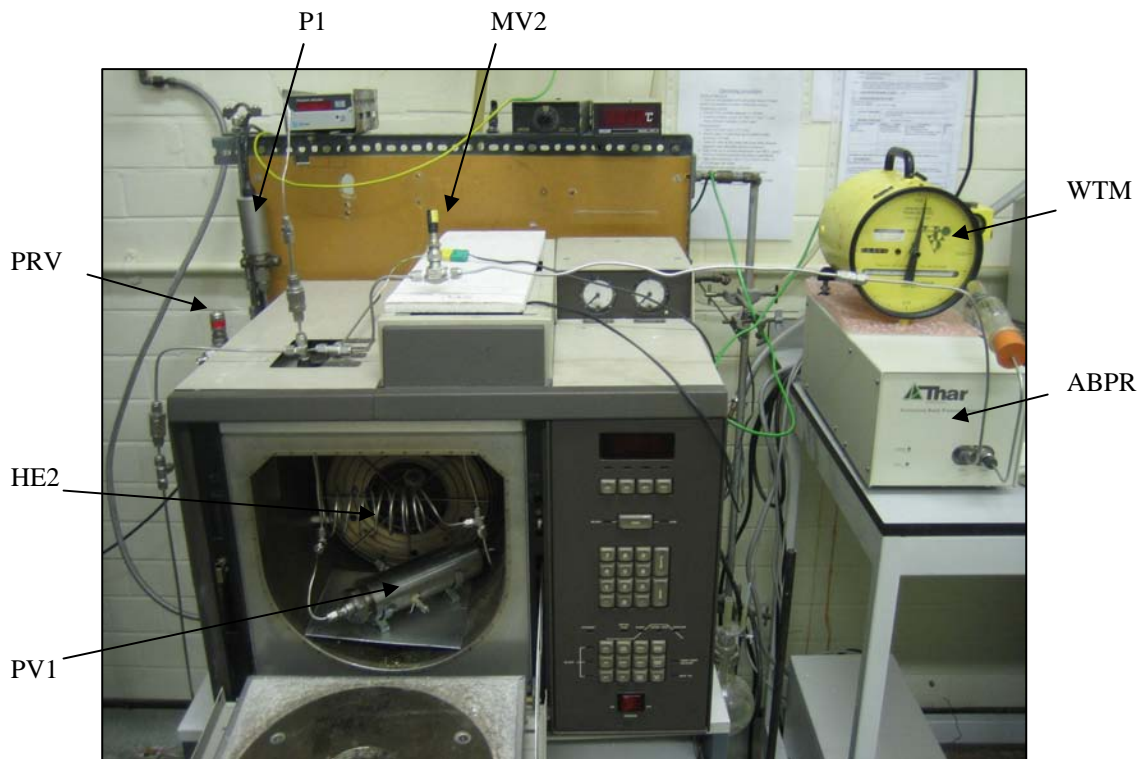


Figure 2.2 Photograph of the experimental apparatus detailed in the ‘drying section’ and the ‘depressurisation section’, where: PV1 = reaction pressure vessel; HE2 = heat exchanger; PRV = safety pressure relief valve; P1 = pressure gauge; MV2 = micrometering valve; WTM = wet test flow meter; ABPR = automated back pressure regulator.

2.3.2 Initial sample characterisation and preparation of carrots

A cork borer was used to cut cylindrical pieces (length = 25 mm and diameter = 4 mm) from carrots. The core (xylem) and cortex (phloem) have been shown by Srikatden and Roberts (2006) to have different moisture transfer properties at different temperatures therefore only the cortex was used to ensure consistency – for clarification this is the part of the carrot labelled ‘phloem’ in Figure 2.3. The xylem transports water and dissolved minerals from the roots throughout the plant body and is composed of four cell types: vessel elements, tracheids, parenchyma cells and fibers. The phloem transports sugars throughout the plant and like the xylem is composed of four cell types: sieve tube members, companion cells, parenchyma cells and fibers. The boundary between the cortex and the central core is known as the stele.

For each experiment seven carrot cylinders were cut from one whole carrot: four were used in a drying experiment; three were used to determine the initial average total moisture content of the carrot. The initial moisture content of the carrot pieces was measured by drying the samples in an oven, at 80°C to constant mass and comparing to the original mass (Tedjo *et al* 2002). The initial moisture content typically was found to be ~90% w/w which is expected for vegetables of this kind (Doymaz 2004). A secondary method was also used, where carrot samples were dried over the drying agent, magnesium sulphate (MgSO₄), at room temperature and pressure, until a constant weight was reached. This technique confirmed that the weight loss recorded using the high temperature, oven method, could be assumed to be water and any weight loss from other compounds such as volatile matter was insignificant. Therefore, the oven method was the favourable method for moisture content determination (due to its speed and ease) and is used throughout this work.

Both cooked and raw carrot samples were used in this work. Cooking was carried out by placing the carrot piece in boiling water for 600 seconds.

The water content in this work is mainly reported as normalised moisture content (NMC) - a dimensionless value - which allows the water content after drying and rehydration to be comparable with the initial pre-processed water content (equation 2.2). There may be some variability in the initial water content of carrots, so this method guarantees that the extent of drying or rehydration (compared with the original water content) is measured, rather than just an arbitrary water loss or gain which may vary depending on the initial carrot moisture content.

The moisture content was calculated on a dry basis (d.b.), as the ratio of the amount of water, to the amount of dry solids in the sample:

$$X = \frac{m - m_s}{m_s} \quad (2.1)$$

where X is the moisture content of the sample (d.b.) (g water/g dry matter), m is the total mass of the sample at time t (g) and m_s is the mass of the dry solids (g).

The NMC may then be calculated using the following equation:

$$NMC = \frac{X_d}{X_0} \quad (2.2)$$

where NMC is the normalised moisture content, X_d is the moisture content following the drying experiment (g water/g dry matter) and X_0 is the initial moisture content (g water/g dry matter). Carrots had an average initial moisture content of 9.01 ± 1.78 g water/g dry matter.

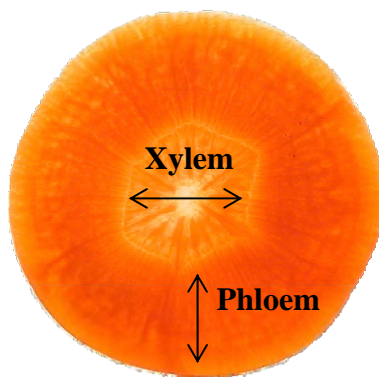


Figure 2.3 A photograph of a horizontal cross section through a carrot, illustrating the different tissues of the carrot: phloem (cortex) and xylem (core).

2.3.3 Method for supercritical drying of carrot pieces using supercritical carbon dioxide

Four samples for each experiment were placed in a purpose built sample holder which held the material in the centre of the pressure vessel (Figure 2.4). This was to protect them from any wall effects of the CO_2 flow, that may occur at the inside walls of the vessel. The samples were also held in a parallel arrangement which was found to be preferential to a sequential arrangement for gaining similar moisture contents in samples throughout drying. The sample holder was placed inside the pressure vessel and closed. CO_2 was introduced into the apparatus and then pressurised to the desired pressure. The temperature was then raised, using an oven set to the required temperature. Once stable conditions had been reached, the exit micrometering valve was opened to achieve the desired flow rate, monitored by the WTM. EtOH, if required, was also added at this point and programmed to pump at a rate that would result in the desired molar ratio of EtOH to CO_2 passing through the pressure vessel. The average EtOH concentration used and the calculation used to work out the rate of addition of EtOH are detailed in the next section.

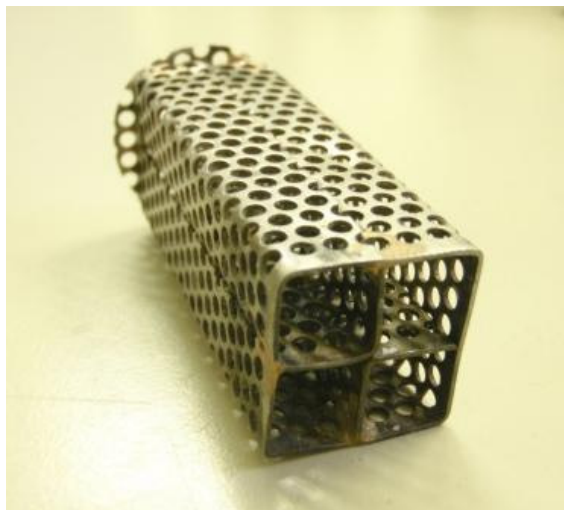


Figure 2.4 A photograph of the purpose built sample holder, designed to hold four cylindrical pieces of carrot in a parallel arrangement, in the centre of the pressure vessel.

Several experiments were carried out to investigate the rate of drying, allowing estimation of the drying times required to reach specified moisture contents. Upon reaching this time, the computer controlled APBR was set to depressurise at a controlled rate of 0.4 MPa/minute. This depressurisation rate was chosen for initial experiments because it was slow and therefore would be expected to minimise damage upon depressurisation, which may occur due to fast expelling of the gas from the dried structure. Additionally, the depressurisation rate of 0.4 MPa/minute was viable practically i.e. depressurisation from 20 MPa would take ~3000 seconds. Depressurisation rate is investigated in more detail in the following chapter (section 3.4.4). All experiments were carried out in triplicate, each involving four pieces of carrot.

It is noteworthy to mention that it was difficult to consistently achieve exactly the same moisture content by drying for a specified time. The final moisture content achieved through drying for a specified time is dependable on many factors, including the initial moisture content of the carrot, slight fluctuations in the scCO_2 flow rate, the temperature, the pressure, and the mol% of co-solvent. Furthermore, moisture contents could only be determined after depressurisation, at the end of the experiment. Additionally, there was also some variation in the final moisture content of the four samples dried in each individual experiment. Therefore, there is expected to be some variability in the moisture content of carrot pieces which were dried for microstructural analysis and rehydration studies, and this is considered later, in the appropriate sections.

2.3.3.1 Addition of ethanol as a co-solvent

Initial experiments showed that higher quantities of EtOH in the scCO₂ resulted in more water being removed in a specified time, indicating a favourable increase in water solubility (Figure 2.5). However, addition of a co-solvent also alters the critical temperature and critical pressure (Table 2.1). Increasing the co-solvent (in this case EtOH) quantity also causes an increase in the critical temperature and pressure required to obtain a supercritical phased system. High temperatures, such as those typically used in air drying (65-85°C), cause thermal damage therefore it is favourable that we dry below these temperatures. An EtOH concentration of 6 mol% was used in these experiments as it enabled supercritical experiments to be carried out at temperatures of ~50°C but also gave reasonable improvement on NMCs (following 5400 seconds of drying) compared to those obtained when 0 mol% EtOH was used (Figure 2.5). It should be noted that at an EtOH concentration of ~8 mol% the system was below the critical point therefore a supercritical phase was not reached at 50°C.

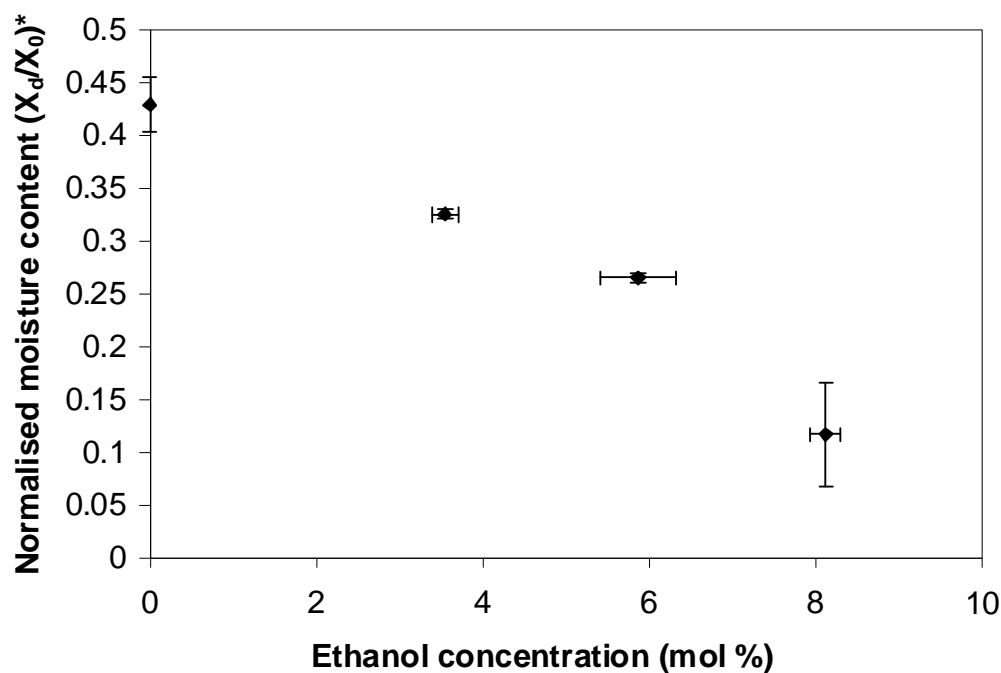


Figure 2.5 Plots showing the moisture content of carrot pieces, dried for 5400 seconds using $\text{scCO}_2(\text{EtOH})$ over a range of EtOH concentrations (20 MPa, 50°C). Note, however, that at ~8 mol% EtOH the system was not in the supercritical phase. Each point represents the overall mean from three independent drying experiments \pm one standard deviation of the mean (vertical error bars). Horizontal error bars indicate variability in EtOH concentration \pm one standard deviation of the mean.

*Normalised moisture content is the moisture content following the experiment (g water/g dry matter) \div the initial moisture content (g water/g dry matter) (equation 2.2).

The rate of EtOH addition from the HPLC pump required to reach 6 mol% was calculated for different CO_2 flow rates, at STP. Examples of rates used are shown in Table 2.2.

Table 2.2 Examples of average CO_2 and EtOH flow rates required to reach 6 mol% EtOH, at STP.

Average flow rate of CO_2 (l/minute)	Average EtOH concentration (mol %)	Average EtOH flow rate (ml/minute)
1	6	0.164
2	6	0.328
3	6	0.491

The calculations used to calculate the mole percent of EtOH used in each experiment are stated below.

All gas volumes recorded in experiments were corrected to STP so that local variations in air temperature and atmospheric pressure were accounted for, as per equation 2.3:

$$V_{STP} = V_{EXP} \cdot \frac{273.15}{T_{lab}} \cdot \frac{P_{lab}}{1} \quad (2.3)$$

where V_{STP} is the corrected volumes in litres, V_{EXP} is the experimentally measured volume from the WTM, T_{lab} is the local temperature in K, and P_{lab} is the local atmospheric pressure in atm.

The calculated volume of CO_2 at STP was then converted to moles using the following expression:

$$n = \frac{V_{STP}}{22.4} \quad (2.4)$$

where n is the number of moles of CO_2 and V_{STP} is the volume of CO_2 at STP in l .

The moles of EtOH required for 6 mol% concentration could then be calculated using equation 2.5:

$$mol\% = \frac{n_{EtOH}}{(n_{EtOH} + n_{CO_2})} \times 100 \quad (2.5)$$

where n_{EtOH} is the moles of EtOH and n_{CO_2} is the moles of CO_2 .

The moles of EtOH can then be converted into a volume in millilitres by using the molar mass of EtOH (46 g/mol) and the density of EtOH (0.79 g/ml). This value had to be estimated for each experiment since the lab temperature and pressure varied from day to day, and also the flow rate fluctuated by small amounts throughout the experiment.

When EtOH was used in an experiment, an additional 1800 seconds phase in which $scCO_{2(pure)}$ was passed over the samples was also included, at the end of the required processing time. This accounted for 1800 seconds of the total drying time reported and was necessary to ensure that all

EtOH was removed from the system prior to depressurisation thus preventing the carrots from being wetted by residual solvent.

As seen for drying with $\text{scCO}_{2(\text{pure})}$ the moisture content achieved in a specified time could not be replicated exactly therefore there was some variation seen over experiments and within experiments themselves. This was due to the same reasons that were explained in section 2.3.3.

2.3.4 The use of liquid carbon dioxide for drying experiments

Experiments were carried out with liquid CO_2 to compare the rate of drying using different phase systems.

SCFs are advantageous to conventional solvents: they are compressible and therefore the solvent properties can be easily tuned by small changes in the temperature or pressure. This causes significant changes in the density and hence the solvating properties of the fluid. SCFs have a much higher density than the equivalent substance in a gaseous state and therefore have an improved solvating power. Much research has been carried out on the solubility of various substances into SCFs at different temperatures and pressures, particularly for supercritical extraction of compounds, where solubility is very important (Haaraus *et al.* 1995; Reverchon 1997).

Since the density is such an important parameter when it comes to solute solubility, the same solvent density was used during experiments with liquid CO_2 as that which had been used for $\text{scCO}_{2(\text{pure})}$. This allowed comparison of the water solubility in the CO_2 fluid. However, it is important to note that achieving a liquid phase at the same density as the supercritical phase required reducing the temperature and pressure of the system. Reducing the temperature of the system also causes a reduction in the vapour pressure of solute (water), thereby potentially reducing its solubility in the CO_2 . It is therefore difficult to independently examine the effect of the phase change of CO_2 on water solubility.

At conditions of 20 MPa and 50°C the density of the supercritical fluid was 0.784 kg/dm^3 . For the liquid CO_2 system, conditions of 25°C and 8.3 MPa were required to achieve the same density.

2.3.5 Method for air drying of carrot pieces

Air drying was carried out at various temperatures (40, 50 and 60°C) in a fan oven. Four cylindrical samples were held in a sample holder (the same as that used for the supercritical experiments) and the moisture content was monitored. The samples were briefly removed at regular intervals and their mass determined over time until <0.1 NMC was reached. The moisture content at each time point was calculated from the total initial moisture content and the mass lost, during drying. It was assumed that all mass loss was due to water removal. All drying experiments were carried out in triplicate.

2.3.6 X-ray micro-computed tomography for the analysis of microstructure

X-ray micro-CT was used to study the microstructure of air, and supercritically dried carrot pieces immediately after drying, allowing for non-invasive analysis of the samples' internal structure. The samples were scanned using a high resolution desktop x-ray micro-CT system (Skyscan 1072, Skyscan, Belgium), consisting of a microfocus sealed x-ray tube with a spot size of 5 µm, operating at a voltage of 100 kV and current of 96 µA. X-ray radiograph images were captured and then reconstructed using a filtered back-projection algorithm which converts the single image into many 2-D horizontal slices through the cylindrical sample, allowing the internal structure to be visualised.

2.3.7 Method for rehydration of carrot pieces

Air and supercritically dried carrot pieces (6-10% w/w moisture content) were immersed in a glass beaker containing 100 ml distilled water, maintained at 50 ± 3°C or 80 ± 5°C. The samples were removed at regular time intervals (~every 300 seconds), blotted on tissue paper, and their mass determined over a total period of 2400 seconds. Each experiment was carried out at least six times (on two pieces of carrot from each of three independent drying experiments), at both of the rehydration temperatures. Results are reported in terms of NMC which is defined using the following equation:

$$NMC = \frac{X_r}{X_0} \quad (2.6)$$

where NMC is the normalised moisture content (for rehydration), X_r is the moisture content following the rehydration experiment (g water/g dry matter) and X_0 is the initial moisture content before drying (g water/g dry matter). Carrots had an average initial moisture content of 9.01 ± 1.78 g water/g dry matter.

2.3.8 Light microscopy for microstructural studies

An Olympus BX50 microscope (Olympus Optical Co., Middlesex, UK) with a JVC TK-1070E video camera (JVC London, UK) mounted on the microscope was used to study carrot microstructure, on a computer monitor. Single images were then captured on the computer using Leica QWin software. Air dried and supercritically dried carrots were rehydrated and thin slices taken from the samples were analysed using this technique.

2.3.9 Cryo-scanning electron microscopy for microstructural analysis

A Philips XL30 field-emission gun environmental scanning electron microscope (FEG-ESEM) (Philips Electronics UK Ltd., UK) with an Oxford Inca 300 energy dispersive spectrometer (EDS) system was used to study the internal cellular structure of rehydrated carrot, allowing comparison of wet samples with unprocessed carrot. Since the instrument additionally has a PolarPrep 2000 cryo-stage system, the rehydrated samples could be rapidly frozen in liquid nitrogen and then fractured within the scanning electron microscopy (SEM) chamber. Samples were then etched at -90°C for 300 seconds and coated with gold for imaging. Air and supercritically dried-rehydrated carrot samples were viewed in this way.

2.3.10 A texture analysis method to measure the hardness of carrot pieces

A texture analyser (TA-XT2i, Stable Micro System, UK) with a cylinder probe (2 mm diameter) was used for puncture compression test analysis. The probe was used to measure the maximum force required to penetrate an individual rehydrated cylindrical piece of carrot, positioned horizontally over a heavy duty platform, to a depth of 2.5 mm. The speed of approach of the probe was 1 mm/second and a 5 kg load cell was used. Three independent experiments (each comprising at least three carrot pieces) were performed for each drying method and rehydration

temperature. The mean maximum force (Newtons) was recorded, and the standard error of the mean calculated for each drying condition.

2.3.11 A method for colour measurement of carrot pieces

Colour analysis was carried out on dried and rehydrated carrot pieces using a scanner, Photoshop 6.0, and the 'L*a*b*' colour model (CIELAB). The 'L*a*b*' colour model can be viewed as a 3-D space with the L* value varying between 0 (black) and 100 (white) and 'a*' representing the red/green shift and 'b*' representing the yellow/blue shift. This is based on the principal that a colour cannot be both red and green, or blue and yellow. The 'a*' axis is green at one extreme (represented by $-a^*$) and red at the other (represented by $+a^*$). Likewise, the 'b*' axis has blue at one end ($-b^*$), and yellow ($+b^*$) at the other. The centre of each axis is 0. The furthest from the central L* axis, the more intense the colour is. The model is illustrated in Figure 2.6. The purpose of the model is to allow a coloured product to be given an exact 'L*a*b*' colour specification which may be compared and duplicated as necessary.

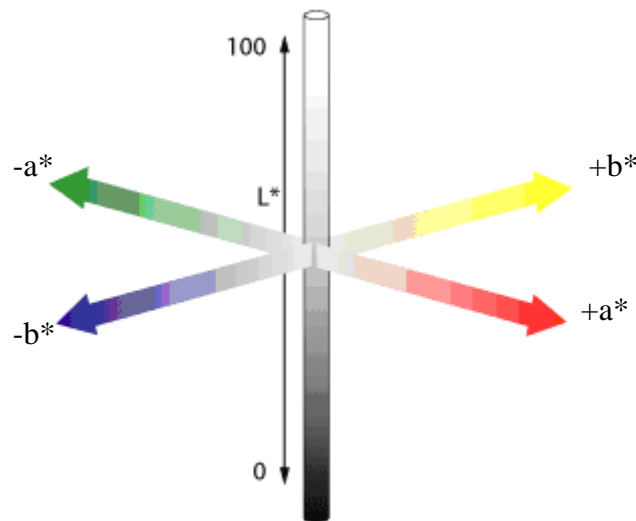


Figure 2.6 An illustration of the 'L*a*b*' colour model (CIELAB), showing the vertical "lightness" (L*) axis ranging from values of 0-100 and the two horizontal axis representing the red and green (a*) and the blue and yellow (b*) colour shift.

The difference in colour between two samples, ΔC can be expressed numerically:

$$\Delta C = \sqrt{(\Delta L^*)^2 + (\Delta a^*)^2 + (\Delta b^*)^2} \quad (2.7)$$

For each experiment, four samples were analysed and an L^* , a^* , and b^* value taken from three points on each carrot piece: top, middle and bottom. An average value of L^* , a^* and b^* , and the standard error of the mean was calculated for samples from each experiment.

Raw carrot was used as the control and the 'ideal' colour from raw carrot, averaged from 10 samples ($L^* = 48.17 \pm 1.02$, $a^* = 36.83 \pm 1.62$, $b^* = 46.62 \pm 2.50$), was used to calculate the colour change, by using the equation above (equation 2.7). This was carried out for samples dried by different air and supercritical drying methods, both before and after rehydration

2.3.12 Statistical analysis techniques

In all statistical analyses, one of the most significant decisions that must be made is whether to use a parametric or a non-parametric method. There are however several restrictions on using parametric methods (for example, the two-sample t test): a moderately large sample size is required, the variances in the treatment groups should be equal, and the data should be from populations that are normally distributed.

Therefore, a non-parametric Mann-Whitney U test was used here to compare two independent sets of data which may be of a smaller size. The only assumption required for this test is that the populations from which the two sets of data have been derived are similar - this is the statement of the null hypothesis. In addition, the null hypothesis also states that the magnitudes of the values in the two treatments groups are similar.

For statistical testing of the differences between three or more samples, analysis of variance (ANOVA) is the parametric method of choice. However, as mentioned above this is only applicable when the assumptions of the test are met. The non-parametric equivalent to one-way ANOVA is the Kruskal-Wallis test, and this was therefore used here for statistical analysis of three or more samples.

Both tests involve ranking the data, calculation of a test statistic and finally examination of the validity of the null hypothesis. The chosen level of significance for both tests was $\alpha = 0.05$.

Rejection of the null hypothesis following the Kruskal-Wallis test informs the analyst that the three or more populations differ but no conclusions may be drawn about the differences between the individual pairs of the populations. Therefore a post hoc statistical test (Nemenyi's test) was used to measure the origin of the proposed differences.

2.4 Results and discussion

An overview of this section is initially outlined here to guide the reader through the results. The first part of this section compares the results of supercritical drying times with air drying times, and some estimated drying rates are discussed briefly.

Several parameters were changed and the effects on supercritical drying times were investigated: co-solvent (EtOH) was added to the SCF, liquid CO₂ was used to dry instead of scCO₂, and the drying temperature was varied. These experiments enabled favourable conditions to be chosen which were used for the rest of the experiments completed in this chapter.

Also, in this chapter, the effect of pre-cooking the carrot before drying, changing the solvent flow rate and increasing the sample surface area, on drying times was studied. These experiments in particular gave us an idea of the mechanism by which water was being removed in this system, at the conditions studied. This is discussed in section 2.4.1.8.

The main focus of this chapter was a study of the effect of the drying technique on the product structure and properties. Section 2.4.2 contains microscopy and x-ray micro-CT images of the dried and rehydrated product. Texture, rehydration and colour were also investigated, as important properties for measuring the quality of foods. Supercritically dried samples were compared with air dried samples.

2.4.1 Drying profile for air and supercritically dried carrot pieces

Drying profiles for carrots, dried with scCO_{2(pure)}, with scCO_{2(EtOH)} and by air drying, are presented in Figure 2.7.

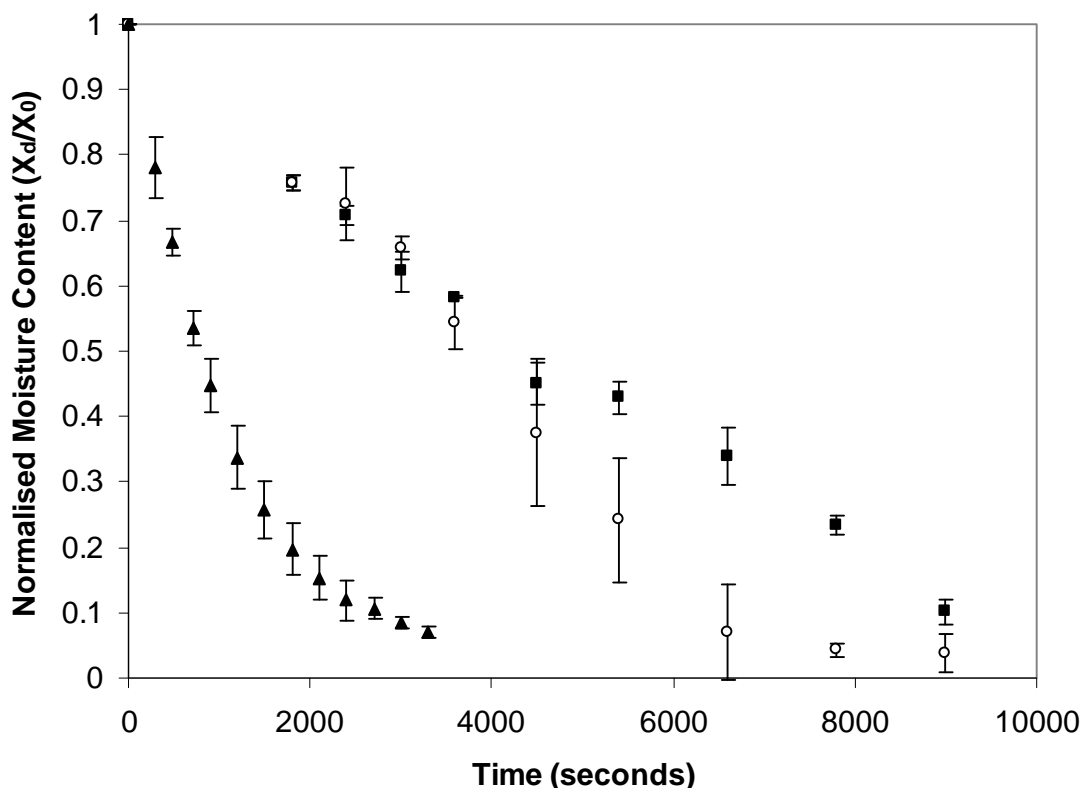


Figure 2.7 Drying profiles for raw carrot pieces dried in air (▲), scCO₂(pure) (■) and scCO₂(EtOH)* (○). Supercritical experiments were carried out at 20 MPa and 50°C and air drying was carried out at 50°C. Each point represents the overall mean from at least three independent sets of measurements \pm one standard deviation of the mean.

*1800 seconds of each time point includes drying without EtOH to purge the system of this solvent before depressurisation (see section 2.3.3.1).

2.4.1.1 Addition of ethanol as a co-solvent during supercritical drying

The inclusion of EtOH can be seen to increase the overall rate of drying in the supercritical systems (Figure 2.7). The Mann-Whitney U-test was used to examine the differences between data at each of the time points for scCO₂(pure) and scCO₂(EtOH). The chosen level of significance, α , was 0.05. The differences in moisture content between carrots dried in scCO₂(pure) or scCO₂(EtOH) became statistically significant at, and beyond, 5400 seconds.

As discussed in more detail in the introduction (section 1.1.3), addition of a co-solvent can favorably influence the solubility of polar substances in scCO₂ (Berna *et al.* 2001; Bae *et al.*

2004). Their mechanism of action is thought to involve specific chemical and physical interactions that exist between the co-solvent and solute, including hydrogen bonding and dipole-dipole attractions (Ekart *et al.* 1993; Ke *et al.* 1997). The co-solvent (EtOH) has also been reported to interact with the scCO₂ (Lalanne *et al.* 2001). Therefore, the increased extent of moisture removal seen over a 5400 second drying period when EtOH was added, was expected. It should be noted however, that carrots processed in an environment of scCO_{2(pure)} also experienced considerable moisture loss. Over half the original moisture content of the carrot was lost over this time, indicating that drying with scCO_{2(pure)} alone is possible.

Before this time, the effects of EtOH addition are less obvious for two main reasons: firstly, the times indicated include the 1800 second purge time, during which scCO_{2(pure)} alone is passed over the sample to remove EtOH from the system before depressurisation. Thus, a 2400 second experiment for example, involves exposing the samples to scCO_{2(EtOH)} for only 600 seconds. Secondly, it takes time for the EtOH concentration within the pressure vessel to become fully established, as scCO_{2(EtOH)} replaces the scCO_{2(pure)} present in the vessel at the beginning of an experiment.

The effect of co-solvent addition on the structure of the carrot pieces is discussed later in section 2.4.2.

2.4.1.2 Comparison of supercritical drying with air drying

At the conditions used, drying to any moisture content was seen to take longer for supercritical drying than for air drying, although comparisons of this nature must be treated with caution due to the different flow regimes employed for each. Nevertheless, estimated drying rates were calculated from the slope of the drying curves (moisture content plotted against time, Figure 2.8) to give a rough comparison of drying rates.

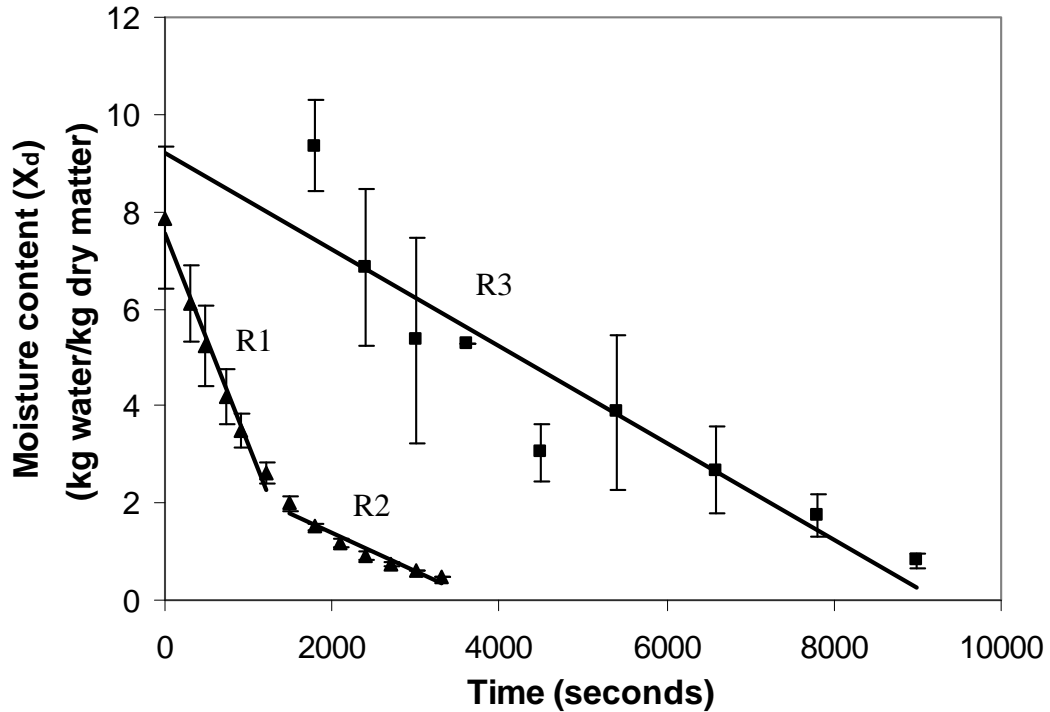


Figure 2.8 Moisture content plotted against time for raw carrot pieces dried in air (▲) and $\text{scCO}_{2(\text{pure})}$ (■). Average regression lines have been plotted to allow calculation of the drying rates (R1-R3). Supercritical experiments were carried out at 20 MPa and 50°C and air drying was carried out at 50°C. Each point represents the overall mean from at least three independent sets of measurements \pm one standard deviation of the mean.

The drying rate is:

$$\frac{dx}{dt} = \frac{X_2 - X_1}{\Delta t} \quad (2.8)$$

where Δt = time difference between time points 1 and 2; X_2 = moisture content at time point 2; X_1 = moisture content at time point 1.

However, here the rates were averaged from the regression line on the graph (Figure 2.8). The shape of the drying profiles in Figure 2.7 and Figure 2.8 were seen to differ between air and supercritical drying with $\text{scCO}_{2(\text{pure})}$. Supercritical drying experienced a constant rate of drying throughout therefore one rate was calculated from the drying curve (R3). Air drying however,

experienced a falling rate therefore two drying rates were calculated: an initial (faster) rate of drying (R1) and a slower drying rate, after about 1500 seconds (R2). Drying rates are displayed in Table 2.3.

Table 2.3 Drying rates for supercritical and air drying, calculated from regression lines plotted on moisture content against time curves (Figure 2.8)

Type of drying	Rate ((g/g)/second)
Air drying (R1)	4.38×10^{-3}
Air drying (R2)	8.00×10^{-4}
Supercritical drying (R3)	9.95×10^{-4}

Therefore, although air drying is initially considerably faster than supercritical drying, after a certain time period, when air drying becomes much slower due to the falling rate, supercritical drying in fact becomes faster than air drying.

A plot of the natural logarithm (\ln) of the moisture content (X_d) versus time for air drying is a straight line, indicating that air drying kinetics follow a 1st order relationship (Figure 2.9).

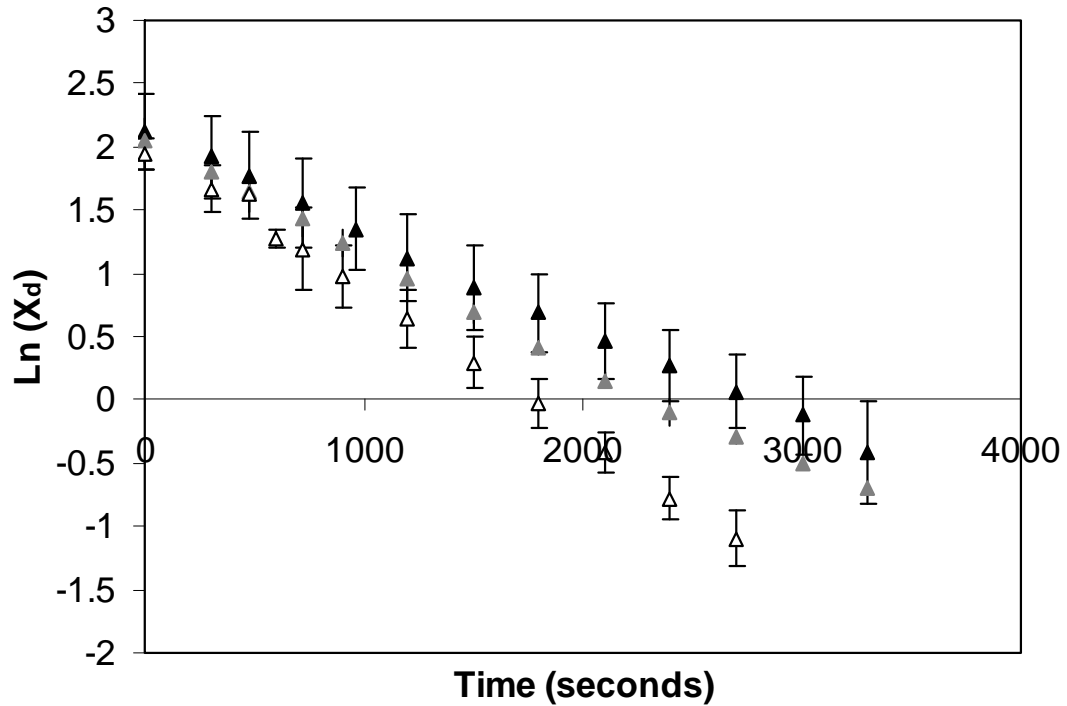


Figure 2.9 A plot of $\ln(X_d)$ versus time for carrot pieces, air dried at 40°C (▲), 50°C (▲) and 60°C (△). Each point represents the overall mean from at least three independent sets of measurements \pm one standard deviation of the mean.

The first-order rate law equation is:

$$-\frac{d(X)}{dt} = k(X) \quad (2.9)$$

which when integrated is:

$$\ln(X) = -kt + \ln(X)_0 \quad (2.10)$$

therefore the slope of the graph ($\ln(X)$ plotted against time) is equal to $-k$ (the rate constant).

This is consistent with the falling rate period, commonly associated with the latter part of air drying, where the rate of transport of moisture through the food matrix, determined by the mechanism of internal moisture transport, becomes limiting (Krokida *et al.* 2003; Mujumdar and Devahastin 2000). A preceding constant drying rate period may be present in the earliest stages

of the drying experiment. However, this is commonly never seen during the drying of food materials, particularly those with high water content (Arévalo-Pinedo and Murr 2006). In the case of supercritical drying with $\text{scCO}_{2(\text{pure})}$, the straight line relationship between moisture content and time indicates zero order kinetics.

It is more difficult to examine the kinetics for the data obtained when drying with $\text{scCO}_{2(\text{EtOH})}$. As discussed above, early time-point experiments carried out with this fluid include a substantial contribution from $\text{scCO}_{2(\text{pure})}$ alone. It appears that, at the investigated conditions, supercritical drying with $\text{scCO}_{2(\text{pure})}$ proceeds via a different mechanism to that occurring during air drying. This hypothesis is discussed later in more detail in section 2.4.1.8. The significance of longer drying times for scCO_2 drying, compared with air drying, is also discussed in section 2.4.1.8.

2.4.1.3 Drying with liquid carbon dioxide

To analyse the effects and advantages and disadvantages of working in the supercritical phase, drying in liquid $\text{CO}_{2(\text{pure})}$ was also investigated for comparison. Liquid CO_2 may also offer a more economical alternative to supercritical processing, since it does not require such extreme operating pressures may therefore offer reduced capital and operating costs.

The conditions used were 25°C and 8.3 MPa which as discussed earlier, in the apparatus and methodology section (2.3.4), resulted in the same fluid density as the supercritical drying conditions used (Table 2.4).

Comparison of liquid CO_2 and scCO_2 has been investigated for the use in metal recovery, for electroplating baths, where liquid CO_2 was shown to perform equally as well as scCO_2 (Laintz *et al.* 1998). A CO_2 process that uses CO_2 in a liquid state has also been developed for fabric cleaning and has been mentioned in a report on emerging technologies (Blake-Hedges 1998). Liquid CO_2 has also been reported independently for the use in extraction of essential oils (Tuan and Ilangantileket 1997). However, limited research exists on direct comparison of liquid CO_2 and scCO_2 for other industrial processes, such as drying and extraction.

Liquids physically differ from SCFs – they have lower diffusivities, higher viscosities and may have higher densities (Table 1.1). For liquid CO_2 used here, the same fluid density has been used

but it will have a lower diffusivity and higher viscosity than scCO₂. This potentially means that the fluid may have more difficulty diffusing in and out of the sample, and therefore drying the carrot sample. The assumed and perceived benefits of using scCO₂ compared with liquid CO₂ may explain why limited research on the use of liquid CO₂ for extraction and drying has been carried out.

Table 2.4 Experimental conditions used to achieve CO₂ liquid and supercritical phases for drying, while maintaining the same density.

Temperature (°C)	Pressure (MPa)	Density (kg/dm ³)	Phase
25	8.289	0.784	Liquid
50	19.98	0.784	Supercritical

Results showed that using liquid CO_{2(pure)} decreased the amount of moisture that could be removed in a specified time when compared with scCO_{2(pure)}, suggesting that water is more soluble in the supercritical solvent (Figure 2.10). Namatsu *et al.* (1999) observed that water was more soluble in scCO₂ than in liquid CO₂.

This observed difference in water removal is not due to a density difference between the different phased (liquid or supercritical) systems since this is kept constant. Therefore, changes that may influence the solute solubility are the temperature, pressure, and subsequently the vapour pressure. Additionally, the properties of the resulting system in which processing takes place, such as viscosity and diffusivity, may also influence solubility. Therefore, the decreased solubility seen in liquid CO_{2(pure)} here is expected to be due to, either the decrease in vapour pressure of the solute at the lower experimental temperature used, or due to the lower diffusivity of the liquid phased system compared with the supercritical phase system (a solvent with a higher diffusivity may be expected to diffuse into and out of the carrot pieces more efficiently and therefore dry them faster). The effect of the vapour pressure on water solubility is also discussed in section 2.4.1.4 - where the effect of temperature on water removal is examined (Figure 2.11).

However, when the liquid CO₂ was modified with 6 mol% EtOH (liquid CO_{2(EtOH)}), the same drying rates were observed as those seen when using scCO_{2(EtOH)}. It is expected that the addition of a co-solvent such as EtOH would enhance the solute solubility and therefore increase the rate of water removal, as discussed in sections 1.1.3 and 2.4.1.1 (Berna *et al.* 2001; Bae *et al.* 2004). This co-solvent effect is seen here for both liquid and supercritical systems, but interestingly the effect seems to be considerably higher for the liquid system, since the rate of drying with liquid CO_{2(pure)} has gone from being lower than the drying rate with scCO_{2(pure)} to the same drying rates for liquid CO_{2(EtOH)} and scCO_{2(EtOH)}. It may be hypothesised that with the addition of EtOH the interactions between the co-solvent and the solute/solvent may be more influencing on the drying rate than the affect of the solute vapour pressure or solvent diffusivity.

In conclusion, water removal with scCO_{2(EtOH)} appears to go via a different mechanism to that of scCO_{2(pure)} drying, involving specific chemical interactions and therefore increased solute solubility, regardless of whether the system is a liquid or supercritical phase.

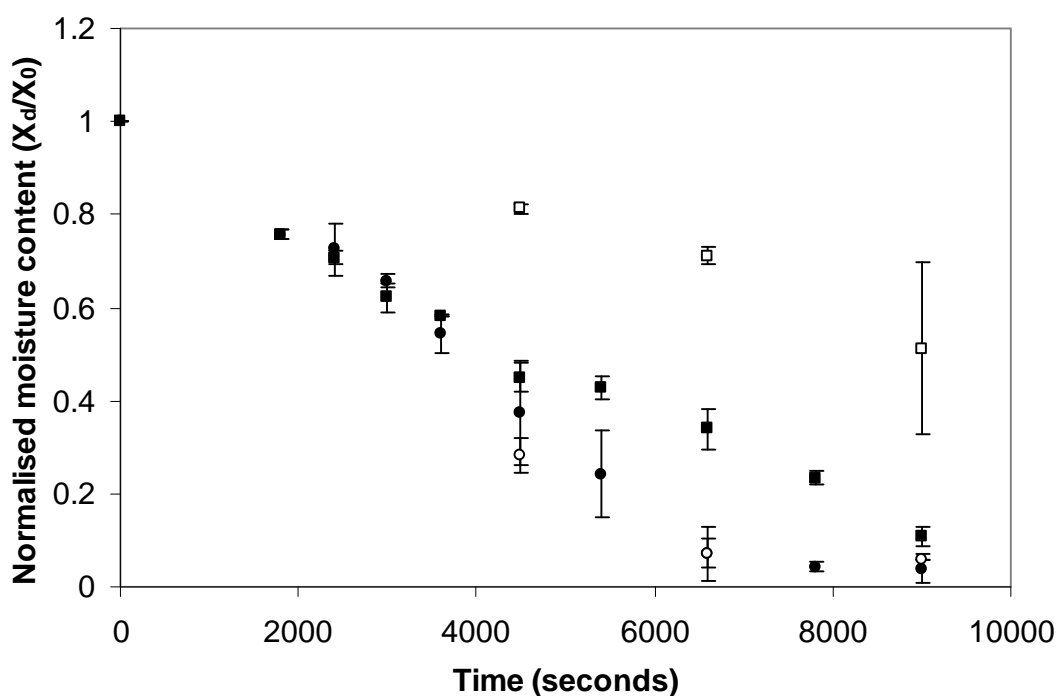


Figure 2.10 Drying experiments carried out using liquid CO_{2(pure)} (□); liquid CO_{2(EtOH)} (○) (8.3 MPa, 25°C); scCO_{2(pure)} (■) and scCO_{2(EtOH)} (●) (20 MPa, 50°C), all using a flow rate of 2 l/minute. Each point represents the overall mean from at least three independent sets of measurements ± one standard deviation of the mean.

These results confirm that for improved moisture removal using $\text{CO}_{2(\text{pure})}$ it is beneficial to work in the supercritical region. However, there is no difference when $\text{CO}_{2(\text{EtOH})}$ is used. It is interesting to note that it is therefore possible to work at lower temperatures and pressures and still achieve reasonable moisture loss, if liquid $\text{CO}_{2(\text{EtOH})}$ is used. The resulting microstructure following liquid CO_2 drying has not been investigated here since drying was generally more efficient when carried out in the supercritical phase, and a key aim of this work was to establish the effect (and any potential benefits) of drying in the supercritical phase, on carrot microstructure.

2.4.1.4 The effect of temperature on drying rate

The effect of temperature on air and supercritical drying using $\text{scCO}_{2(\text{pure})}$ was investigated between 40 and 60°C (Figure 2.11).

The effect of temperature on drying with $\text{scCO}_{2(\text{EtOH})}$ has not been studied here due to results reported in section 2.4.1.3 that found little difference in water removal between samples dried in a supercritical phase and those dried in a liquid phase (both with EtOH added as a co-solvent), which (due to the phase difference) operated at different temperatures and pressures. This suggested that the temperature did not have such an influence on drying rate when EtOH was used as a co-solvent, to assist drying.

The results were statistically examined using the Kruskal-Wallis non-parametric statistical hypothesis test (chosen level of significance, $\alpha = 0.05$). For air dried samples the difference between NMCs achieved at different temperatures became statistically significant at $t = 2100$ seconds and beyond. For supercritically dried samples there was a statistical difference between all the time points that were investigated for more than one temperature i.e. 3000, 4500, 6600 and 9000 seconds.

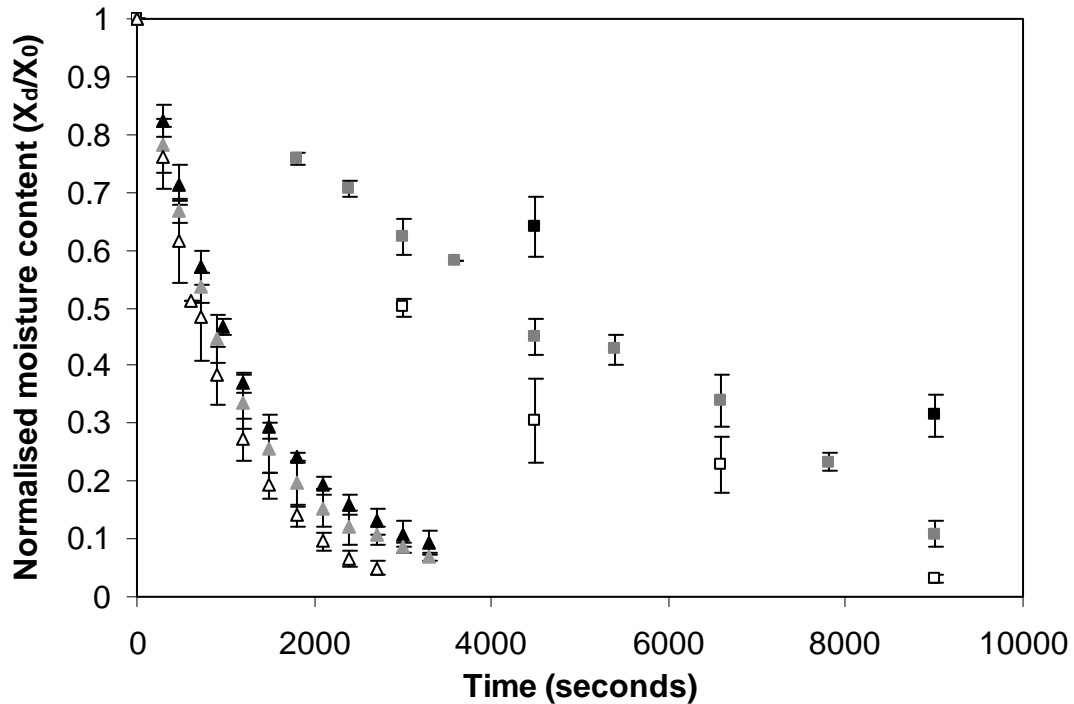


Figure 2.11 Comparison of carrot drying profiles at 40°C (▲), 50°C (▲) and 60°C (△) using air drying or drying with $\text{scCO}_2(\text{pure})$ (40°C (■), 50°C (■), 60°C (□)) at 20 MPa. Each point represents the overall mean from at least three independent sets of measurements \pm one standard deviation of the mean.

Greater moisture removal, at comparable time points, was achieved by increasing the temperature for both air and supercritical drying (Figure 2.11). For air drying this is as expected and is in line with the results reported by others. For example, Krokida *et al.* (2003) showed that air temperature had a greater effect than air humidity or air velocity on the drying rates of several different types of vegetables. In the case of supercritical drying, such a relationship is supported by the work of King *et al.* (1992), Sabirzyanov *et al.* (2002) and Sabirzyanov *et al.* (2003), who showed that the solubility of water in compressed CO_2 increases with temperature, at pressures from 20 MPa down to 5 MPa (solubility below this pressure was not reported). King *et al.* (1992) described solubility as a function of vapour pressure. It is likely that the increased solubility seen with increasing temperature here is due to the increased vapour pressure of the solute. This may also explain the increased rate of water removal seen when using scCO_2 , compared with liquid CO_2 , since higher temperatures were used to achieve a supercritical phase at the same density (section 2.4.1.3).

The supercritical system used in these experiments is expected to be above its crossover point, since at the pressure investigated here (20 MPa) water solubility is more dependent on vapour pressure than changes in density. At pressures below the crossover point, density decreases with increasing temperature and therefore would be expected to reduce the water solubility (Haarhaus *et al.* 1995), which is in contrast to what is seen here. Crossover points are discussed in more detail, with relation to solubility during supercritical extraction, in section 1.2.1.

Despite the beneficial effects of increased temperature on the moisture removal, the elevated temperatures may also have a negative effect on the product quality through thermal damage. For example, thermal damage may take place in the form of undesirable changes in colour, nutritional value, and texture during drying particularly for fruit and vegetables which contain high water content (Maharaj and Sankat 1996; Lin *et al.* 1998; Aguilera *et al.* 2003). Nagaya *et al.* (2006) reported that a temperature below 49°C was shown to preserve colour and maintain vitamin content during drying of vegetables using a desiccant-based low-temperature drying technique.

Therefore, for further supercritical experiments reported here, 50°C was chosen as a standard temperature that allowed acceptable water removal but also would result in minimal thermal damage.

2.4.1.5 The effect of cooking on drying rate

To examine the mechanism of supercritical drying, the effect of pre-cooking the carrots in boiling water (100°C) for 600 seconds before drying was investigated (Figure 2.12).

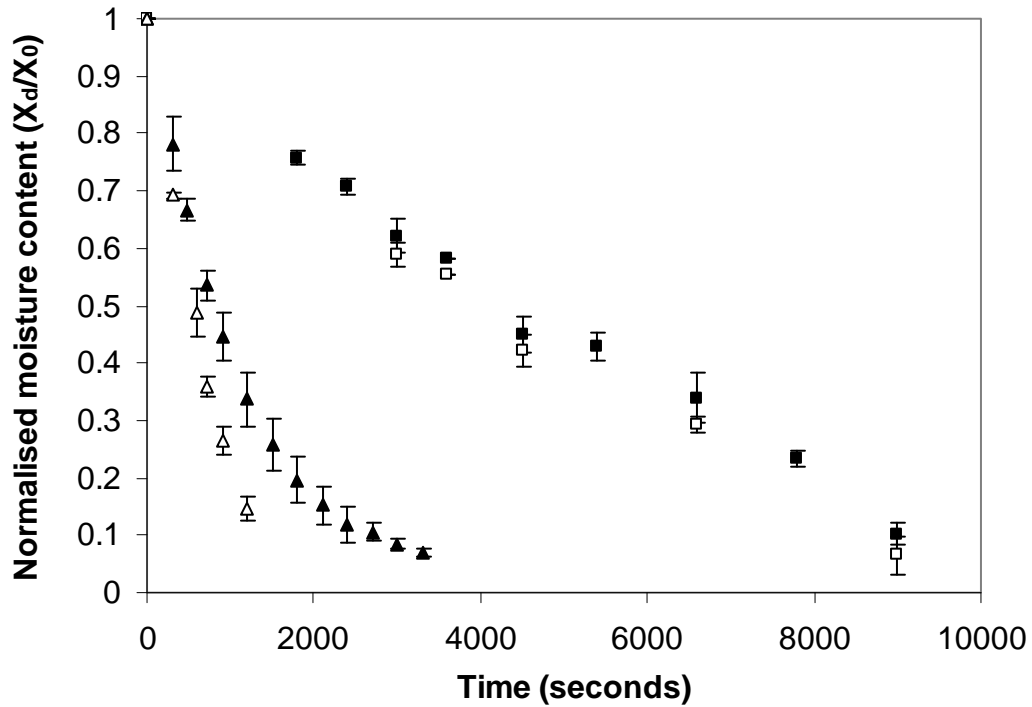


Figure 2.12 Comparison of carrot drying profiles for cooked (Δ) and raw samples (\blacktriangle) dried using air drying, and cooked (\square) and raw (\blacksquare) samples dried with $\text{scCO}_{2(\text{pure})}$. All experiments were carried out at 20 MPa and 50°C. Each point represents the overall mean from at least three independent sets of measurements \pm one standard deviation of the mean.

The Mann-Whitney U-test was used to statistically examine differences between moisture contents at each time point (chosen level of significance, $\alpha = 0.05$). For air drying, pre-cooking was shown to have a statistically significant effect on the moisture content achieved at all comparable time points, and the overall time required to dry to low moisture content was reduced by pre-cooking.

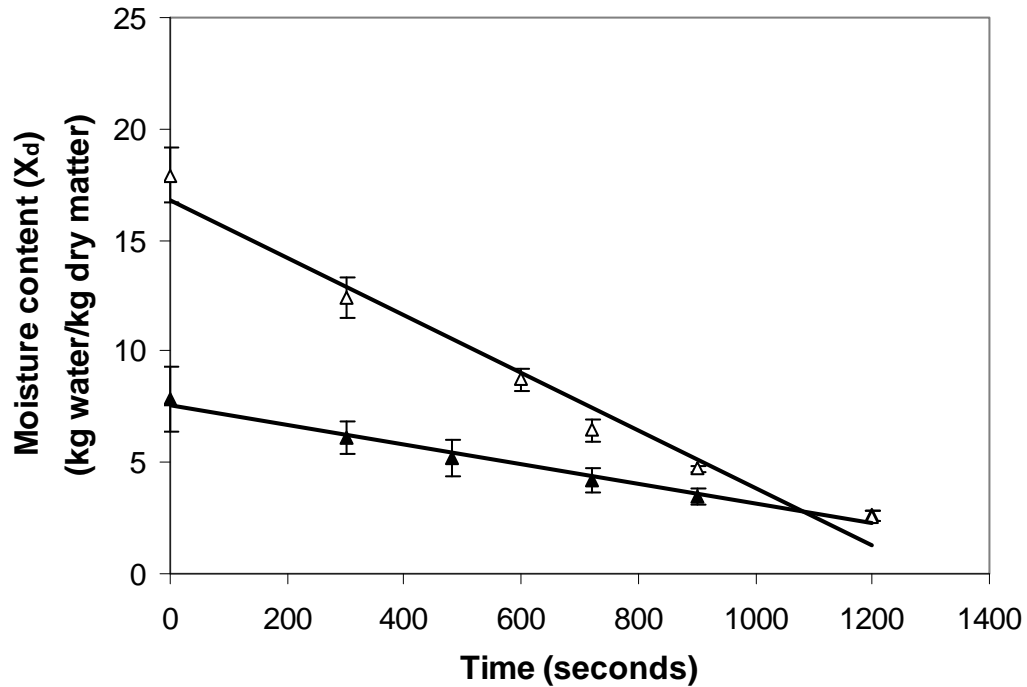


Figure 2.13 Moisture content plotted against time for cooked (Δ) and raw carrot pieces (\blacktriangle) dried using air drying (50°C), in the initial stages of drying. Regression lines have been plotted to calculate the rate of drying. Each point represents the overall mean from at least three independent sets of measurements \pm one standard deviation of the mean.

The rate of drying was also calculated for the initial stages of air drying (<1200 seconds), from a regression line plotted on the moisture content versus time curve (Figure 2.13). The rate of drying cooked carrot was calculated as 1.29×10^{-2} (g/g)/second, while the rate of drying raw carrot was 4.38×10^{-3} (g/g)/second. The drying rate for cooked carrot is therefore almost 3 times faster than for raw carrot in the initial stages of drying.

High temperature processing ($>90^{\circ}\text{C}$) or cooking of carrots causes thermal texture degradation due to wall component dissolution (solubilisation and depolymerisation) (Greve *et al.* 1994; Sila *et al.* 2006). Cell wall separation may also occur during cooking, in addition or independently to cell wall degradation (Aguilera 2005). The breakdown of cell wall pectins by β -elimination reactions is responsible for some of this texture loss. Pectin polysaccharide solubilisation in grape tissue (induced by a drying pre-treatment rather than cooking) has been reported to help increase the drying rate of grapes (Femenia *et al.* 1998).

In plant tissue the water is mainly contained within the cells and during drying loss of this water occurs through transportation across the cell membrane and cell wall (Ahrné *et al.* 2003). The breakdown of cell wall components is expected to cause an increase in the water diffusivity within the product during drying therefore increasing the drying rate, as seen by Femenia *et al.* (1998). Therefore, this may explain the increase in drying rate seen for cooked, air dried carrot pieces.

The latter stages of air drying takes place in what is known as a 'falling rate' period. The rate limiting step in this stage is the diffusion of internal moisture to the sample surface, where it can be transferred to, and removed by the air. In cooked samples, there is less internal resistance and therefore higher water diffusivity, due to the breakdown of cellular components. Consequently, results show a reduction in the time taken for water to be removed in the 'falling rate' period of drying.

In contrast, such effects were not seen when drying with scCO_2 : Figure 2.12 shows no difference in the moisture content versus time curves of cooked and uncooked carrot, suggesting that the internal structure of the carrot does not control the rate of moisture removal during supercritical drying. At these conditions therefore, it is hypothesised that supercritical drying with $\text{scCO}_{2(\text{pure})}$ is instead externally controlled by the supercritical solvent properties, or controlled by the rate of mass transfer from the surface of the samples.

A small number of experiments were also carried out, drying cooked carrots with $\text{scCO}_{2(\text{EtOH})}$ for comparison (Figure 2.14). Results were in agreement with the results seen for drying with $\text{scCO}_{2(\text{pure})}$ - cooking has no effect on the efficiency of drying.

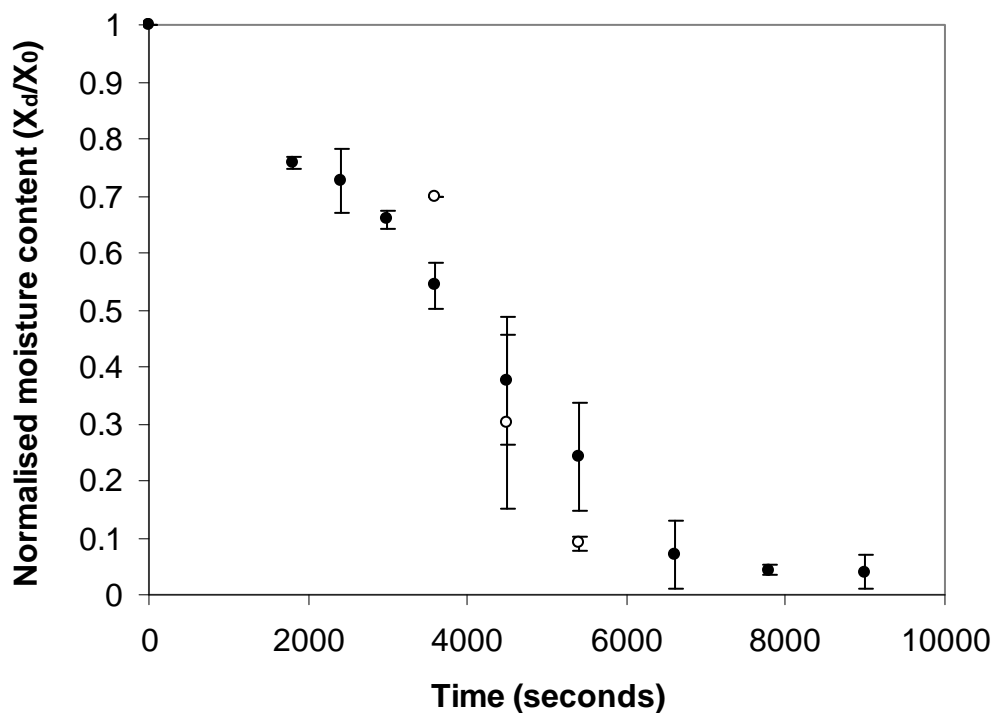


Figure 2.14 Comparison of carrot drying profiles for cooked (○) and raw samples (●), dried using $\text{scCO}_2(\text{EtOH})$. All experiments were carried out at 20 MPa and 50°C. Each point represents the overall mean from at least three independent sets of measurements \pm one standard deviation of the mean.

2.4.1.6 The effect of flow rate on supercritical drying

The amount of water removed in a specified time during supercritical drying was shown, in the previous section, to be influenced by the properties of the supercritical fluid (i.e. temperature, pressure, density, co-solvent addition), or the solute properties (i.e. vapour pressure), rather than the internal structure of the product being dried. It was shown that modifying the scCO_2 with small quantities of EtOH or increasing the temperature (at 20 MPa), increased the amount of water removed. In this section the effect of the flow rate was explored to investigate the mechanism of drying further (Figure 2.15).

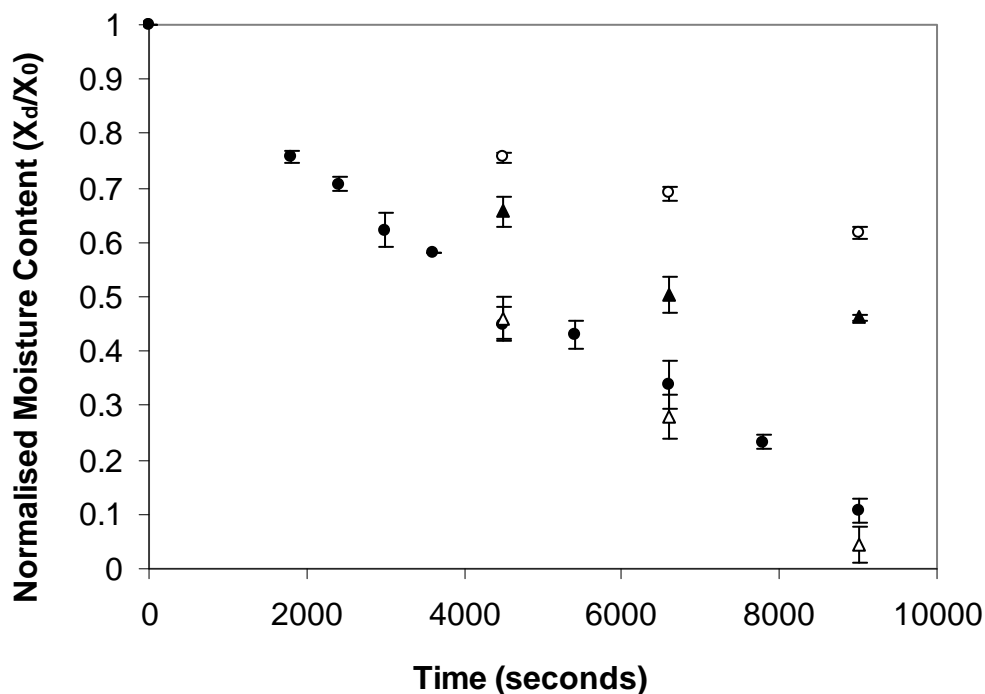


Figure 2.15 Drying profiles for carrot pieces dried with $\text{scCO}_{2(\text{pure})}$, using flow rates of 0.5 l/minute (○), 1 l/minute (▲), 2 l/minute (●) and 3 l/minute (△). All experiments were carried out at 20 MPa and 50°C. Each point represents the overall mean from at least three independent sets of measurements \pm one standard deviation of the mean.

The results showed that increasing the flow rate increases the rate of drying, but only up to a certain point. Increasing the flow rate from 1 l/minute to 2 l/minute increases the amount of water that can be removed by the $\text{scCO}_{2(\text{pure})}$, but at 2 l/minute a limit is reached and if the flow rate is increased further it has no effect on the amount of water removed in a specified time. It is therefore concluded, that at lower flow rates than 2 l/minute the drying is limited externally by mass transfer resistances. This is also supported by the results of drying cooked carrot which showed that internal structure has no effect on how much water is removed. Above 2 l/minute the water removal is controlled by something else. The rate limiting step at 3 l/minute may be internally diffusion limited or the water removal may be controlled by the mass transfer of water from the sample into the solvent. This was investigated further in the next section (2.4.1.7).

Han *et al.* (2009) reported that during extraction of safflower seed oil using scCO_2 , extraction was initially limited by the solubility of the oil in the SCF, however, later in the extraction

process, the limitation was the mass transfer of the less accessible oil, out of the seed since the accessible oil has already been extracted. It appears that the mass transfer of the solute (for example, during extraction or drying), out of the material, is only a limiting factor when the solute is inaccessible, or the material has high mass transfer resistances. This may or may not be the case during supercritical drying of carrots, discussed here. However, the results reported by Han *et al.* (2009), are in agreement with results reported in this thesis that show higher flow rates generally were associated with higher extraction rates, and the increased volume of CO₂ enabled removal of a higher volume of oil or water. A suggested mechanism for the water removal during supercritical drying of carrots is discussed further in section 2.4.1.8.

2.4.1.7 The effect of increased surface area on drying rate

The effect of increased surface area for moisture removal was studied at several different flow rates (Figure 2.16). The same quantity of carrot was used as in previous experiments but was grated. This was expected to give more information on whether the movement of the solvent into and out of the sample was a limiting factor, at higher flow rates. The results were compared with drying experiments carried out on pieces of carrot (Figure 2.16).

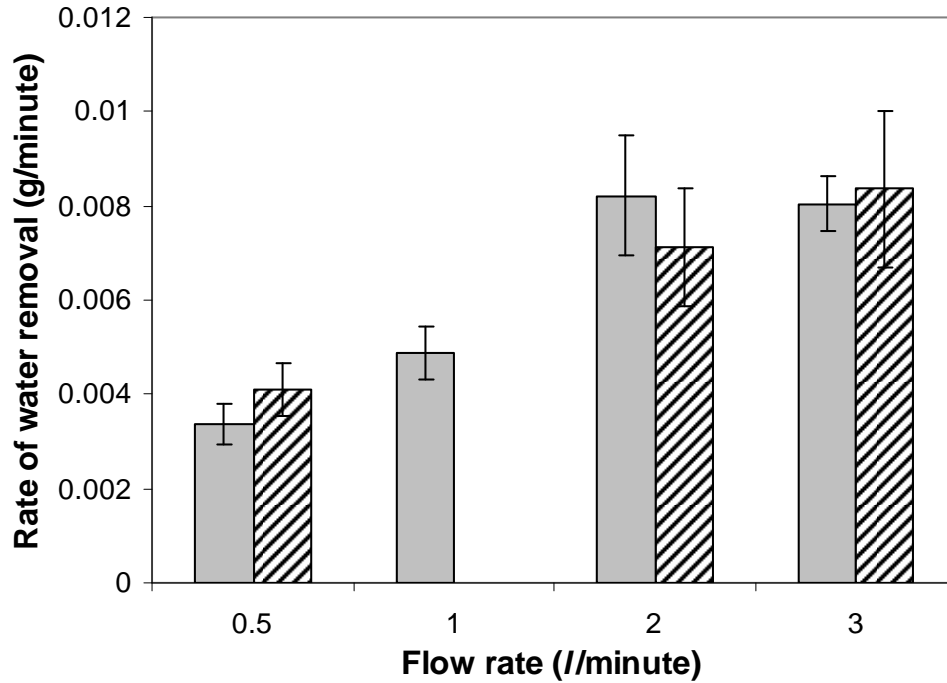


Figure 2.16 Graph showing the rate of water removal for pieces of carrot (grey bars) and grated carrot (striped bars), dried in $\text{scCO}_2(\text{pure})$ at varying flow rates. The supercritical conditions used were 50°C and 20 MPa .

Interestingly, grated carrot (Figure 2.16 (grey bars)), at all flow rates investigated, showed no differences in rate of water removal when compared with that seen for pieces of carrot (Figure 2.16 (striped bars)), despite more ‘surface water’ being available. Based on these results, it appears that the limiting factor at all flow rates is not internal diffusion of the water, or the movement of the SCF into or out of the sample. The results suggest that the limiting factor lies with the transport of the available water (whether surface or internal) into the SCF.

A further graph was plotted, displaying actual moisture loss against the possible water loss (calculated from solubility data in the literature (Sabirzyanov *et al.* 2002)), at different flow rates, to illustrate the extent of water saturation in the SCF. This was illustrated for both grated and pieces of carrot.

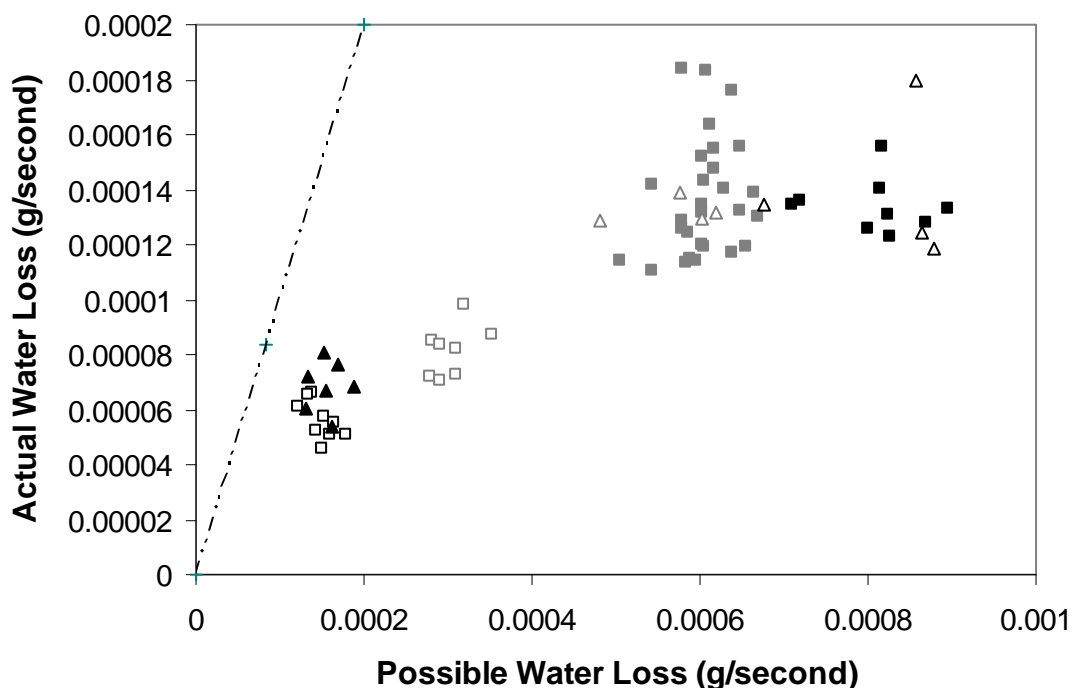


Figure 2.17 Plot showing the actual water loss against the possible water loss (calculated from water solubility in $\text{scCO}_{2(\text{pure})}$ at 50°C and 20 MPa , assuming the $\text{scCO}_{2(\text{pure})}$ becomes saturated) for pieces of carrot, at flow rates of 0.5 l/minute (\square), 1 l/minute (\square), 2 l/minute (\blacksquare), 3 l/minute (\blacksquare), and grated carrot, at flow rates of 0.5 l/minute (\blacktriangle), 2 l/minute (\triangle) and 3 l/minute (\triangle). The line ($-\cdot-\cdot-$) indicates the theoretical line on which the results should fit, taken from solubility data of water in $\text{scCO}_{2(\text{pure})}$ (Sabirzyanov *et al.* 2002).

The results showed that the actual water loss was a lot less than if the $\text{scCO}_{2(\text{pure})}$ had been fully saturated (Figure 2.17 ($-\cdot-\cdot-$)). At lower flow rates the water loss is closer to the expected value, but at higher flow rates the values move further away. This is likely to be due to the $\text{scCO}_{2(\text{pure})}$ having less chance to become fully saturated at higher flow rates. However, the $\text{scCO}_{2(\text{pure})}$ is able to carry away more water, but does not increase at the same proportion to the flow rate i.e. at 0.5 l/minute around $6.7 \times 10^{-5}\text{ g/second}$ was removed but at double this flow rate (1 l/minute) only around $8.3 \times 10^{-5}\text{ g/second}$ was removed. Between 2 and 3 l/minute there is no increase in the water removal, despite the flow rate increase. This was discussed earlier in section 2.4.1.6 and illustrates the point at which the water removal is no longer limited externally by how much water the solvent can remove, or hold.

Although the $\text{scCO}_{2(\text{pure})}$ is never saturated with water, there is a limit with how much can be carried which varies with flow rate (as different volumes of $\text{scCO}_{2(\text{pure})}$ are used) and therefore different degrees of saturation are reached. It is also interesting to remember that above 2 l/minute there is still a constant rate of moisture removal (seen in Figure 2.15 as a straight line), suggesting that despite the $\text{scCO}_{2(\text{pure})}$ not being saturated, it reaches a maximum capacity for how much water it can remove.

It may be that, the $\text{scCO}_{2(\text{pure})}$ that is in contact with the samples does become saturated, while some $\text{scCO}_{2(\text{pure})}$ which is not in direct contact with the sample remains unsaturated and therefore does not aid water removal. This would explain the deviation from the possible water removal, which could be removed if all of the $\text{scCO}_{2(\text{pure})}$ was saturated.

2.4.1.8 A proposed mechanism for supercritical drying

By examining the various experiments that have been discussed in the previous sections, a mechanism for the moisture removal using $\text{scCO}_{2(\text{pure})}$ is proposed and is discussed here.

At the conditions investigated, several conclusions may be drawn:

- At the flow rate investigated (2 l/minute) the internal cellular structure of the carrot was not seen to affect supercritical drying rate, since cooked carrot possessed the same drying characteristics as raw carrot. Therefore the cellular structure is not acting as an internal resistance to water removal.
- Below a flow rate of 2 l/minute the drying rate is externally controlled, since the drying rate is seen to increase with increasing flow rate, as external resistances for mass transfer are reduced. At 2 l/minute and above, the rate limiting step is no longer externally controlled as the drying rate does not increase with flow rate.
- At the flow rate investigated (2 l/minute), increased surface area does not affect supercritical drying rate, since grated carrot, with more surface water available experienced the same water removal when compared with carrot pieces. Therefore, internal diffusion is not a rate limiting step at these conditions.

Therefore, below 2 l/minute the rate is limited by external mass transfer resistances. At 2 l/minute and above, since increasing the flow rate does not increase drying rate and the process is not limited by internal diffusion, the rate limiting step can only be the transfer or solubilisation of the water into the SCF. It has however been shown in section 2.4.1.7 (Figure 2.17) that the SCF is not fully saturated but there appears to still be a limit to how much water it can hold, depending on the flow rate used.

This limit on how much water the SCF can hold could be increased by addition of a co-solvent (EtOH) or by drying at an increased temperature. Addition of co-solvent increases water solubility in the SCF by changing the properties of the SCF, while increasing the temperature, increases the vapour pressure of the solute (water).

The suggestion that supercritical drying, at flow rates of 2 l/minute, is limited by the transfer or solubilisation of the water into the SCF explains why a constant drying rate is seen, as opposed to a falling drying rate period, such as that seen during air drying, where the rate is limited by internal diffusion of the water out of the sample.

The process of water removal is expected to occur as a consequence of the SCF entering the product that is being dried. Upon exiting, the SCF is thought to carry away some water, thereby drying the product. The presence of the SCF within the product during water removal may aid volume retention during drying, since it is one-way diffusion of liquid water out of the product that causes collapse during air drying. This is discussed further in section 2.4.2.2, in relation to product structure.

The water present in the sample is solubilised into the scCO₂ and as the SCF exits the sample it carries some water with it. Tassaing *et al.* (2004) studied the interactions of water-CO₂ mixtures at various temperatures and a pressure of 25 MPa: at temperatures below 100°C, water was reported to exist in a monomeric form, as solitary water surrounded by CO₂ molecules.

The process of water removal would be expected to be fast as it is known that SCFs have high mass transfer properties, but the amount of water carried out of the sample also depends on the solubility of the water in the scCO₂, at the temperatures and pressures investigated.

The nature of the phase change(s) during supercritical drying is also thought to assist in volume retention of the dried product. Figure 2.18 illustrates the phase changes occurring during air drying (green arrow); freeze drying (blue arrow); and supercritical drying (red arrow). The black dot is the critical point, above which the supercritical region exists. Freeze drying occurs in the low temperature, low pressure region while supercritical drying typically occurs in the high pressure, high temperature region. However, the use of CO₂ as a SCF allows the critical point to be reached at a temperature of 31.1°C, which is considered low in terms of drying temperatures, since most industrial air drying applications use temperatures of 65-85°C (Ratti 2001). For both freeze and supercritical drying, ambient conditions are only reached once the product is dry, preventing some product collapse post-processing.

Food products that are freeze dried generally experience minimal shrinkage. The product is initially frozen, before removal of the water by sublimation therefore the water passes from a solid substance directly to a gaseous substance. So, although a phase boundary exists, the nature of the boundary is different to that experienced during air drying and therefore capillary forces and liquid water diffusion out of the product are avoided, which can cause collapse during air drying.

During supercritical drying, the water within the product being dried may be expected to go from a liquid into a supercritical single phased mixture with scCO₂ (a supercritical binary mixture). It is also possible that the liquid water may be 'carried' away by the supercritical solvent but remain in a liquid state. It is suggested that the phase change (or lack of phase change) of liquid water that takes place during supercritical drying does not cause as much shrinkage or collapse to the structure as the phase change that takes place during air drying. This may be because capillary forces and liquid water diffusion out of the product are also avoided during supercritical drying, in addition to freeze drying.

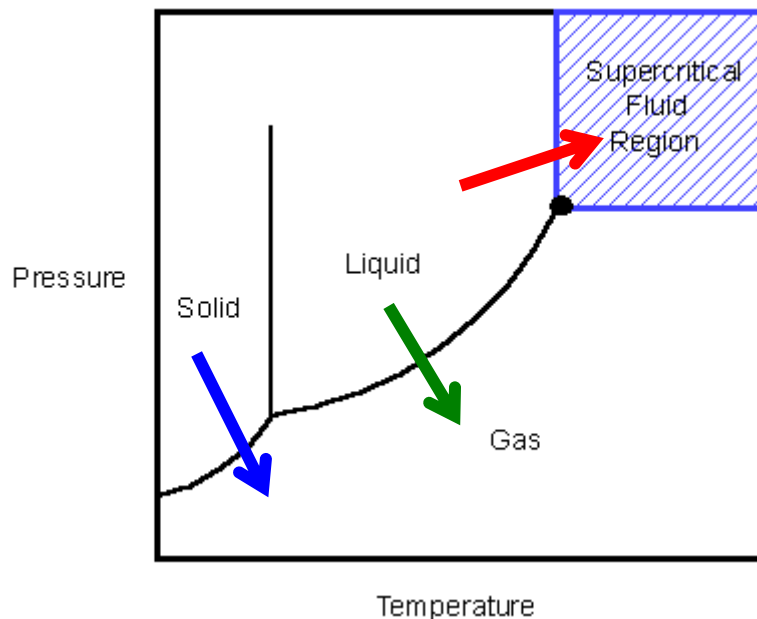


Figure 2.18 An illustration of the phase boundaries crossed for air (green arrow), freeze (blue arrow) and supercritical (red arrow) drying. The black dot is the critical point of the solvent, above which the supercritical phase exists.

Alternative methods of supercritical drying processes have been reported, where the water is first exchanged for an organic solvent which is more soluble in $\text{scCO}_{2(\text{pure})}$, then this solvent is ‘washed away’ with the SCF. Liquid CO_2 is often used to displace the solvent first, and then the temperature and pressure is increased to achieve a supercritical phase. The scCO_2 is then released as a gas by venting the SCF to ambient pressure. Several variations of this method exist (Laudise and Johnson 1986). The mechanism by which this occurs has been reported as an extraction process of the organic solvent by the scCO_2 (Abecassis-Wolfovich *et al.* 2003). Shrinkage during the depressurisation step has been observed in gels dried using this method, enforcing the idea that the SCF helps to maintain the material volume during ‘drying’ (i.e. removal of the organic solvent or water), prior to depressurisation, in supercritical drying methods (Rangarajan and Lira 1991). Additionally, the high porosity of materials produced in this way indicates that the SCF is inherent in the sample during drying. These observations support the proposed mechanism of water removal, discussed above (for supercritical drying without the use of an intermediate organic solvent), which states that the SCF enters the product

that is being dried and upon exiting, carries away some water within a binary supercritical mixture.

Despite the supercritical drying process (by direct removal of water, without a previous stage to exchange the water for an organic solvent) being an overall slow drying process, by comparison with air drying (Figure 2.7), there is scope for increasing the drying rate. It was proposed in section 2.4.1.8 that when supercritical drying at flow rates <2 l/minute the rate is limited by external mass transfer resistances and at flow rates >2 l/minute the rate is limited by transfer of the water into the supercritical solvent therefore several options exist for increasing the drying rate: experimentation with different supercritical solvents, addition of alternative co-solvents, addition of other additives which may affect the SCF properties, and/or manipulation of the processing conditions such as flow rate, temperature and pressure. However, care should be taken, since solvent choice may affect the final sample structure. EtOH addition was shown to have a significant influence on the carrot structure, in addition to increasing the drying rate, and is discussed further in the following section (2.4.2). Drying rate is important not only from a practical perspective but also economically, as a longer process is likely to be more costly.

2.4.2 Structural analysis

2.4.2.1 Microscopy: light microscopy and cryo-scanning electron microscopy for analysis of wet carrot microstructure following rehydration

Qualitative analysis of the carrot microstructure was carried out to determine the effect of the drying method on the internal, cellular structure. This is of great importance as changes on the microstructural level will also relate to changes at a macrostructural level such as density, texture and rehydration properties.

Light microscopy

Light microscopy was shown to give a good indication of the cellular microstructure within the rehydrated products (Figure 2.19). Samples dried using $scCO_2$ and then rehydrated have been compared with that of raw carrot. The structure of dried samples was not observed using this technique since the light microscopy equipment would not allow substantial light through a thin

slice of the dried sample. The viewing of dried samples was therefore not possible. However, the internal structure of dried samples could be viewed very well using x-ray micro-tomography, so this method was used instead (section 2.4.2.2).

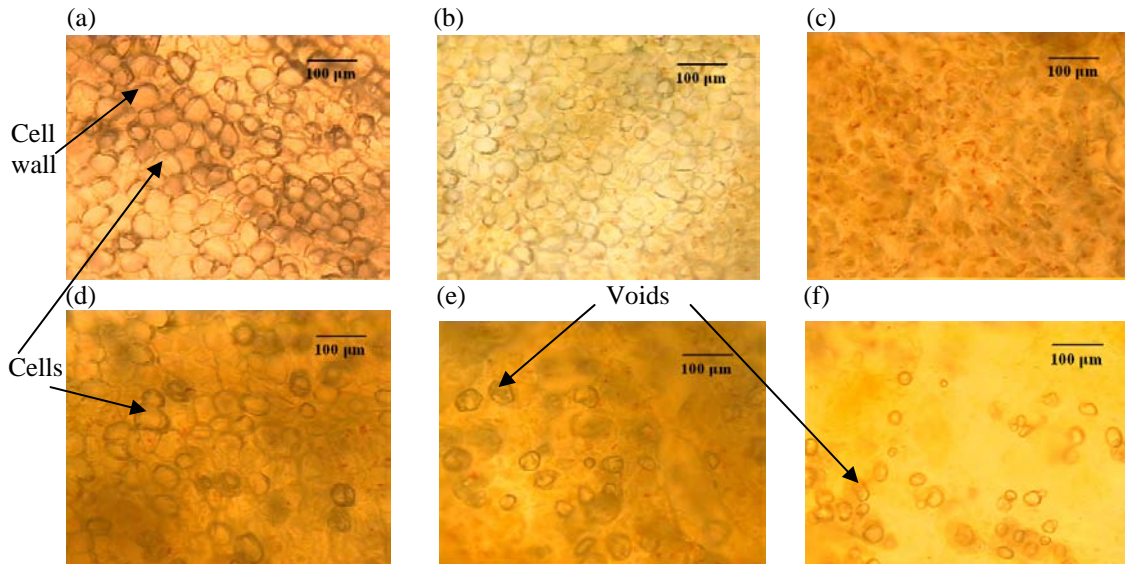


Figure 2.19 Light microscopy images showing: (a) raw carrot (b) raw carrot dried with $\text{scCO}_2(\text{pure})$ at 50°C & rehydrated at 50°C ; (c) raw carrot dried with $\text{scCO}_2(\text{pure})$ at 50°C & rehydrated at 80°C ; (d) raw carrot dried with $\text{scCO}_2(\text{EtOH})$ & rehydrated at 50°C ; (e) raw carrot dried with $\text{scCO}_2(\text{EtOH})$ & rehydrated at 80°C ; (f) cooked carrot dried with $\text{scCO}_2(\text{pure})$ at 50°C & rehydrated 50°C .

Raw carrot is shown before cooking and drying, to illustrate the initial cellular structure of carrot (Figure 2.19 (a)). This cellular structure was also visible in those samples dried using $\text{scCO}_2(\text{pure})$ and rehydrated at 50°C (Figure 2.19 (b)). However, during cooking, rupturing or separation of some of the cell walls may occur, causing structure loss (Verlinden *et al.* 2009). Certainly, during cooking all of the cell wall components will undergo thermal texture degradation due to wall component dissolution (which occurs during cooking) as discussed in section 2.4.1.5. High temperature processing will also have a similar effect to that of cooking, especially if the sample is exposed to these high temperatures for a significant length of time (Greve *et al.* 1994; Sila *et al.* 2006). For example, samples that had been rehydrated at 80°C (Figure 2.19 (c)) no longer exhibited a complete cellular structure, much like those that had been cooked prior to drying (Figure 2.19 (f)).

Samples dried using $\text{scCO}_2(\text{EtOH})$ appeared to have additional structural entities present, although these were not clear in the samples rehydrated at 50°C (Figure 2.19 (d)) since it was difficult to distinguish between cellular structure and the additional voids that were formed. However, the voids were still present in samples that had been rehydrated at 80°C (Figure 2.19 (e)), proving that they were in fact not part of the original cellular structure and had been induced during the drying process. These were also evident in cooked samples, dried with $\text{scCO}_2(\text{pure})$ (Figure 2.19 (f)), but not in raw carrot that had been dried in the same manner (Figure 2.19 (b)). The voids were also visible using cryo-SEM (Figure 2.20), confirming that they were not simply an artefact of the light-microscopy technique.

These results indicate that the addition of EtOH as a co-solvent had an effect on the microstructure formed during supercritical drying, causing the creation of voids. Supercritical drying using $\text{scCO}_2(\text{pure})$ (without EtOH) was also seen to change the carrot structure in the same way and cause voids to be created. However, this was only observed in carrot that had been pre-cooked and not on those samples that hadn't been cooked prior to drying. These voids are expected to be formed during depressurisation and may be the consequence of gas bubbles, formed as the pressure in the vessel is released, causing the $\text{scCO}_2(\text{pure})$ to change from a supercritical to a gaseous state. The release of this gas from the carrot structure could result in formation of bubbles or voids. Depressurisation may also rupture the cells, as seen by Louka *et al.* (2004) during decompression experiments, which may cause voids to be formed. These voids are then only visible in samples that have been pre-cooked or processed using $\text{scCO}_2(\text{EtOH})$. The selectivity of this phenomenon may be due to the carrot structure being made weaker and therefore easier to manipulate, for example due to breakdown of components in the cell wall upon pre-cooking. EtOH addition during supercritical drying may also cause some component breakdown. The structure, following drying with $\text{scCO}_2(\text{EtOH})$, is discussed in more detail in the following sections but it should be noted that following longer processing times with $\text{scCO}_2(\text{EtOH})$, the carrot sample was seen to fall apart (Table 2.5 (e)). These results suggest that some breakdown of the carrot structure took place under continued exposure to $\text{scCO}_2(\text{EtOH})$.

In summary, both cooked and raw carrot pieces may be prone to structural changes during drying with $\text{scCO}_2(\text{pure})$ and $\text{scCO}_2(\text{EtOH})$, respectively. It is hypothesised that these structural

changes take place during the depressurisation stage and that the pre-cooking or processing with $\text{scCO}_2(\text{EtOH})$ assists the void formation by ‘weakening’ the structure.

Cryo-SEM

Cryo-SEM is a technique where wet samples are rapidly frozen, preserving their natural state and then the internal cellular structure is exposed by fracturing the sample. The advantage of this technique is that vulnerable biological structures are well preserved during the rapid freezing stage and freeze fracturing causes the material to break clean along weak edges, for example membranes, without causing much deformation to the internal structure. Preparation techniques for conventional SEM require dehydration of the sample, making it difficult to observe wet structures without a further processing step, which may cause damage (collapse and shrinkage) to the structure.

Carrots have successfully been viewed in the past using cryo-SEM (Sanjuán *et al.* 2005). A cellular matrix may be observed as an artefact of this technique due to the accumulation of soluble solutes during etching which form a continuous matrix of cells. This is known as the eutectic artefact or aggregation phenomena. However, viewing of the cellular carrot structure is also possible using this technique including details such as fractured and non-fractured cells, cell walls, cell-cell contacts and voids, caused by cell detachment.

Here, samples dried using various techniques (all at 50°C) were then rehydrated at 50°C or 80°C and the internal structure viewed using cryo-SEM (Figure 2.20 (b)-(e)). Raw carrot was used as a control (Figure 2.20 (a)). The cryo-SEM image of raw carrot observed here however was different to that of fresh carrot phloem reported by Sanjuán *et al.* (2005) which had been viewed by the same technique. The image shown here (Figure 2.20 (a)) appeared to contain some non-fractured cells, while the fresh carrot sample reported by Sanjuán *et al.* (2005) only contained fractured cells. This discrepancy may be due to different fracturing temperatures used; the nature of the fracture can be determined by the temperature used during fracturing. Samples frozen in liquid nitrogen will reach about -200°C but then must be transferred to the fracturing chamber, in which the sample temperature cannot be tightly controlled. Both images of raw carrot however show cellular structures which contain cells that are well joined along their cell walls, indicating a well preserved structure with limited structural damage.

Air dried samples (rehydrated at 50°C) (Figure 2.20 (b)) and those dried with $\text{scCO}_2(\text{pure})$ (rehydrated at 50°C) (Figure 2.20 (c)), show cells which appear to be fractured - the surface of the sample appears flat compared with the non-fractured, 'raised' cells seen in raw carrot (Figure 2.20 (a)). Therefore, some cellular changes had occurred in carrot samples during air/supercritical drying and rehydration.

The cell walls are not as visible in the supercritically dried sample (Figure 2.20 (c)) as they are in the air dried sample (Figure 2.20 (b)), indicating that some cellular structure or cell wall components may have been lost during $\text{scCO}_2(\text{pure})$ processing. However, the images are of varying quality therefore it is difficult to say if these differences seen are due to the image quality or the actual microstructure of the sample.

Samples dried with $\text{scCO}_2(\text{EtOH})$ (rehydrated at 50°C) exhibited creation of a porous structure with some voids present (Figure 2.20 (d)). These voids were also present, and more plentiful in samples that had been dried with $\text{scCO}_2(\text{EtOH})$ but rehydrated at 80°C (Figure 2.20 (e)). The presence of voids in samples that had been exposed to $\text{scCO}_2(\text{EtOH})$ is supported by results seen using light microscopy (Figure 2.19).

The formation of voids in carrot tissue were also seen by Sanjuán *et al.* (2005), caused by conventional blanching of the carrot (submitted to 95°C water for 60 seconds, followed by 26°C water for 300 seconds) which resulted in cell detachment and therefore voids. According to the author these are a common feature of such samples. Cell wall separation has also been observed in carrot which has been blanched and cooked, independently (Sanjuán *et al.* 2005; Fuchigami *et al.* 1995). Cell wall separation may also contribute to void formation. However, although cell detachment or cell wall separation may be expected to occur during rehydration at 80°C, this does not explain the formation of voids in those samples that were processed with $\text{scCO}_2(\text{EtOH})$ but rehydrated at 50°C (Figure 2.20 (d)). This suggests that it is not just the high temperature rehydration that is responsible for the void formation. Additionally, samples that had been exposed to $\text{scCO}_2(\text{pure})$ and rehydrated at 80°C did not exhibit void formation when examined under the light microscope (Figure 2.19 (c)). In conclusion, it is expected that the addition of EtOH as a co-solvent that is contributing to the formation of voids by 'weakening'

the structure. This is in agreement with results seen in the previous subsection (on light microscopy analysis) and is discussed further there.

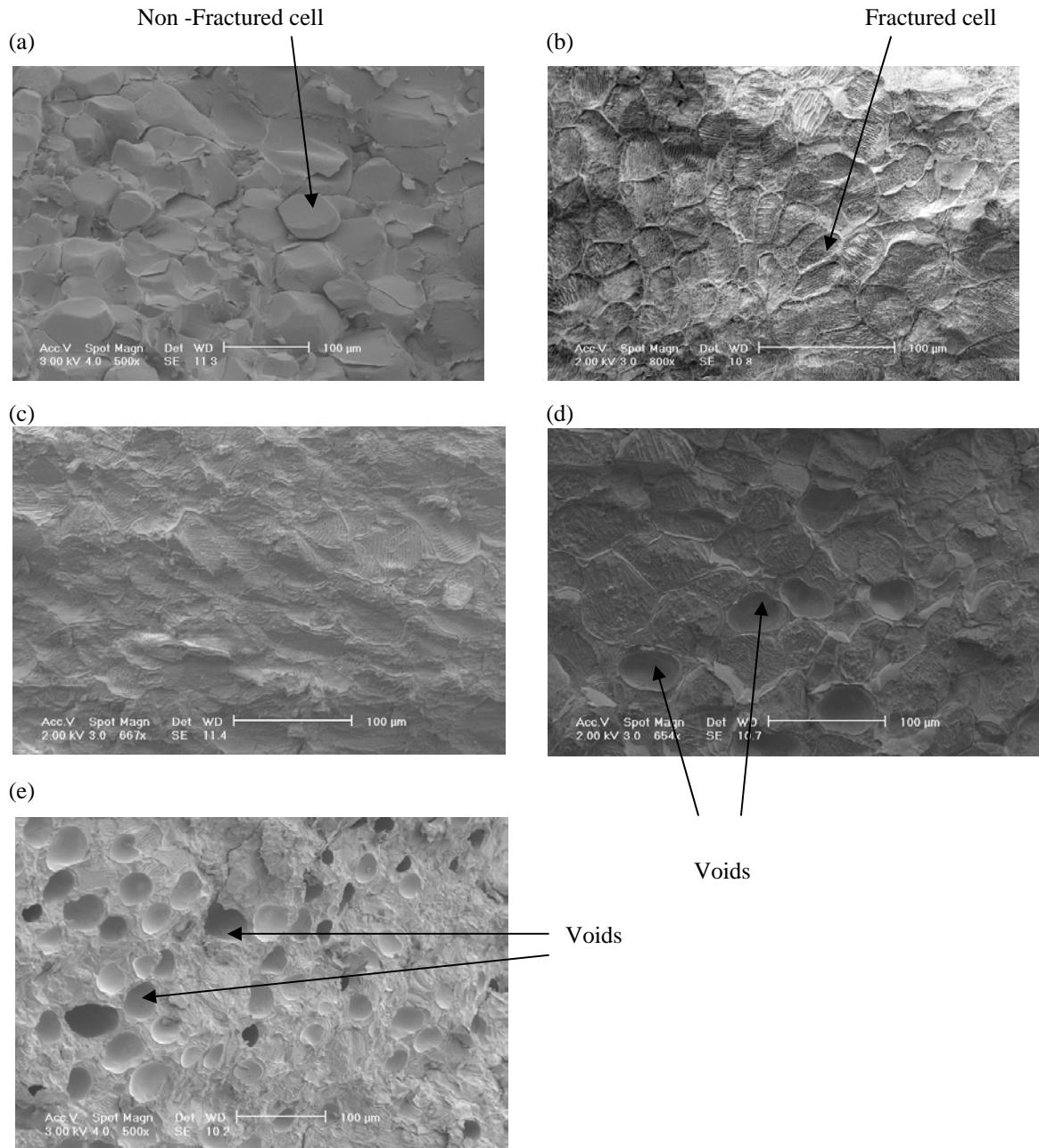


Figure 2.20 The internal microstructure of carrot pieces, imaged using cryo-SEM: (a) Raw carrot; (b) air dried carrot, rehydrated at 50°C; (c) scCO₂(pure) dried carrot, rehydrated at 50°C; (d) scCO₂(EtOH) dried carrot, rehydrated at 50°C; (e) scCO₂(EtOH) dried carrot, rehydrated at 80°C. All samples were dried at 50°C.

2.4.2.2 X-ray micro-computed tomography for analysis of the dried carrot structure

X-ray micro-CT was used to view the internal structure and cross section morphology of both supercritical and air dried carrots (Figure 2.21). This technique was not suitable for the viewing of wet samples - as discussed in section 1.5.2, high water content results in limited contrast between the water and the sample structure. This is illustrated in Figure 2.21 (a), where the structure of wet, raw carrot is not visible by x-ray analysis due to the high water content present (~90%). It may also give misleading results for the density of the sample since the sample appears much darker, due to the ability of the water to strongly absorb the x-rays. However, a darker image normally equates to a higher density product, when comparing samples of the same water content, since the x-rays are more strongly absorbed by a higher density sample. Consequently, this technique was limited here to the viewing of dried samples only. The structures of wet, rehydrated samples were viewed using alternative techniques: light microscopy and cryo-SEM. X-ray micro-CT has however been used to view air-water systems, using the high x-ray absorption of water as an advantage for this technique (Hubers *et al.* 2005).

Shadow radiograph images for each sample were initially collected and then reconstruction of this data allowed 2-D horizontal slices through the cylindrical sample to be viewed (Figure 2.21).

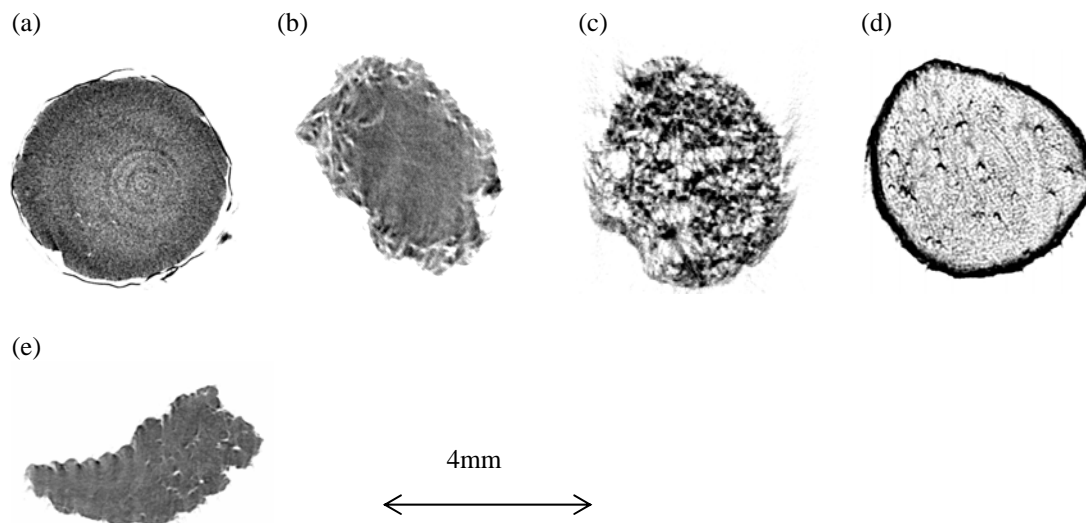


Figure 2.21 Reconstructed 2D cross-sectional x-ray images of (a) raw carrot and uncooked carrot pieces dried using: (b) $\text{scCO}_{2(\text{pure})}$ at 50°C ; (c) $\text{scCO}_{2(\text{pure})}$ at 60°C ; (d) $\text{scCO}_{2(\text{EtOH})}$ at 50°C ; (e) air at 50°C . Before drying each carrot piece was circular in cross-sectional shape and the original size as the raw carrot sample (a).

The general shape of the slice through the sample indicates the degree of shrinkage, and the darkness of the image gives an indication of the density of the dried pieces, as mentioned above. Note, however, that these images are a reverse of the actual x-ray image produced. Originally, the background appears black (where x-rays have reached the detector) and the sample being viewed is white (where the x-rays have been unable to penetrate the sample) but images were reversed to allow easier viewing of the structural entities.

During air drying, shrinkage and collapse of the product was observed, producing a dense closely-packed cellular structure with limited intercellular spaces (Figure 2.21 (e)). During air drying heat is applied to the surface of the product being dried which diffuses into the solid, primarily by conduction. Diffusion of the water occurs in the opposite direction, out of the sample, causing the shrinkage which is seen here. Capillary and tension forces are also present at the interface between the liquid water and the air, which damages delicate structures such as cells.

The sample dried in $\text{scCO}_{2(\text{pure})}$ at 50°C (Figure 2.21 (b)) appears to have a comparable density to the air dried sample. Note, however, that the deviation from cross-sectional circularity is less

pronounced after the supercritical drying, indicating that the original structure was maintained to a greater extent using this technique. In addition to the preservation of cross-sectional geometry, the overall volume of the carrot pieces dried in the SCF was visually observed to be closer to that of the original. It was previously suggested that the movement of the scCO_2 into the carrot during drying helped to maintain the sample volume while the water was removed, which prevented some collapse. Drying with a SCF may also reduce surface tension and capillary forces which can cause shrinkage and damage during air drying (Lee *et al.* 2007; Namatsu *et al.* 1999). Certainly the nature of the phase boundary during supercritical drying appears to be more favourable than the liquid-gas phase boundary present during air drying which causes surface tension and capillary forces. This has been discussed in section 2.4.1.8.

Upon depressurisation the remaining scCO_2 exits the sample as a gas and leaves behind the dried structure which is more stable and therefore does not collapse. Experiments where depressurisation was initiated before the samples were fully dried resulted in collapse of the samples, indicating the importance of low moisture content at depressurisation for volume and structure retention.

Drying with $\text{scCO}_2(\text{EtOH})$ (Figure 2.21 (d)) ensured even greater retention of the original volume and shape. This low density, porous structure with increased intercellular space may help explain rehydration properties seen later. However, the volume was not always retained indefinitely. Some shrinkage, resulting in a volume reduction of the structures dried with $\text{scCO}_2(\text{EtOH})$, was seen after leaving the dried samples for a few hours at room temperature and pressure. Similarly, highly porous materials, prepared by freeze drying are susceptible to post-drying collapse when optimal conditions for storage are not maintained (Levi and Karel 1995). Therefore, optimisation of storage conditions following drying may prevent the collapse seen - those samples that were x-rayed and placed in the warm ($\sim 40^\circ\text{C}$) x-ray micro-CT chamber, immediately after drying, did not collapse. The collapse therefore may be due to the small amounts of water still present within the open, porous structure. A possible solution to this would be to introduce a rapid heating step following drying, to remove any final moisture.

The appearance of a denser outer layer was present in all samples that had been dried using $\text{scCO}_2(\text{EtOH})$ and may be due to the outer edge of the sample in fact being denser than the central

region. However, little collapse was seen in samples dried with $\text{scCO}_2(\text{EtOH})$, suggesting that increased density due to collapse of the sample surface was unlikely. A further explanation however, may be that some solutes within the carrot were concentrated in the outer layer of the carrot piece which would account for the higher density seen. Carrots contain alcohol soluble and alcohol insoluble solutes as part of their total solid content, including small amounts of protein, ash, reducing sugars, hydrolysable sugars, starch, and cellulose (Carpenter 1940; Lee 1945). Since this phenomenon was not seen in those samples dried with $\text{scCO}_2(\text{pure})$, it is suggested that the EtOH may play some part in moving solutes to the sample surface but without actually removing them from the carrot piece. This may be due to partial solubility of solutes in the alcohol for example, or just generally high molecular mobility of solutes - which has previously been reported in food products with high water content (Witrowa-Rajchert and Lewicki 2006).

Generally, drying times were chosen that would result in similar low moisture contents of products (<0.1 NMC). However, the same drying times were used for supercritical experiments carried out at 50°C and 60°C . As discussed earlier (section 2.4.1.4), higher temperatures in supercritical drying resulted in a higher rate of water removal, therefore carrot pieces dried at 60°C contained less water than those dried for the same time at 50°C . A lower moisture content product may give a misleading x-ray image which could also be assigned to a less dense product. The density difference seen here, between samples dried with $\text{scCO}_2(\text{pure})$ at 60°C (Figure 2.21 (c)) and the samples dried with $\text{scCO}_2(\text{pure})$ at 50°C , may therefore be due to a small moisture content difference. Ideally, the moisture content would have been more closely controlled, and only structural comparison of samples containing the same moisture content would take place.

Some research has been carried out, looking at the effect of the temperature of supercritical drying on the structure of niobia and silica aerogels (Brodsky and Ko 1996; Wang *et al.* 1991). Higher temperatures, and the introduction of MeOH during drying were seen to alter the gel structure when compared with $\text{scCO}_2(\text{pure})$ drying at lower temperatures (Wang *et al.* 1991). This suggests that temperature of supercritical drying and addition of a co-solvent may affect the dried products structure. However, that research is limited and only reports the effects on gel, not food structure. Brodsky and Ko (1996) report evidence of accelerated gel aging at higher

drying temperatures, or even aggregation of one of the components. However, the extent of structure alteration during drying largely depends on the initial gel network, so direct comparisons of temperature effects cannot be made with the differing material (carrot) dried here.









Samples dried at 60°C also exhibited less shrinkage and collapse, as well as a lower density, when compared with those dried at 50°C. The reduced shrinkage and collapse seen is likely to be due to the samples having lower moisture contents, preventing collapse upon depressurisation. This may be due to the products T_g . A sugar-water mixture, which was used as a model for the water phase of fruits, showed that the T_g decreases with increased water content; water acts as a plasticiser for sugars (Nijhuis *et al.* 1998). Drying of foods increases their T_g and therefore may account for some of the decreased mobility seen here since foods that are stored below their T_g are more stable once they transition to a glassy state.

These differences have been discussed in relation to the rehydration properties observed in the following section (2.4.2.3).

2.4.2.3 Rehydration properties of dried carrot pieces

Dried samples were rehydrated at both 50°C and 80°C. Their appearance was observed and documented before and after rehydration (Table 2.5). The moisture gain due to rehydration was also studied (Figure 2.22).

Table 2.5 Photographs illustrating the appearance of dried carrot pieces using various drying techniques, followed by rehydration, where possible: (a) Raw carrot; (b) air dried carrot at 50°C and then rehydrated at 50°C; (c) $\text{scCO}_2\text{(pure)}$ dried at 50°C and then rehydrated at 50°C; (d) $\text{scCO}_2\text{(EtOH)}$ dried at 50°C and then rehydrated at 50°C; (e) $\text{scCO}_2\text{(EtOH)}$ dried at 50°C to a lower moisture content of < 0.01 NMC.

Drying method	Visual appearance	After rehydrating (at 50°C)
(a) Raw carrot		N/A
(b) Air dried, 50°C		
(c) $\text{ScCO}_2\text{(pure)}$ dried, 50°C		
(d) $\text{ScCO}_2\text{(EtOH)}$ dried, 50°C		
(e) $\text{ScCO}_2\text{(EtOH)}$ dried, 50°C (dried to a lower moisture content, < 0.01 NMC)		Sample not rehydrated

Photographic results (Table 2.5) show that carrot samples dried with air (Table 2.5 (b)), $\text{scCO}_2\text{(pure)}$ (Table 2.5 (c)), and $\text{scCO}_2\text{(EtOH)}$ (Table 2.5 (d)) could be rehydrated to a comparable appearance to that of the original raw carrot (Table 2.5 (a)). Rehydrated samples, particularly those that were dried using $\text{scCO}_2\text{(EtOH)}$, are arguably lighter in colour than the raw carrot but this difference was not significantly noticeable to the naked eye. Colour during drying and rehydration is discussed in section 2.4.2.5 in more detail.

The photographs in Table 2.5 also confirm the degree of drying-induced shrinkage that was observed in the x-ray micro-CT images (air dried > scCO_{2(pure)} dried > scCO_{2(EtOH)} dried). Although, interestingly, all of the samples appear to regain the majority of their original volume, upon rehydration, illustrated by comparison with the photograph of raw carrot (Table 2.5 (a)). The photographs also illustrate the damage that can be caused by drying using scCO_{2(EtOH)} to complete dryness. Carrot samples were seen to fall apart upon continued exposure to scCO_{2(EtOH)} and therefore were unable to be dried intact to <0.01 NMC using this method. The voids seen using light microscopy and cryo-SEM may be responsible for the structure breaking apart, especially if longer exposure times caused more voids to be formed within the carrot structure.

Rehydration curves were initially plotted of NMC against rehydration time. The NMC for rehydration was calculated using equation 2.6.

This enabled the extent of rehydration to be observed easily, since a NMC value of 1 would require the dried sample to have rehydrated back to its original (pre-dried) moisture content and would be the 'ideal' situation. However, comparison of rehydration curves such as Figure 2.22 became difficult, as many of the samples that had been dried by different techniques began rehydration with different NMC values. There was also some variability across the samples that had been dried in the same way, resulting in large error bars. The moisture content prior to rehydration may affect the rehydration properties and therefore give unreliable and misleading results if grouped together and averages are taken. Due to the nature of the supercritical drying it was impossible to consistently dry all samples to exactly the same moisture content. This has been discussed earlier in section 2.3.3. Therefore, the results were re-plotted as single experiments (raw data) displayed as NMC, after rehydration (X_r/X_0) against initial NMC, before rehydration (X_d/X_0). This enabled easier comparison of results, since the variation in starting moisture contents was accounted for and therefore samples that exhibited more/less favourable rehydration properties could be identified.

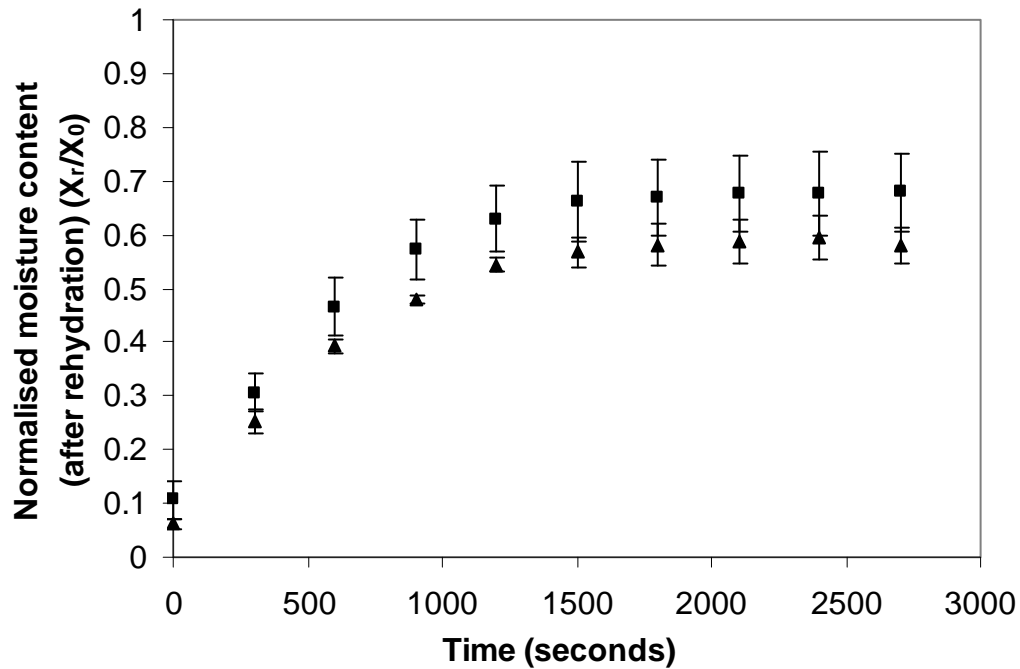
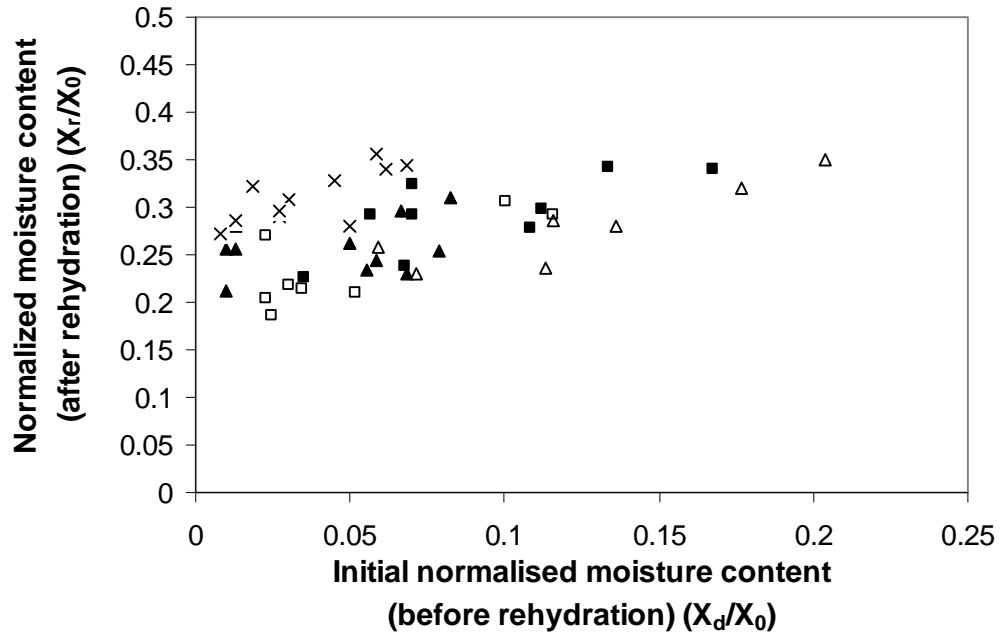


Figure 2.22 A rehydration curve of samples that were air dried at 50°C (▲) and dried with $\text{scCO}_2(\text{pure})$ at 50°C (■), followed by rehydration at 50°C. Each value represents the overall mean from at least three independent experiments (each involving at least three pieces of carrots) \pm one standard error of the mean.

Rehydration results (for samples rehydrated at 50°C) were plotted as data points for each individual experiment, at rehydration times of both 300 seconds (Figure 2.23 (a)) and 2400 seconds (Figure 2.23 (b)). Time points of 300 seconds and 2400 seconds were chosen to give an indication of the measure of the initial rehydration rate (at 300 seconds), and also at a time when the EMC had been, or was very close to being reached (at 2400 seconds).

Figure 2.23 shows the NMC (after rehydration) plotted against the initial NMC (before rehydration), for cooked and raw carrot pieces dried with air, $\text{scCO}_2(\text{pure})$, or $\text{scCO}_2(\text{EtOH})$. All results were obtained following rehydration at 50°C. The results are shown for both 300 seconds and 2400 seconds rehydration times, in Figure 2.23 (a) and Figure 2.23 (b), respectively. Note, that different scales for NMC on the y axis have been used, in order to display the results in a clearer manner.

(a)



(b)

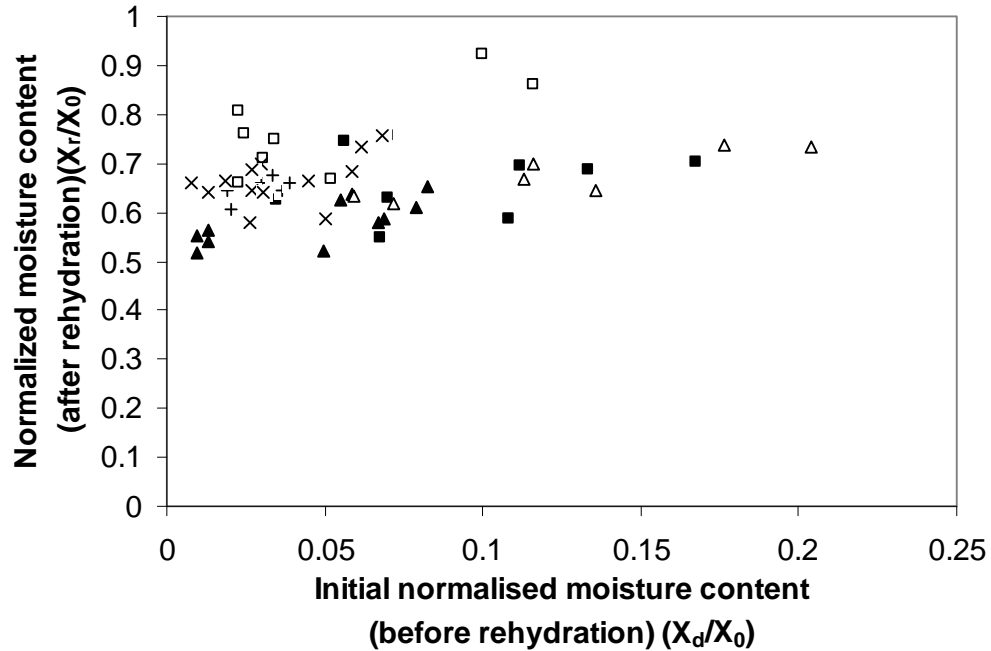


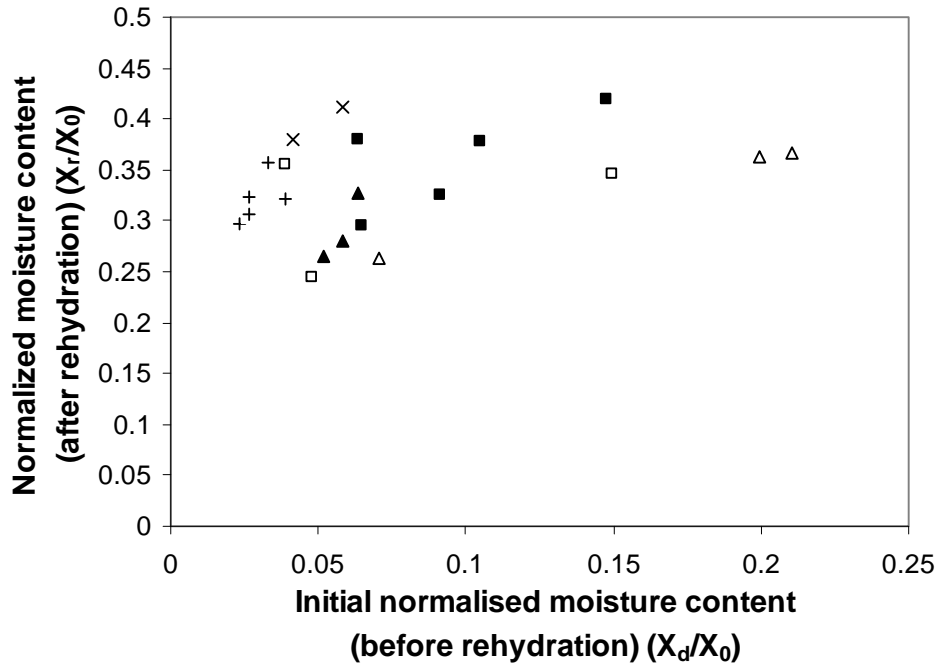
Figure 2.23 NMC, during rehydration at 50°C, plotted against initial NMC, before rehydration at a) 300 seconds and b) 2400 seconds. Samples were dried using: air drying at 50°C (▲), $\text{scCO}_{2(\text{pure})}$ at 50°C (■), $\text{scCO}_{2(\text{EtOH})}$ at 50°C (x), air drying (after cooking) at 50°C (Δ) and $\text{scCO}_{2(\text{pure})}$ (after cooking) at 50°C (□). Each point is a measurement from a single piece of carrot.

For rehydration after 300 seconds, no conclusive differences between samples dried via different techniques can be seen. However, the observed trends suggest that the extent of rehydration for carrot pieces dried with $\text{scCO}_2(\text{EtOH})$ may be slightly greater than for the others. A potential explanation for this is discussed later in this section. However, after 2400 seconds of rehydration these differences in NMC had disappeared, suggesting samples dried using $\text{scCO}_2(\text{EtOH})$ may have a faster ‘instant’ rehydration rate than those samples dried using the alternative techniques.

Furthermore, although pre-cooking increased the rate of air drying, its effects did not persist with respect to rehydration i.e. no difference was seen between the NMCs obtained for air dried, cooked and air dried, uncooked carrot, at either 300 or 2400 seconds rehydration time (Figure 2.23 (a) and (b)). In contrast, cooking was seen to affect the rehydration properties of supercritically dried carrot pieces, with higher NMCs being observed with pre-cooked samples, but only after 2400 seconds of rehydration (Figure 2.23 (b)). A significant difference is however debatable.

The temperature employed during supercritical drying had no effect on the amount of moisture subsequently gained after 300 seconds or 2400 seconds of rehydration, and is shown in a separate figure for clarity (Figure 2.24 (a) and (b)).

(a)



(b)

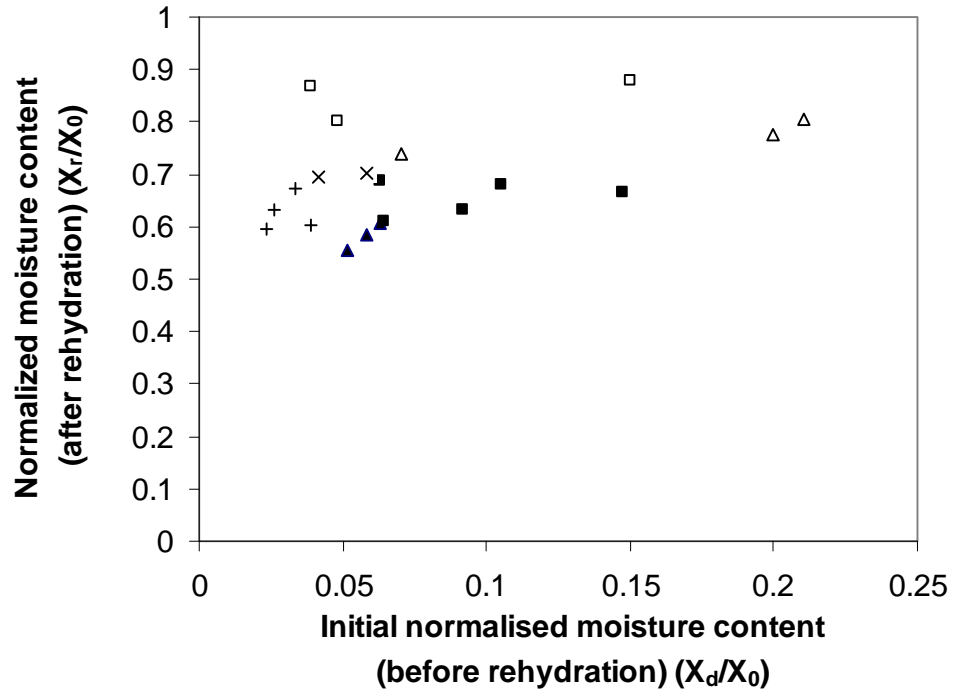


Figure 2.25 NMC, during rehydration at 80°C, plotted against initial NMC, before rehydration at a) 300 seconds and b) 2400 seconds. Samples were dried using: air drying at 50°C (\blacktriangle), $\text{scCO}_2(\text{pure})$ at 50°C (\blacksquare), $\text{scCO}_2(\text{pure})$ at 60°C (+), $\text{scCO}_2(\text{EtOH})$ at 50°C (x), air drying (after cooking) at 50°C (\triangle) and $\text{scCO}_2(\text{pure})$ (after cooking) at 50°C (\square). Each point is a measurement from a single piece of carrot.

Interestingly, results for equivalent rehydration experiments, carried out at 80°C were very similar to those conducted at 50°C. The NMCs after 300 seconds and 2400 seconds rehydration are shown in Figure 2.25 (a) and Figure 2.25 (b) respectively.

The similarity of results obtained at 80°C rehydration, with those obtained at 50°C rehydration contradicts the results of Krokida and Marinos-Kouris (2003), who showed that rehydration temperature of various dehydrated fruits and vegetables had a significant effect on both the rate of rehydration and the EMC achieved. It is suggested that this difference may be due to several factors: the use of different drying temperatures to dehydrate the material (50°C was used in this work, compared with 70°C used in the work reported by Krokida and Marinos-Kouris (2003)); the use of different sample sizes (the volume of pre-dried carrot pieces reported here were a tenth of those used by Krokida and Marinos-Kouris (2003)); and/or the use of different drying methods (supercritical drying was used in this work, compared with air drying used in the work reported by Krokida and Marinos-Kouris (2003)). Different drying temperatures and techniques would consequently result in changes to the physical structure, for example porosity. Such changes have been shown to influence rehydratability (Nikhuis *et al.* 1998). It may also be that changes in rehydration at different temperatures do exist, but on the small scale used here, they are not significant enough to be identified. Direct comparison of these results is therefore unreliable.

Drying with $\text{scCO}_2(\text{EtOH})$ produced low density, porous structures with increased intercellular space and showed great retention of the original volume and shape (Figure 2.21). The production of voids was also observed in light microscopy images (Figure 2.19). This may explain the slightly higher NMCs seen for these samples, in the early stages of rehydration (after 300 seconds) (Figures 2.23 (a) (x) and 2.25 (a) (x)), and also the fact that they floated during rehydration, when compared with other samples which had lower NMCs after 300 seconds of rehydration, and sank during rehydration. Sanjuán *et al.* (2005) also saw the creation of voids in carrots, during blanching, which also resulted in a slightly higher EMC being achieved upon rehydration, as the voids were expected to be filled with water. The looser structure (through cell wall separation) was also mentioned as an explanation for a higher rehydration diffusion coefficient seen. Sanjuán *et al.* (2005) suggested that water may be able to enter this looser structure more quickly therefore aiding rehydration. There was no evidence for cell wall

separation during drying with $\text{scCO}_2(\text{EtOH})$. However, carrot pieces that had been cooked and then dried with $\text{scCO}_2(\text{pure})$ exhibited both cell wall component breakdown (potentially cell wall separation) and the creation of voids (Figure 2.19 and 2.20). They also appeared to have slightly higher NMCs than other samples, after 2400 seconds of rehydration (Figure 2.23 (b) (□) and Figure 2.20 (b) (□)), suggesting void formation and cell wall degradation enabled a slightly higher degree of water to be re-gained upon rehydration. It is therefore proposed that these voids may facilitate the movement of water into the internal structure of the sample and cell wall breakdown may also enable more water to be held within the rehydrated sample structure. It is anticipated that these minor differences may be more noticeable if drying and rehydration was carried out on larger samples.

Air dried samples would be expected to exhibit poor rehydration properties due to their collapsed and shrunken structure which may restrict intercellular diffusion of water into the product. However, despite air dried samples appearing more collapsed than those that had been dried with $\text{scCO}_2(\text{pure})$ (Figure 2.21), no difference was observed in the rehydration properties. The air dried samples regained much of the original volume of the pre-dried sample, upon rehydration, suggesting some of the shrinkage and collapse may have been reversible. This would explain why air dried samples exhibited similar rehydration properties to samples dried with $\text{scCO}_2(\text{pure})$.

Some structural differences between samples dried with $\text{scCO}_2(\text{pure})$ at 50°C and 60°C, were observed in x-ray micro-CT images (Figure 2.21). However, these differences were not extended to their rehydration properties. As discussed earlier (section 2.4.2.2), the structural differences seen between those samples dried at 50°C and 60°C may be due to small differences in the moisture content of the samples, which don't appear to have a distinguishable effect on the rehydration properties.

2.4.2.4 Texture analysis of rehydrated carrot pieces to measure hardness

Texture properties of foods, particularly fruits and vegetables, are important to the consumer. To assess the impact of microstructural changes during drying on a macrostructural property (texture), puncture force analysis was performed on rehydrated samples following 2400 seconds

rehydration at either 50°C or 80°C. Figure 2.26 shows a photograph of the TA-XT2i texture analyser used to obtain these results.



Figure 2.26 TA-XT2i, texture analyser from Stable Micro System, UK, used to obtain puncture force results for carrot pieces, following rehydration.

Initially as a control experiment, carrot pieces were cooked in boiling water (100°C) to mimic the cooking of carrot in a consumer environment, and that of foods that may be rehydrated at home using boiling water. The force required to puncture the samples was monitored over cooking time (Figure 2.27).

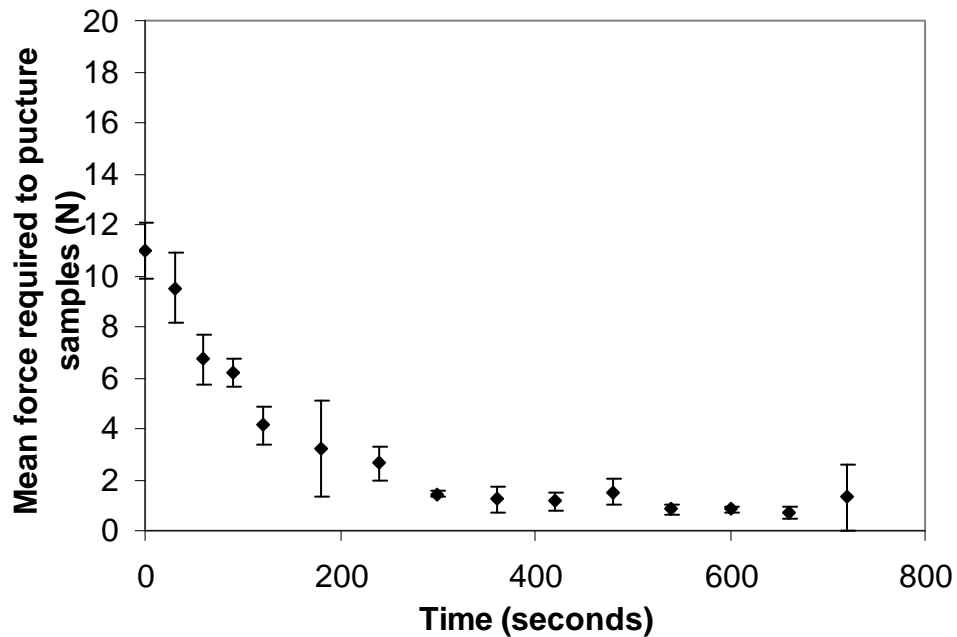


Figure 2.27 Graph showing the force required to puncture cylindrical raw carrot pieces that had been cooked (in water at 100°C) for different amounts of time. Each point represents the overall mean from at least three independent sets of measurements \pm one standard deviation of the mean. The same y axis scale is used as that for the texture results (Figures 2.28 and 2.29), to allow easy comparison.

The reduction in force required to puncture samples was reduced greatly after 300 seconds of cooking, indicating that breakdown of the rigid cellular wall structure and/or cell wall separation had occurred. These results gave a useful indication of the expected force required to puncture raw and cooked carrot. These values are used in Figures 2.28 and 2.29 for comparison with carrot samples dried using different techniques, and then rehydrated.

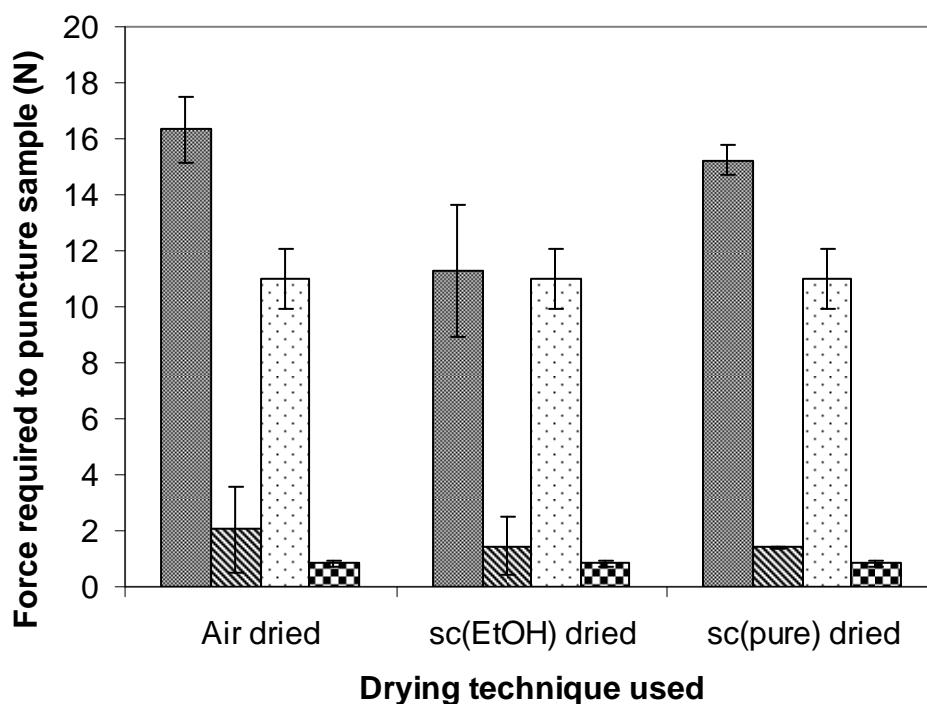


Figure 2.28 Puncture testing of carrot samples, dried using different techniques (all at 50°C) and rehydrated at 50°C (dark bars) or 80°C (diagonal dark stripes). Raw carrot (spots) and cooked carrot (checks) are shown for comparison. Each value represents the overall mean from at least three independent experiments (each involving at least three pieces of carrots) \pm one standard error of the mean.

Figure 2.28 shows the results of the puncture test, used as an indicator of textural properties of the dehydrated-rehydrated samples. Fresh raw carrot (Figure 2.8 (spots)) and cooked carrot (Figure 2.8 (checks)) were used as controls. The structural and textural properties of fruits and vegetables relate highly to the integrity of cell wall components (Ng *et al.* 1998). For example, heat-induced texture degradation is attributed to cell wall pectin solubilisation and pectin depolymerisation, via β -elimination (Georget *et al.* 1998; Lin *et al.* 1998; Sila *et al.* 2006). Rehydrating at 80°C was seen to have an equivalent effect to pre-cooking, on the required force to puncture, presumably as both lead to cell wall degradation. As such, trends relating process conditions to puncture force are best seen for samples rehydrated at 50°C. At this rehydration temperature, the maximum average puncture force values decreased in the following order: air drying > drying with $\text{scCO}_2(\text{pure})$ > drying with $\text{scCO}_2(\text{EtOH})$. Application of the Kruskal-Wallis test to these data sets indicated that any difference between the three was right on the limit of

statistical significance, at $\alpha = 0.05$. However, the general trends relate well to the density and porosity of the various dried samples, suggesting that the more porous, low density dried samples (i.e. those dried with $\text{scCO}_2(\text{EtOH})$) have a softer texture when rehydrated than those with low porosity and high density (i.e. those subjected to air drying).

Puncture forces in this work were similar to those reported by Lin *et al.* (1998). Air dried slices produced by these authors required a force of 18.1 N to puncture them, a force comparable to that required to puncture air dried carrot cylinders rehydrated at 50°C in this work (16.32 ± 1.17 N). The force required in this work to puncture rehydrated carrots that had been dried using $\text{scCO}_2(\text{EtOH})$, 11.27 ± 2.38 N, is comparable with the value of 11 N obtained by Lin *et al.* (1998) for samples dried using MVD.

Case-hardening during drying was stated to be the reason for the differences seen between samples dried by air drying and MDV (Lin *et al.* 1998). This phenomenon is associated with systems where water removal from the surface is faster than the rate at which water migrates from the interior. The surface therefore dries to form a hard layer containing previously-dissolved solutes. In MVD heat is generated within the product, resulting in *in situ* vaporisation of water which is able to rapidly diffuse out of the tissue without carrying dissolved solutes that contribute to case-hardening. Lin *et al.* (1998) also related their findings to sensory analysis, with samples dried by MVD receiving the better sensory ratings for texture (in both dried and rehydrated states). Given the similarities between the puncture forces associated with MVD and samples dried with $\text{scCO}_2(\text{EtOH})$, it is anticipated that the texture of the latter may also be preferable to the air dried equivalents, although sensory evaluations are required to confirm this.

While case-hardening may contribute to some of the harder texture seen with the air drying, the textural properties relating to drying with $\text{scCO}_2(\text{pure})$ cannot yet be fully explained. The suggested mechanism (section 2.4.1.8) for supercritical drying would not facilitate case hardening. It is worth noting that puncture force analysis was performed through 2.5 mm of the cylindrical sample, which was a total of 4 mm in diameter (pre-dried), hence a degree of the puncture measurement would have been contributed from the internal texture too.

As mentioned earlier, the texture is also thought to be related to the density of the dried product, which does explain why the rehydrated puncture force of $\text{scCO}_{2(\text{pure})}$ dried carrot is higher than that of $\text{scCO}_{2(\text{EtOH})}$ dried carrot.

Air dried and $\text{scCO}_{2(\text{pure})}$ dried carrot pieces both required an increased force to puncture the sample than that of pre-dried raw carrot, which can be explained by the incomplete rehydration of the samples back to the original moisture content. In the case of samples dried using $\text{scCO}_{2(\text{EtOH})}$, incomplete rehydration would also be expected to result in a higher rehydrated puncture force to that of raw carrot. However, results show that the puncture force is actually very similar to that of raw carrot. This may be explained by the counteracting texture effect of the voids present in the sample, expected to lower the carrot hardness. Therefore, modification of the scCO_2 with EtOH reduced the puncture force of the rehydrated product to more closely resemble that of raw carrot. Sanjuán *et al.* (2005) also reported that the creation of voids in carrot, created a looser structure which consequently reduced the puncture force of the carrot.

Air dried and $\text{scCO}_{2(\text{pure})}$ dried samples, dried at 50°C (Figure 2.28) and 60°C (Figure 2.29) had very similar puncture forces for samples rehydrated at both 50°C and 80°C . Therefore, small changes in the drying temperature do not appear to influence the texture, following rehydration.

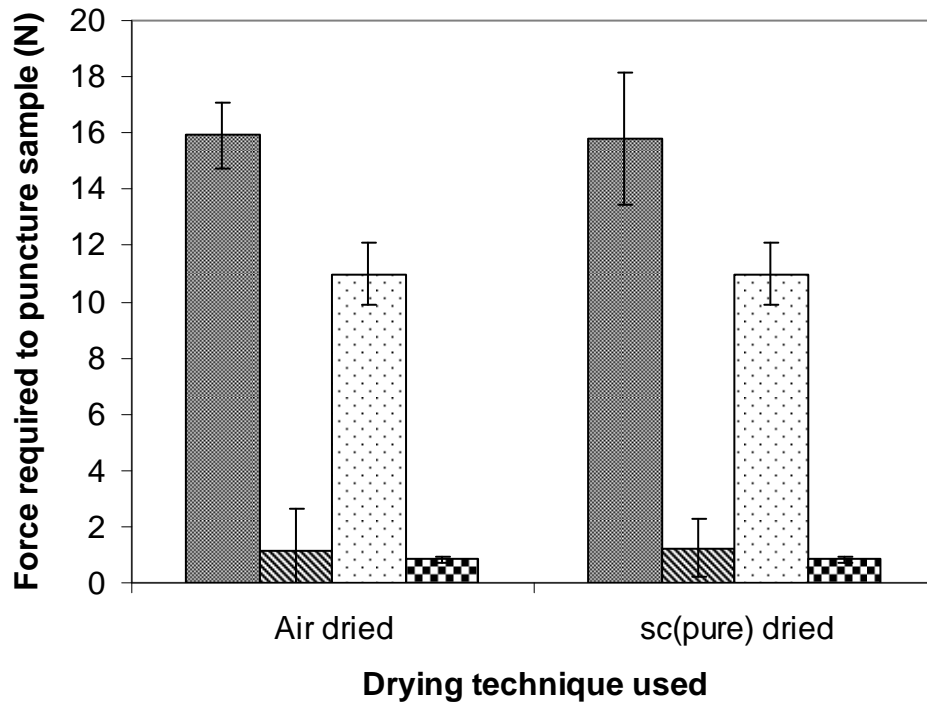


Figure 2.29 Puncture testing of carrot samples, dried using air and $\text{scCO}_{2(\text{pure})}$ (both at 60°C) and rehydrated at 50°C (dark bars) or 80°C (diagonal dark stripes). Pre-dried raw carrot (spots) and cooked carrot (checks) are shown for comparison. Each value represents the overall mean from at least three independent sets of measurements \pm one standard deviation of the mean.

2.4.2.5 Colour analysis of carrot pieces

The colour of carrot samples was measured as described in section 2.3.11, using a scanner, Adobe Photoshop 6.0, and the 'L*a*b*' colour model (CIELAB). A similar method for colour analysis of food has been reported by Kiliç *et al.* (2007).

Figure 2.30 illustrates the set up in the scanner used to obtain the images. Scanners often have a built in colour correction, so the scan must be done over a wide range of colours, to avoid different results for different samples. In an attempt to overcome this, paint sample cards were used to try and give a reproducible colour range over which the scan was done. These images were then imported into Adobe Photoshop where L*a*b* values were recorded using the Info Palette. Measurements were taken at different points on the sample and an average calculated. This was repeated over three experiments. Finally, the total colour change (ΔC) from the

standard colour of raw carrot (before drying) was calculated (equation 2.7). Raw carrot was used at the 'ideal' colour and deviation from this colour was represented in the total colour change value. The colour change was measured directly after drying and also after rehydrating at both 50°C and 80°C. The results are shown in Figure 2.31.



Figure 2.30 An example of scanned dried carrot pieces (air dried, 80°C) used to obtain $L^*a^*b^*$ values in Adobe Photoshop.

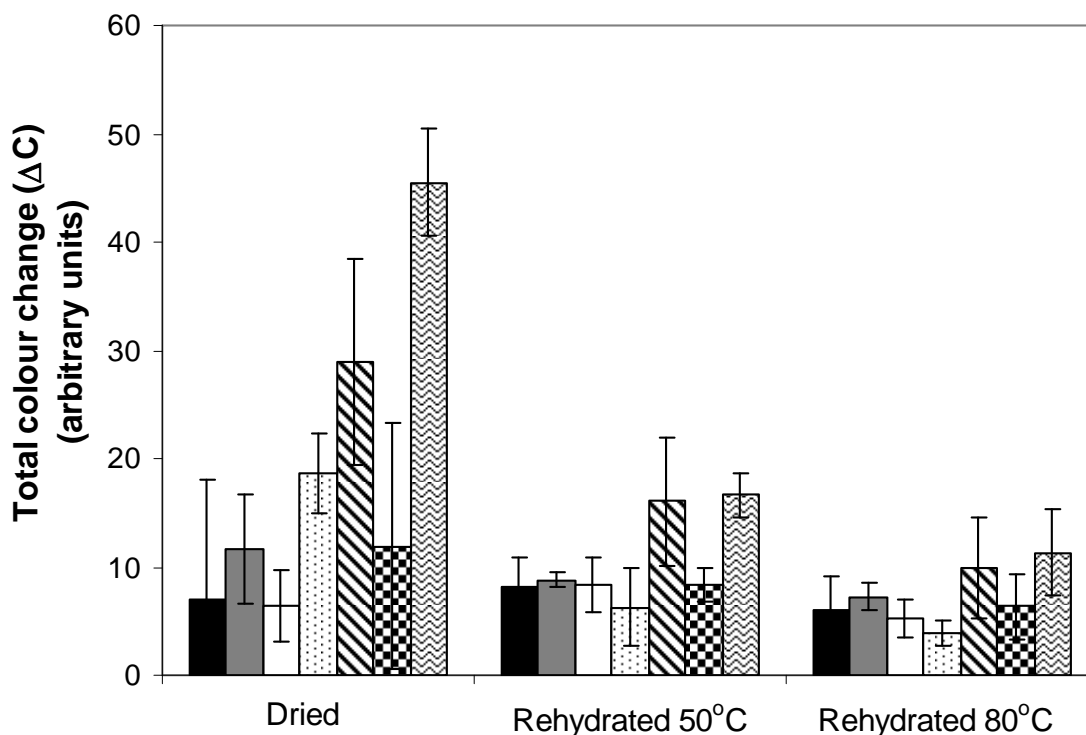


Figure 2.31 Comparison of the total colour change (ΔC), following drying and rehydration at 50°C and 80°C, for samples dried using various techniques: air dried, 50°C (black); air dried, 60°C (grey); cooked carrot, air dried, 50°C (white); scCO₂(pure) dried, 50°C (spots); scCO₂(pure) dried, 60°C (diagonal stripes); cooked carrot, scCO₂(pure) dried 50°C (checks); scCO₂(EtOH) dried 50°C (zigzags). Each bar represents the overall mean from at least three independent measurements taken from at least three individual pieces of carrots \pm standard error of the mean.

Following drying, carrots that had been dried with scCO₂, especially scCO₂(EtOH), appeared to be paler in colour than raw carrot. Initially it was hypothesised that this was due, primarily to the extraction of carotenes (α - and β -carotenes), as these substances are known to be soluble in scCO₂ (Cynarowicz *et al.* 1990; Nijhuis *et al.* 1998; Reverchon 1997). Upon rehydration however, the colour returned significantly so that the difference between fresh and dried carrot became almost indistinguishable to the naked eye (Table 2.5). This suggests carotene extraction had not been as extensive as first expected. Instead, it is suggested that supercritical drying led to a decrease in the transparency of the cell walls, that was reversible on rehydration. This may be due to extraction or alteration of compounds in the cell wall or cell membrane, due to supercritical processing. An alternative explanation may also be that the location of the

carotenes has changed during supercritical processing, influencing the appearance of the colour of the dried sample. However, investigative analysis on carotene content in dried samples would be required to draw firm conclusions. In contrast, air dried samples were darker in colour than fresh raw carrot. The collapse of the cellular structure, shrinkage and therefore increased carotene concentration within a specific area provides an explanation for this.

These hypotheses are also supported by the fact that a smaller average colour change is seen in cooked carrot which is subsequently dried using $\text{scCO}_2(\text{pure})$. Upon cooking, the cellular structure is broken down which may allow more visibility of the carotene after drying than when raw carrot is dried. Also, some collapse of the structure upon cooking also occurs which would provide concentration of the carotene within a specific area, similar to that seen with air dried samples. The largest colour change was associated with carrot dried using $\text{scCO}_2(\text{EtOH})$ which were also the samples experiencing the least collapse or shrinkage on a macrostructural level, and therefore also less cellular microstructural collapse. Collapse or rupture of the cell structure during drying appears to be necessary to enable the carotene to be visible in dried samples.

Temperature of air drying did not appear to affect the colour change following drying and rehydration – similar results were observed for both 50°C and 60°C. However, supercritical drying with a higher temperature of 60°C caused an increase in deviation from the ‘ideal’ colour after drying, and after rehydration, at both temperatures, although the colour change was more visible following drying. This may be due to lower moisture contents after drying at 60°C, when compared with those dried at 50°C. The same drying time was used for 50°C and 60°C drying and hence during higher temperature drying, the samples would have been dried faster. This would contribute to lower moisture content and less cell wall transparency (as discussed above the dried samples experienced more colour loss which returned upon rehydration), weakening the carotene colour observed upon analysis. This difference in initial NMC is illustrated in the rehydration results (Figure 2.24) and some of the same samples were used for both rehydration and colour comparison experiments. Future analysis would therefore only involve colour comparison on those samples with the exact same moisture content.

2.5 Conclusion

It has been demonstrated that carrots can be dried with $\text{scCO}_2(\text{pure})$ and $\text{scCO}_2(\text{EtOH})$, promoting improved retention of original sample volume than air drying. This novel technique has also been shown to produce less dense microstructural characteristics, especially in samples dried using $\text{scCO}_2(\text{EtOH})$. The additional creation of voids during drying with $\text{scCO}_2(\text{EtOH})$ and drying pre-cooked carrot with $\text{scCO}_2(\text{pure})$ may increase the total moisture gained during rehydration, at 300 seconds and 2400 seconds, respectively. This may enable manipulation of rehydration rates in both the early and latter stages. The subsequent texture of rehydrated samples, dried with $\text{scCO}_2(\text{EtOH})$, was closer to the original texture of raw carrot, than those samples dried via air drying or using $\text{scCO}_2(\text{pure})$, suggesting the discussed structural changes had a positive impact on the texture, following rehydration. It is anticipated that such microstructural differences may favorably alter sensorial properties of dehydrated-rehydrated foods.

Although some colour loss was observed following drying with the supercritical systems this was found to be largely reversible on rehydration. However, the reason for this observation is not currently known.

A mechanism for supercritical drying, at the conditions investigated, was also suggested. The scCO_2 was thought to diffuse into the sample and maintain the sample volume while the water was removed. The water present in the sample was expected to be dissolved into, or carried out by the SCF which subsequently exited the sample. This explained the ability of supercritically dried samples to retain their circularity well – since the scCO_2 was able to occupy volume that was originally occupied by water. Upon drying, the scCO_2 was expelled from the sample, at which point the dried structure was more stable and less prone to significant shrinkage. However, depressurisation of samples that were not fully dried did experience some shrinkage.

Below 2 l/minute the drying rate was limited by external mass transfer resistances, since increasing the flow rate (up to 2 l/minute) was shown to increase the drying rate. Above 2 l/minute however, the rate of drying was not improved with increased flow rate and additionally, internal structure did not affect the drying rate. Therefore it was hypothesised that >2 l/minute the drying rate was limited by the scCO_2 instead, and how much moisture it can hold. This hypothesis was supported by the increased moisture removal seen when EtOH was

added as a co-solvent and also the increased removal of moisture when temperature was increased, which were both expected to change the solubility properties of the SCF.

A potential drawback of this method is the longer drying times involved when compared with conventional methods such as air drying (Figure 2.7). This is not only practically inconvenient, but a longer process may also incur higher costs. However, increasing the supercritical drying rate by: addition of a co-solvent; increasing drying temperature; and/or increasing scCO₂ flow rate; has been illustrated here and may offer a favourable solution to this problem.

3.0 Drying of biopolymer gels using supercritical carbon dioxide

ABSTRACT

The method used previously to dry carrots with unmodified supercritical carbon dioxide ($\text{scCO}_2(\text{pure})$) or ethanol modified scCO_2 ($\text{scCO}_2(\text{EtOH})$) was used here to remove water from agar gel, containing varying concentrations of sucrose (0-10%). The effect of sucrose concentration and supercritical drying conditions (co-solvent addition, flow rate and depressurisation rate) on gel microstructure was evaluated and compared with air and freeze dried gels. X-ray micro-computed tomography was used to determine the voidage (percentage open pore space) of the dried structures. Additionally, rehydration and mechanical properties were investigated. For formulations containing sucrose, which displayed the best structural retention, voidage was found to increase in the order: air drying (4%) < supercritical drying with $\text{scCO}_2(\text{pure})$ (48%) < supercritical drying with $\text{scCO}_2(\text{EtOH})$ (68%) < freeze-drying (76%). During supercritical drying CO_2 flow rate (1 l/minute and 3 l/minute) and depressurisation rate (0.4 and 1.6 MPa/minute) were not found to have any effect on the dried microstructure. Gels that had been supercritically dried displayed similar rehydration properties to those that were air dried. However, upon rehydration supercritically dried gels showed more favourable textural properties than those that had been air or freeze dried.

Fourier transform infrared spectroscopy was used to investigate proposed interactions that may be responsible for the different structures produced during supercritical drying with and without ethanol. An agar- CO_2 interaction was detected which appeared to be lost upon ethanol addition to partially wet gel. It was proposed that water-agar and ethanol- CO_2 interactions, thought to occur in this system may have jointly prevented the agar- CO_2 interaction from occurring. Additionally, an explanation for the structural changes observed upon ethanol addition was proposed. However, further experiments are required to prove or disprove these hypotheses.

3.1 Introduction

The use of $\text{scCO}_{2(\text{pure})}$ and $\text{scCO}_{2(\text{EtOH})}$ for drying carrots was investigated in chapter 2. In this chapter the method is extended to gel systems that are often used in processed food systems. The effects of sucrose addition on the dried gel structure and gel properties such as texture and rehydration have also been examined.

The wide importance of gelling agents in the food industry stems from their ability to be added to processed foods such as meat, cheese, yogurt and confectionary products, allowing manipulation of sensorial attributes (Renard *et al.* 2006). In particular, the texture of such products may be altered with the use of gel networks. Gel networks consist of space filling networks of cross linked polymers and it is this microstructure that is important for texture and flavour perception in such systems.

In this chapter the drying of agar gels is primarily investigated. Agar gels form strong gels with as little as 1% agar in water, and are thermoreversible. This means that upon heating (above 85°C) and cooling (below $30\text{-}40^{\circ}\text{C}$) the gel may be melted and set an infinite amount of times. Interactions between the polymer chains stabilise the gel structure and allow water to be immobilised within the network. The gel network structure has an influence on the mobility of the incorporated water, and therefore will influence drying properties.

Upon removal of water from a gel network under atmospheric conditions the structure becomes susceptible to structural manipulation and shrinkage, due to tension forces created at the liquid-vapour interface. Freeze drying avoids this problem by removal of water through sublimation (the water goes directly from a solid to a gaseous phase). However, although structure and volume is retained, freeze dried gels are commonly brittle and fragile. The technique is also expensive and therefore a need exists for a new drying technique that may solve some of these problems.

Sucrose addition was also investigated in this chapter as a method to potentially enhance the gel structure. The addition of sucrose to biopolymer gels has been reported by Suzuki *et al.* (2001) to have an effect on gel network structure which consequently affects the mechanical properties of the gel (Normand *et al.* 2003).

Supercritical drying has been investigated here, as a new way to dry these complex structures, after showing promising results in chapter 2. There has also been significant research reported on the use of supercritical drying for the creation of aerogels and highly porous structures, without structure collapse (Higginbotham *et al.* 2003; Namatsu *et al.* 1999; Rangarajan and Lira 1991; Takishima *et al.* 1997; von Behren *et al.* 1997). However, this has not yet been extended to food products.

The addition of a co-solvent (EtOH) during drying was investigated as a method to increase drying rate, and perhaps more importantly, to manipulate the gel microstructure. Comparison of supercritical drying with conventional drying techniques, including air and freeze drying was carried out.

In summary, addition of gels into food products allows exciting new structures and mouthfeels to be created. Therefore, the drying of biopolymer gels is of importance in terms of both structure maintenance and structure manipulation, to favorably influence sensorial perception. The addition of sucrose to the gel network, prior to drying, and the addition of co-solvent to the scCO₂, during supercritical drying, may also assist in this quest to create new exciting gel structures.

3.2 Materials

3.2.1 Rig components

Details of the rig components and the materials used for the experimental rig are detailed in chapter 2 (section 2.2.1).

3.2.2 Gel preparation

The biopolymer gel used in this research was agar, and was chosen due to its wide usage in the food industry. The uses of biopolymers in the food industry, and more specifically the use of agar, are discussed in sections 1.3.5 and 1.3.5.1, respectively. Sucrose addition to gels is also discussed in section 1.3.5.3. Agar (product number A1296) and sucrose (product number S9378) were purchased from Sigma Aldrich (Poole, UK).

The gels were prepared by initially dissolving sucrose in deionised water to the required concentration (0%, 1% and 10% w/v). The agar powder (2% w/v) was then stirred with the sucrose solutions and boiled for 120 seconds, to ensure complete dissolution of the agar. The solution was left to cool and de-gas by standing for a few minutes, before pouring into a plastic mould with cylindrical recesses (length = 12 mm and diameter = 5 mm). The gels were left to cool at room temperature for at least one hour to set, before removing the gels from the mould.

Four gel cylinders were used in each drying experiment, while three others were used to determine the initial average total moisture content, by drying to constant mass overnight in an oven at 80°C. Gels containing 0% sucrose were used as a control.

The moisture content in this work is reported as NMC. Discussion of NMC, the reasons for its choice, and the equation used to calculate it (equation 2.2) have been included in chapter 2 (section 2.3.2).

3.2.3 Carbon dioxide and ethanol

CO₂ (liquid withdrawal) was supplied by BOC (Guildford, UK). Absolute ethanol (99.9% pure) was supplied by Fisher Scientific (Loughborough, UK) and was of Analar grade.

3.3 Apparatus and methodology

3.3.1 High pressure drying equipment

The experimental rig is described in chapter 2 (section 2.3.1) and a schematic representation has been detailed in Figure 2.1

3.3.2 Method for supercritical drying of gel pieces using supercritical carbon dioxide

Drying using scCO₂ was carried out using the equipment outlined in chapter 2 (section 2.3.1), used for carrot drying. Experiments were carried out in the same way as described in section 2.3.3, for carrot pieces (using a 2 l/minute flow rate and a 0.4 MPa/minute depressurisation rate, at 20 MPa and 50°C). However, the effect of process conditions was also investigated in this chapter. Experiments were carried out at a constant temperature and pressure of 50°C and 20

MPa, respectively. Two CO₂ flow rates (1 l/minute and 3 l/minute) and two depressurisation rates (0.4 MPa/minute and 1.6 MPa/minute) were additionally investigated.

ScCO_{2(pure)} and scCO_{2(EtOH)} (containing 6 mol% EtOH) were used as the solvents for gel drying experiments, similarly to those experiments carried out in chapter 2. The amount of EtOH that was required to achieve 6 mol% was dependent on the CO₂ flow rate and was calculated for each experiment using the method outlined in section 2.3.3.1.

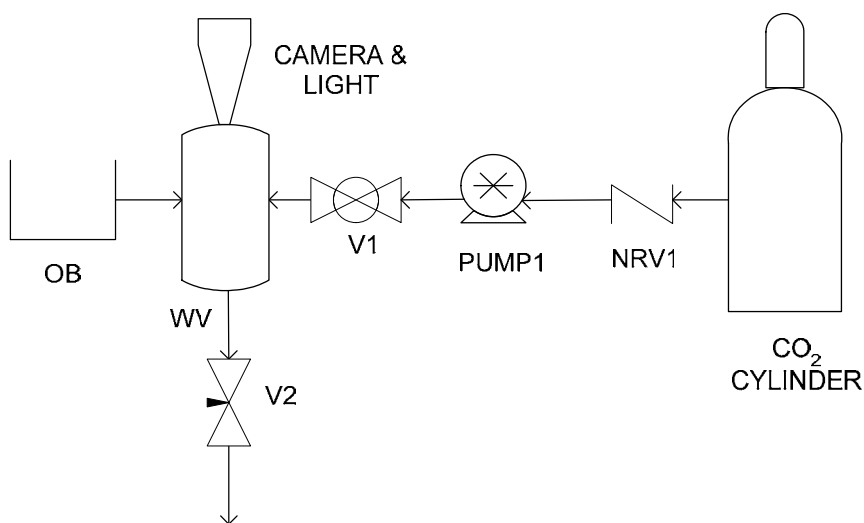
Initial experiments were carried out to determine a drying time that resulted in gels being dried to a low moisture content (<0.1 NMC). 10800 seconds was found to be sufficient time to obtain gels dried to this level when using scCO_{2(pure)}, while 7800 seconds was sufficient when using scCO_{2(EtOH)}.

Depressurisation was controlled at a steady rate by a micrometering valve which was a component of the computer controlled ABPR (Thar Technologies Inc., Pittsburgh, PA, USA).

All drying experiments (each involving four pieces of gel) were carried out in triplicate.

3.3.3 High pressure windowed pressure vessel

In addition to drying experiments, a high pressure vessel with a view cell was used to observe the behaviour of the gel pieces at supercritical conditions, and during depressurisation. A schematic of the experimental apparatus is shown in Figure 3.1.



Key:

OB = oil bath	V1 = ball valve
WV = windowed pressure vessel	V2 = micrometering valve
PUMP1 = HiP pressure generator	NRV1 = non-return valve

Figure 3.1 Schematic representation of the experimental set up used to view gels during exposure to supercritical conditions and on subsequent depressurisation.

This rig consisted of a high pressure vessel (60 ml) with a view cell, through which a light and camera was set up enabling images to be captured throughout supercritical processing. A HiP pressure generator (Model number: 62-6-10, High Pressure Equipment Company, Erie, PA, USA) was used to achieve the desired pressure. An enclosed circulating oil bath (OB) surrounded the vessel and was used to obtain the desired temperature. The temperature and pressure were measured within the vessel using a thermocouple and a pressure gauge, respectively. For experiments using $\text{scCO}_2(\text{EtOH})$, EtOH was added to the windowed pressure vessel (WV) prior to pressurisation, in quantities required to achieve a 6 mol% concentration (at 20 MPa and 50°C). Gel pieces were mounted in the centre of the vessel, to ensure the EtOH was only in contact with the gel when part of a binary mixture with scCO_2 . This supercritical equipment did not allow flow rate through the pressure vessel. Gels were monitored through the view cell, at various temperatures and pressures, and also during depressurisation.

Depressurisation was controlled by opening and closing of a micrometering valve (V2) at the vessel's exit.

3.3.4 Method for air drying of gel pieces

Gels were placed in an oven, at 50°C and upon reaching NMCs below 0.05 (after ~3600 seconds drying time) the gels were removed for x-ray micro-CT analysis, texture analysis and rehydration studies. All experiments were carried out in triplicate.

3.3.5 Method for freeze drying of gel pieces

Freeze drying experiments were carried out using a VirTis (New York, US) freeze dryer. The samples were frozen to -55°C for 14400 seconds, and then dried for 30000 seconds at a temperature of 0°C and a chamber pressure of 1×10^{-4} MPa (1000 mTorr). Final sample temperature was 25°C. All samples were dried to NMCs below 0.01 and experiments were carried out in triplicate.

3.3.6 X-ray micro-computed tomography for the analysis of gel microstructure

X-ray micro-CT was used to study the microstructure of the dried gel pieces immediately after drying. Details of this technique are outlined in section 2.3.6.

Quantitative 3-D analysis was additionally carried out on gel pieces, using the CTan (version 1.7.0.0) analysis software. The whole of each sample was included in the analysis and was therefore referred to as the 'volume of interest' (VOI). Global thresholding on the VOI was carried out ('binarisation'), in order to segregate the solid and the open structure of the sample. To ensure that every detail of the surface was included in the subsequent calculations, the region of interest (ROI) was selected to be slightly larger than the surface of the sample and the 'ROI shrink-wrap' feature was used in order to shrink it to the boundary of the binarised object.

The percentage object volume was measured which is reported here as percentage solid object. The percentage open space could then be calculated as percentage total object (100%) minus percentage solid object. This is taken here as a measure of the voidage of the gel.

3.3.7 Method for rehydration of gel pieces

Dehydrated gel pieces were immersed in a glass beaker containing 50 ml distilled water, kept at room temperature ($21 \pm 2^\circ\text{C}$). The samples were removed at regular time intervals, blotted on tissue paper to remove excess water, and their mass determined until the EMC had been reached. Three results were obtained from each experiment (from three individual gel samples) and this was carried out in triplicate, with samples derived from three independent experiments. Results are reported in terms of NMC (equation 2.6).

3.3.8 A texture analysis method to measure the hardness of gel pieces

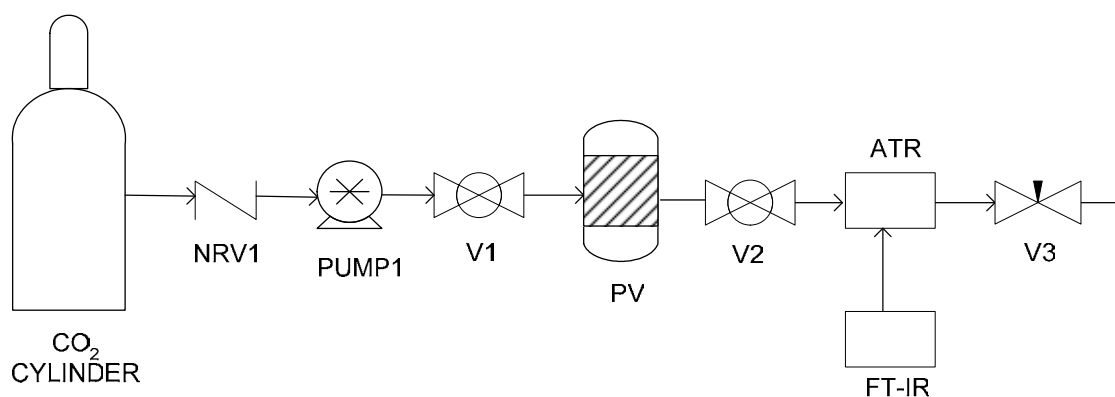
A texture analyser (TA-XT2i, Stable Micro System, Godalming, UK) was used as outlined in section 2.3.10. Six results were obtained from each experiment (two results from three individual gel samples) and this entire procedure was carried out in triplicate, with samples derived from three independent experiments. The mean maximum force (N) was recorded, and the standard error of the mean calculated for each drying condition.

Supercritically dried samples were dried further using the freeze drying method discussed in section 3.3.5, to the same, negligible moisture content as the freeze dried samples (<0.01 NMC), before texture analysis was carried out. This was carried out to ensure any texture differences observed were due to the drying technique and not the moisture content. X-ray micro-CT analysis was carried out before and after this additional step to confirm no visible changes in microstructure had occurred (Table 3.1). Any textural differences between the samples could then be associated with the initial drying method used to remove the bulk of the water. Texture analysis could not be carried out on air dried samples, as extreme shrinkage resulted in a too low gel volume for puncture and compression.

3.3.9 Fourier transform infrared analysis of gel pieces in the presence of supercritical carbon dioxide

ATR-IR spectroscopy with FT-IR transmission was used to study the interactions of the supercritical solvent with the agar gel, through *in situ*, real time monitoring. FT-IR spectra of dried gel pieces, in the presence of scCO_2 , were recorded using an FT-IR-

6300, Jasco, Great Dunmow, UK), equipped with a KBr beam splitter and KRS-5 lense. A golden gate ATR optical unit (golden gateTM, part number: 10586, Specac Ltd., Orpington, UK) with a high pressure attachment (SCF golden gateTM ATR top plate, part number: 10585, Specac Ltd., Orpington, UK) were used in conjunction with the spectrometer. A schematic of the experimental set up is shown in Figure 3.2.



Key:

NRV1 = non-return valve	V1, V2 = ball valves
PV = pressure vessel	V2 = micrometering valve
PUMP1 = HiP pressure generator	ATR = ATR golden gate (with high pressure attachment)
FT-IR = FT-IR spectrometer	

Figure 3.2 Schematic representation of the experimental set up used for FT-IR analysis of agar gels, during exposure to $scCO_2$ and $scCO_{2(EtOH)}$.

The analysis area of the top plate consisted of an ATR-IR diamond element mounted in a tungsten carbide plate, giving one reflection at an angle of 45° . The SCF top plate had an integrated heater which was controlled by a 4000 seriesTM temperature controller (Specac Ltd., Orpington, UK) and allowed for temperatures up to $300^\circ C$. Pressures of up to 41.4 MPa could be reached in the cell which had a volume of 28 μl .

The sample was mounted in the top plate, upon the diamond element, so that good contact was made between the sample and the surface of the crystal. Compressible graphite gaskets were positioned between the cell and the tungsten carbide plate, to ensure good contact was made,

and there was no CO₂ leakage. The temperature was then raised using the heating plate and CO₂ was delivered from a CO₂ cylinder at 5 MPa, before manually compressing to the desired pressure using a HiP pressure generator (Model number: 62-6-10, High Pressure Equipment Company, Erie, PA, USA). For experiments requiring EtOH as a co-solvent, a pressure vessel (PV) was employed in between the CO₂ pump and the top plate. The desired quantity of EtOH was deposited in the vessel, prior to pressurisation, which upon pressurisation (to 20 MPa and 50°C), produced a 6 mol% concentration of EtOH in scCO₂. This was passed over the gel sample, held in the top plate, to mimic the exposure of the gel to scCO₂(EtOH) in the same way that gels were exposed to scCO₂(EtOH) during drying experiments. This enabled interactions between the gel and SCF to be monitored. The scanning range used was 500-4000 cm⁻¹ wavenumbers, with 64 scans obtained for each sample.

3.4 Results and discussion

3.4.1 Drying protocols: drying times and normalised moisture contents achieved

Gels were typically dried to <0.1 NMC, since low moisture content is important for preservation of foods and components of food. However, water activity is thought to be more important than the total amount of water present, for the stability and quality of the food (Maltini *et al.* 2003). The water activity was not measured here, but low moisture contents were achieved through drying, in an effort to achieve product stabilisation and preservation. However, due to limitations of the drying techniques (discussed in the subsections below), some variability was seen in the final dried moisture content of samples. This is expected to have an influence on the quality parameters of the dried product, such as microstructure and rehydration. The implications of the final NMC of dried samples on material properties is considered in later sections and has also been discussed in relation to drying of carrot pieces in sections 2.3.3 and 2.4.2.2.

Air drying

Gels were air dried in an oven and upon reaching <0.05 NMC the gels were removed. During air drying, moisture content of samples could be monitored and measured at any point during the

drying process. However, there was some variability over the batch and estimated times were used therefore some variability in moisture content still existed. During air drying, gels at low moisture contents are dried in the 'falling rate' period therefore at lower moisture contents the rate of drying is slower. To achieve very low moisture contents, comparable with those experienced in freeze drying, samples would have to be dried for a very long time and this also affects the product quality, since extensive shrinkage occurs during air drying. Therefore NMCs below 0.01 were not achieved using this method.

Freeze drying

Moisture contents in the case of freeze drying were fairly consistent over the batch and were generally dried to NMCs below 0.01. Freeze drying was capable of drying down to very low moisture contents, and unlike air drying the moisture content could only be determined after drying. Small amounts of moisture remaining in freeze dried product has been shown to cause collapse (Levi and Karel 1995) therefore in the case of freeze drying, samples were dried overnight to lower moisture contents than air or supercritically dried gel pieces.

Supercritical drying

Similarly to freeze drying, moisture contents of supercritically dried gels could only be determined following depressurisation, at the end of the experiment. Due to the nature of supercritical experiments, moisture contents were sometimes variable between experiments and there was also some variability between samples from the same experiment (seen for both $\text{scCO}_2(\text{pure})$ and $\text{scCO}_2(\text{EtOH})$). Therefore, estimated drying times were selected for supercritical experiments, to dry gels down to similar NMCs (<0.1). Given more time, gels would have been dried further, to lower and therefore more comparable (to each other and also to that of freeze dried samples) moisture contents.

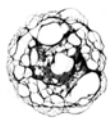
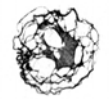
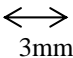
NMCs of supercritically dried gels were generally between 0.02 and 0.09 NMC (where 1 equals 100% of the total original moisture content).

As seen in chapter 2 (section 2.4.1.1), the addition of co-solvent increased the rate of drying with scCO_2 . This was supported here by observation of the drying times required to reach

specific moisture contents: low NMCs (<0.1) could be reached within 10800 seconds of drying with $\text{scCO}_2(\text{pure})$, or within 7800 seconds when using $\text{scCO}_2(\text{EtOH})$ (a flow rate of 3 l/minutes was used for both experiments). Drying times could be extended by one hour to dry the gels further (<0.04 NMC) and this prevented overnight collapse which was often seen in some of the gels that were dried between 0.04 and 0.1 NMC. However, for the purpose of these experiments NMCs between 0.04 and 0.1 were agreed to be an acceptably low level for preservation, and microstructural analysis was carried out before any collapse occurred. X-ray micro-CT analysis took place in a warm chamber ($\sim 40^\circ\text{C}$) which was seen to prevent gel collapse in the long term, thought to be due to the removal of the last traces of moisture in the sample during analysis. This observation has been discussed in more detail in section 2.4.2.2.

As mentioned in the methods section here (section 3.3.8), prior to texture analysis of supercritically dried samples, gel pieces were subjected to freeze drying to remove any last traces of moisture. This enabled texture comparison of gels predominantly dried using scCO_2 or freeze drying methods, and texture differences would therefore relate to the drying technique and not the moisture content of the dried sample. However, in order to confirm that this final drying step did not have an effect on the gel microstructure, gels that had been dried using $\text{scCO}_2(\text{EtOH})$ were observed in the x-ray micro-CT, immediately after drying, and also following a further freeze drying step to remove the last traces of moisture (Table 3.1). The supercritically dried gel, that had been further freeze dried (Table 3.1 (b)), looked slightly smaller than the sample that had been immediately examined by x-ray micro-CT (Table 3.1 (a)), suggesting that some collapse had occurred before the freeze drying step (owing to small amounts of water present in the sample). However, it is argued that the similarity in microstructure for the two gels provide evidence that removal of the final traces of moisture, in either the x-ray chamber or freeze drier was unlikely to affect the structure, since both structures looked the same.

Table 3.1 X-ray micro-CT, 2-D images of gels dried using $\text{scCO}_2(\text{EtOH})$, which were dried further to remove the final traces of moisture: (a) using the warm x-ray micro-CT chamber, and (b) via freeze drying.

	2-D x-ray image	Initial drying method	Method to remove final traces of moisture
(a)		$\text{ScCO}_2(\text{EtOH})$ dried	X-ray micro-CT chamber ($\sim 40^\circ\text{C}$)
(b)		$\text{ScCO}_2(\text{EtOH})$ dried	Freeze drying (0°C)
			

3.4.2 Visual appearance of dried gels and the effect of sucrose addition

Appearance and structure

The visual appearance of air, freeze, and supercritically dried gels were compared (Figure 3.3). For supercritical drying, the addition of 10% sucrose to the agar gel significantly improved the appearance and dried structure of the gel, resulting in less volumetric shrinkage than the control gel (0% sucrose). Gels dried using $\text{scCO}_2(\text{EtOH})$ (Figure 3.3 (d)) had a similar volume to those dried without co-solvent (Figure 3.3 (c)), although bubbles at the gel surface were visible for samples dried using co-solvent (Figure 3.3 (d)), suggesting some structural differences existed which are discussed later in section 3.4.3. Freeze dried samples had excellent volume retention at both 0% (Figure 3.3 (e)) and 10% sucrose concentration (Figure 3.3 (f)). In contrast, air dried samples exhibited extensive shrinkage at both 0% (Figure 3.3 (g)) and 10% (Figure 3.3 (h)) sucrose concentrations. Supercritically dried samples displayed a volume in between that seen for air and freeze dried: those containing 0% sucrose behaved like air dried gels, exhibiting extensive shrinkage (Figure 3.3 (b)), while those containing 10% sucrose behaved more freeze dried gels, maintaining considerable volume during drying (Figure 3.3 (c)).

It is also worth noting that the total starting solid mass was retained throughout the supercritical experiments (for both $\text{scCO}_2(\text{pure})$ and $\text{scCO}_2(\text{EtOH})$), providing evidence that neither sucrose or agar was extracted in the supercritical drying process.

Mechanisms

Freeze dried samples were able to maintain their original volume, avoiding shrinkage, without any sucrose addition (Figure 3.3 (e)). Therefore, sucrose addition to freeze dried gels does not appear to have a favourable effect on the visible gel structure, and thus any interactions that may occur between the gel and the sucrose do not have a significant effect on the dried structure. The freeze drying mechanism, by which gel collapse is avoided, is thought to be due to the gel network being frozen until it is dry, preventing helix aggregation and therefore gel collapse. Although sucrose addition did not affect the visual appearance and dried volume of freeze dried gels, its effect on gel rehydration and texture is discussed in sections 3.4.6 and 3.4.7, respectively.

In the case of supercritical drying, sucrose does favorably affect the gel structure during drying, enabling considerably more volume to be retained in those gels containing sucrose (Figure 3.3 (c) and (d)). The sucrose may act as an inert filler, retaining some volume in the gel during drying, and therefore influencing the final dried microstructure. However, interactions between polymers, water and sucrose have been reported in similar systems and Nussinovitch *et al.* (2000) have provided evidence that sucrose does not purely act as an inert filler in freeze dried sucrose-infused gels: increases in density of the gel could not be predicted by corresponding stoichiometric relations of the amount of sucrose added. Additionally, interactions of sucrose with agarose and agar gels have been reported in the literature by several authors (Normand *et al.* 2003; Nussinovitch *et al.* 2000; Pongsawatmanit *et al.* 1999). Interactions observed through sucrose addition to gels include: a reduction in the extent of helix aggregation, increased cross linking of the polymer chains and increased elasticity (the theory of which is discussed in section 1.3.5.3). These interactions are therefore expected to contribute to a more open, elastic gel structure, explaining the ability of the sucrose to prevent gel shrinkage and collapse during supercritical drying, while still allowing the scCO₂ to move into and out of the structure. Therefore, in contrast to freeze drying (where gels are frozen and therefore held rigid during drying), the gel network is thought to be mobile and elastic during supercritical drying in a SCF environment. This is discussed further in section 3.4.4, and the potential interaction of the agar gel with the scCO₂ is also speculated.

Air dried gels show some improvement in structure with the addition of sucrose, prior to gel drying (Figure 3.3 (h)), suggesting similar interactions to those discussed for supercritically dried gels may be occurring. However, sucrose addition was most favourable, for structure improvement of agar gels dried with scCO_2 .

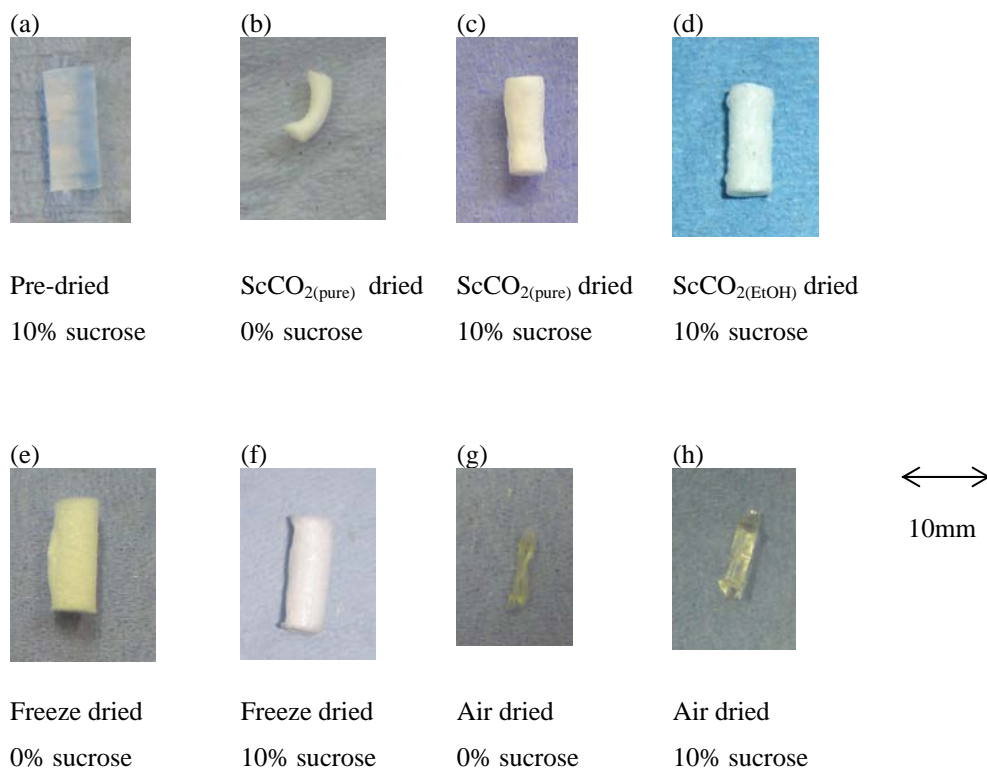


Figure 3.3 Photographs comparing the visual appearance of: (a) 2% agar gels before drying; and ((b)-(h)) 2% agar gels dried using different techniques. Supercritical drying was carried out at 50°C, 20 MPa, 1 l/minute flow rate and 0.4 MPa/minute depressurisation rate. Air drying was carried out at 50°C. Freeze drying was carried out at 0°C for 30000 seconds, following initial freezing at -55°C for 14400 seconds. Note that colour differences are due to variation in the lighting, at the time of photographing are not related to differences between the gels.

3.4.3 X-ray micro-computed tomography analysis

X-ray micro-CT allows viewing of the internal structure, following drying. It also gives an indication of the degree of shrinkage of the gel, density of the gel, and a quantitative measure of

gel voidage (percentage open space). Comparison of the internal gel structure after drying by air, freeze and supercritical methods are shown in Table 3.2, supporting visual, photographic information seen in Figure 3.3. Shadow radiograph images for each sample were initially collected and then reconstruction of this data allowed 2-D horizontal slices through the cylindrical sample to be viewed.

Qualitative observations

Air dried gels were dense, with a shrivelled and low porous structure (Table 3.2 (d)). Freeze dried gels were of a low density and kept their circularity well throughout the drying process, at both 0% (Table 3.2 (e)) and 10% (Table 3.2 (f)) sucrose concentrations. Supercritically dried gels lay somewhere between air and freeze dried gels, in terms of both size and density when 10% sucrose was present (Table 3.2 (b)). However, when no sucrose was present during supercritical drying, the gels shrank and behaved in a similar way to air dried gels (Table 3.2 (a)). These observations were the same as those that had been made from visual analysis of the external volume of the gel pieces, discussed in section 3.4.2. However, more importantly, x-ray micro-CT allowed viewing of the internal structure and any structural entities that may be present. For example, addition of a co-solvent during supercritical drying had the effect of adding more voids into the structure (Table 3.2 (c)), when compared with $\text{scCO}_{2(\text{pure})}$ dried gels (Table 3.2 (b)). The differences between using $\text{scCO}_{2(\text{pure})}$ and $\text{scCO}_{2(\text{EtOH})}$ for drying are discussed in more detail in section 3.4.4, and may provide an explanation for this observation.

Quantitative analysis

Quantitative analysis of x-ray micro-CT images is also possible, allowing values to be obtained for percentage open space (voidage) and percentage solid object, for each dried gel piece. Table 3.2 shows the percentage open space (voidage) of the agar gels dried via different drying methods.

Freeze dried samples had the biggest percentage open space (76%), while in contrast air dried had a negligible percentage open space (4%). Percentage open space values for supercritically dried gels lay between those for air and freeze dried samples. These results could be linked to the amount of shrinkage that was seen in these samples through visual observations (qualitative



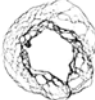



analysis) of the x-ray micro-CT images. For example, freeze dried gels maintained the largest volume during drying and also resulted in the highest percent open space value (76%), while air dried gels lost the largest volume and also exhibited the smallest open space value (4%). Supercritical gels were in between air and freeze dried gels for both shrinkage and open space (48%) measurements.

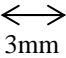
Interestingly, gels dried using $\text{scCO}_2(\text{EtOH})$ had a very similar open space to that of freeze dried (68%), and a higher percentage open space than those dried using $\text{scCO}_2(\text{pure})$ (48%). However, the only statistically different results were those of air and freeze dried samples, calculated at a 0.05 significance level using a Kruskal-Wallis and Nemenyis *post-hoc* non-parametric multiple comparison tests. The previous observation, of a ‘bubbled’ structure in the gels dried using $\text{scCO}_2(\text{EtOH})$, explains the higher percentage open space observed, compared with those samples that were dried with $\text{scCO}_2(\text{pure})$. Possible reasons for these differences seen with the addition of EtOH as a co-solvent are discussed in section 3.4.4.

All of the dried gel structures containing 0% sucrose, except those that were freeze dried, had a negligible percentage open space. Again, this correlated with the degree of shrinkage visually observed in the samples containing 0% sucrose.

Measurements of percentage open space, reported here, are discussed in relation to rehydration properties, in section 3.4.6.

Table 3.2 X-ray micro-CT 2-D images of air, freeze and supercritically dried gels. The flow rate and depressurisation rate employed for supercritical drying were 1 l/minute flow rate and 0.4 MPa/minute depressurisation, respectively. Percentage open space values represent the overall mean from at least three independent experiments \pm one standard deviation of the mean (with the exception of sample (a) where only one result was collected).

	2-D x-ray image	Drying method	Percentage sucrose (%)	Percentage open space (%)
(a)		ScCO ₂ (pure) dried	0	7
(b)		ScCO ₂ (pure) dried	10	48 \pm 7
(c)		ScCO ₂ (EtOH) dried	10	68 \pm 3
(d)		Air dried	10	4 \pm 0.1
(e)		Freeze dried	0	79 \pm 6
(f)		Freeze dried	10	76 \pm 6



3mm

3.4.4 Effect of supercritical process conditions on gel structure

Flow rate has already been investigated in chapter 2 (section 2.4.1.6) in relation to drying rate: an increase in flow rate was shown to increase the rate of drying. However, here, the effect of the processing conditions on gel microstructure was the focus of interest.

Changes in processing conditions, namely flow rate and depressurisation rate, were carried out during supercritical drying of gels. It was hypothesised that changing these variables would manipulate and influence the dried gel structure. For example, different depressurisation rates have been reported to affect foaming and final pore size of plasticized or melted polymers, due to the ability of the depressurisation rate to control the nucleation and growth of pores, during depressurisation (Liang and Wang 2000; Xu *et al.* 2007; Tsivintzelis *et al.* 2007a). Plasticisation of polymers is discussed later in this section.

However, the potential also exists for damage of the gels structure, especially through large increases in depressurisation rate. For example, Takishima *et al.* (1997) reported that damage of aerogels could be caused in all stages of the supercritical drying process and recommended that quick changes in composition, pressure and temperature should be avoided, especially for large aerogels.


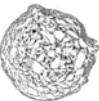
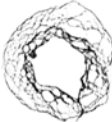
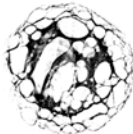
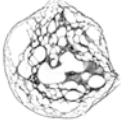
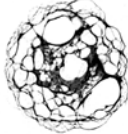
Changing the flow rate (between 1 l/minute and 3 l/minute) and the depressurisation rate (between 0.4 MPa/minute and 1.6 MPa/minute) had no significant effect on the resultant microstructure produced, when $\text{scCO}_{2(\text{pure})}$ was used as the solvent (Table 3.3 (a) and (b)). This visual observation was supported quantitatively by measuring the percentage open space at the different flow rate and depressurisation rates, from the x-ray micro-CT images. No significant differences were measured, suggesting the structure is not mobile and is not affected by flow rate or depressurisation rate when $\text{scCO}_{2(\text{pure})}$ is used for drying. However, this may be favourable in terms of drying kinetics, since the rate of drying could be increased, by increasing flow rate (Figure 2.15), without influencing the dried structure.

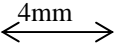
It should also be remembered, that despite no structural differences being observed at these conditions, this may not be the case if larger flow rates and depressurisation rates were investigated. Also, any ‘bubbling’, or other effects of depressurisation and/or flow rate on the structure may not be permanent structural changes, which therefore may not have been present when x-ray micro-CT analysis was carried out some time after depressurisation. For example, a higher depressurisation rate may cause larger voids/bubbles to be formed which collapse immediately after depressurisation, meaning they would not be captured in the x-ray micro-CT image.

Changing the flow rate and depressurisation rate during drying with $\text{scCO}_2(\text{EtOH})$ also did not cause any visible, or statistically significant differences when examined using quantitative x-ray analysis (Table 3.3 (c)-(f)). However, the addition of EtOH as a co-solvent was seen here to radically change the resultant gel structure (Table 3.3 (c)-(f)), when compared with gels dried using $\text{scCO}_2(\text{pure})$ (Table 3.3 (a)-(b)), resulting in a more open ‘bubbled’ structure. This can also be seen quantitatively in Table 3.3 through the measured percentage open space values (and was previously observed in section 3.4.3). Statistically significant open space values were found between samples dried with $\text{scCO}_2(\text{pure})$ (Table 3.3 (b)) and $\text{scCO}_2(\text{EtOH})$ (Table 3.3 (c)), calculated at a 0.05 significance level using a Kruskal-Wallis and Nemenyis *post-hoc* non-parametric multiple comparison tests.

Interestingly, similar observations of the effect of $\text{scCO}_2(\text{EtOH})$ mixtures on polymer structures have been reported in the literature: $\text{scCO}_2(\text{EtOH})$ mixtures were found to act as a much more efficient blowing agent than $\text{scCO}_2(\text{pure})$ for foaming polymers (Tsivintzelis *et al.* 2007b). The report however, does not give a clear conclusion as to the reason for increased foaming efficiency when EtOH is present.

Table 3.3 X-ray micro-CT 2-D images of supercritically dried gels (all containing 10% sucrose), dried using various processing conditions. Percentage open space values represent the overall mean from at least three independent experiments \pm one standard deviation of the mean (with the exception of sample (e) where only one result was collected).

	2-D x-ray image	Supercritical solvent	CO ₂ Flow rate	Depressurisation rate	Percentage open space
(a)		ScCO ₂ (pure)	1	4	48 \pm 7
(b)		ScCO ₂ (pure)	3	16	42 \pm 12
(c)		ScCO ₂ (EtOH)	1	4	68 \pm 3
(d)		ScCO ₂ (EtOH)	3	16	61 \pm 1
(e)		ScCO ₂ (EtOH)	1	16	60
(f)		ScCO ₂ (EtOH)	3	4	62 \pm 5



There are several possible explanations why differences were seen in the gel structure when $\text{scCO}_2(\text{EtOH})$ was used for drying, compared with $\text{scCO}_2(\text{pure})$.

Plasticisation of the gel may occur, due to sorption of CO_2 into the polymer which is known to induce swelling and plasticisation. Plasticisation is evidenced by a reduction in the T_g or T_m of the polymer. A reduction in the viscosity is also observed due to this plasticisation effect which results from a transition of the polymer from a glassy to a rubbery state, where polymer chains can move more freely. CO_2 exhibits significant specific interactions with many polymers mainly due to its large quadrupole moment and also the ability of CO_2 to act as a Lewis acid or base.

Co-solvent addition has been reported to enhance the plasticisation properties of scCO_2 for polymers and consequently the mobility of the polymer chains (Gendron *et al.* 2006; Hirogaki *et al.* 2005; Tsivintzelis *et al.* 2007b). The addition of a small amount of organic solvent, as a co-solvent, increases the affinity between the scCO_2 and the polymer, which may increase the solubility of the CO_2 in the polymer therefore expecting to also increase the polymer-plasticising capacity of scCO_2 .

A reduction in the T_m (and therefore melting of the polymer), or swelling may be an indication of plasticisation of the polymer. The agar gels were observed in a windowed vessel (a high pressure vessel which contained a view cell), in $\text{scCO}_2(\text{pure})$ or $\text{scCO}_2(\text{EtOH})$ mixtures, at 20 MPa, and temperatures up to 100°C , to observe if swelling or melting of the polymer was taking place under these conditions. Shrinkage of the gels was observed, due to water loss, but there was no evidence of swelling or melting, which would indicate that plasticisation is taking place (Table 3.4).

It was interesting to note that the gel began as a transparent cylindrical sample, which following some water loss became opaque. This may also be observed in the photographic images displayed in Figure 3.3. A small pressure drop, which occurred during processing with $\text{scCO}_2(\text{EtOH})$ (Table 3.4 (ii)), also caused the transparent gel to appear cloudy, this was due to the formation of bubbles in the gel, due to gas expansion, which were later seen to disperse, leaving a transparent gel once again. This phenomenon may contribute to the formation of the ‘bubbled’ structure seen during drying with $\text{scCO}_2(\text{EtOH})$. It is likely that this structure is formed during

depressurisation, and the EtOH present makes the gel structure more susceptible to the 'bubbling' effect, since the effect is not seen to the same extent in the gels dried with $\text{scCO}_2(\text{pure})$.

In addition to the experiments observed in the windowed vessel, differential scanning calorimetry (DSC) experiments could also not clearly confirm a melting point, below 100°C , for wet gels containing 10% sucrose, despite agar gel having a reported melting point of approximately 85°C . This may be due to an increase in the melting point of the gel, with sucrose addition, which has been reported by Normand *et al.* (2003). The melting point increase is thought to be due to an increase in cross linkages, created by hydrogen bonds, between hydroxyl groups in sucrose and agar and therefore would explain why a melting point is not seen below 100°C .

Therefore, it is assumed that the addition of $\text{scCO}_2(\text{EtOH})$ solvent to the gel does not cause a melting point depression below the experimental drying conditions investigated here (20 MPa, 50°C), and overall there were no visual signs of plasticisation, at these conditions.

The behaviour of polymers in the presence of scCO_2 depends on many factors: the polymers physical properties of the polymer (T_g , crystallinity, and crosslinking); the nature of the interactions between the SCF and the polymer; the experimental temperature and pressure; and also the chemical nature of the polymer. Agar has a rigid structure maintained by cross links or 'junction zones', involving non-covalent binding of chains in ordered conformations (Arnott *et al.* 1974; Lahaye and Rochas 1991). This inflexible arrangement may account for the inability of scCO_2 to permeate between the polymer chains and plasticise the agar. Water molecules are expected to participate in a hydrogen bonding system in the agarose cavity which contributes to the stability of the double helix. The helices are also believed to be extensively aggregated, with the gel framework composed of many side-by-side rigid chains of large cross-section, compared with a single polysaccharide chain. A suggested schematic representation of an agarose gel network compared with a random chained polymer (Figure 3.4) also gives a clearer understanding of why a polymer with random cross-linking may plasticise more readily than agarose, the gelling fraction of agar.

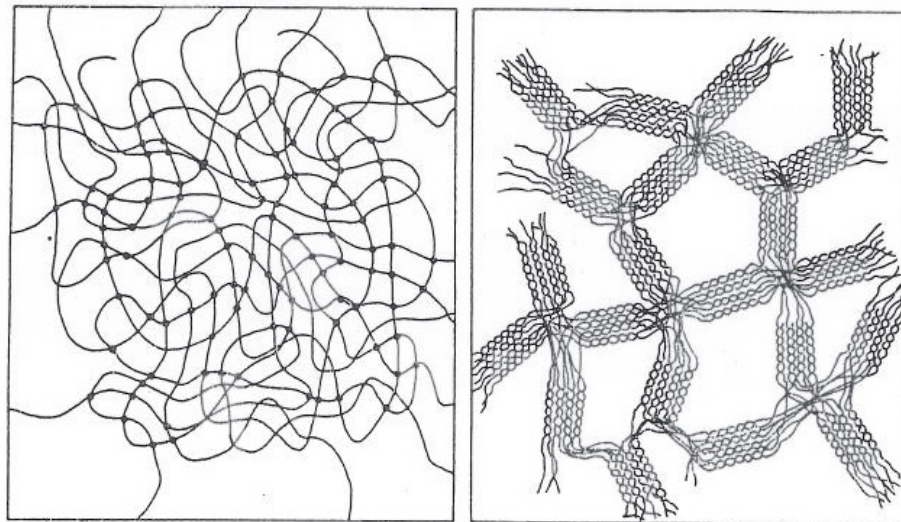


Figure 3.4 A schematic representation of the agarose gel network (right), in comparison with a network formed from random polymer chains (left) at a similar polymer concentration (Arnott, Fulmer and Scott (1974)). Note that the aggregates in agarose gel may actually contain 10 to 10^4 helices rather than the smaller numbers shown here.

There are several possible explanations, other than plasticisation, for the difference in microstructure produced by using $\text{scCO}_2(\text{pure})$ and $\text{scCO}_2(\text{EtOH})$ and these are discussed below.

The dissolution of the polymer in the SCF may occur, facilitated by the addition of EtOH as a co-solvent. Low molecular weight polystyrene dissolution into $\text{scCO}_2(\text{EtOH})$ mixtures has been observed, which was not seen in $\text{scCO}_2(\text{pure})$ (Lalanne *et al.* 2001). However, there is no evidence to suggest that dissolution of agar occurs here, as the same amount of solid material is present at the start and end of the drying process. Additionally, agar has a high molecular weight and is therefore unlikely to dissolve in the scCO_2 , in the same way that low molecular weight polystyrene might.

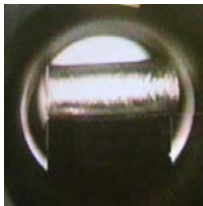







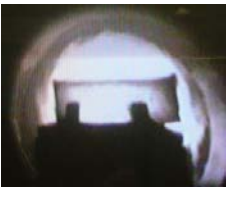
Adsorption or partitioning of the co-solvent in the polymer may also occur which could alter the chemical nature of the polymer. Specific interactions such as hydrogen bonding of the co-solvent, which can act as a proton donor to basic sites on the polymer, can contribute to adsorption of the co-solvent. These factors were discussed by Kazarian *et al.* (1998) in relation to the degree of partitioning of co-solvents into cross-linked polymers. It is likely that adsorption or interaction of the EtOH with the agar may be occurring here, altering bonding, and causing

structural changes to occur during the experiment (which then don't change under ambient conditions/upon EtOH removal). Certainly, the EtOH may compete for hydrogen bonding sites on the agar, which would otherwise hold together the rigid agar structure, and therefore could cause some structural disruption.

The solubility of agar in aqueous EtOH solutions has been previously discussed by Lahaye and Rochas (1991), in terms of the ability of the solvent to disrupt the ordered conformation of agar, which also depends on the precise chemical structure of the agar. Moreover, this review confirms that interactions between EtOH and agar can occur, which could then theoretically disrupt the ordered structure of agar.

These hypotheses were investigated further using FT-IR analysis (section 3.4.5).

Table 3.4 Images taken inside a pressure vessel of wet agar gel (containing 10% sucrose), exposed to: (i) $\text{scCO}_2(\text{pure})$; and (ii) $\text{scCO}_2(\text{EtOH})$. Images were captured before pressurisation, at maintained pressure, and after depressurisation. Note, that the cloudy appearance of the gel during the co-solvent experiment (ii) is due to a small pressure drop which caused bubbles to appear in the gel.

	0.1 MPa, 50°C	20 MPa, 50°C	20 MPa, 70°C	20 MPa, 100°C	After depressurisation
(i)					
(ii)					No photo available

3.4.5 Fourier transform infrared spectroscopy to investigate molecular interactions

FT-IR has been widely used in the past for monitoring polymer-CO₂ interactions by evaluation of specific bending modes, which may infer polymer plasticisation. This has been discussed previously in section 1.2.3.1.

Here, FT-IR has been used to investigate the interaction of scCO₂ with agar gel in order to study the interactions that occur during gel drying and which may account for the different structures achieved when drying with scCO₂ versus scCO₂(EtOH). Experiments included:

- The effect of pressure on the band intensity of agar.
- Study of CO₂ and EtOH alone (without agar present) to determine if any interactions involving the two solvents were present.
- The effect of scCO₂(pure) exposure to agar (both dry and partially wet) gels.
- The effect of scCO₂(EtOH) exposure to agar (both dry and partially wet) gels
- Study of agar and EtOH alone (without CO₂ present) to determine if any interactions were occurring between them.

The results of these experiments are summarised in Table 3.5 and discussed in more detail in the text. A hypothesised mechanism by which interactions may occur has been outlined at the end of this section.

Table 3.5 A table summarising the results of FT-IR experiments. Further discussion can be found in the text.

Study	Interaction Present?	Evidence of interaction
Agar with scCO ₂ (effect of pressure)	N/A	Figure 3.5 - an increase in the band intensity with increasing pressure was observed.
ScCO ₂ with EtOH	Yes – between CO ₂ and EtOH.	Literature – a doublet was seen for the CO ₂ bending absorption band, indicating an interaction between the CO ₂ and EtOH (Cabaço <i>et al.</i> 2005).
Agar with scCO ₂	Yes – between agar and CO ₂ .	Figure 3.8 – the CO ₂ bending and stretching modes changed from singlets to doublets in the presence of agar.
Agar with scCO ₂ (EtOH)	Yes – proposed to be between the EtOH and the CO ₂ .	Figure 3.9 – the CO ₂ stretching mode changed from a doublet to a singlet upon EtOH addition (explained in Figure 3.11).
Agar with EtOH	None observed.	Figure 3.10 – no changes in the absorption bands when EtOH was or was not present.

In the first study the effect of pressure increase on the IR spectrum was observed. A pressure increase alone (while using the same drying solvent and keeping other conditions constant) was seen to cause an increase in the intensity of the absorption bands but the peaks retained the same shape and the same band centre. This is illustrated in Figure 3.5 (where %T on the y axis is the percentage transmittance). The increase in band intensity is purely an effect of increased medium density (CO₂) with increasing pressure and has previously been observed by Lalanne *et al.* (2001).

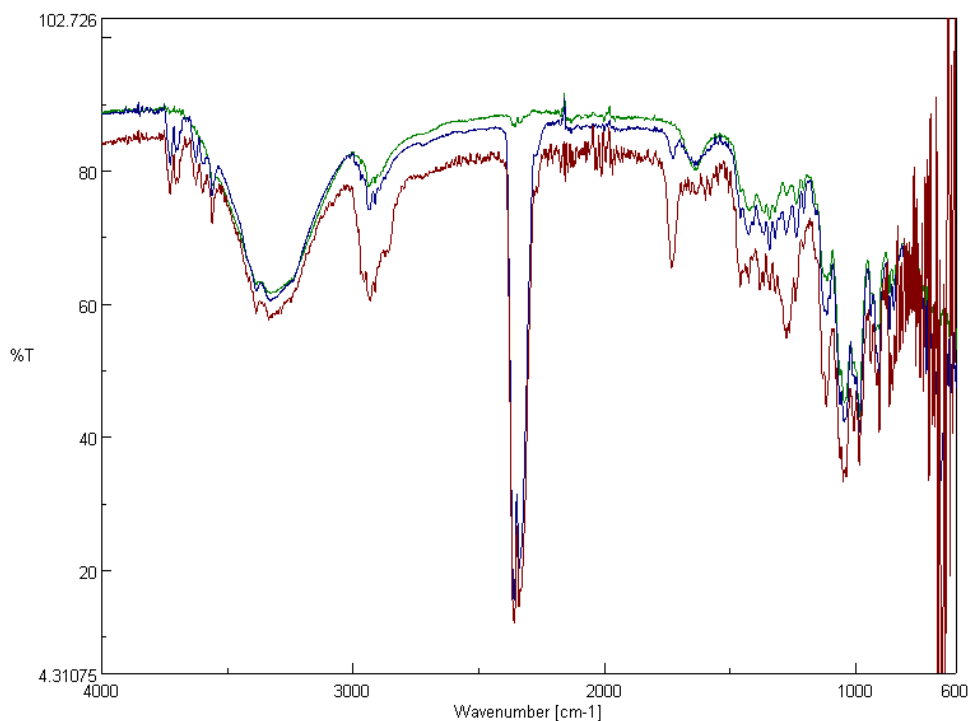


Figure 3.5 FT-IR spectra of dried 2% agar gel, containing 10% sucrose, exposed to $\text{scCO}_2(\text{pure})$ at 0.1 MPa/50°C (green line), 12 MPa/50°C (blue line), and 16.5 MPa/50°C (red line).

To study if an interaction between CO_2 and EtOH was present, scCO_2 was first observed alone, followed by scCO_2 in the presence of EtOH. The IR active bending and stretching modes of CO_2 were observed and results showed that scCO_2 alone (with no gel present) had a single peak at 660 cm^{-1} and a single peak at 2337 cm^{-1} , corresponding to the CO_2 , bending mode (ν_2) and the asymmetric stretching (ν_3) mode, respectively. $\text{ScCO}_2(\text{EtOH})$ was then observed using FT-IR. Interestingly, the EtOH was not visible in these quantities (6 mol%) in the IR spectrum, and the spectrum was identical to that for CO_2 alone (Figure 3.6). However, upon depressurisation of the same mixture, the EtOH was observed in the spectrum (Figure 3.7).

The bands that were present during depressurisation were not indicative of an interaction occurring between CO_2 and EtOH since the bands remained in the same place as when CO_2 and EtOH were observed separately. Additionally, under supercritical conditions, no changes in the CO_2 peaks were observed upon EtOH addition which may also infer there is no interaction between CO_2 and EtOH. However, CO_2 is known to interact with EtOH and this interaction has been proven using Raman spectroscopy by Cabaço *et al.* (2005). These authors report that an

EDA (electron donor-acceptor) 1:1 complex in which the carbon atom of CO_2 is the electron acceptor centre and the oxygen atom of the hydroxyl (EtOH) is the electron donor centre is formed. This was reported to result in two, in-plane and out-of-plane, bending modes being observed as seen with polymer- CO_2 interactions. The interactions observed by Cabaço *et al.* (2005) were observed in a liquid CO_2 -EtOH phase, therefore it is likely that interactions did occur between the supercritical CO_2 and EtOH observed here but they were not seen in the FT-IR spectra in this system. This could be due to the CO_2 being in large excess to the EtOH and therefore the EtOH is not observed by FT-IR, until depressurisation, when the EtOH drops out of the binary SCF mixture and exists as a liquid on the ATR crystal where it can be detected. CO_2 -EtOH interactions reported in the literature by Lalanne *et al.* (2001) and Cabaço *et al.* (2005) were seen when EtOH was present in higher concentrations (>30% by weight) therefore at lower concentrations of EtOH the interaction may not be seen. Additionally, Kazarian *et al.* (1996) reported that substances present in the bulk CO_2 may not be observed by the ATR crystal and therefore would not appear in the IR spectrum. Consequently, interactions between such substances may also not be seen.

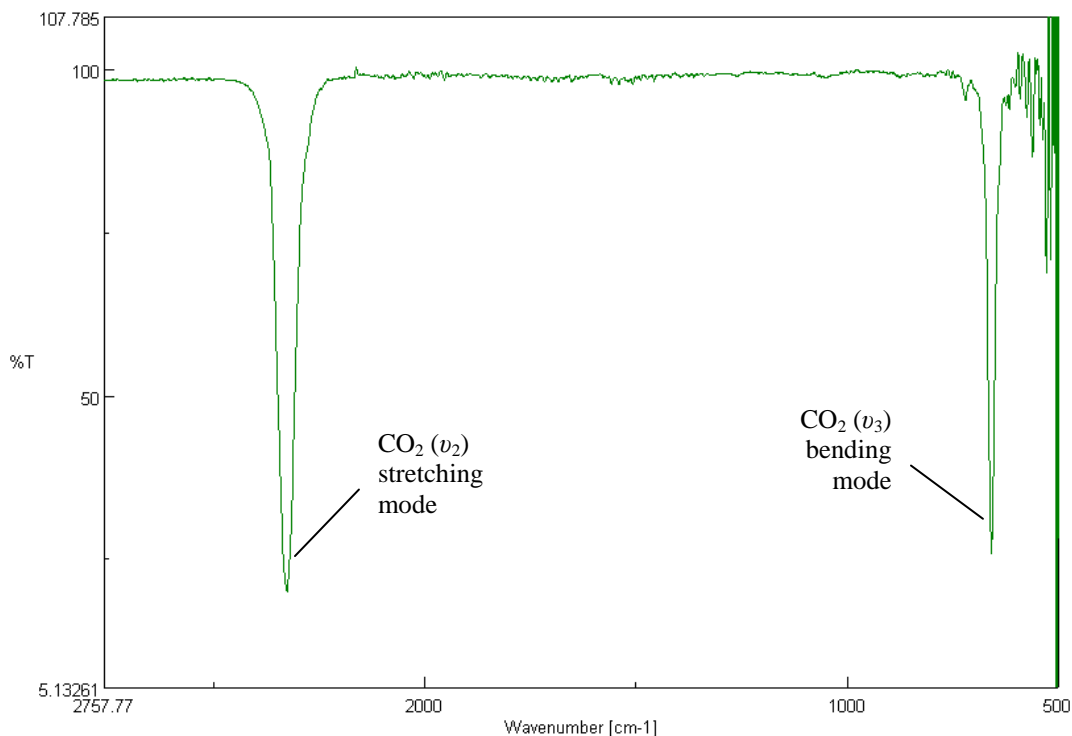


Figure 3.6 FT-IR spectrum of $\text{scCO}_2(\text{pure})$ and $\text{scCO}_2(\text{EtOH})$ at 20 MPa/50°C.

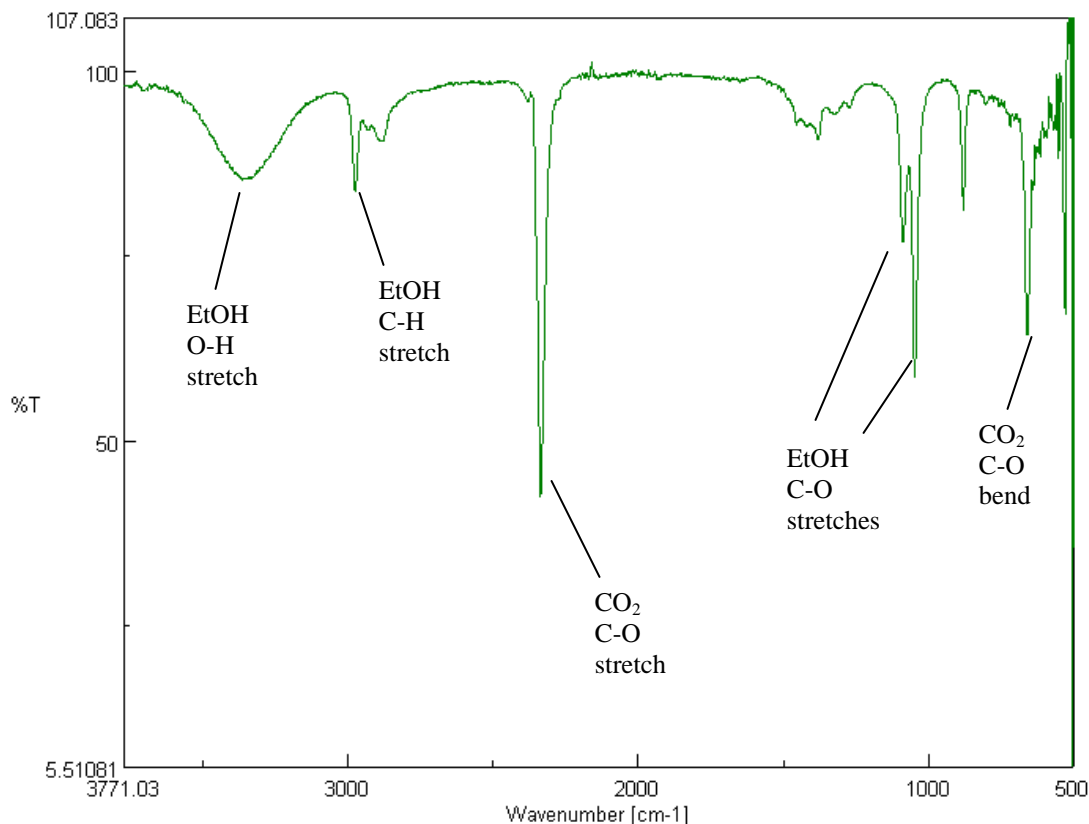


Figure 3.7 FT-IR spectrum of $\text{scCO}_2(\text{EtOH})$, during depressurisation.

The next study investigated the interaction of scCO_2 with agar gel. In the presence of agar gel (for both dried and partially wet gel, containing 10% sucrose) the CO_2 bending (ν_2) mode was split into a doublet - two bands were observed at 669 and 659 cm^{-1} in the FT-IR spectra. This is illustrated in Figure 3.8 (circled in red) for partially wet agar gel (at two different processing conditions), compared with $\text{scCO}_2(\text{pure})$ alone and agar alone. The CO_2 absorption bands were much broader which may be due to the increased absorbance associated with this region (known as the “fingerprint region”) when agar gel was present, and also could be indicative of the scCO_2 being in a different environment.

More importantly, the splitting of the CO_2 bending mode indicates that the degeneracy of the molecule is lost. Degeneracy arises when the symmetry of the molecule is such that certain fundamental frequencies are equal (one energy level corresponds to two or more states of motion). The two peaks seen here can be assigned individually to the in-plane and out-of-plane CO_2 bending modes, indicating that some interaction between the agar polymer and scCO_2 is

occurring, causing their frequencies to differ. This is usually because the molecules ability to rotate has been restricted in some way, for example by forming an EDA complex.

Splitting of this band has been previously reported and assigned to a Lewis acid-base type interaction of the CO₂ with chemical groups on polymers, in particular carbonyl groups, but also ester and ether groups (Kazarian *et al.* 1996; Nalawade *et al.* 2006a; Nalawade *et al.* 2006b). Kazarian *et al.* (1996) reported that interactions causing a T-shaped geometry or a 'bent' T-shape configuration with the CO₂ would release the degeneracy of the ν_2 mode, due to the symmetry of 'free' CO₂ no longer existing.

Agar contains ether groups which are located on the agar backbone (Figure 1.5). These groups may take part in a Lewis acid-base interaction with the CO₂.

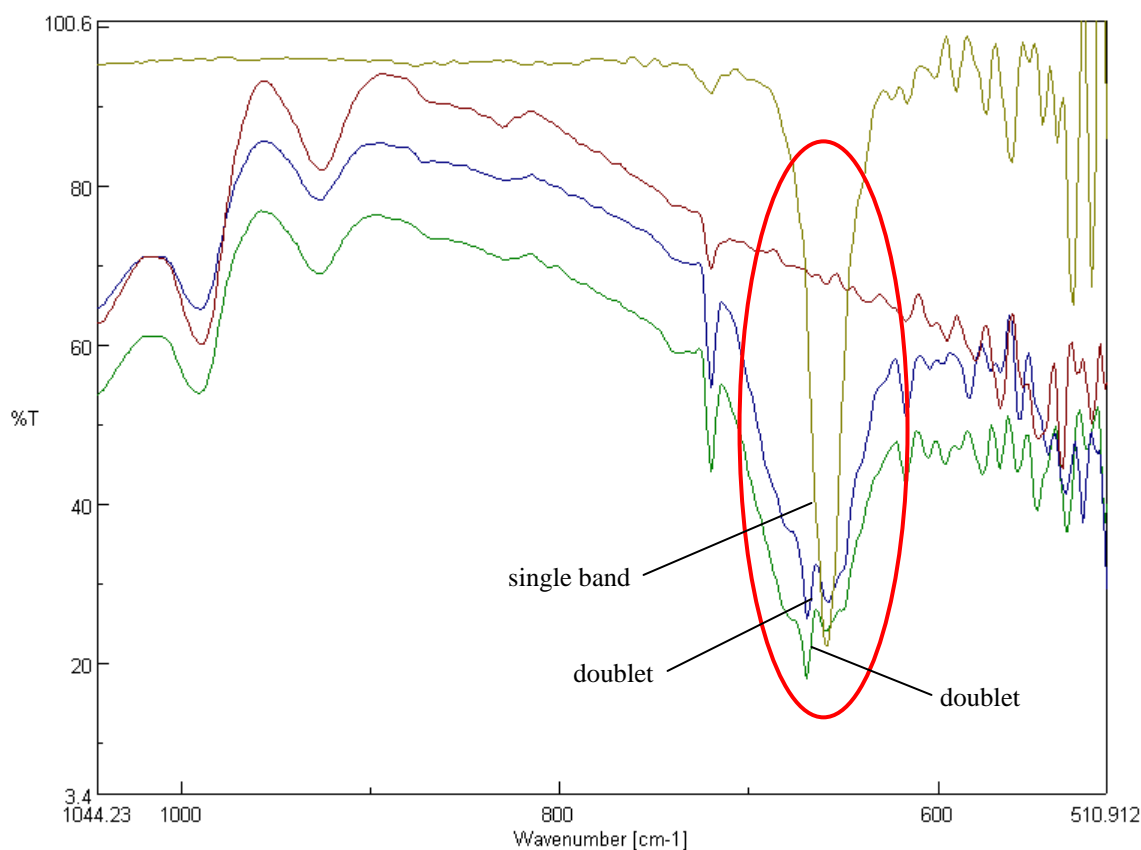


Figure 3.8 FT-IR spectra of partially dried 2% agar gel, containing 10% sucrose, exposed to scCO_{2(pure)} at 10 MPa/50°C (blue line) and 20 MPa/50°C (green line), compared with scCO_{2(pure)} alone at 20 MPa/50°C (brown line) and the agar gel before exposure to scCO_{2(pure)} (red line). Note that the IR spectra lines have been moved apart to allow easier viewing.

The band corresponding to the asymmetric stretching (ν_3) mode at 2337 cm^{-1} was also seen to split into two bands at 2338 and 2359 cm^{-1} (in the same way as shown in Figure 3.9 (blue and red lines)) (for both dry and partially wet gels) but was not shown here due to the CO_2 spectrum having a very strong absorption band in this region which did not illustrate the interaction well. The asymmetric stretching band for CO_2 is not doubly degenerate therefore the splitting of this band is not due to the loss of degeneracy that was seen with the CO_2 bending mode. However, the appearance of additional bands in FT-IR spectra may be due to the scCO_2 being present in different environments which can cause a shift in the band. If the molecule is present in more than one environment, two bands may be seen, which appear as a doublet.

The next study investigated the interaction of agar with $\text{scCO}_{2(\text{EtOH})}$. Interestingly, with the addition of EtOH to scCO_2 and agar, the previous doublet (for the CO_2 absorption band at $\sim 660\text{ cm}^{-1}$) changed to a singlet, suggesting CO_2 exists in a 'free' state and agar- CO_2 interactions were no longer present (Figure 3.9). The asymmetric CO_2 stretching mode, ν_3 , on the other hand remained as a doublet, upon $\text{scCO}_{2(\text{EtOH})}$ addition to both dry and partially wet gels. However, upon extended exposure of $\text{scCO}_{2(\text{EtOH})}$ to *partially wet* agar gel, the two bands (at 2338 and 2359 cm^{-1}) combined to form a single band (2337 cm^{-1}) (Figure 3.9 (green line)). This return to a single band indicates that the CO_2 no longer exists in two environments.

This phenomenon (combining of the CO_2 stretching bands at 2338 and 2359 cm^{-1} to form a single band) however was not seen when EtOH was added to *dried* gel. After EtOH exposure to dried gel, a single band was observed for the CO_2 bending mode at $\sim 660\text{ cm}^{-1}$ and a doublet was observed for the stretching mode at 2338 and 2359 cm^{-1} , which did not change upon extended exposure to EtOH. Interactions that may be responsible for these changes in the IR spectrum are discussed later in this section.

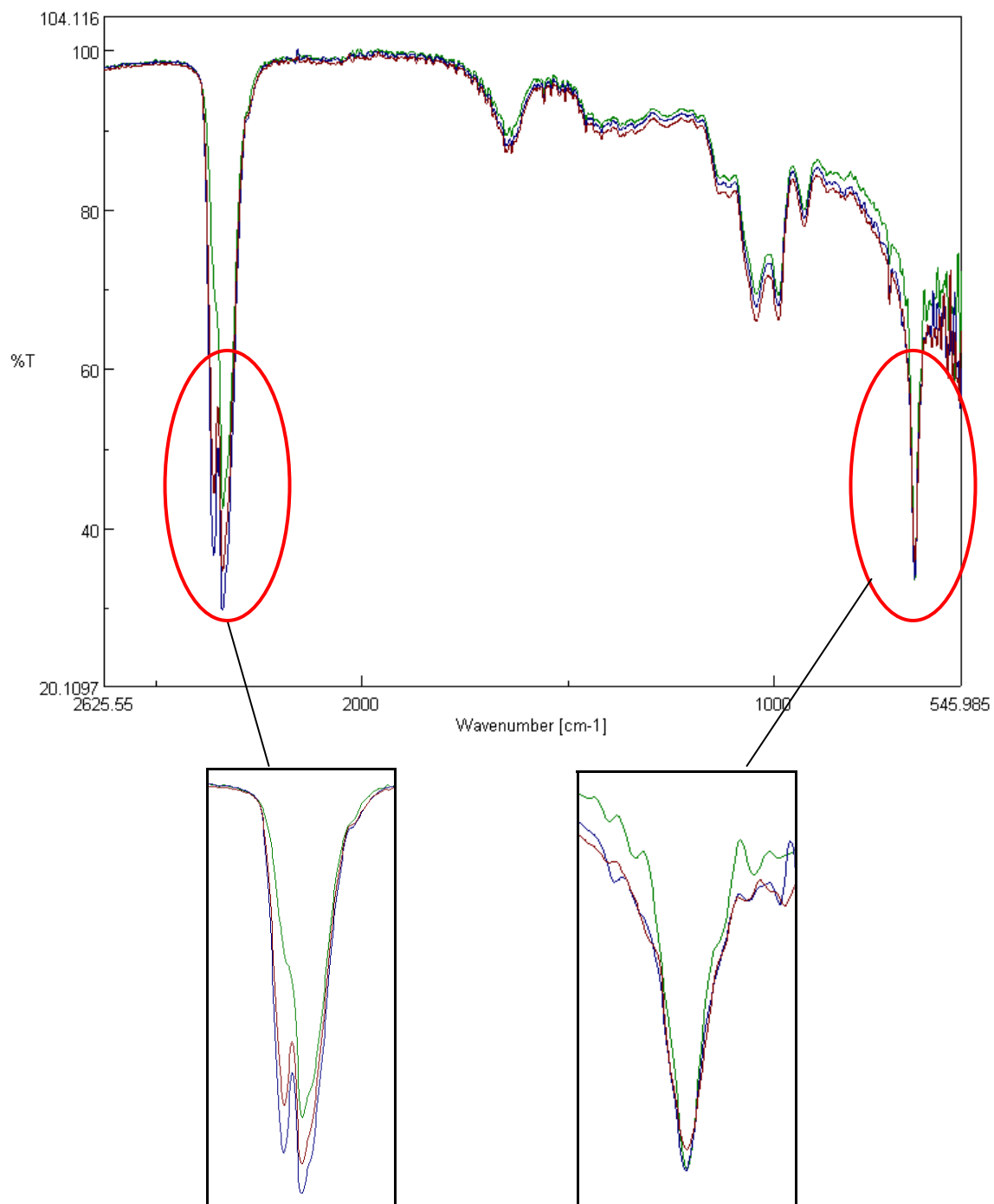


Figure 3.9 FT-IR spectra of partially dried 2% agar gel, containing 10% sucrose, exposed to scCO₂ at 20 MPa/50°C after EtOH addition for 60 seconds (blue line), 420 seconds (red line) and 1500 seconds (green line).

Finally, agar and EtOH were observed by FT-IR analysis alone (without CO₂) present to understand if there were any interactions occurring between the agar gel and the EtOH in this system. The spectra are presented in Figure 3.10. The band absorptions for the individual components retained the same band frequencies when they were mixed together, indicating that the two components were not interacting at the conditions investigated (21°C and 0.1 MPa). However, an interaction cannot be discounted: there may be an interaction present which is just not visible in the IR spectrum and/or the interaction may only occur at supercritical conditions.

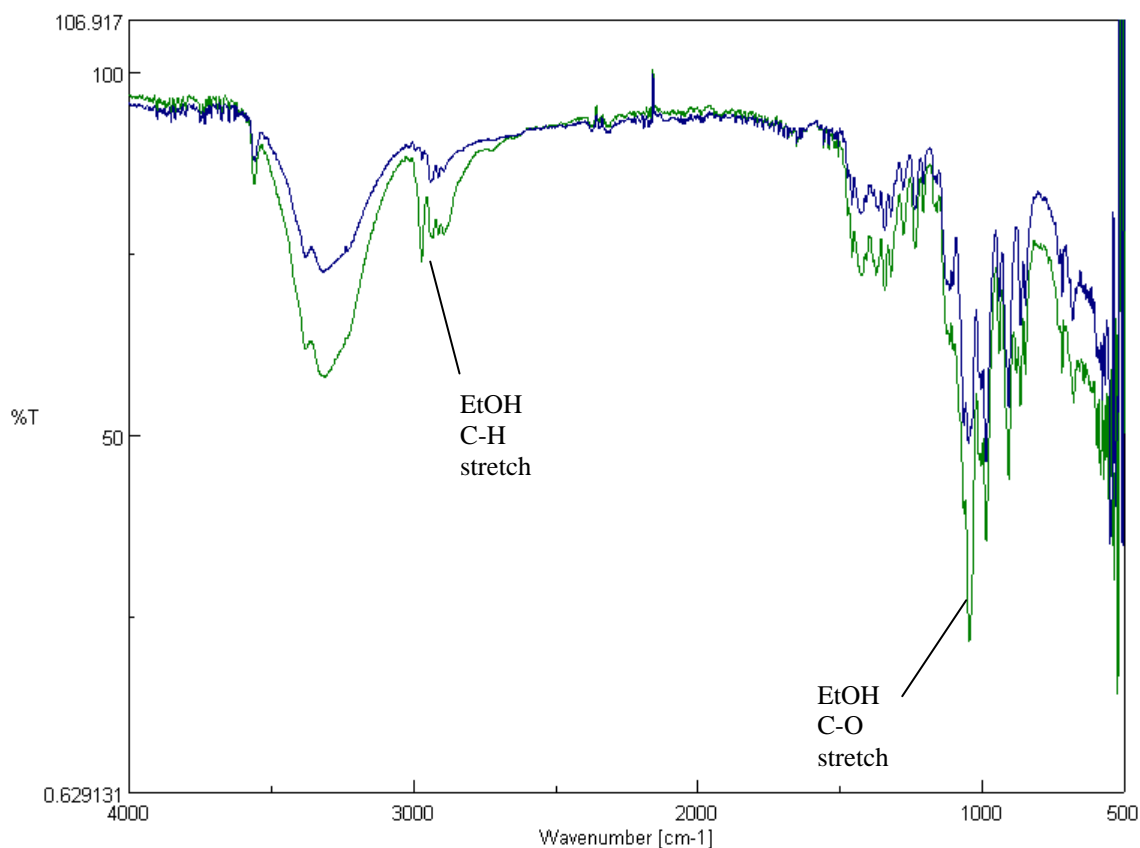


Figure 3.10 FT-IR spectra of supercritically dried 2% agar gel, containing 10% sucrose at 0.1 MPa/21°C with (green line) and without EtOH present (blue line).

An explanation for the loss of the doublets (representing the CO₂ stretching and bending modes) upon EtOH addition to agar and scCO₂

Results discussed above showed evidence of an interaction occurring between the scCO₂ and the agar gel, causing the splitting and loss of degeneracy of the ν_2 bending mode and also evidence

that the scCO_2 may exist in more than one environment, causing two bands to be seen for the ν_3 stretching mode. However, upon EtOH addition the interaction may be lost and the scCO_2 present in the second environment may also be removed. This is in contrast to what might be expected, since the addition of a co-solvent might be expected to increase the affinity between a polymer and the scCO_2 . Additionally, the removal of scCO_2 from a second environment upon EtOH addition is also dependent on whether or not water is present.

It is hypothesised here that the EtOH competes for interaction sites on the agar and interacts with the scCO_2 , disrupting the original agar- scCO_2 interaction. A suggested mechanism for these interactions is illustrated in Figure 3.11 which shows potential sites of interaction on the agar gel e.g. Lewis acid-base, electron donating-accepting sites.

Upon $\text{scCO}_{2(\text{pure})}$ addition to the agar gel, a doublet absorption band for the CO_2 stretching band is exhibited in the FT-IR spectrum (Figure 3.11 (a)). This is thought to be due to the scCO_2 being present in two environments, once of which may involve interactions with the agar gel. In the case of the partially wet gel, some of the interaction sites on the gel are expected to be interacting with water and therefore unavailable to interact with scCO_2 (Figure 3.11 (c)). However, it is hypothesised (from the FT-IR results) that there are still enough sites interacting with the scCO_2 to allow the scCO_2 to exist in two environments, and therefore the existence of two bands which appear as a doublet absorption band in the FT-IR spectrum.

It is assumed that despite no evidence of CO_2 -EtOH interactions in the FT-IR spectra displayed here, interactions *are* likely to occur as several authors have reported such interactions in the literature (Lalanne *et al.* 2001; Cabaço *et al.* 2005). Potential reasons for the CO_2 -EtOH interaction not being seen here in the IR spectra have been discussed earlier. Following EtOH addition, the dried gel may therefore lose some interactions with the CO_2 molecules, since it is now competing with CO_2 's ability to interact with EtOH and the EtOH may also be interacting with the agar (Figure 3.11 (b)). However, there appears to still be some scCO_2 interacting with the agar, and present in a second environment which results in two stretching absorption bands (even upon extended exposure times to EtOH). In comparison, there are expected to be less interaction sites on partially wet agar gel that bind with CO_2 , due to some already interacting with water (Figure 3.11 (d)). Therefore, with increased exposure to EtOH the fewer interacting

CO₂ molecules may be removed, resulting in loss of the scCO₂ in the second environment and a single absorption band is seen instead.

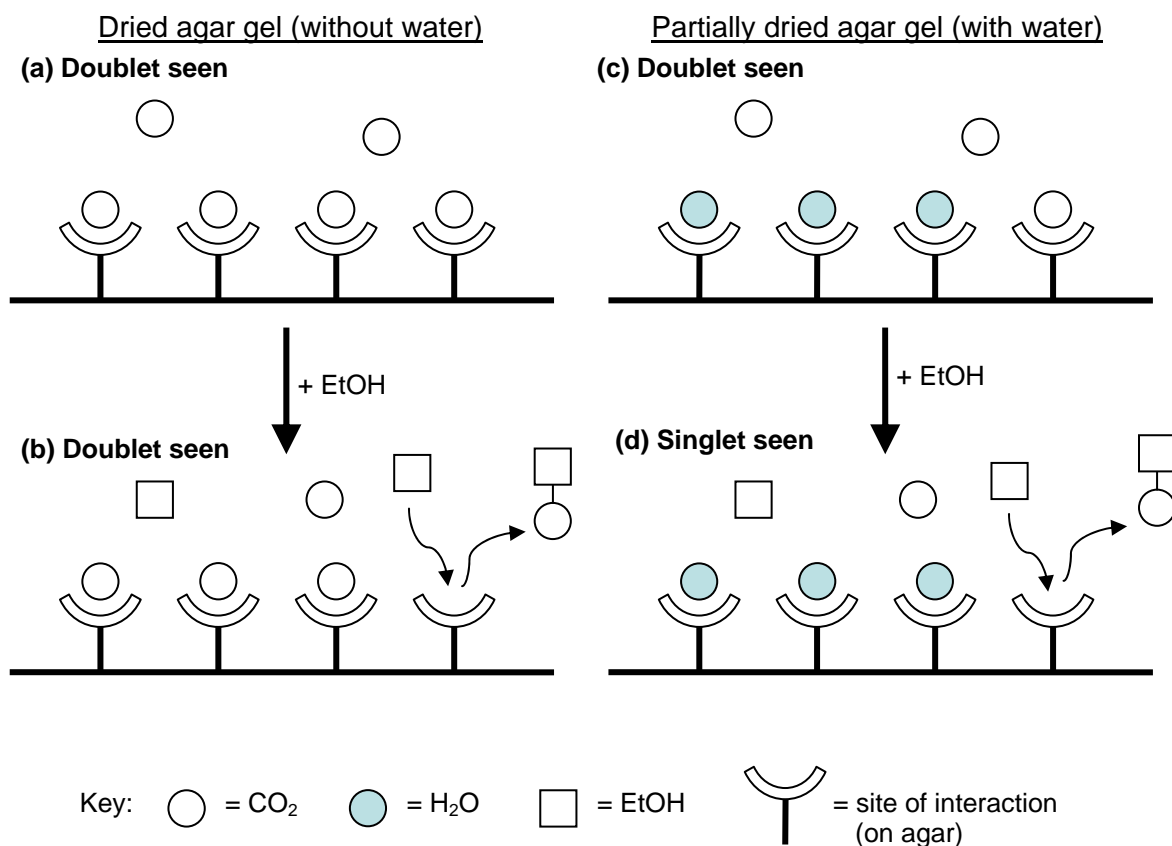


Figure 3.11 An illustration of the proposed interactions that may occur during exposure of (dried and partially wet) agar gel to scCO₂ and scCO₂(EtOH) which resulted in a singlet (d) or a doublet ((a)-(c)) for the absorption band associated with the CO₂ stretching mode.

In contrast, the doublet for the CO₂ *bending* mode was always lost upon EtOH addition, to both dried and partially wet gels. This is likely to be due to the different reasons for the formation of the doublets and therefore the loss of them also i.e. upon EtOH addition, the CO₂ molecules may lose the interaction that restricts their bending mode but not the removal of the scCO₂ from a second environment, where different interactions may be occurring. The removal of the scCO₂ from a second environment requires further EtOH to remove the additional band seen (for the CO₂ stretching mode) from the FT-IR spectrum. Strengths of any interactions may also vary and affect the sensitivity of the mode. Most authors use the CO₂ bending mode to infer CO₂-polymer interactions due to the bending mode having a higher sensitivity than the CO₂ stretching mode.

(Kazarian *et al.* 1996). Therefore, the bending mode may be more sensitive to EtOH addition (and therefore disruption of the interaction) than the stretching mode. This work has been discussed in the literature (Brown *et al.* 2010).

An explanation for the differences in agar structure seen upon EtOH addition to agar and scCO₂ during drying

In section 3.4.4 it was suggested that agar-EtOH interactions may occur that could disrupt the ordered confirmation of agar e.g. hydrogen bonding. This would explain why a different structure was created during drying with scCO₂(EtOH) compared with those dried with scCO₂(pure) (Table 3.3). It is also possible that EtOH interacts with water (both bound and unbound) in the agar structure. The double helices that make up agar are known to be stabilised by the presence of water molecules bound inside the double helical cavity. Additionally, exterior hydroxyl groups allow aggregation of these helices to form a tertiary structure. Therefore, disruption of these interactions by EtOH may de-stabilise the rigid agar helix and result in changes to the tertiary agar structure (Hui 2005). Consequently, changes in the tertiary structure of agar will have an affect on the chemical and physical properties of the gel (Rees and Welsh 1977).

The FT-IR spectra displayed in Figure 3.10 showed no evidence of an agar-EtOH interaction and IR experiments have not been carried out to observe if EtOH-water interactions were present. However, it may be hypothesised that EtOH-water interactions such as those illustrated in Figure 3.12 could influence the agar structure during drying with scCO₂(EtOH).

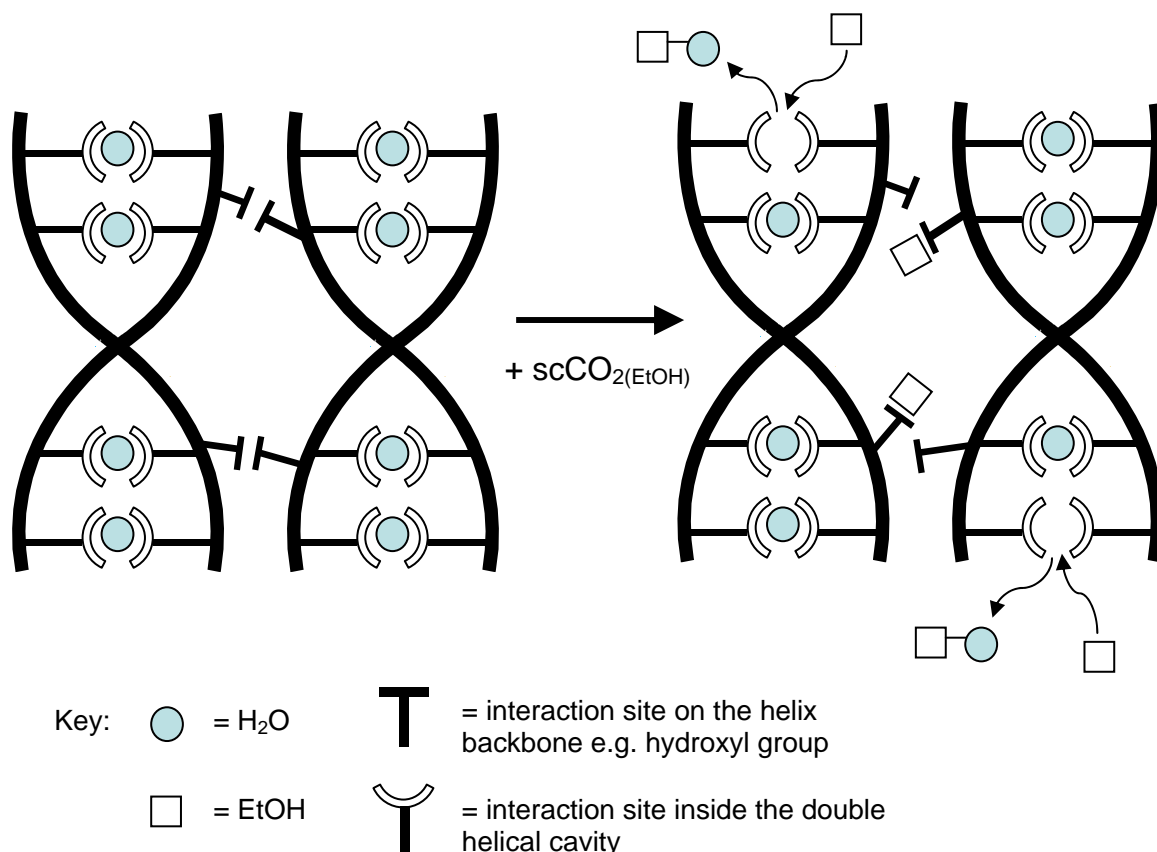


Figure 3.12 An illustration of the proposed interactions that may occur between the agar helices during exposure of agar gel to $\text{scCO}_2(\text{EtOH})$ which could cause disruption to the molecular structure.

Considering the results discussed above, and no evidence of plasticisation (indicated by swelling or melting of the polymer) observed previously in the windowed vessel, it is unlikely that plasticisation occurs here. Addition of a co-solvent would be expected to increase the affinity between a polymer and the scCO_2 , and therefore also increase the plasticising capacity of scCO_2 . However, it appears that the opposite is seen here and in fact the affinity between the polymer and the scCO_2 is decreased upon EtOH addition (Figure 3.11).

In conclusion, the results discussed here are not fully conclusive. It appears that interactions with the CO_2 and agar do exist, which may be disrupted when EtOH is added, leading to loss of a doublet in the FT-IR spectrum for CO_2 which is indicative of the CO_2 -agar interaction. The EtOH is also thought to disrupt interactions within the agar structure by interacting with water within the agar structure and/or interacting with hydroxyl groups on the agar backbone which stabilise the tertiary gel structure. These suggested interactions may be the reason for different

structures achieved upon drying with $\text{scCO}_2(\text{EtOH})$ compared with those dried with $\text{scCO}_2(\text{pure})$. It is also thought that plasticisation does not occur here. Further experiments are required to confirm the presence of specific interactions.

3.4.6 Rehydration properties of dried gel pieces

Dried samples were rehydrated at $21 \pm 2^\circ\text{C}$ and their moisture gain, over time, due to rehydration was studied (Figure 3.13).

Despite clear differences in structure, volume, and voidage measurements between the gels dried by supercritical and air drying, no difference in rate of rehydration or final equilibrium NMC, following rehydration was observed (Figure 3.13). The air dried gels were able to swell considerably during rehydration, explaining their ability to absorb similar quantities of water to those that were supercritically dried, despite the supercritically dried samples having a much larger volume to begin with. The extreme shrinkage observed during air drying was therefore not entirely irreversible.

Freeze dried gels had the largest volume and voidage to begin with and subsequently showed the fastest rehydration to much higher EMCs than air and supercritically dried gels (Figure 3.13 (a) and (b)). Interestingly, despite no statistically significant differences between percentage open space values of the dried gels containing 0% sucrose (Table 3.2 (e)) and those containing 10% sucrose (Table 3.2 (f)), the sucrose addition did result in improved rehydration properties. Samples with added sucrose were able to reach comparable moisture contents of the pre-dried gel (Figure 3.13 (b)). Addition of sucrose to agar gel has been shown to decrease the size of ice crystals upon freezing (Fuchigami and Teramoto 2003; Arunvanart and Charoenrein 2008). As sucrose concentration was increased, the amount of water in the gel and freezing temperatures decreased which shortened the freezing time. The ice crystals were seen to be smaller in those gels containing higher sucrose concentration and texture was improved. Higher rates of freezing were also linked to the formation of smaller ice crystals and smaller ice crystal distribution in various freeze dried foods, not containing any sucrose (Mousavi *et al.* 2007). During freeze drying, voids are then created in spaces that were originally occupied by these ice crystals. However, results here seem to be in disagreement with observations made by Fuchigami and

Teramoto (2003), and Arunvanart and Charoenrein (2008). Freeze dried gels seen here, containing 10% sucrose (Table 3.2 (f)) in fact appear to have larger voids than those containing 0% sucrose (Table 3.2 (e)) when observed visually from the x-ray 2-D images, which could account for the improved rehydration properties seen in those gels containing 10% sucrose. The voids created, through the formation and removal of ice crystals, during freeze drying therefore can be related to the rehydration properties of the dried gel pieces. However, the interconnectivity and pore structure of these voids is also important, as this is an indication of the porosity of the material and higher porosity values can be related to improved rehydration properties (Marabi and Saguy 2004; Torringa *et al.* 2001). Voidage alone may only give information about closed porosity, which is not expected to influence the rehydration properties in the same way as open porosity, or pore connectivity would. Marabi and Saguy (2004) reported that the rehydration ratio of dry food particulates increased with bulk and open porosity, but was not affected by closed porosity. Hence, while both open and closed porosity are important product characteristics, only open pores are important in water uptake. Therefore, the voidage alone cannot be expected to affect the rehydration properties, and discussion of the voidage, with regards to rehydration properties would therefore be more accurate, if the void contribution to open or closed porosity is known.

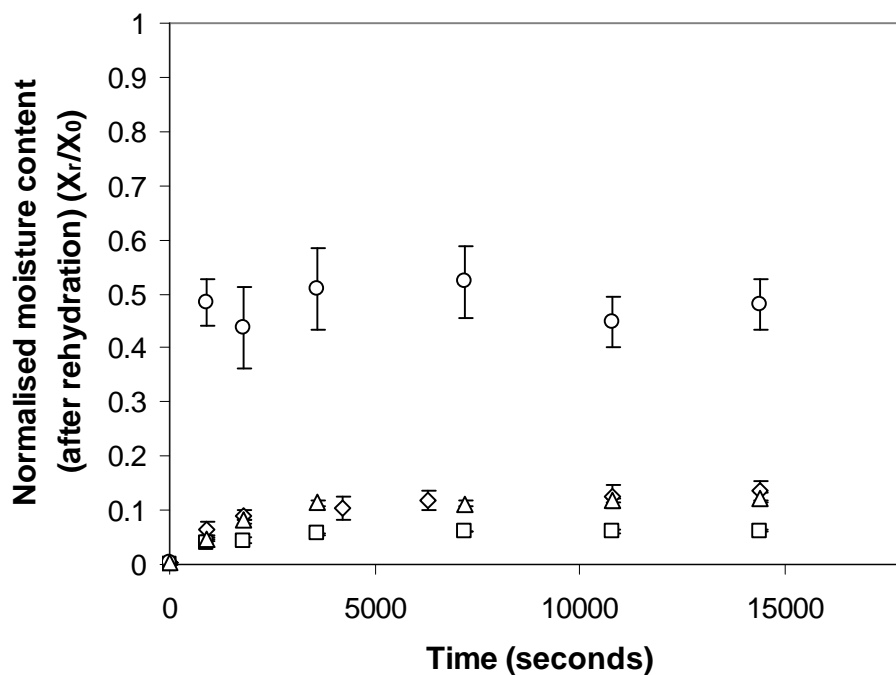
The results for supercritically dried-rehydrated gel pieces agreed with this argument, that voidage values would not allow prediction of rehydration properties: despite gels dried with $\text{scCO}_2(\text{EtOH})$ possessing similar voidage values and volumes to freeze dried gels, their rehydration properties were not comparable. Also, no differences in the rehydration of gels supercritically dried using $\text{scCO}_2(\text{pure})$ or with $\text{scCO}_2(\text{EtOH})$ were seen, despite the structural differences seen and a significant quantitative difference in their voidage values. The moisture content of these gels at saturation did not reach the moisture content of the pre-dried gel, indicating that the supercritical drying process is not reversible.

As mentioned above, the porosity of the material should also be considered, since the interconnectivity of the pores inside the gel is more important than simply the amount of space inside the gel. Despite the supercritically dried gels having an open structure similar to that of the freeze dried gels, it is possible that the pores are not as accessible and could relate to closed porosity rather than open porosity. The voids left through the removal of ice crystals, during

freeze drying, may be expected to infer a more open porosity than supercritical drying, which removes the water using a diffuse SCF, having the ability to diffuse quickly and easy through narrow pore networks. The structure of scCO₂ dried gels was also more elastic and less rigid than the freeze dried gels (and is discussed further in section 3.4.7), allowing for collapse of some pores following the drying process. Had time allowed, values for pore connectivity would have been calculated through subsequent 3-D x-ray micro-CT analysis or alternatively by mercury porosimetry, as reported by Portsmouth and Gladden (1991).

Despite supercritical drying bringing about no beneficial improvement to the rehydration properties of agar gels when compared with those that were air dried, the retention of volume during drying is an important quality factor in the appearance of dried food stuffs (Khalloufi and Ratti 2006). The higher percentage open space value of supercritically dried gels is also anticipated to result in a more desirable gel texture than air dried gels which exhibit low open space values, having experienced a high degree of shrinkage. Texture of the air dried gels could consequently not be measured due to the lack of significant volume to carry out the analysis on.

(a)



(b)

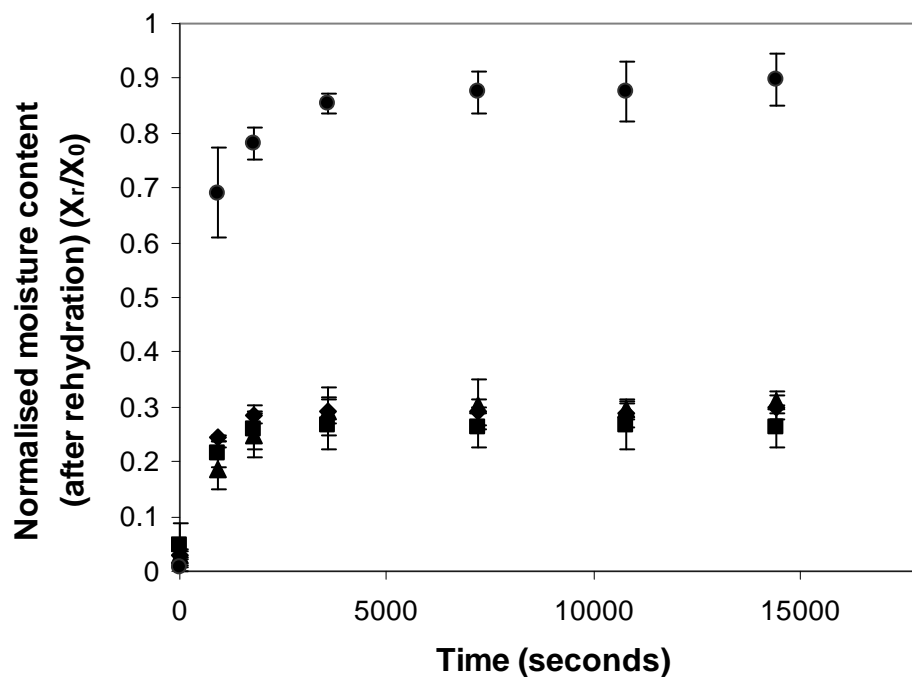


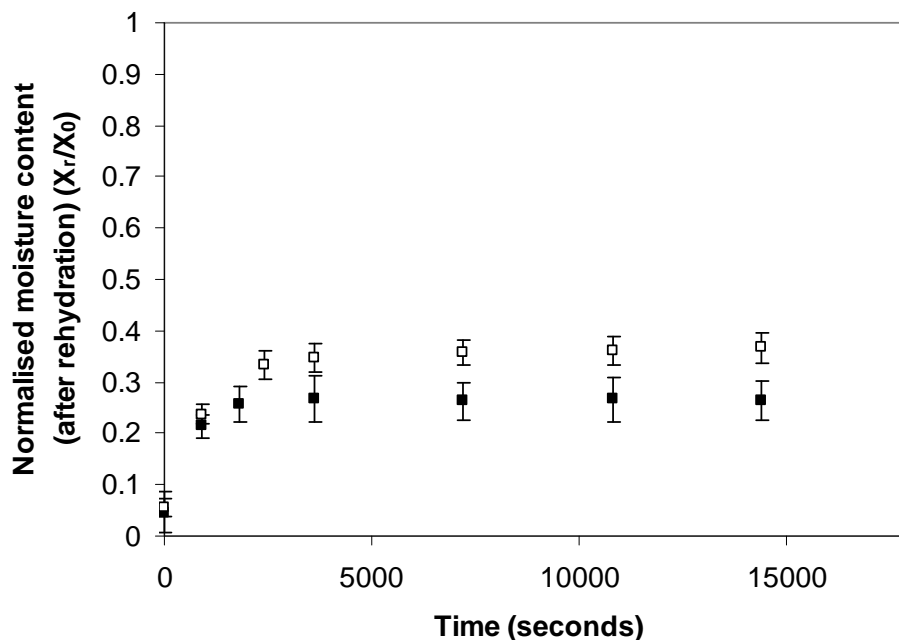
Figure 3.13 Graphs showing the rehydration (25°C) of dried gels containing, (a) 0% sucrose, and (b) 10% sucrose, which were dried with $scCO_2(pure)$ (squares); $scCO_2(EtOH)$ (diamonds); air (triangles) and freeze dried (circles). Supercritical drying conditions used were 1 l/minute flow rate and 0.4 MPa/minute depressurisation. Each point represents an overall mean of four gel samples from one independent experiment \pm one standard deviation (vertical error bars).

Rehydration of supercritically dried gels that had been processed using alternative scCO_2 flow rates (between 1 l/minute and 3 l/minute) and depressurisation rates (between 0.4 MPa/minute and 1.6 MPa/minute) were also investigated. The rehydration rates were similar for all flow rates and depressurisation rates, with the most significant difference being observed between those gels that had been dried at 1 l/minute flow rate, 0.4 MPa/minute depressurisation rate and 3 l/minute flow rate, 1.6 MPa/minute depressurisation rate – the latter having slightly improved rehydration properties. This was seen for both $\text{scCO}_{2(\text{pure})}$ and $\text{scCO}_{2(\text{EtOH})}$ (Figure 3.14). It was not clear if this small difference was due to flow rate, depressurisation rate, or both, since results for 1 l/minute flow rate and 1.6 MPa/minute depressurisation rate, and 3 l/minute flow rate and 0.4 MPa/minute depressurisation rate gave varied results for rehydration rates (in between those for 1 l/minute flow rate, 0.4 MPa/minute depressurisation, and 3 l/minute flow rate, 1.6 MPa/minute), depending on if $\text{scCO}_{2(\text{pure})}$ or $\text{scCO}_{2(\text{EtOH})}$ was used. However, as discussed in section 3.4.4 there was no significant difference between percentage open space values observed at the different processing conditions. The small differences that were seen, in fact showed that gels dried at 1 l/minute and 0.4 MPa/minute depressurisation actually had a higher percentage open space than those gels dried at 3 l/minute and 1.6 MPa/minute depressurisation which is in contrast to what would be expected, since a higher flow rate and higher depressurisation rate may be expected to open up the structure, through more vigorous processing, than lower flow rates and depressurisation rates. The rehydration results suggest that this may be the case, but the changes due to processing conditions is not exhibited in the percentage open space measurements. The improved rehydration properties at higher flow rate and depressurisation rate may therefore be due to increased interconnectivity of the voids which is not exhibited in the percentage open space values, albeit in a small way, for the conditions used here. Additionally, the lower percentage open space values for gels dried at higher flow rate and depressurisation rates may be indicative of smaller, narrower pores that could facilitate water uptake more readily than larger pores due to capillary action.

It is also noteworthy to mention that the sucrose was seen to leach from the gel matrix, during rehydration in water, suggesting that the sucrose is weakly bound within the agar matrix (despite interactions between the agar and sucrose expected, as discussed in section 3.4.2). The leaching of solids is a common observation during rehydration of dried food (Sun 2008). Both the

nutritional quality of the food product and its water uptake can be affected during this process. Hence, leaching should be considered during rehydration, especially when studying the kinetics of the process. However, changing the concentration of solids in the rehydration solution may prevent or even reverse the leaching process and could be considered as a solution to this problem. However, since the sucrose was added to the product before drying, leaching of the material is not as important as leaching of a nutritional substance that already existed in the material, pre-drying. The addition of sucrose also was shown to improve rehydration properties here therefore a potential negative effect of leaching, on water uptake (rehydration) is unimportant here.

(a)



(b)

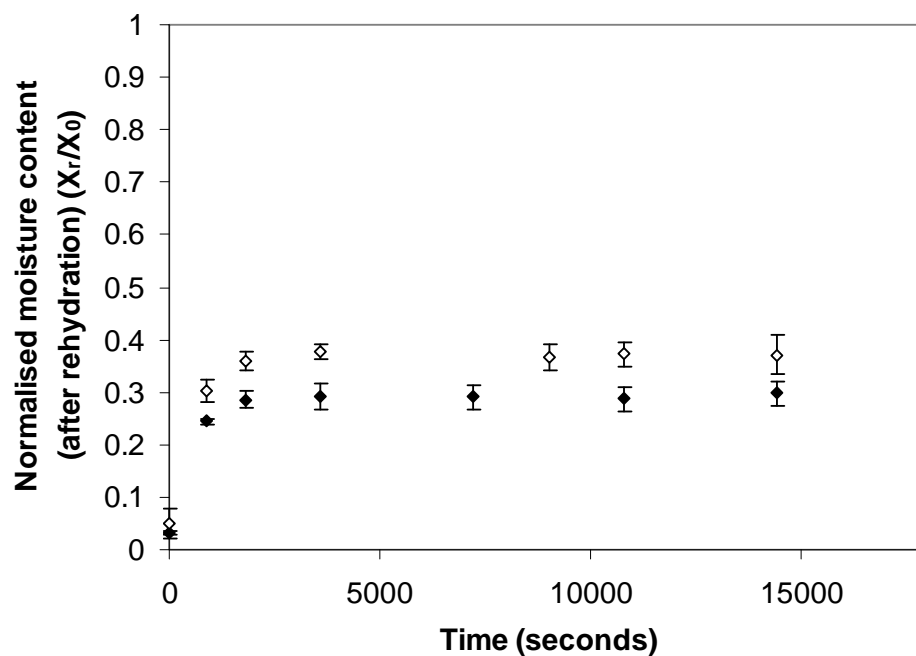


Figure 3.14 Graphs showing the rehydration (25°C) of supercritically dried gels, containing 10% sucrose, dried using (a) $\text{scCO}_{2(\text{pure})}$ (squares) and (b) $\text{scCO}_{2(\text{EtOH})}$ (diamonds). Conditions used were: 1 l/minute flow rate and 0.4 MPa/minute depressurisation rate (black points); and 3 l/minute flow rate and 1.6 MPa/minute depressurisation rate (open points).

Each point represents the overall mean from at least three independent measurements taken from at least three individual pieces of carrots \pm standard error of the mean.

3.4.7 Texture analysis of dried gel pieces to measure hardness

Texture is closely related to sensory perception of a food product. Dried food products may also be eaten without rehydrating first, increasing the importance of the dried product texture. Mechanical properties are also important when it comes to transporting and storing the dried product as dried gels, especially those with low solid content can become fragile and brittle.

Texture analysis of gel pieces was carried out in the same way as in chapter 2 (section 2.3.10 and 2.4.2.4). A puncture compression test was used to measure the force to puncture which is related to the gel hardness. Figure 3.15 shows the results for supercritically and freeze dried samples. For freeze dried samples, as the sucrose concentration was increased the gel hardness also increased. This is due to the higher concentration of solid present in the gel and therefore allowing for a more dense dried gel network. For supercritically dried samples (dried with the use of a co-solvent), the force required to puncture the gel is similar to that of freeze dried samples that contain 10% sucrose. However, interestingly when $\text{scCO}_2(\text{pure})$ is used for drying, the force required to compress the gel is significantly larger. Some increase in hardness could be due to the smaller volume of the gels dried with $\text{scCO}_2(\text{pure})$, compared with freeze dried gels and those dried with $\text{scCO}_2(\text{EtOH})$, and therefore an increased density. The structure produced during supercritical drying is also expected to influence the force required to puncture samples, which is related to the volume of the gel pieces, following drying.

This reduced volume of the gel would be expected to be related to the voidage and porosity of the gel, and some correlation is seen between the voidage (percentage open space) measurements (Table 3.2) and the texture analysis measure of hardness (Figure 3.15). Both freeze dried gels and those dried with $\text{scCO}_2(\text{EtOH})$ have a higher value for percentage open space than the gels dried with $\text{scCO}_2(\text{pure})$, and therefore a more open internal structure. This increased porosity, whether open or closed, would be expected to result in a decrease in the hardness of the gel, which is seen here. Agar gels that were filled with CO_2 bubbles also showed a decrease in the mechanical and compressive strength of the gel, suggested to be due to local rupture, produced during bubble formation and growth, acting as sites for failure propagation (Nussinovitch *et al.* 1992). The bubbles formed during drying with $\text{scCO}_2(\text{EtOH})$ may therefore be

responsible for the reduction in puncture force measured, compared with gels dried using $\text{scCO}_2(\text{pure})$ that exhibited a higher puncture force.

It is also interesting to note that upon compression of the supercritically dried samples a smooth puncture force curve was observed, while for freeze dried samples the curve was much more jagged, indicating fracturing of a brittle gel when put under pressure (Figure 3.16). This same phenomenon was also seen by (Nussinovitch *et al.* 1993), during the measurement of stress-strain relationship for freeze dried alginate gels.

This difference in brittleness may be related to the arrangement of the sucrose within the gel which when dried quickly, or at high temperatures, by freeze drying or air drying, respectively, takes on a non-crystalline, amorphous state which is very brittle (Beckett 2008; Mathlouthi and Reiser 1994). In contrast, slower drying of a sucrose solution results in a crystalline sugar and therefore is expected to occur during supercritical drying. If this is the case, supercritical drying may offer a unique drying method, where a sugar solution within a gel system can be dried to its original dried crystalline state, offering different textural properties to those achieved through freeze drying or air drying. This however, requires further investigation to prove, since sugar crystallisation depends on several other factors including temperature, heat transfer, mass transfer, and phase transition phenomena (Ben-Yoseph and Hartel 2006).

This brittleness observed in freeze dried samples is associated with a more rigid, non-elastic structure which was shown to rehydrate better, as would be expected. However, brittle dried structures that are produced during freeze drying do not store or transport well due to their fragile structures, offering another advantage of supercritical drying.

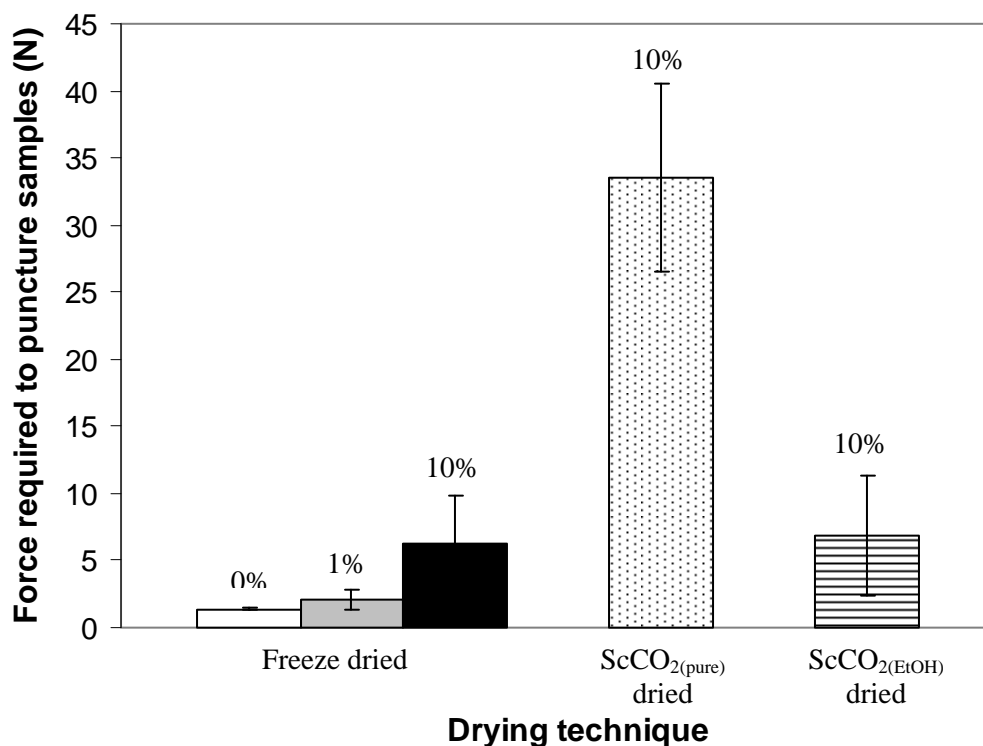


Figure 3.15 Chart illustrating the force required to puncture agar gel pieces measured in Newtons (N). Freeze dried samples contained 0% sucrose (white); 1% sucrose (grey); and 10% sucrose (black). Supercritically dried (with scCO₂(pure)) samples contained 10% sucrose (spots) and supercritically dried (with scCO₂(EtOH)) contained 10% sucrose (stripes). Each value represents the overall mean from at least three samples taken from three independent experiments \pm one standard error of the mean (vertical error bars).

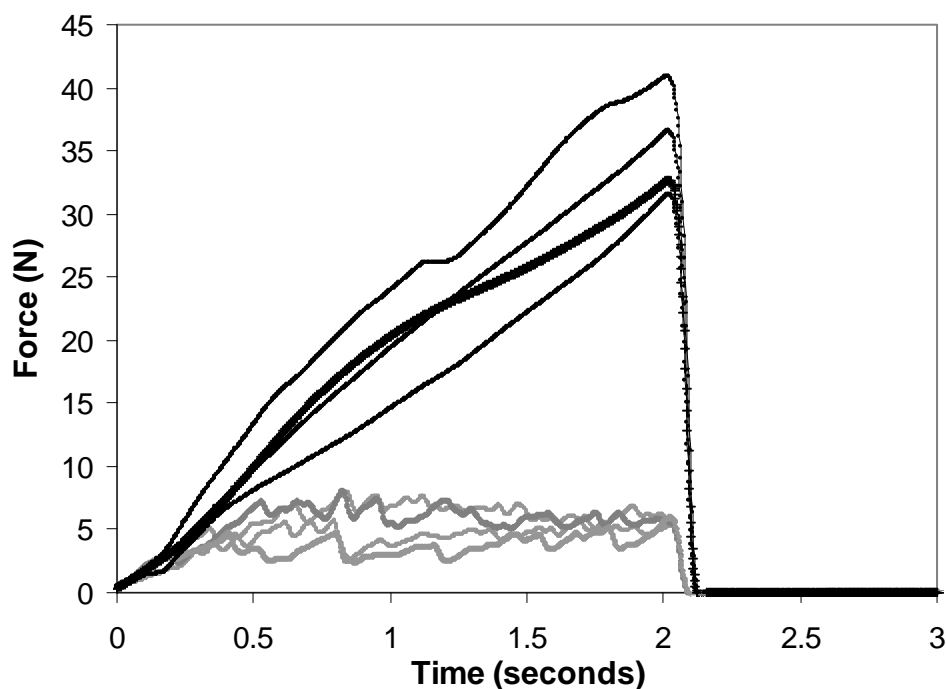


Figure 3.16 Texture analysis traces, illustrating the force, in Newtons (N), required to puncture gel pieces dried with $\text{scCO}_{2(\text{pure})}$ (black lines) and freeze dried gel pieces (grey lines). Each gel piece was taken from the same supercritical, or freeze drying experiment. Supercritical processing conditions used were 3 l/minute flow rate and 0.4 MPa/minute depressurisation. Freeze drying was carried out at 0°C for 30000 seconds.

3.5 Conclusion

It has been shown that agar gel can be dried using scCO_2 , to low moisture contents.

The addition of sucrose was shown to improve the volume retention and dried structure of gels, following supercritical drying which was thought to be due to a combination of reduced helix aggregation, increased cross linking of polymer chains and increased gel elasticity.

Addition of EtOH during the supercritical drying process gave rise to microstructural differences which was thought to be due to interactions occurring between the EtOH and agar. However, investigation by FT-IR analysis (of the bending mode, ν_2 , of CO_2) suggested that possible interactions seen between $\text{scCO}_{2(\text{pure})}$ and agar were in fact lost or disrupted when EtOH was added, and no further interactions were proven. Therefore the reason for the microstructural

change was unclear. Further experiments are required to confirm the presence of specific interactions and to deduce whether plasticisation is occurring or not.

No microstructural changes were observed due to changes in CO₂ flow or depressurisation rate, suggesting the gel was not mobile during the processing stages, and also showing that drying rate could be improved with increased flow rate without compromising the gel structure, at the conditions investigated here.

The percentage open space for supercritically dried gels was calculated as 48% for those dried with scCO_{2(pure)} and 68% for those dried with scCO_{2(EtOH)}. Rehydration results suggested that percentage open space values were related to closed porosity rather than open porosity since despite volume retention during drying being similar to that of freeze dried gels, the rehydration was not comparable. Some small differences in rehydration properties were seen between samples dried at varying flow rates and depressurisation rates, despite no differences seen in their percentage open space values, suggesting the processing conditions may affect the open porosity. Although this was not very significant here, it may be of more importance on an industrial scale where processing conditions are more extreme and can be varied on a larger scale.

The puncture force of samples were measured and the highest measurements were for samples dried with scCO_{2(pure)}, due to a more dense gel network than that of samples dried using scCO_{2(EtOH)} and freeze dried samples.

In summary, it has been shown that agar gels can successfully be dried using scCO₂, with creation of a unique microstructure which can be modified with addition of a co-solvent. This consequently affects the textural but not the rehydration properties. Supercritical drying potentially offers an alternative method, with the use of mild temperatures to dry biopolymers for the use in food products. There may also be potential to tune known interactions that occur during supercritical drying, with and without co-solvents, and to use this knowledge to manipulate the structure in a favourable way. However, further research is necessary.

4.0 Drying of agar gel on pilot plant scale equipment using supercritical carbon dioxide

ABSTRACT

The method used previously to dry carrots and agar with supercritical carbon dioxide (scCO₂) on a laboratory scale (using a 50 ml pressure vessel) was extended here to pilot plant scale equipment (using a 3 litre pressure vessel), in order to investigate the potential of using this drying technique on a larger scale. Bigger gel pieces and more gel pieces were able to be dried in one single experiment than those carried out in chapter 3. Flow rates of up to 1200 l/hour were used which allowed comparison of more significant flow rate changes than those that had previously been studied. Depressurisation rate however could not be tightly controlled and fast depressurisation rates were shown to cause damage to the gel structure.

Agar gel pieces containing sucrose or Glucidex 21D were dried and the structure and gel properties were compared with air and freeze dried gels. Gels containing Glucidex 21D exhibited similar properties to those containing the same quantity of sucrose, although rehydration properties were improved slightly. Generally, gels containing higher sugar concentrations exhibited less gel shrinkage upon supercritical drying and rehydration properties were similar to those of air dried gels, but their texture was more favourable than both air and freeze dried gels. Flow rate changes during supercritical drying suggested that a slower drying regime may be favourable for rehydration properties of the dried gel. However, structure and texture did not appear to be affected by flow rate changes during supercritical drying.

Supercritical drying on this scale therefore enabled larger changes in process parameters to be investigated which may influence the rehydration properties of the gel. Results, however, suggest that supercritical drying on pilot plant scale equipment is comparable to drying on laboratory scale equipment, implying that this technique could potentially be suitable for industrial scale drying.

4.1 Introduction

The use of scCO₂ for drying agar gels was investigated in chapter 3. The aims of the work described in this chapter were:

- To investigate the supercritical drying of agar gels using scCO_{2(pure)} on pilot plant scale equipment, located at the industrial sponsor (Unilever), in order to consider the potential of using this drying technique on a larger scale, in industry.
- To compare these results observed here with those results obtained on smaller scale equipment, in chapter 3, in terms of gel dried structure, subsequent rehydration properties and mechanical properties (of the dried and rehydrated gel).
- To examine and compare the effect of sucrose addition and also an alternative sugar, Glucidex 21D on the gel's dried structure, rehydration properties and mechanical properties (before and after rehydration) – it was hypothesised that a longer chain sugar (Glucidex 21D) may influence the final dried gel structure in a different way to sucrose by interacting differently with the helical agar structure.
- To compare the effect of the supercritical drying technique on the gel's dried structure, subsequent rehydration properties and mechanical properties (of the dried and rehydrated gel) with freeze drying and air drying techniques.
- To investigate the effect of larger flow rate changes (compared with small flow rate changes made in chapter 3) on gel properties.

4.2 Materials

4.2.1 Rig components

Work was carried out using Unilever's pilot plant scale supercritical drying equipment which was supplied by Feyecon (www.feyecon.com) and has been described further by Khalloufi *et al.* (2010). Details of specific components have been omitted for confidentiality reasons.

4.2.2 Gel preparation

Agar (product number A1296), sucrose (product number S9378) and Glucidex 21D were purchased from Sigma Aldrich (Poole, UK).

The gels were prepared by initially dissolving sucrose or Glucidex 21D in deionised water at the required concentration (0%, 1% 2%, 5% 10%, 20% or 30% w/v). The agar powder (2% w/v) was then stirred with the sugar solutions and boiled, using a microwave, to ensure complete dissolution of the agar.

The solution was left to cool, and de-air by standing for a few minutes, before pouring into a glass petri dish. The gels were left to cool at room temperature for at least one hour to set, before cutting the gels into 20 mm x 10 mm x 10 mm cuboid pieces and removing from the dish. In a second set of experiments, cylindrical moulds were used which measured length = 12 mm and diameter = 5 mm; the same size as in chapter 2. Likewise, these gels were left to cool for at least one hour before de-moulding. The samples were then dried using supercritical, air and freeze drying methods and rehydrated in deionised water at room temperature.

Ten gel cylinders, at each sugar concentration, were used in each drying experiment, while three others at each sugar concentration were used to determine the initial average total moisture content, by drying to constant mass overnight in an oven at 80°C. Gels containing 0% sugar solution were used as a control.

Moisture content in this work is reported as NMC. Discussion of this unit of measurement, the reasons for its choice, and the equation used for calculation of the NMC (equation 2.2) has been included in chapter 2 (section 2.3.2).

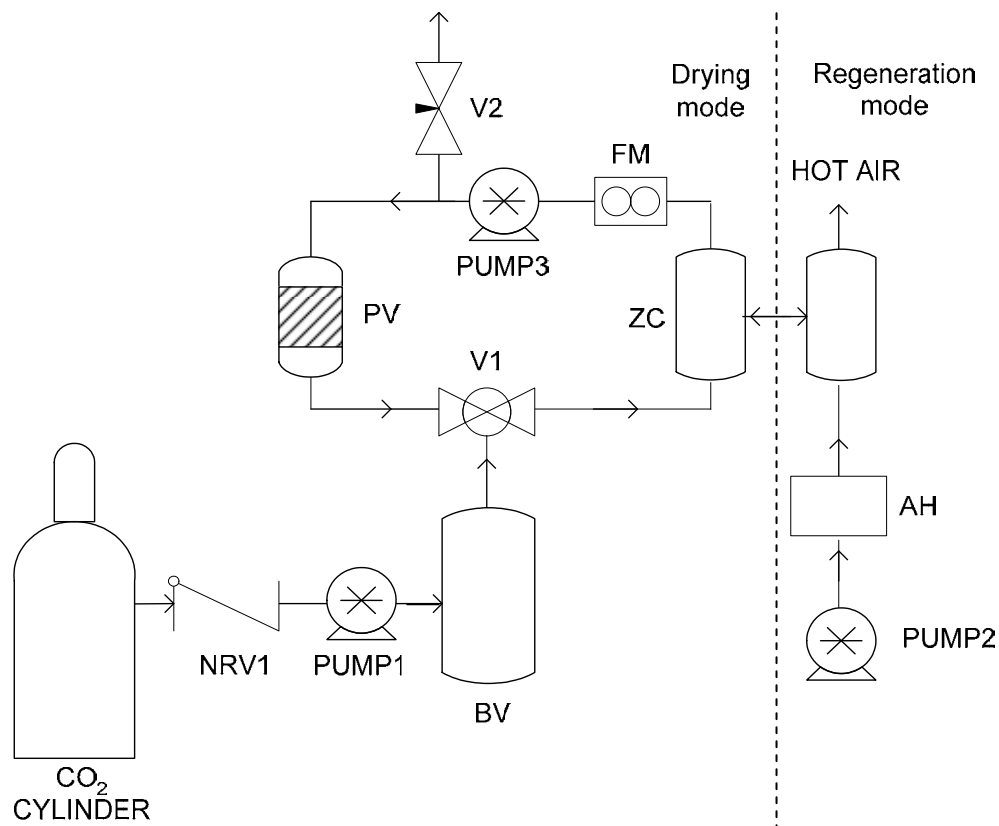
4.2.3 Solvents

CO₂ (liquid withdrawal) was supplied by BOC (The Netherlands).

4.3 Apparatus methodology

4.3.1 Equipment

The experimental rig for carrying out the supercritical drying experiments is shown in Figure 4.1. Notation used in the diagram is referred to throughout the following sections. The main differences between the equipment used here and the equipment used in chapters 2 and 3 (described in section 2.3.1) were the incorporation of a recirculation loop enabling re-use of the same scCO_2 , and a drying column that regenerated the 'wet' scCO_2 . Due to the presence of a drying column, co-solvent addition was not possible using this equipment, therefore $\text{scCO}_{2(\text{pure})}$ was studied alone.



Key:

PV = reaction pressure vessel with in built heater	PUMP1 = pneumatic liquid CO ₂ pump
V1 = ball valve	PUMP2 = air pump
V2 = micrometering valve	PUMP3 = circulation pump
ZC = zeolite column	AH = hot air heater
BV = buffer vessel	FM = flow meter
NRV1 = non-return valve	

Figure 4.1 Schematic representation of the experimental apparatus used for supercritical drying (to the left of the dotted line) and subsequent regeneration of the zeolite, following drying experiments (to the right of the dotted line). More details on the equipment set up can be found in *Khalloufi et al. (2010)*.

4.3.2 Method for supercritical drying

Liquid CO₂ was supplied from a 25 kg cylinder to a buffer vessel (BV), and was compressed to the desired pressure using a pump (PUMP1). The CO₂ was then fed into the drying part of the

Chapter 4: Drying of agar gel on pilot plant scale equipment using supercritical carbon dioxide

rig directly from the BV, controlled using a ball valve (V1), until the desired pressure was reached in the pressure vessel (PV). The CO₂ was also heated at this point to the desired temperature using an in-line heating mechanism. Supercritical drying experiments were carried out by constant circulation of the CO₂ using a pump (PUMP3). Flow rate could be measured using a flow meter (FM), incorporated into the high pressure tubing. The scCO₂ was circulated past the sample, held in the PV, and then passed over a drying agent (zeolite) which was held in a second vessel known here as the zeolite column (ZC). This removed moisture from the circulating scCO₂ and increased the drying capacity of a constant volume of CO₂, by allowing it to be recirculated. Depressurisation was initiated by opening a micrometering valve (V2) and the rate of depressurisation could be controlled by way of opening and closing this valve. Following depressurisation, the ZC was moved into 'regeneration mode'. The zeolite was regenerated by blowing hot air through the column, using a pump (PUMP2) and a hot air heater (AH) which heated the zeolite to high temperatures (>200°C), to release the bound water, prior to re-using for further experiments.

The first sets of experiments were carried out at a pressure and temperature of 10 MPa and 40°C, respectively. A single flow rate of between 1100 and 1200 l/hour was used and the depressurisation rate was set between 0.1 and 0.15 MPa/minute. Drying times of 18000-21600 seconds could be achieved using these conditions which allowed gels to be dried to low NMCs (typically <0.05, where 1 equals 100% of the total original moisture content). As mentioned earlier, due to use of the zeolite as a drying agent and the recirculation of CO₂, co-solvent experiments could not be carried out using this equipment.

Each individual experiment was only carried out once, however the large volume of the pressure vessel (3 litres) allowed ten duplicates of each gel to be dried per experiment.

In the second sets of experiments, a pressure and temperature of 14 MPa and 50°C were used, respectively. Flow rate was varied between 200 l/hour and 900 l/hour, and an individual experiment where 200 l/hour was followed by 900 l/hour was also investigated.

Depressurisation rate was not varied in either set of experiments due to the possibility of damaging the seals if high depressurisation rates were used. Instead depressurisation was controlled at a slow rate of about 0.1-0.15 MPa/minute.

4.3.3 Air drying method

Gels were dried in a hot air oven for 7200 seconds at 70°C, followed by leaving overnight at 50°C until gels reached <0.05 NMC. All experiments were carried out in triplicate.

4.3.4 Freeze drying method

Gels were freeze dried in an industrial freeze drier. Gels were frozen to -55°C for 14400 seconds, and then dried for 2 days at a temperature of 0°C and a chamber pressure of 1×10^{-4} MPa (1000 mTorr). Final sample temperature was 25°C. All samples were dried to <0.05 NMC and experiments were carried out in triplicate.

4.3.5 X-ray micro-computed tomography for the analysis of gel microstructure

X-ray micro-CT was used to study the microstructure of the dried gel pieces after drying. Details of this technique are outlined in section 2.3.6. X-ray radiograph images were captured and reconstructed to give a 2-D horizontal slice through the cylindrical sample.

4.3.6 Method for rehydration of gel pieces

Dehydrated gel pieces were immersed in beakers containing 50 ml distilled water, kept at room temperature ($21 \pm 2^\circ\text{C}$). The samples were removed at regular time intervals, blotted on tissue paper to remove excess water, and their mass determined. Samples were left overnight to determine the rehydration end point. Three results were obtained from each experiment (from three individual gel samples). Results are reported in terms of NMC (equation 2.6).

4.3.7 A texture analysis method to measure the hardness of gel pieces

A texture analyser (TA-XT2i, Stable Micro System, Godalming, UK) was used as outlined in section 2.3.10.

Three independent experiments (each comprising at least three gel pieces) were performed for each drying method and sugar concentration, before and after rehydration. The mean maximum force (N) was recorded, and the standard error of the mean calculated for each drying condition.

4.4 Results and discussion

4.4.1 The effect of sucrose addition on the drying and rehydration of agar gel pieces, dried using air, freeze and supercritical drying techniques

The effect of sucrose addition on the drying and rehydration of cuboid agar gel pieces is discussed here. Comparison with Glucidex 21D, and also the subsequent effect of sugar addition on the structure and mechanical properties is discussed in the following sections.

As discussed in section 3.4.1, some moisture content variability existed between the different drying techniques. However, since the supercritical drying method used in this chapter allowed drying to lower moisture contents than the method used in chapters 2 and 3, results were more comparable for supercritical, air and freeze dried gels.

Figure 4.2 shows photographic images of the air dried, freeze dried and supercritically dried gels, containing 5%, 10%, 20% and 30% sucrose, before and after rehydration. In air dried and supercritically dried gels the addition of sucrose to the agar gel significantly improved the appearance and dried structure of the gel, resulting in less volumetric shrinkage. Slightly less shrinkage was observed for gels which had been supercritically dried compared with air dried gels. However, air dried gels expanded to similar volumes of supercritically dried gels, following rehydration. Those gels containing 0% sucrose exhibited a high degree of shrinkage and structural damage which was not reversible upon rehydration. This was also previously observed in chapter 3 (section 3.4.3), for gels dried on a smaller scale, where suggested mechanisms for increased structural retention, upon sucrose addition, were discussed. However, for freeze dried gels, all gels exhibited minimal shrinkage, including those containing 0% sucrose. This is expected of freeze drying which is known to produce highly porous dried products and is in agreement with results seen in section 3.4.3. In fact, the most shrinkage and damage (albeit minimal) was observed in freeze dried gels containing 30% sucrose. This is discussed in relation to rehydration properties, below.

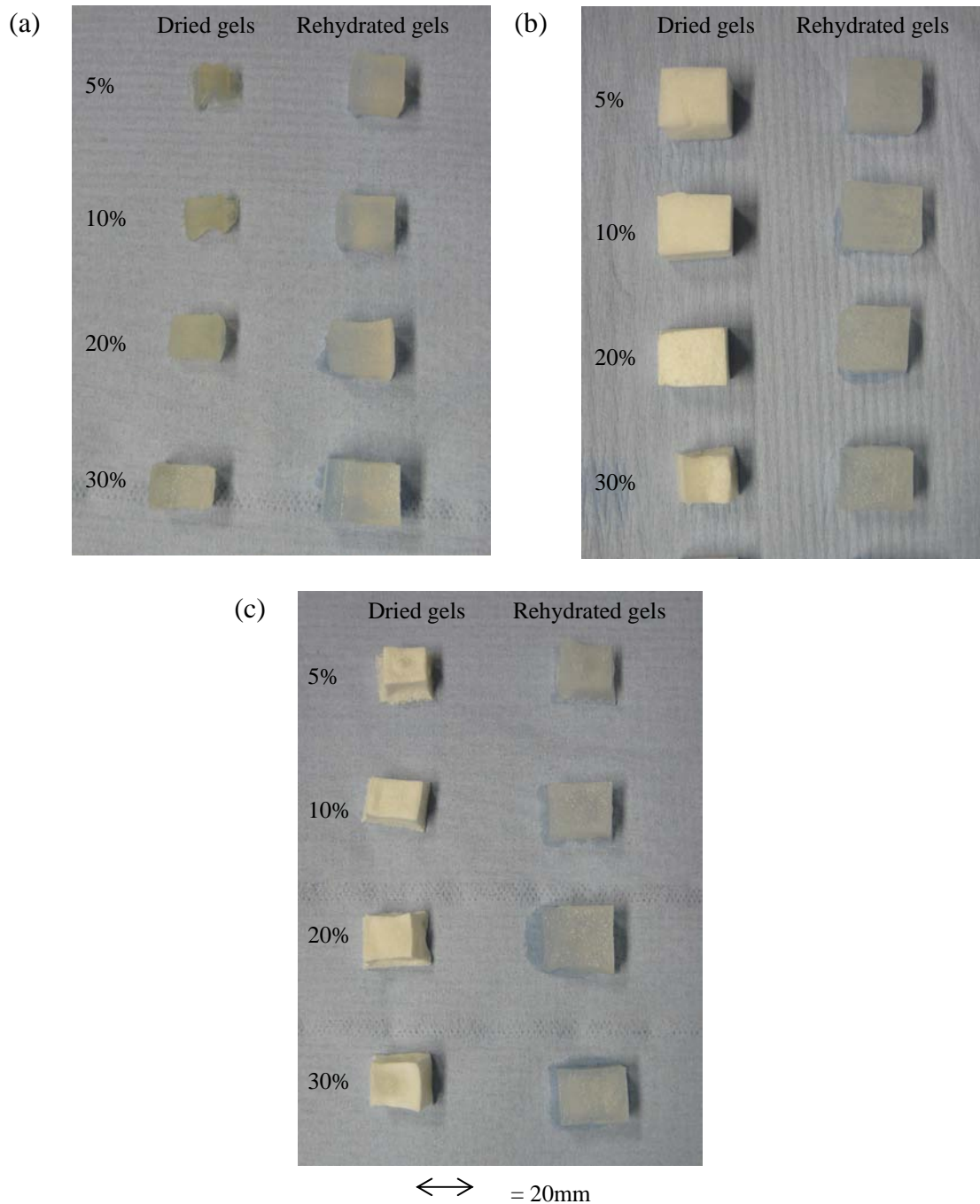


Figure 4.2 Photographs comparing the visual appearance of (a) air dried, (b) freeze dried and (c) supercritically dried 2% agar gel pieces, before and after rehydration (84000 seconds, 21°C), made up with different concentrations of sucrose (5%, 10%, 20% or 30%).

Upon rehydration, freeze dried gels regained the largest volume (up to 100%) compared with air dried and supercritically dried gels which regained some volume, but never 100% of the original pre-dried gel volume (Figure 4.2 (a), (b) and (c)). This is not illustrated pictorially in Figure 4.2

as no image of the pre-dried gel (to scale) is available. However, some indication of the level of volume regained is given by the extent of rehydration, indicated by the NMC (where 1 equals the initial moisture content before drying), illustrated in Figure 4.3, since those gels that up took more water generally also regained a larger volume.

Freeze dried gels experienced fast rehydration to similar NMCs of the pre-dried gel (Figure 4.3 (b)). Air dried gels and supercritically dried gels experienced rehydration of up to 60% and 65% of the original moisture content, respectively – the most being associated with those gels containing increased levels of sucrose (Figure 4.3 (a) and (c)). However, in the case of freeze dried gels, containing 20% and 30% sucrose, rehydration was slightly inhibited. This was thought to be due to the increased shrinkage seen in the photographic images for freeze dried gels containing 30% sucrose, compared with freeze dried gels containing <30% sucrose (Figure 4.2 (b)). It was hypothesised that too much sucrose may in fact have a detrimental effect on the structure achieved during freeze drying. Nonetheless, addition of up to 10% sucrose was shown to assist rehydration of freeze dried gels, both here and in chapter 3 (section 3.4.6).

The addition of sucrose has been shown to decrease freezing times of agar since less water is available and therefore the size of ice crystals upon freezing are reported to be smaller in systems with a higher sucrose concentration (Fuchigami and Teramoto 2003; Arunvanart and Charoenrein 2008). During freeze drying, voids are then created in spaces that were originally occupied by these ice crystals therefore smaller ice crystals may results in smaller voids which could restrict rehydration and would explain rehydration results observed here.

It is also possible that the addition of >20% sucrose causes some disruption to the gel network and/or reduced gel porosity, for example through competition of water binding between agar and sucrose solvation. However, the effect of this ‘damage’ on rehydration properties is minimal and >0.9 NMCs are still reached for all samples after 30000 seconds (Figure 4.3 (b)).

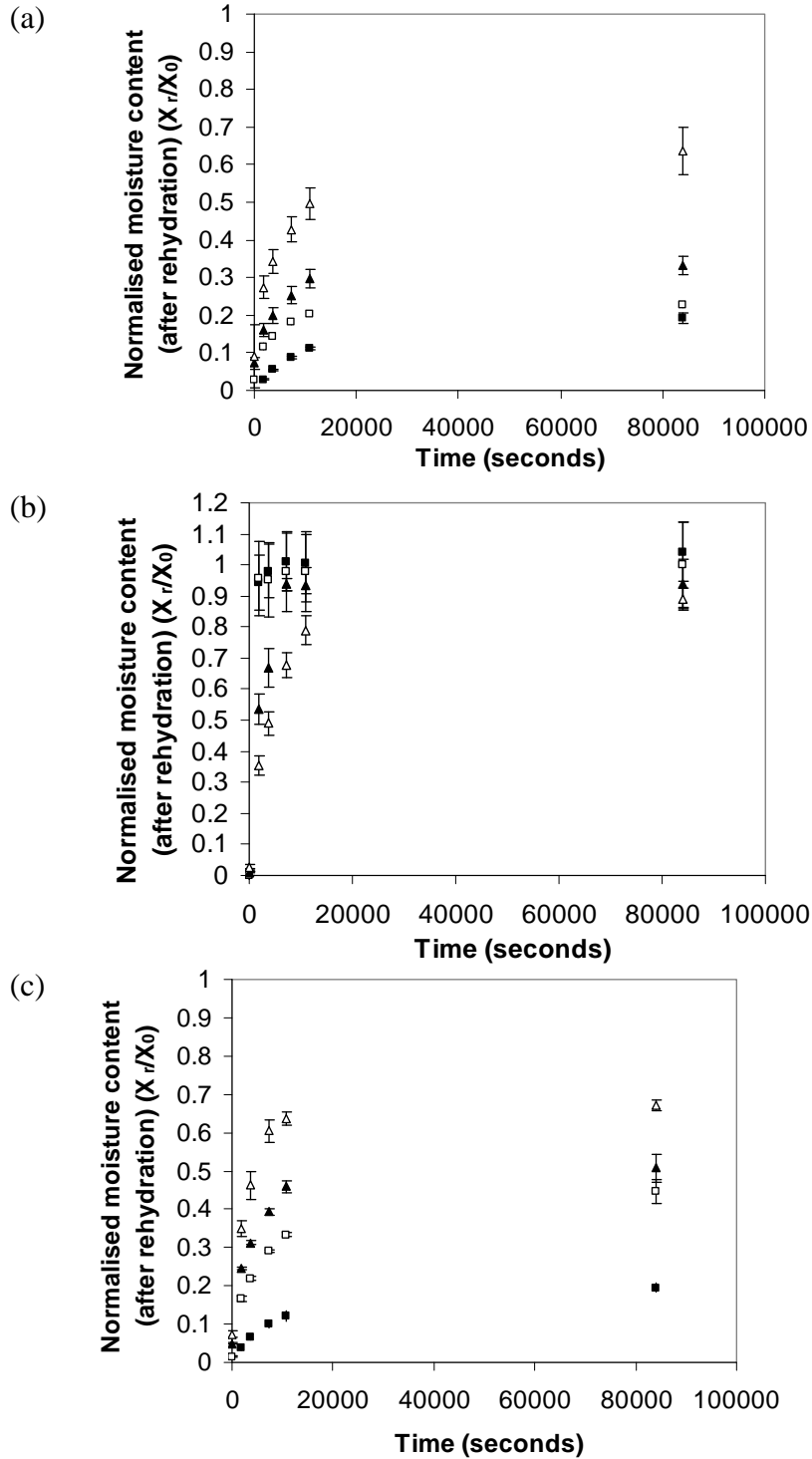


Figure 4.3 Rehydration (at 21°C) of (a) air dried, (b) freeze dried and (c) supercritically dried sucrose-infused agar gels, containing: 5% sucrose (black squares); 10% sucrose (open squares); 20% sucrose (black triangles); and 30% sucrose (open triangles). Note: NMC scale for (b) freeze dried gels goes from 0 to 1.2 rather than 0 to 1.

Rehydration properties of air dried gels were similar to those seen in chapter 3 for gels containing 10% sucrose, although the values cannot be directly compared due to the difference in the size of the gel pieces: here a maximum value of 0.2 NMC was reached, compared with a value of 0.3 NMC for the equivalent gels dried in chapter 3. Addition of a higher concentration of sucrose (30%) was also investigated in this chapter to see the influence on the rehydrated NMC and how much of the original moisture content (NMC = 1) could be achieved through rehydration. A significant increase in rehydration potential was observed in gels containing 30% sucrose, allowing 0.6 NMC to be achieved after 84000 seconds rehydration. In contrast, only 0.2 NMC could be reached at 5% sucrose (Figure 4.3 (a)). Similar results were obtained for supercritically dried gels: addition of 30% sucrose to the agar gel pieces enabled 0.65 NMC to be achieved, upon rehydration.

In conclusion, there was no advantage in the rehydration properties of gels dried using $\text{scCO}_2(\text{pure})$ when compared with those dried by air drying or freeze drying. However, the effect of the drying technique in relation to structure and mechanical properties is discussed in the following sections (4.4.3 and 4.4.4).

4.4.2 The effect of Glucidex 21D addition (and comparison with sucrose addition) on the drying and rehydration of agar gel pieces, dried using air, freeze and supercritical drying techniques

An alternative sugar, Glucidex 21D, was added to agar gels and is compared here to agar gels containing sucrose with respect to drying and rehydration properties. Experiments were not carried out for gels made up with a solution of 30% Glucidex 21D, but comparison of the gels containing 5%, 10% and 20% sugars were made.

Glucidex 21D is a polysaccharide, having a much longer sugar chain than sucrose which is simply a disaccharide. It was therefore hypothesised that Glucidex 21D would behave differently to sucrose when added to 2% agar gel and may therefore experience different drying and rehydration properties. This would allow potential tuning and manipulation of gel properties during drying

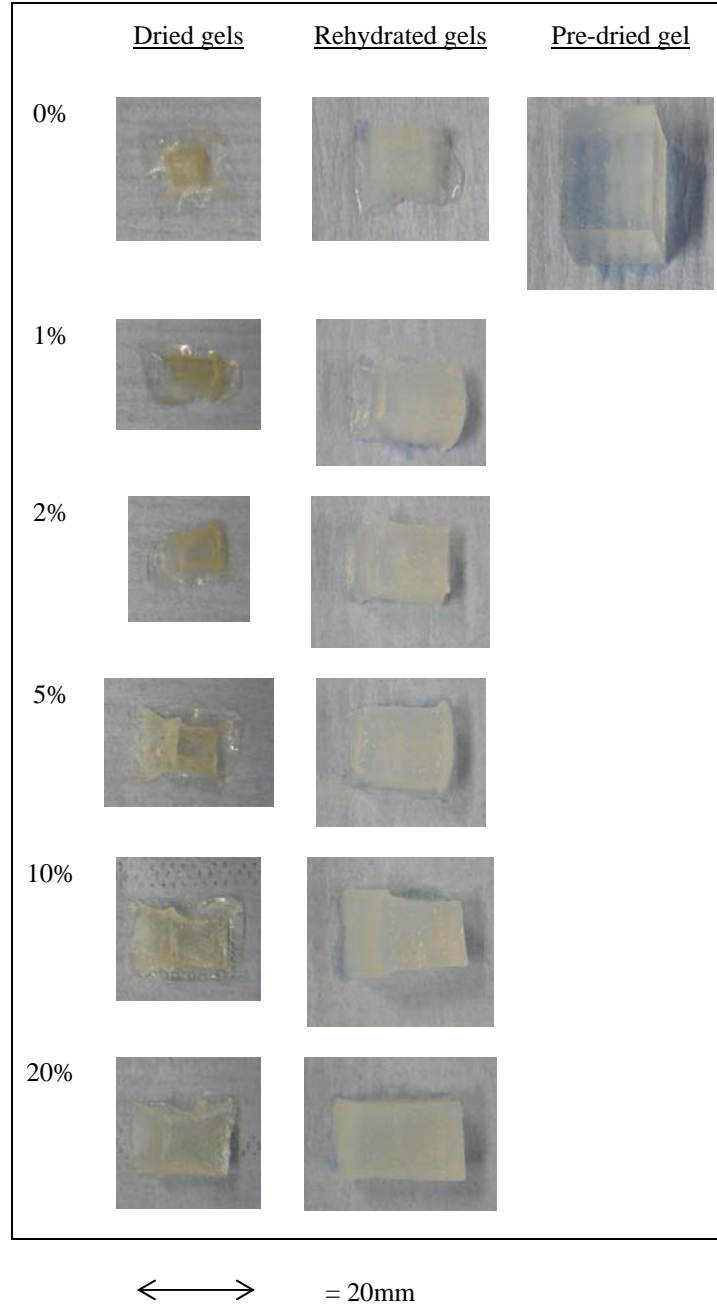


Figure 4.4 (a) Photographs comparing the visual appearance of air dried 2% agar gel pieces, before and after rehydration (84000 seconds, 21°C), made up with different concentrations of Glucidex 21D (0%, 1%, 2%, 5%, 10% or 20%).

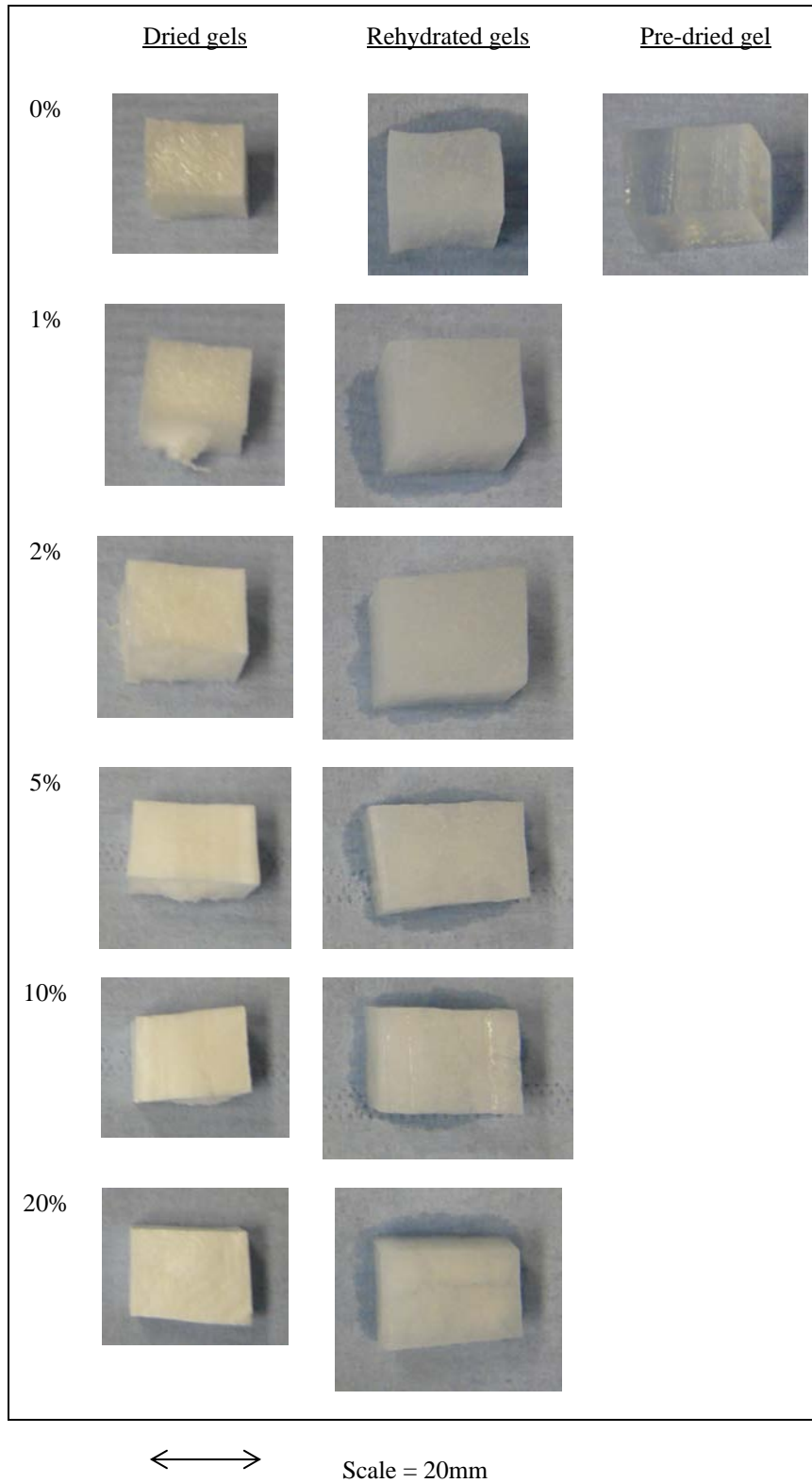


Figure 4.4 (b) Photographs comparing the visual appearance of freeze dried agar gel pieces, before and after rehydration (84000 seconds, 21°C), made up with different concentrations of Glucidex 21D (0%, 1%, 2%, 5%, 10% or 20%).

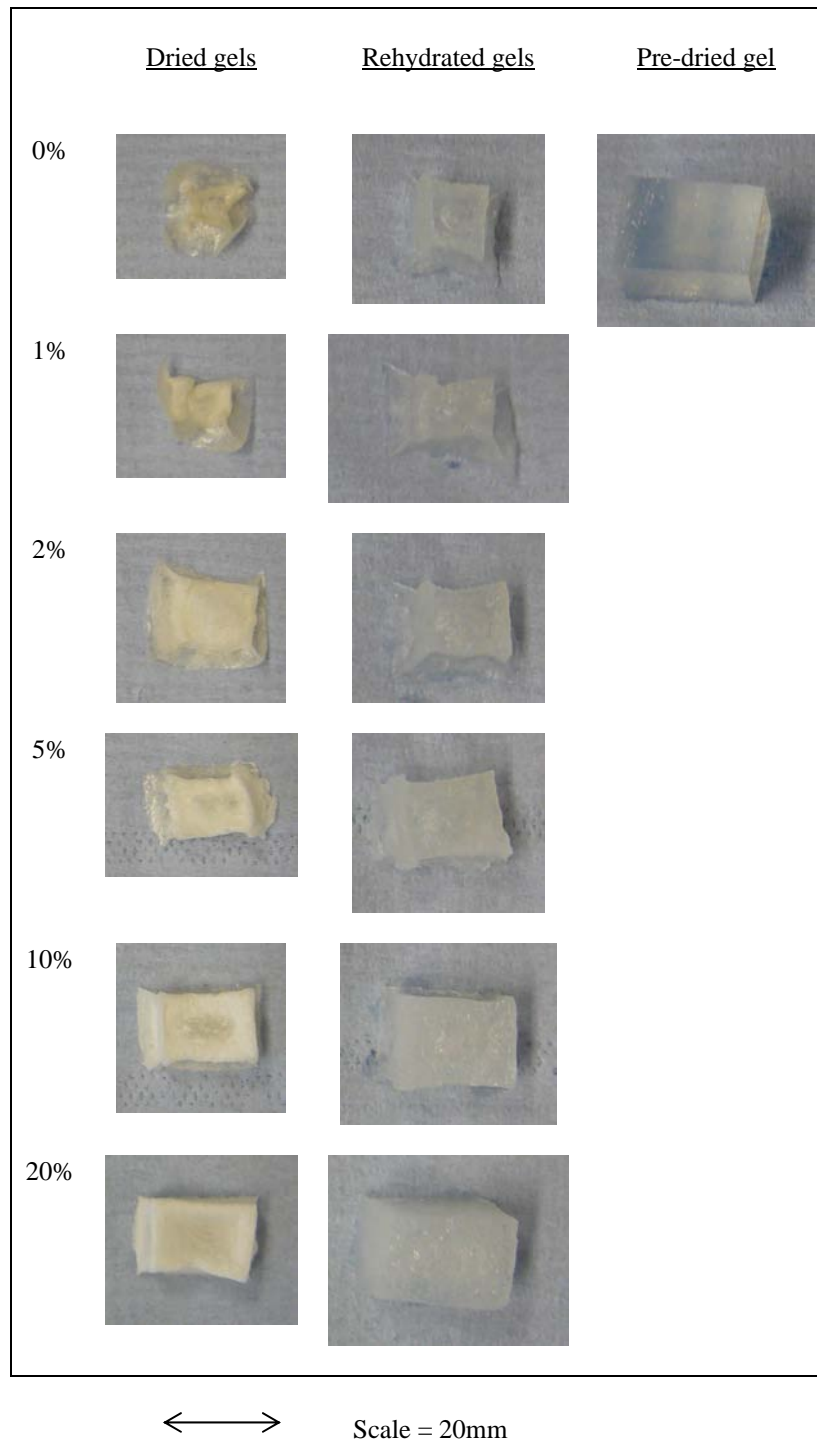


Figure 4.4 (c) Photographs comparing the visual appearance of supercritically dried 2% agar gel pieces, before and after rehydration (84000 seconds, 21°C), made up with different concentrations of Glucidex 21D (0%, 1%, 2%, 5%, 10% or 20%).

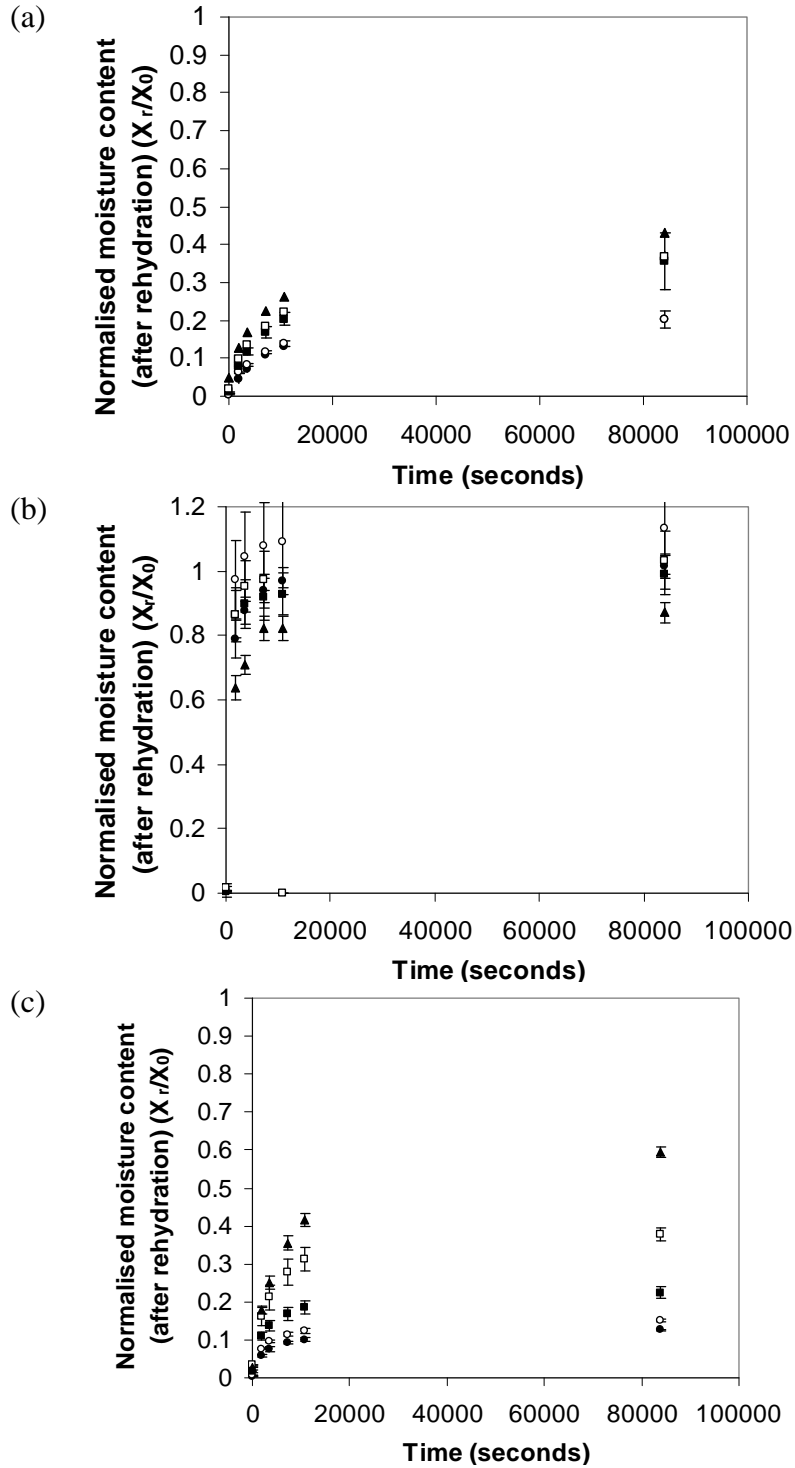


Figure 4.5 Rehydration (at 21°C) of (a) air dried, (b) freeze dried and (c) supercritically dried Glucidex 21-D-infused agar gels, containing: 1% Glucidex 21D (black circles); 2% Glucidex 21D (open circles); 5% Glucidex 21D (black squares); 10% Glucidex 21D (open squares); and 20% Glucidex 21D (black triangles). Note: NMC scale for (b) freeze dried gels goes from 0 to 1.2 rather than 0 to 1.

Chapter 4: Drying of agar gel on pilot plant scale equipment using supercritical carbon dioxide

The 21D gives a value for the sugars' dextrose equivalent (DE) which is a measure of the reducing power of the sugar. Dextrose is a synonym of D-glucose and refers to the pure, crystalline monosaccharide obtained after the total hydrolysis of starch. The reducing power of a sugar is measured by its ability to reduce solutions of alkaline copper sulphate (Fehling's solution) to cuprous oxide. Pure dextrose is defined with a DE of 100, therefore other sugars DEs are calculated as a percentage of the reducing value of pure dextrose.

Photographs of pre-dried, dried and rehydrated gels that were dried by air drying, freeze drying and supercritical drying are compared in Figure 4.4. Images were comparable to those obtained with gels containing sucrose: for air and supercritically dried gels, the most shrinkage was observed for those that had lower sugar levels; for freeze dried gels minimal shrinkage was exhibited for all sugar concentrations. For air and supercritically dried gels that contained 20% sugar, much of the volume and original water content was regained upon rehydration: supercritically dried gels containing 20% Glucidex 21D were able to reach 0.6 NMC (Figure 4.5 (c)), while those made up with 20% sucrose only reached 0.5 NMC (Figure 4.3 (c)); air dried gels containing 20% Glucidex 21D (Figure 4.5 (a)) were able to reach 0.4 NMC, while those made up with 20% sucrose reached 0.3 NMC (Figure 4.3 (a)). This slight improvement in rehydration properties was also seen for gels containing <20% sugar.

Freeze dried gels containing Glucidex 21D also showed increased NMCs of up to 1.2 upon rehydration (Figure 4.5 (b)) when compared with the sucrose equivalent gels which reached up to 1 NMC (Figure 4.3 (b)). Interestingly, this infers that the gels take on more water than they originally held before drying. This was however only seen for gels containing 2% Glucidex 21D. Gels that contained 20% Glucidex 21D, exhibited hindered rehydration, in the same way that freeze dried gels containing 20% and 30% sucrose did. 100% of the total original moisture content was never reached for these gels. However, rehydration was still good and 100% of the original moisture content was reached for all other samples in less than 30000 seconds.

A possible explanation for the improved rehydration seen with Glucidex 21D is that the longer chain sugar (Glucidex 21D) has the ability to maintain a more open gel structure than a shorter chained sugar, such as sucrose, enabling improved rehydration properties. The interactions, expected to occur between agar and sucrose (increased cross linking of the polymer chains and

reduced helix aggregation, which are discussed further in section 3.4.3) may also be occurring in a stronger and/or exaggerated way with Glucidex 21D. For example, the longer chain sugar molecules in Glucidex 21D may increase the cross linking and reduce the helix aggregation further.

Specific dried and rehydrated properties of gels containing sucrose and Glucidex 21D are discussed in the following sections, including mechanical textural properties (section 4.4.3) and internal gel structure (section 4.4.4).

4.4.3 Texture analysis of rehydrated gel pieces, containing sucrose and Glucidex 21D, to measure hardness

As discussed in section 3.4.7, texture is an important attribute of foods for sensorial perception, transport, and storage of the product. Measurement of the mechanical properties of a food, such as hardness, gives an indication of the food texture. The force required to puncture gels, containing between 5% and 30% sucrose and 0% and 20% Glucidex 21D were measured before drying and after air, supercritical and freeze drying followed by rehydration, to indicate the impact of the process upon the hardness of the gel (Figure 4.6).

For both sucrose and Glucidex 21D-containing gels, freeze drying appeared to cause a loss in gel hardness compared with the pre-dried gel (Figure 4.6 (a) and (b) (diagonal striped bars)). Rehydrated gels had a puncture force of about 0.1 N, compared with ~0.5 N before drying-rehydrating. The puncture force was very consistent and did not change with the percentage of added sugar – all concentrations of sugar required low forces to puncture the samples. This was thought to be due to the freeze drying technique, which causes open, porous, fragile structures. In chapter 3, the puncture force of the dried gel was investigated and linked to the voidage of the dried gels, measured by x-ray micro-CT. The voidage was higher in freeze dried gels compared with those dried using $\text{scCO}_2(\text{pure})$, which had a lower voidage and exhibited a higher puncture force.

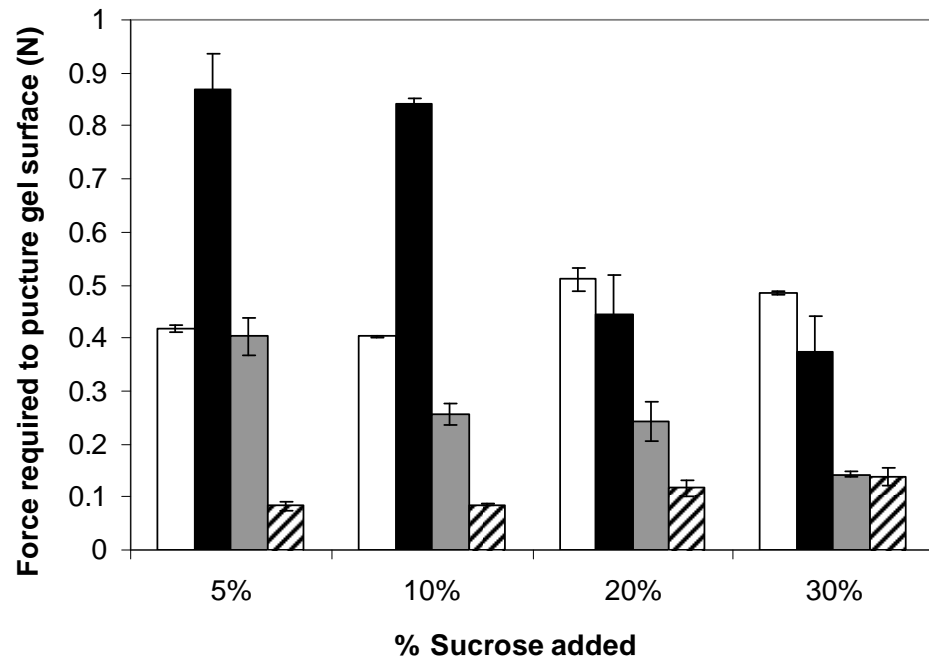
In contrast, rehydrated air dried gels that contained <20% sugar (sucrose or Glucidex 21D) exhibited a significant increase in the force required to puncture the gel, when compared with that for pre-dried gels (Figure 4.6 (a) and (b) (black bars)). This observation is thought to be due

to occurrence of irreversible shrinkage and case hardening. For gels containing 20% and 30% sugar, the puncture force was comparable to that of the pre-dried gel, suggesting that sugar addition may have a favourable effect on maintaining the texture of the original gel. This is likely to be due to reduced shrinkage and case hardening, upon sugar addition.

Rehydrated supercritically dried gels experienced the closest puncture forces (when compared with air and freeze dried-rehydrated gels) to those of the pre-dried gel, at the widest range of sugar concentrations (Figure 4.6 (a) and (b) (grey bars)). Similarly to air dried gels, higher puncture forces were associated with lower concentrations of sugar. This is thought to be due to the effect of sugar levels on gel volume retention during drying – higher sugar levels were previously shown to visibly reduce the shrinkage of gels (observed in Figure 4.2 and Figure 4.4 for sucrose and Glucidex 21D, respectively) and therefore were expected to result in a more open, less dense gel network, with a lower associated puncture force. This effect however, was more exaggerated in air dried-rehydrated gels. The extra contribution of case hardening and also increased shrinkage (compared with supercritically dried gels), particularly at lower sugar concentration, during air drying is expected to account for this.

Overall, supercritically dried-rehydrated gels exhibited more comparable puncture forces to those of the pre-dried gel. This was particularly the case at lower sugar concentrations (5-20%). However, at sugar concentrations >20% air dried-rehydrated gels exhibited closer puncture forces to those of the pre-dried gel. Therefore, supercritical drying followed by rehydration appears to result in a more favourable gel texture to that produced through freeze drying followed by rehydration, since it is more comparable to the pre-dried gel texture. Supercritically dried-rehydrated gels also exhibit a more favoured gel texture compared to air dried-rehydrated gels, but only at particular sugar concentrations.

(a)



(b)

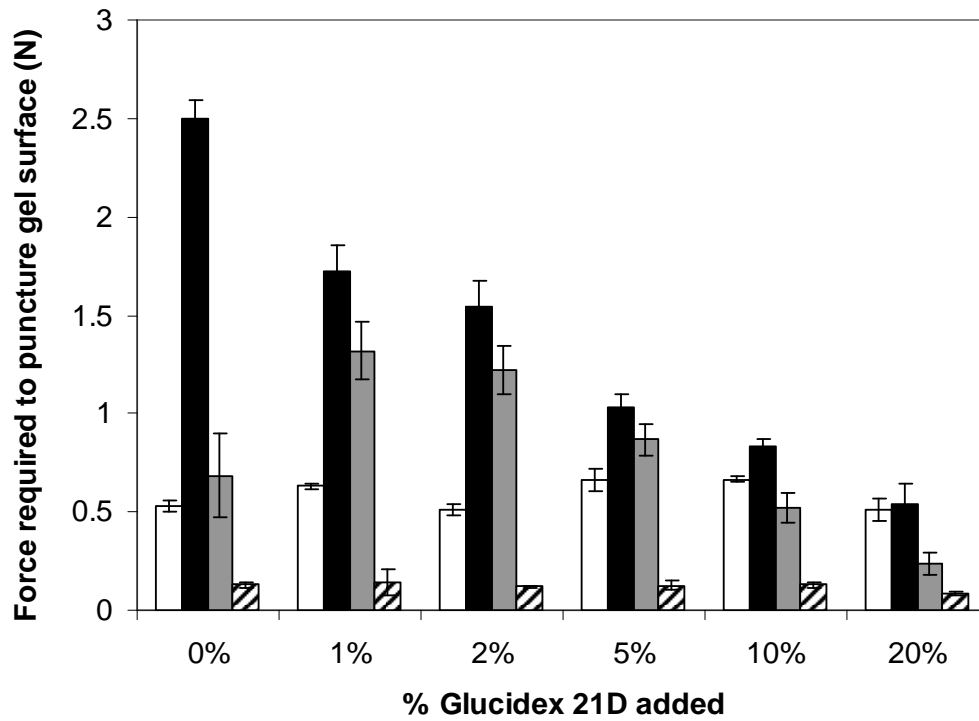


Figure 4.6 Comparison of the force required to puncture 2% agar gel pieces before drying (white), and after air (black), supercritical (grey) and freeze (diagonal stripes) drying, all followed by rehydration. Gels were made up with varying concentrations of (a) sucrose (5-30%) or (b) Glucidex 21D (0-20%).

4.4.4 X-ray micro-computed tomography for analysis of the structure of gels containing sucrose and Glucidex 21D

X-ray micro-CT images of air, freeze and supercritically dried agar gel pieces containing 0%, 20% and 30% sucrose and 0% and 20% Glucidex 21D are shown in Figure 4.7. Shadow radiograph images for each sample were initially collected and then reconstruction of this data allowed 2-D horizontal slices through the cuboidal sample to be viewed.

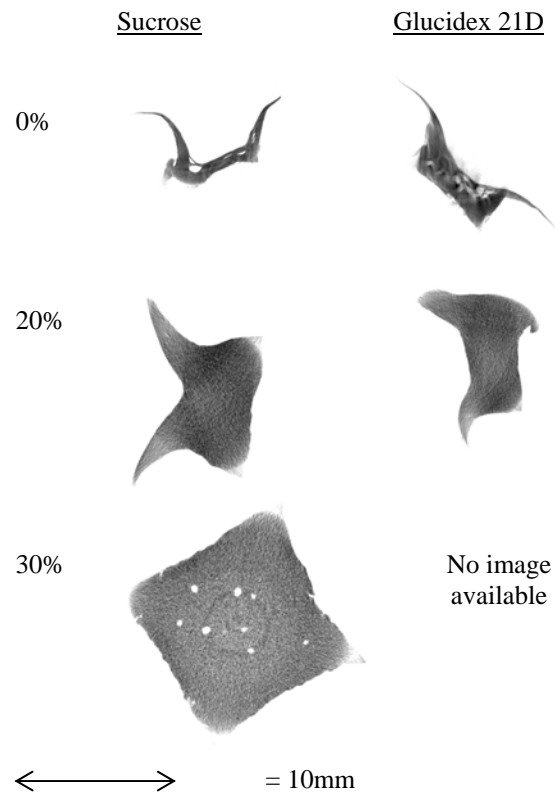


Figure 4.7 (a) 2-D x-ray micro-CT images (taken horizontally through the gel) of air dried agar gels, containing (0, 20 or 30%) sucrose or (0 or 20%) Glucidex 21D.

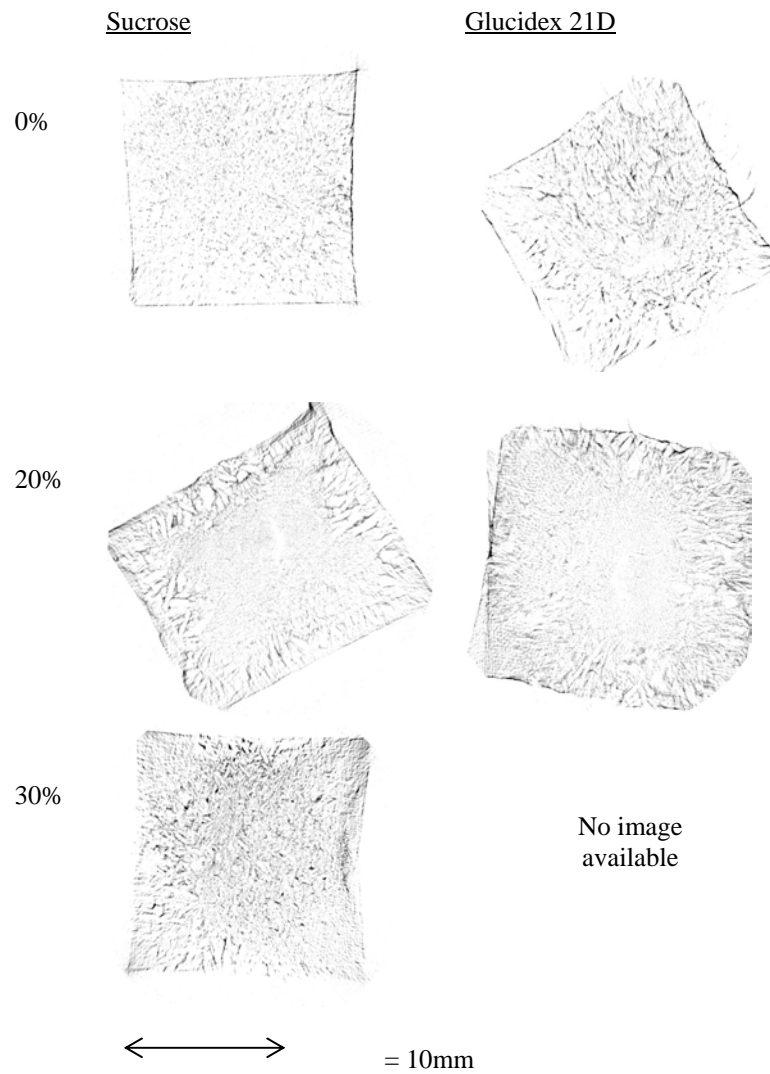


Figure 4.7 (b) 2-D x-ray micro-CT images (taken horizontally through the gel) of freeze dried agar gels, containing (0, 20 or 30%) sucrose or (0 or 20%) Glucidex 21D.

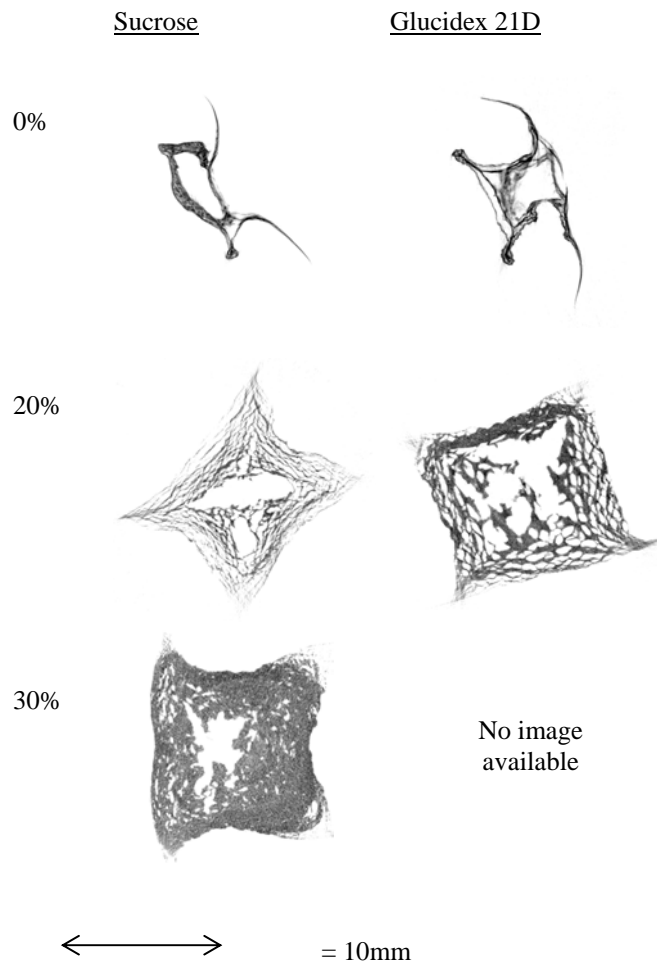


Figure 4.7 (c) 2-D x-ray micro-CT images (taken horizontally through the gel) of supercritically dried agar gels, containing (0, 20 or 30%) sucrose or (0 or 20%) Glucidex 21D.

As seen in chapter 3 (Table 3.2), air dried gels containing 10% sugar were shrivelled and very dense compared with the supercritically and freeze dried equivalents. Similarly, gels that were air dried here exhibited collapsed, dense structures, indicated by the darkness of the x-ray images. At lower sugar concentrations, particularly 0% sugar, a high degree of deformation was observed while at higher sugar concentrations less deformation occurred. The mechanism of this effect was discussed in section 3.4.2 and was thought to be due to interactions occurring between the sucrose and the agar structure: reducing the extent of helix aggregation, increasing the cross linking of the polymer chains, and increasing the elasticity of the polymer. Alternatively, the sugar may simply act as an inert filler, taking up some of the gel volume and therefore preventing the complete collapse of the structure.

Chapter 4: Drying of agar gel on pilot plant scale equipment using supercritical carbon dioxide

At 30% sucrose, even gels that had been air dried (which typically causes shrinkage and collapse), retained their initial cuboidal shape, despite some shrinkage occurring. However, the gels were dense and appeared to have undergone some structural changes – evidenced by the creation of pores/holes, observed in the x-ray image of the dried structure (Figure 4.7 (a)). These may assist in the uptake of water during rehydration. Photographic images in Figure 4.2 illustrate that some of the volume that was lost during drying, was regained upon rehydration.

Freeze drying, in contrast to air drying, results in gels with much lower density (Figure 4.7 (b)). The overall volume of the pre-dried gel was retained and a more uniform structure was obtained. Moreover, the sugar concentration had a minimal effect on the volume achieved following drying. Although, as mentioned earlier (in sections 4.4.1 and 4.4.2), the sugar concentration, particularly higher concentrations, did appear to have an effect on the rehydration properties. This was thought to be due to sugar concentrations affecting the freezing time, during freeze drying, which consequently altered the crystal size formed and therefore the size of the voids formed within the gel structure. Difference in sizes of voids however, cannot be clearly identified in the x-ray images of freeze dried gels in Figure 4.7 (b). This has been discussed further in section 3.4.6, in relation to results obtained in chapter 3.

The supercritical drying process created a different structure to that obtained from both air and freeze drying (Figure 4.7 (c)). Higher sugar concentrations, as with air and freeze drying, were shown to reduce shrinkage during supercritical drying and at the highest percentage (30%) produced a denser gel network. The density of the gel pieces were in between that obtained during air and freeze drying and there were also large voids created in the centre of each of the piece of gel, at all sugar concentrations. The voids may be created during the drying process itself or during the depressurisation step, where expansion of the scCO_2 occurs as it becomes gaseous. Creation of voids, similar to this, had been previously seen during smaller scale supercritical drying but in this case was due to accidental fast depressurisation and/or the use of a co-solvent during drying (Table 3.3 (c)). The depressurisation could not be controlled as accurately on the large scale equipment used here as on the smaller scale equipment used in chapter 3. The depressurisation on the smaller scale equipment was controlled using an ABPR which enabled computer controlled depressurisation. It is therefore likely in the experiments discussed in this chapter that the initial stages of depressurisation were much faster than those

Chapter 4: Drying of agar gel on pilot plant scale equipment using supercritical carbon dioxide

experiments carried out on a smaller scale in chapter 3, providing an explanation for the creation of these voids. Takishima *et al.* (1997) reported that damage of aerogels could be caused during all stages of the supercritical drying process, and suggested that quick changes in composition, pressure and temperature should be prevented, especially for large aerogels.

Nevertheless, rapid depressurisation of plasticised polymers has been used beneficially, to foam polymer scaffolds for tissue engineering. As pressure is released, pockets of gas nucleate and grow in the plasticised polymer. Additionally, as the SCF is released from the polymer, the T_g increases until some point when the T_g is higher than the processing temperature, and the porous structure is set. This has been discussed in section 1.2.3 in more detail. It has not been confirmed whether the agar becomes plasticised here or not. However, it is likely that rapid depressurisation would have an effect on the structure, whether plasticised or not.

An alternative explanation may be that the loss of the water which stabilises the agar double helix may cause the agar structure to be less rigid and therefore break apart during the drying process, or the depressurisation step. Gels here were dried to lower NMCs, using the larger scale equipment, than those achieved in chapter 3, which may explain why this damage was not seen in gels dried on a smaller scale.

Despite differences seen previously, between rehydration properties of gels containing Glucidex 21D, compared with gels containing sucrose, there were not any significant differences visible in the x-ray images of freeze or air dried gels, containing the two different sugars. However, gels dried with $scCO_{2(pure)}$ which contained 20% Glucidex 21D, appeared to have a slightly larger volume than those which contained 20% sucrose, and they were also slightly denser. The volume difference may account for the increased NMC reached upon rehydration (Figure 4.3 (c) and Figure 4.5 (c)).

Overall, freeze dried gels retained the largest volume, resulting in porous open structures, while air dried gels experienced the most shrinkage, resulting in denser gels. Supercritically dried gels were in-between air dried and freeze dried gels, in terms of volume and density. The influence of these structural differences on the rehydration properties and mechanical properties is discussed in sections 4.4.1, 4.4.2 and 4.4.3.

4.4.5 Effect of supercritical process conditions on gel structure

Experiments investigating the effect of processing conditions on the gels' structure and rehydration properties were discussed in chapter 3 (section 3.4.4). It was concluded that no significant differences were seen when changing the depressurisation rate and flow rate. However, a very small change in rehydration rate was seen for gels dried at the lowest flow rate (1 l/minute) and depressurisation rate (0.4 MPa/minute), compared with those dried at the highest flow rate (3 l/minute) and depressurisation rate (1.6 MPa/minute) (Figure 3.14), suggesting that bigger changes in flow rate or depressurisation rate may result in a more significant change in structure or rehydration properties. Due to limitations of the equipment used in chapter 3, higher flow rates and depressurisation rates could not be investigated. However, the pilot plant scale equipment used in this chapter allowed larger changes in flow rate to be investigated. Depressurisation could not be accurately controlled though, and since fast depressurisation may have caused permanent damage to the high pressure seals, this was not investigated. Experiments were carried out on (2% w/v) agar gels, containing varying quantities of sucrose.

4.4.5.1 Drying and rehydration of agar gels containing sucrose

For the previous experiments discussed in this chapter, supercritical drying conditions were set at 10 MPa, 40°C, 1100-1200 l/hour flow rate, and 0.1-0.15 MPa/minute depressurisation rate.

In this section larger changes in flow rate were investigated: 900 l/hour, 200 l/hour and an experiment was also carried out which combined the two flow rates - 200 l/hour for 7200 seconds, followed by 900 l/hour for 10800-14400 seconds. It was hypothesised that the lower flow rate may help to preserve structure, during the earlier stages of drying, where more moisture is available to be removed. Depressurisation rate was maintained 0.1-0.15 MPa/minute.

The experimental set up was also changed slightly, allowing conditions of 14 MPa and 50°C to be reached which were more comparable with those experiments previously seen in chapters 2 and 3. To allow comparison with results discussed in chapter 3, cylindrical gel pieces were used and were of the same size as those pieces used in chapter 3 (length = 12 mm and diameter = 5 mm).

Chapter 4: Drying of agar gel on pilot plant scale equipment using supercritical carbon dioxide

Results for rehydration (at 25°C) of supercritically dried gel pieces (containing varying percentages of sucrose) are shown below, at different flow rates (Figure 4.8). Gels dried at 900 l/minute (Figure 4.8 (a)) which contained 20% sucrose were able to rehydrate to a NMC of ~0.3. Those containing 10% rehydrated to a NMC of 0.2. This is comparable with gels that contained 10% sucrose which were supercritically dried on a smaller scale (1 l/minute CO₂ flow rate and 0.4 MPa/minute depressurisation) (Figure 3.13) and which rehydrated to 0.2-0.3 NMC, suggesting that supercritical drying conditions, or the scale of the drying equipment, did not affect the rehydration properties significantly.

However, gels that were dried at 200 l/hour showed improved rehydration properties, compared to those dried at a flow rate of 900 l/hour, particularly at high sucrose concentrations (Figure 4.8 (b)). At 30% sucrose gel pieces were seen to reach 0.5 NMC, suggesting a slower drying regime may favorably maintain or manipulate the gel structure in a way that improves the rehydration properties.

The increased rehydrated NMC measured for gels dried at 200 l/hour was not seen for the drying regime which started with 200 l/hour flow rate and ended with 900 l/hour (Figure 4.8 (c)). It should be noted that the depressurisation in this experiment was faster (an average of ~0.2 MPa/minute) than the other two experiments (0.1-0.15 MPa/minute), which were more closely controlled. This led to some of the gel pieces becoming physically damaged due to the fast expelling of the CO₂ from the gel structure. This may account for the poorer rehydration seen in comparison to the gels dried at 200 l/hour, and the inability to regain as much water. This however, does confirm that damage to the structure during depressurisation is possible, and may be the cause of voids seen in supercritically dried gels earlier in this chapter (Figure 4.7).

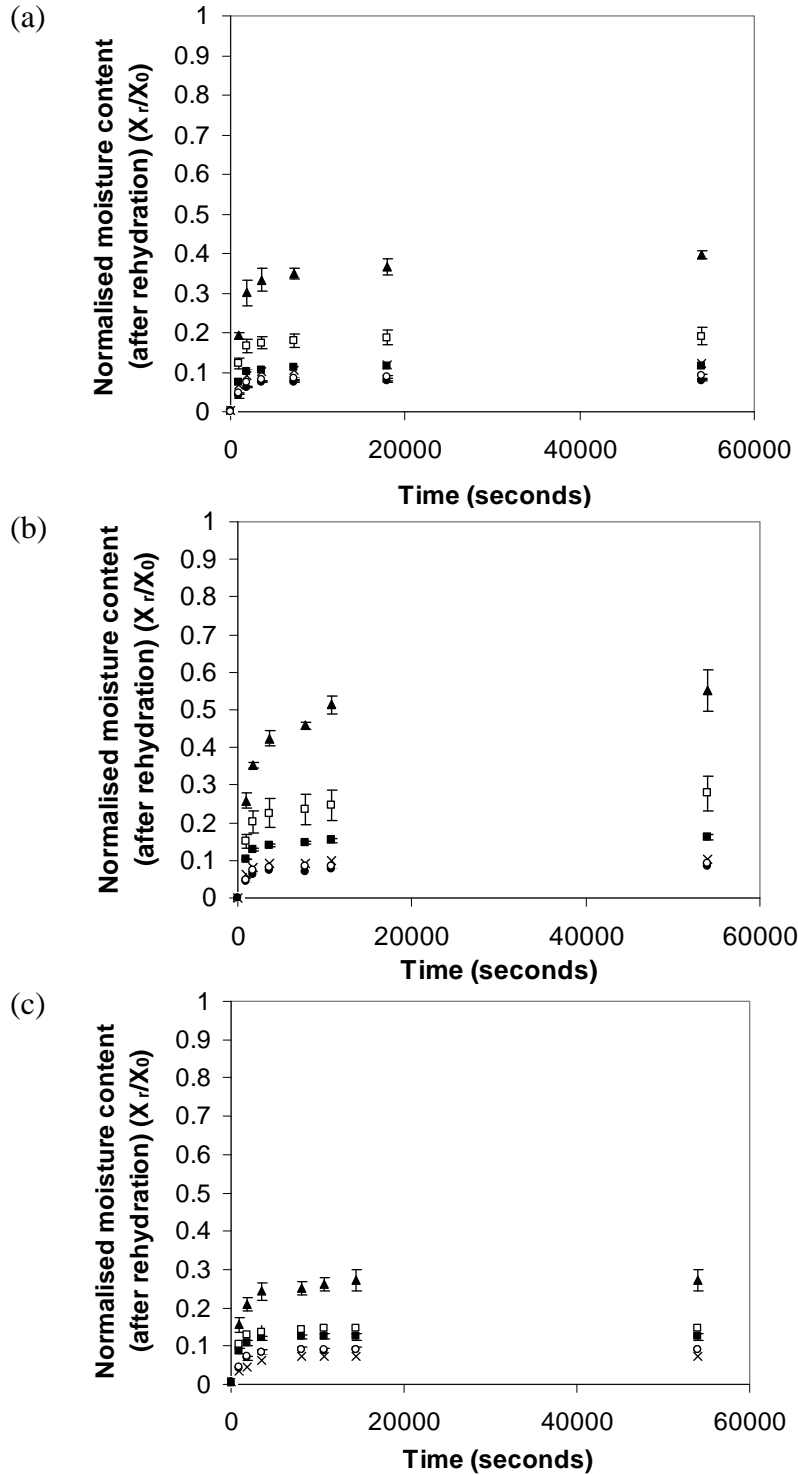


Figure 4.8 Rehydration of sucrose-infused agar gel cylindrical pieces, dried using a scCO₂ flow rate of (a) 900 l/hour, (b) 200 l/hour or (c) 200 l/hour for 7200 seconds, followed by a flow rate of 900 l/hour for 3-4 hours. Gels also contained different concentrations of sucrose: 0% sucrose (crosses); 1% sucrose (black circles); 2% sucrose (open circles); 5% sucrose (black squares); 10% sucrose (open squares); and 20% sucrose (black triangles).

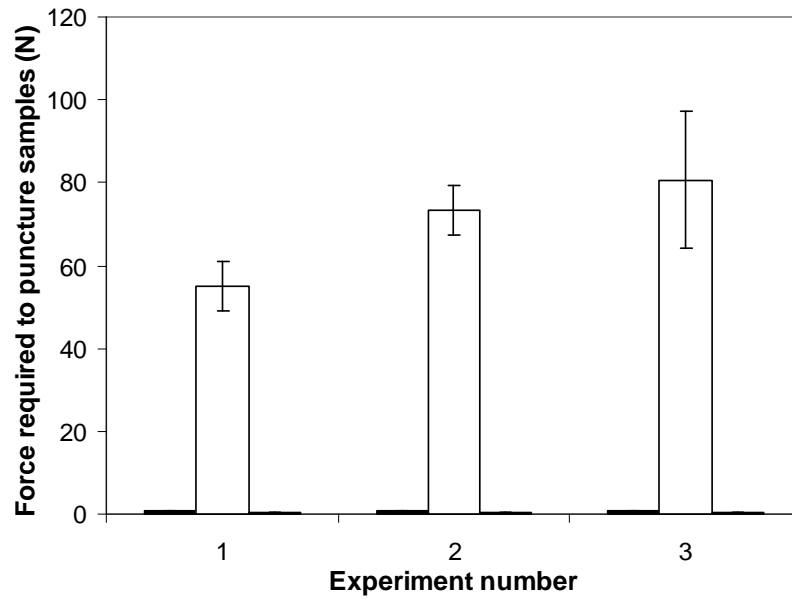
4.4.5.2 Texture analysis of dried and rehydrated agar gel to measure hardness

Gels containing 10% sucrose from each experiment, using different scCO₂ flow rates (900 l/hour, 200 l/hour and 200 l/hour followed by 900 l/hour), were dried and rehydrated. The force required to puncture the cylindrical samples was measured before drying, after drying and after rehydration (Figure 4.9 (a) and (b)). The same analysis was also carried out for gels containing 20% sucrose (Figure 4.9 (c) and (d)). The dried samples, as would be expected, required a much higher force to puncture the samples so are shown on a different scale (Figure 4.9 (a) and (c)). The results for the pre-dried gels and for the samples following rehydration are shown individually in Figure 4.9 (b) and (d).

As seen previously, increasing the sugar concentration causes a decrease in the force required to puncture the gel pieces (Figures 4.6). Results seen here were of a similar magnitude and close to those results observed earlier in this chapter, despite the gel pieces being of a very different size and shape.

For gels containing 10% sucrose, the gel pieces that were dried at 200 l/hour followed by 900 l/hour appeared to require a slightly higher force to puncture them, while the lowest force required to puncture was associated with the gels that were dried at 900 l/hour. This was seen for dried gels before (Figure 4.9 (a)) and after rehydration (Figure 4.9 (b)). However, these differences are very minor and arguably could be down to experimental error, especially since the experiment carried out at 200 l/hour flow rate, followed by 900 l/hour had a faster depressurisation rate than the other experiments (discussed in section 4.4.5.1). Additionally, these differences were not observed in gels containing 20% sucrose, suggesting the flow rate during supercritical drying does not influence the force required to puncture the dried or rehydrated gels.

(a)



(b)

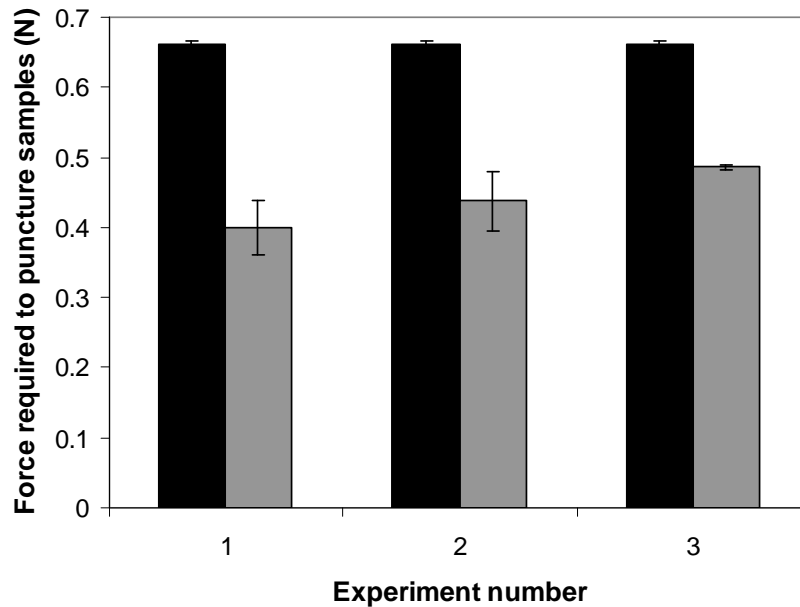
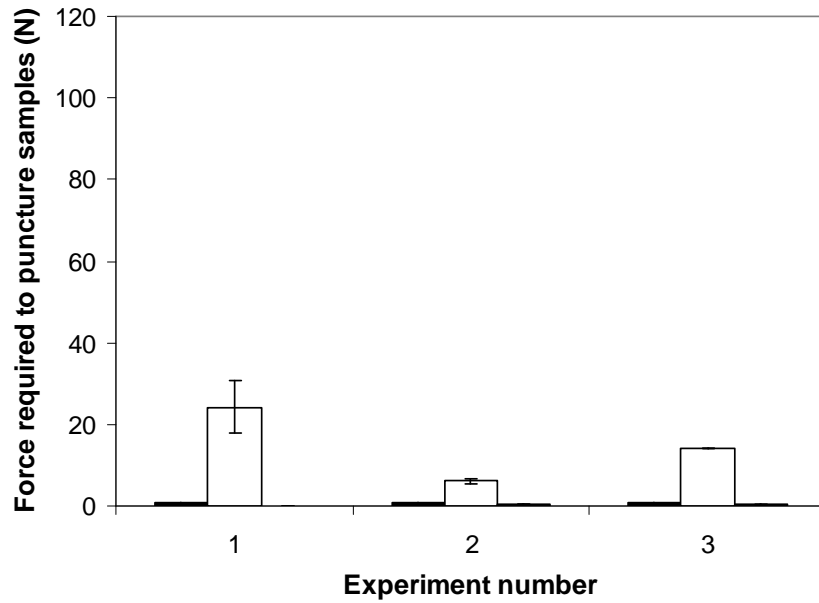


Figure 4.9 (a) & (b) Charts illustrating the force (measured in Newtons (N)) required to puncture agar gel pieces, containing 10% sucrose. Comparison of the texture of gels before supercritical drying (black bars), after supercritical drying (white bars) and after rehydration (grey bars), for experiments at flow rates of: 1. 900 l/hour; 2. 200 l/hour; and 3. 200 l/hour followed by 900 l/hour. Note, that results for before drying and after rehydration can be seen more clearly in chart (b) which is plotted on a different scale.

(c)



(d)

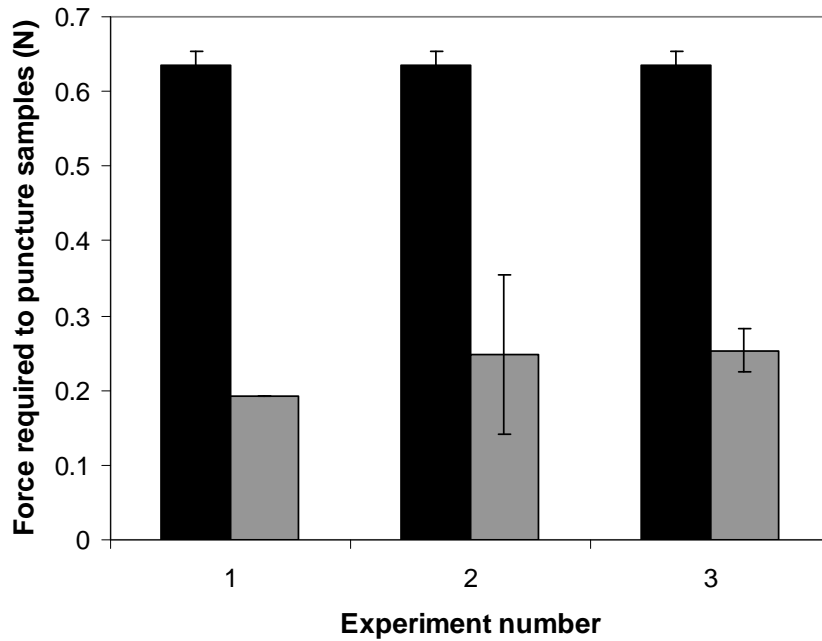


Figure 4.9 (c) & (d) Charts illustrating the force (measured in Newtons (N)) required to puncture agar gel pieces, containing 20% sucrose. Comparison of the texture of gels before supercritical drying (black bars), after supercritical drying (white bars) and after rehydration (grey bars), for experiments at flow rates of: 1. 900 l/hour; 2. 200 l/hour; and 3. 200 l/hour followed by 900 l/hour. Note that results for before drying and after rehydration can be seen more clearly in chart (d) which is plotted on a different scale.

4.4.5.3 X-ray micro-computed tomography and photographic images of cylindrical gels, dried using unmodified supercritical carbon dioxide at varying flow rates

Figure 4.10 and Figure 4.11 show photographic images and x-ray micro-CT images of dried and rehydrated gel pieces, containing varying percentages of sucrose, and dried at different flow rates. The gels are shown to scale, allowing comparison of the degree of shrinkage, and in the case of the photographic images, the gain in volume due to rehydration may also be observed.

There was no visible difference between the volume and appearance of gels dried at 900 l/hour (Figure 4.10 (a)), 200 l/hour (Figure 4.10 (b)), and a combination of 900 l/hour and 200 l/hour (Figure 4.10 (c)), observed in the photographic images. The x-ray micro-CT images however provide more detailed analysis, and a small difference was observed between the appearance of those gels dried at the combined flow rate (of 900 l/hour followed by 200 l/hour) and those dried at a single flow rate (Figure 4.11). This is more significant in gels containing 5% and 10% sucrose which appear to have a more dense structure with fewer voids, than equivalent gels dried at a single flow rate. The small internal structure difference may be a result of the different depressurisation rate employed accidentally. A combination of this structure difference, and the visible damage observed in some of the other gel pieces dried in this experiment (of which x-ray images are not available) are likely to account for the lower rehydration rates that were observed for those gels dried at 200 l/hour, followed by 900 l/hour. However, differences in rehydration properties seen between gels dried at 900 l/hour and those dried at 200 l/hour cannot be explained from x-ray micro-CT analysis, since no differences in the internal structure are seen using this technique.

Increased depressurisation rates (from small scale (chapter 3) to large scale (chapter 4) experiments) were hypothesised to be responsible for the formation of voids in the larger cuboidal gel pieces, during drying (discussed in section 4.4.3). However, the same depressurisation rates (for experiments using 200 l/hour or 900 l/hour) were used in this section, to dry smaller cylindrical gel pieces and no voids were formed. This suggests that the larger gels are more susceptible to void formation during depressurisation. This may be due to the opportunity of larger gels to hold more CO₂ which upon depressurisation becomes gaseous, expands and forms voids.

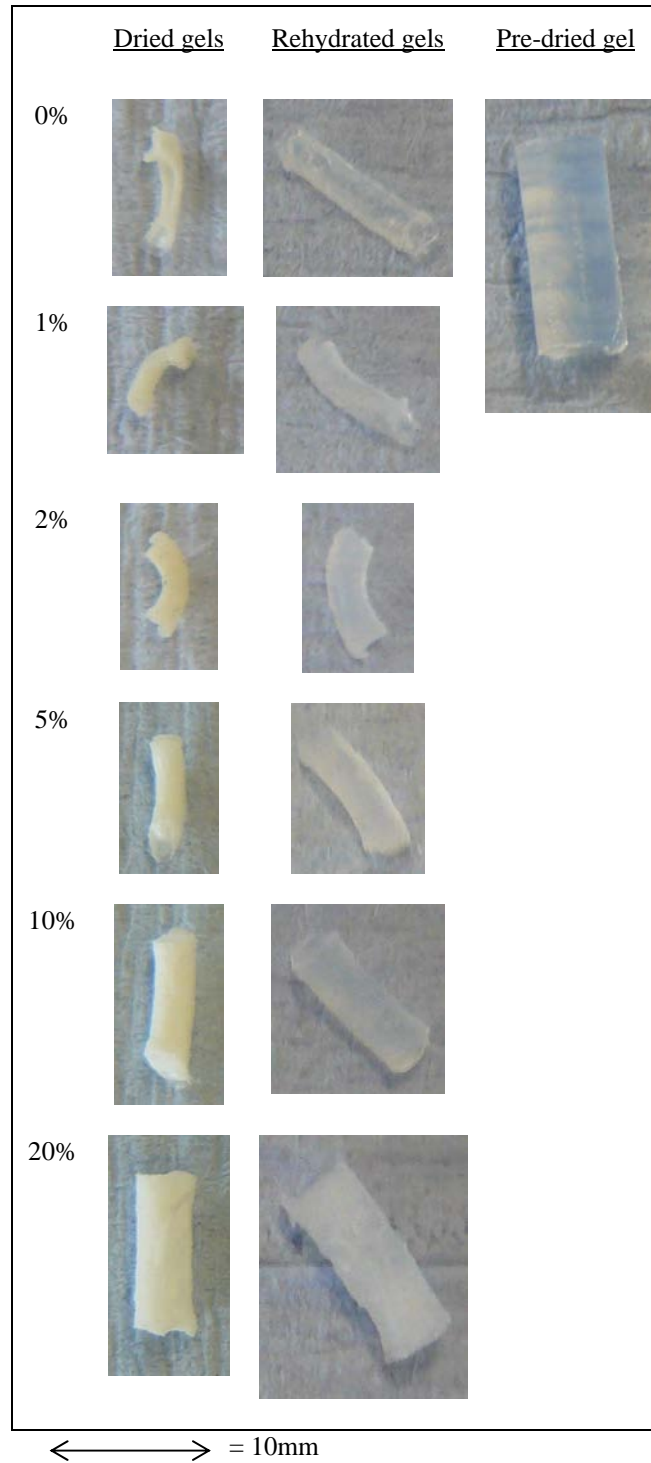


Figure 4.10 (a) Photographic images of supercritically dried agar gels and subsequently rehydrated gels, containing varying concentrations of sucrose (0-20%), dried at a flow rate of 900 l/hour.

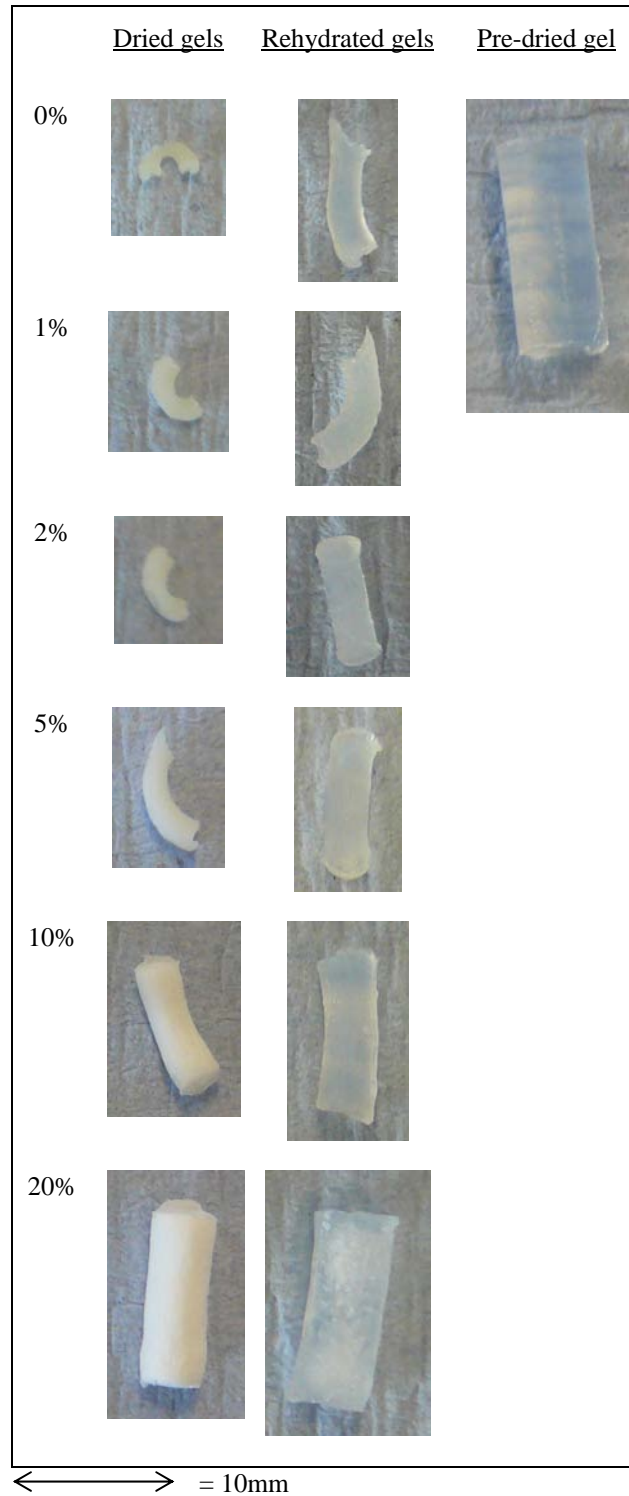


Figure 4.10 (b) Photographic images of supercritically dried agar gels and subsequently rehydrated gels, containing varying concentrations of sucrose (0-20%), dried at a flow rate of 200 l/hour

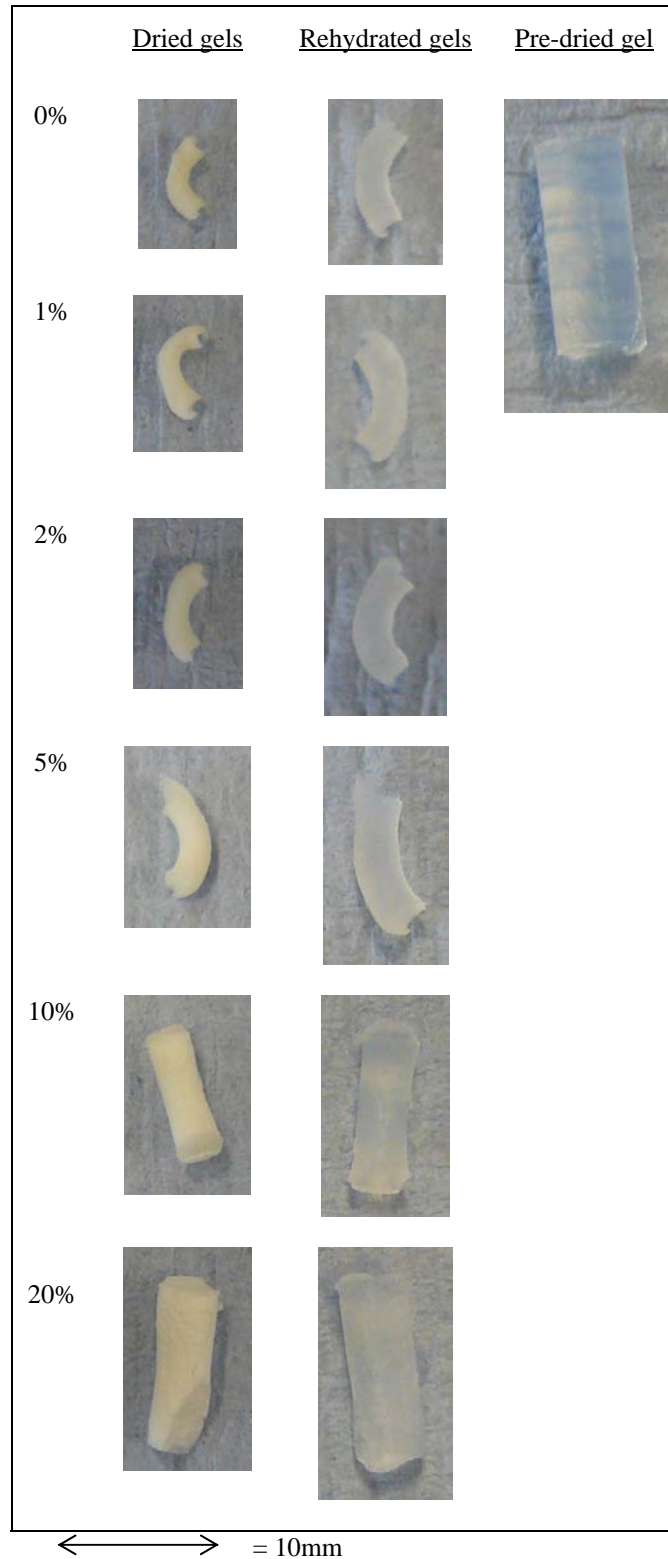


Figure 4.10 (c) Photographic images of supercritically dried agar gels and subsequently rehydrated gels, containing varying concentrations of sucrose (0-20%), dried at a flow rate of 200 l/hour followed by a flow rate of 900 l/hour.

Chapter 4: Drying of agar gel on pilot plant scale equipment using supercritical carbon dioxide

Despite these results being inconclusive, it can be concluded from comparison of the gels dried at 900 l/hour and 200 l/hour that the flow rate does not appear to have an effect on the gel structure, on both a pilot plant scale and a lab based scale (chapter 3, section 3.4.4). This is also consistent with the texture analysis results, discussed in section 4.4.5.2.

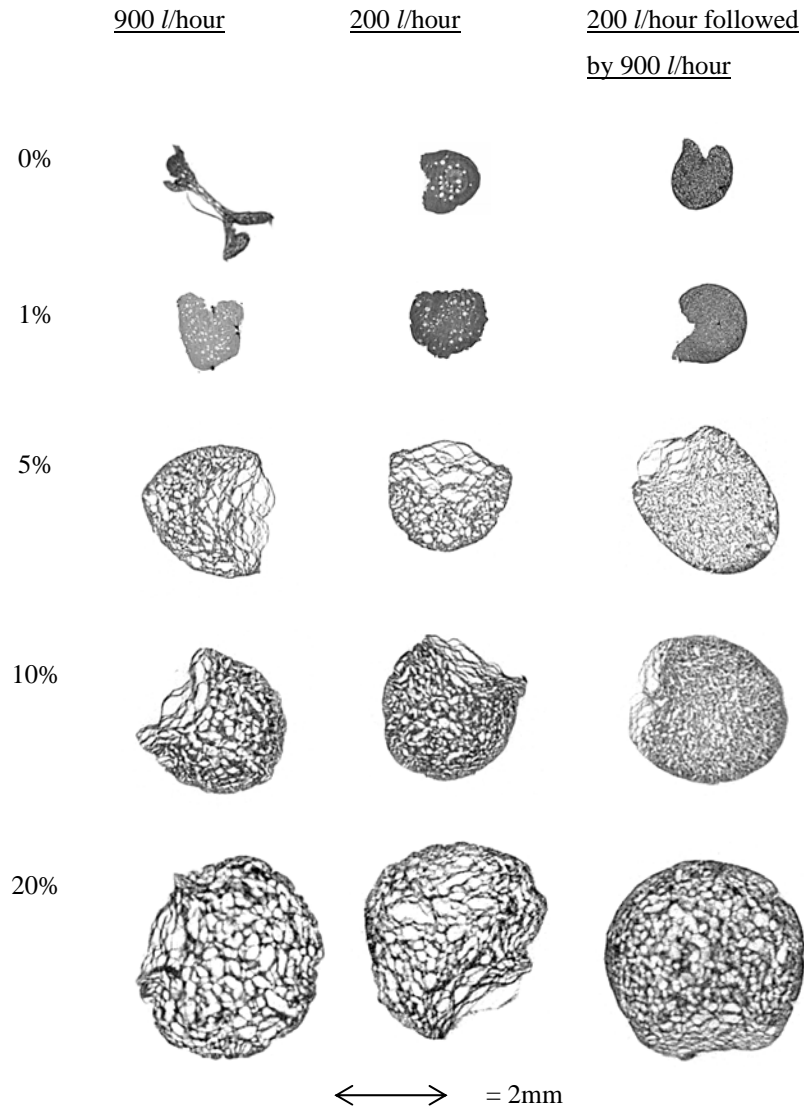


Figure 4.11 X-ray micro-CT images of supercritically dried agar gel pieces, containing varying concentrations of sucrose (0-20%) and also dried at different flow rates (900 l/hour, 200 l/hour, and 200 l/hour followed by 900 l/hour).

4.5 Conclusion

Experiments carried out on larger, pilot plant scale equipment showed similar results to those reported in chapter 3. The main difference observed was the formation of large voids in the centre of the gels pieces, when larger pieces were dried. These were expected to be formed during the depressurisation step, since the depressurisation rate could not be controlled as accurately as those dried on the smaller, laboratory scale equipment, which incorporated the use of an ABPR, allowing computerised control of the depressurisation rate.

For dried gels containing 0-30% sucrose, a lower degree of shrinkage was seen for those gels containing higher sucrose concentrations. Supercritically dried gels retained more volume than air dried gels, but did not show any benefits upon rehydration.

Despite no benefit in the rehydration or volume retention of supercritically dried gels, when compared with freeze dried gels or air dried gels, the texture of the supercritically dried-rehydrated gels did appear to be more similar to the pre-dried gels at sucrose concentrations <20%. Above 20% sucrose, air dried gels behaved more like the pre-dried gels.

Similarly, with the addition of 0-20% Glucidex 21D, the gel texture at sugar concentrations <20% were more like that of the pre-dried gel. The photographic images of the gels also appeared to be the same as the gels containing sucrose and as observed with gels containing sucrose, less shrinkage occurred with increased sugar addition.

The gels containing Glucidex 21D appeared to have very slightly improved rehydration properties compared with the equivalent sucrose containing gels (all results were however within 10% of those seen for sucrose gels). It was suggested that this difference seen was due to the size of the sugar chain and/or the interactions that occurred between the agar and the sugar. Glucidex 21D is a longer chain sugar than sucrose and it therefore may have the ability to maintain a more open gel structure or cause an exaggeration in the interactions that were discussed previously in chapter 3 (section 3.4.2) i.e. increased cross linking and reduced helix aggregation. The slightly larger volume seen for those supercritically dried gels containing Glucidex 21D, compared with gels containing sucrose also confirm that this may be the case, and the larger volume is expected to be responsible for the different rehydration properties seen.

Chapter 4: Drying of agar gel on pilot plant scale equipment using supercritical carbon dioxide

The results for flow rate changes were inconclusive but suggested that a slower drying regime may be favoured, since moisture contents reached during rehydration of gels dried at 200 l/hour were slightly higher than those which were reached for gels dried at 900 l/hour. There were no conclusive differences between the texture (after drying and after rehydration), or structure (after drying) of gels dried at different flow rates. Results also showed that fast depressurisation can lead to structural damage to the dried gel pieces. Unfortunately depressurisation could not be as tightly controlled on the equipment used in this chapter, since depressurisation was controlled by a manual micrometering valve rather than an ABPR, as in chapter 3.

In summary, the addition of sugars (particularly those with longer chains) to gels may improve rehydration and texture following supercritical drying and rehydration. Generally, a balance may need to be reached between: too much sugar which improves rehydration properties but reduces the force required to puncture the gel, and therefore results in a too soft texture; and too little sugar which results in poor structure retention and poor rehydration properties. A suitable sugar concentration, in the middle, was shown to be about 10% or 20% for both sucrose and Glucidex 21D.

Results reported here also confirm that supercritical drying may be carried out on a larger pilot plant scale with comparable results to those produced on laboratory scale equipment, implying that this technique could potentially be suitable for industrial scale drying.

5.0. Overall conclusion and suggestions for future work

5.1 Overall conclusion

The main achievements and conclusions of this work have been discussed below, with reference to the aims outlined in chapter 1:

Process equipment was designed, constructed and optimised for supercritical drying.

Supercritical drying equipment was successfully constructed and used to dry food products. Drying rates were improved by addition of EtOH as a co-solvent to the scCO₂ – a concentration of 6 mol% was found to be optimum. Supercritical CO₂ was also found to be preferable over liquid CO₂ for drying. Changes in experimental process parameters were investigated, including temperature, flow rate and depressurisation rate. Temperature and flow rate could be used to reduce drying times and depressurisation rate could be used to reduce the overall processing time. However, the effect of these parameters on food structure is discussed below. The mechanism of supercritical drying was investigated and it was suggested that the rate of drying at flow rates >2 l/minute was dependent on how much water the SCF could hold at the conditions investigated. Below 2 l/minute however, supercritical drying was limited by external mass transfer resistances and the rate of drying could be increased with increased flow rate. In contrast air drying is controlled by the diffusion of water to the food's surface.

The use of supercritical drying to remove water from foodstuffs, including delicate vegetable structures and biopolymer gels was investigated.

Initially the drying of carrot pieces was investigated as a model system that contained ~90% water and that had a well defined structure in the literature. Experiments were successful and the process was optimised using carrot pieces before applying the technique to agar. Carrots experienced some colour loss during drying with scCO₂(EtOH) however this was reversible upon rehydration. Agar gel (made up with 2% w/v agar) was a more challenging material to dry since

it only contained 2% solid material, therefore the addition of sugar to the gel was investigated as a method to overcome shrinkage during drying.

The potential to manipulate gel microstructure during supercritical drying was investigated and the effect of any structural changes on macrostructural properties was studied

Sugar (sucrose and Glucidex 21D) was added to agar (2% w/v) gel and was shown to improve the dried gel structure and increase volume retention throughout drying. However, this was not necessary during supercritical drying of carrot which contained a higher percentage (~10%) of insoluble material. Glucidex 21D appeared to improve rehydration properties of gel pieces slightly more than sucrose. This was thought to be due to Glucidex 21D being a longer chained sugar than sucrose, which was hypothesised to assist structural retention and therefore improve rehydration properties. The effect however, was minimal.

The addition of EtOH as a co-solvent during supercritical drying assisted in the removal of water but also caused some structural changes to both carrots and agar gels. Voids were formed in carrots that had been dried with $\text{scCO}_2(\text{EtOH})$, while in agar gels the resulting dried structure was more ‘bubbled’ than those that had been dried with $\text{scCO}_2(\text{pure})$. The voids that were formed in carrots during drying were hypothesised to be due to some component breakdown during processing that weakened the carrot structure and enabled voids to be formed during depressurisation. For agar gels, it was thought that the EtOH may disrupt the interactions that hold the agar double helix in a rigid state and therefore enable a ‘bubbled’ structure to be formed during the depressurisation stage of the drying process. These different structures created however, did not have a significant effect on the rehydration properties, although were seen to alter the product’s texture following rehydration.

Changes in flow rate were investigated for the supercritical drying of carrot pieces and did not appear to have an effect on the carrot structure. Additionally, controlled changes in flow rate and depressurisation rate were investigated for the supercritical drying of agar gel pieces and results showed little effect on the gel structure and gel properties. However, fast, uncontrolled depressurisation rates were shown to cause some structural damage to gels and therefore should be avoided during supercritical drying. Structure can therefore not be manipulated in this way.

However, such observations are still useful, since the drying rates may be decreased with increased flow rate, without compromising the product structure.

The supercritical drying technique was compared with air and freeze drying

The rate of supercritical drying was slower than air drying but the supercritical technique displayed comparable, or lower drying times to freeze drying. However, the main reason for comparison of the technique with air and freeze drying was to study the quality of the dried and rehydrated products.

Generally, supercritical drying resulted in improved appearance and reduced shrinkage of both carrot and agar gel pieces when compared with air dried pieces. Freeze dried carrot/gel pieces however, exhibited the least shrinkage during drying. The texture of supercritically dried-rehydrated carrot/agar gel was more favourable than air or freeze dried-rehydrated carrot/gel, since they exhibited a closer texture to that of the pre-dried carrot/gel.

The supercritical drying process was studied on pilot plant scale equipment

Experiments carried out on pilot plant scale equipment showed that this supercritical drying technique is possible on a larger scale and may be suitable for application in industry. Changes were made to the process so that the scCO_2 could be recycled and results were similar to those obtained from laboratory scale experiments. Larger changes in flow rate were investigated but did not appear to affect the gel structure or gel properties.

In conclusion, it has been shown that foods can be successfully dried by a novel drying technique which uses scCO_2 or $\text{scCO}_2(\text{EtOH})$. Supercritical drying may result in a more favourable dried (or dried-rehydrated) product than those produced using conventional drying techniques, making this a valuable technique if the advantages were fully exploited and applied to a suitable food product. Finally, the potential exists for this process to be applied in industry.

5.2 Suggestions for future work

Based on the experimental findings presented throughout this thesis, the following topics are suggested as the most promising areas for future work:

Investigation of supercritical drying with different co-solvents or the addition of different additives to the food/gel to aid drying and/or manipulate the structure

The addition of EtOH to scCO₂ during drying caused structural differences in the product being dried. For agar, this was proposed to be due to some interaction occurring between the EtOH and the agar and/or the water within the agar. Addition of different co-solvents may be a potential way to manipulate structures produced during drying while still aiding water removal. Temtem *et al.* (2006) reported the use of different solvents to foam membranes using a CO₂ assisted phase inversion method. Although this is a different technique to supercritical drying, the author discusses the effect of varying affinities between different co-solvents and scCO₂ on the resulting membrane porosity and pore size, caused by foaming. The co-solvent affinities may affect the product structure during drying, resulting in different structures produced with different co-solvents.

Alternatively, addition of other additives such as surfactants may assist water removal with scCO₂ through the creation of microemulsions (Park *et al.* 2006; Loeker *et al.* 2003; Zhang *et al.* 2004). They have also been reported to prevent collapse during drying of photoresists due to the reduction in capillary forces and therefore may also help retain structure of food during drying (Lee *et al.* 2007).

Investigation of liquid CO₂ drying as an alternative method to supercritical CO₂

ScCO₂ was found to be a better solvent for removal of water than the liquid equivalent (with the same density). However, interestingly when EtOH was added as a co-solvent there was no difference seen between the rate of water removal in the supercritical or liquid system. This discovery could present an interesting opportunity to dry at lower temperatures and pressures, therefore via a more economical process than that required for a supercritical system, but with no detrimental impact on the rate of drying. It may also limit the potential extraction of nutrients

during the drying process. The consequent food structure and food properties obtained using this system have not yet been investigated but it is anticipated that this would be a promising area of future research.

Drying of alternative biopolymer gels or mixed systems

It would be interesting to investigate the supercritical drying of different biopolymers and/or mixtures of biopolymers. Norton and Frith (2001) discussed how mixtures of biopolymers may be used to design microstructures. This knowledge could be used to enable drying of biopolymer gels with known microstructures that could be selected to interact in a favourable way with the supercritical solvent and therefore, in effect design dried microstructures.

Confirmation of the drying mechanism and phase behaviour

A mechanism for supercritical drying has been proposed in chapter 2 however, it would be interesting to map the mass transport and phase behaviour by using MRI, enabling further confirmation of the hypothesised mechanism. Hills (1998) reported the use of MRI to map mass transport and phase behaviour during various processes, including drying.

Modelling of the supercritical drying process

Modelling of the water removal during supercritical drying, which may be thought of as an 'extraction' process, would be useful to predict the drying kinetics for the supercritical drying technique, optimise the technique and also assist scale up. Parameters that should be considered to enable modelling of the process include, the solubility of the solute in the solvent; solvent properties such as temperature pressure, density, flow rate and viscosity; diffusion coefficients; mass transfer coefficients (internal and external); the structure and size/shape of the product being dried; and also shrinkage of the product being dried. Shrinkage may not be important here, since food products dried using supercritical drying were seen to retain much of their volume. Mass balance equations for the solute concentration in the solid and fluid phases may then be defined.

A mathematical model has been derived by Khalloufi *et al.* (2010) (Unilever) to describe the changes in water concentration in a solid food matrix and a fluid carrier while using the same

supercritical drying process and equipment that has been discussed in chapter 4. Parameters considered in the mass balance of the model include the geometry of the dryer, a mass transfer coefficient, a diffusion coefficient, an equilibrium constant between the solid and the fluid, the specific interfacial area of the solid matrix, the porosity of the packed drying vessel and the scCO₂ flow rate. Results reported in chapter 2 of this thesis, on the drying of carrots (Brown et al. 2008) were used to validate the model.

Further FT-IR analysis to determine specific interactions

Interactions between agar, scCO₂, water and EtOH have been proposed based on the results of FT-IR analysis. However, some questions remained unanswered and several assumptions have been made. Further FT-IR analysis could be used to confirm the presence of specific interactions, particularly the interaction of agar (dried and partially wet) with EtOH to determine the reason for the structural changes seen upon EtOH addition. Further FT-IR analysis is also required to confirm the presence of a CO₂-EtOH interaction which could not be seen in this work and may have been absent due to a low concentration of EtOH present in the IR cell.

If evidence of specific interactions occurring during supercritical drying can be collected and linked to the structure of the dried product, the potential exists to tune known interactions that occur during supercritical drying with and without co-solvents, and to use this knowledge to manipulate the structure in a favourable way.

Investigation of the economics of drying

The economics of the drying method is of great importance since an expensive drying technique (such as freeze drying) is only viable for the drying of high value foods which limits its usage considerably.

Compared with low pressure alternatives, SCF drying equipment is deemed expensive, yet this may not be the case when large volume quantities are handled. To make an economic assessment, the equipment cost and the operating costs (manpower, cleaning, energy and fluid consumption, maintenance) would need to be considered. To minimise the cost of CO₂ supply, it

may become important to maximise efficient recovery and recycle the CO₂. The power consumption can be minimised by using efficient heating and cooling systems and a lower pressure also results in lower heating and cooling costs.

No direct economical comparisons between supercritical drying and conventional techniques have been made but it has been suggested that supercritical drying may be less costly than freeze drying (Maltesen and van de Weert, 2008). This may be due to the lower cost required to maintain high pressure, compared with the cost to maintain a vacuum. The length of processing however would have a major influence on the economics of both processes and therefore a cost analysis cannot be performed without industrial scale equipment, and a specific process in place.

Additionally, an economic assessment only becomes important when you can assess the merits of the supercritical method over conventional methods and see if these outweigh any potential extra cost that a supercritical plant may incur. It may then be possible to justify these costs through production of a higher quality product. The work carried out in this thesis goes somewhere towards outlining the advantages and disadvantages of food structures that have been dried using scCO₂ which would influence the feasible cost of a supercritical plant for drying of foods.

6.0 References

- Abecassis-Wolfovich, M., Rotter, H., Landau, M. V., Korin, E., Erenburg, A. I., Mogilyansky, D., and Gartstein, E. (2003). "Texture and nanostructure of chromia aerogels prepared by urea-assisted homogeneous precipitation and low-temperature supercritical drying." *Journal of Non-Crystalline Solids*, 318(1-2), 95-111.
- Achanta, S., Okos, M. R., Cushman, J. H., and Kessler, D. P. (2004). "Moisture transport in shrinking gels during saturated drying." *Bioengineering, Food and Natural Products*, 43(8), 2112-2122.
- Aguilera, J. M., and Stanley, D. W. (1999). "Fundamentals of structuring: polymer, colloid, and materials science." *Microstructural principles of food processing and engineering*, Springer, pp.150-152.
- Aguilera, J. M., Stanley, D. W., and Baker, K. W. (2000). "New dimensions in microstructure of food products." *Trends in Food Science & Technology*, 11(1), 3-9.
- Aguilera, J. M. (2005). "Why food microstructure?" *Journal of Food Engineering*, 67(1-2), 3-11.
- Aguilera, J. M., Chiralt, A., and Fito, P. (2003). "Food dehydration and product structure." *Trends in Food Science & Technology*, 14(10), 432-437.
- Ahrné, L., Prothon, F., and Funebo, T. (2003). "Comparison of drying kinetics and texture effects of two calcium pretreatments before microwave-assisted dehydration of apple and potato." *International Journal of Food Science & Technology*, 38(4), 411-420.
- AOAC (1980). *Official Methods of Analysis (13th ed.)*, Arlington, VA., pp.130-143.
- AOAC (1995). *Official Methods of Analysis (16th ed.) (No. 934.06)*, Arlington, VA., 4.
- Arévalo-Pinedo, A., and Murr, F. E. X. (2006). "Kinetics of vacuum drying of pumpkin (*Cucurbita maxima*): modeling with shrinkage." *Journal of Food Engineering*, 76(4), 562-567.
- Arnott, S., Fulmer, A., Scott, W. E., Dea, I. C. M., Moorhouse, R., and Rees, D. A. (1974). "The agarose double helix and its function in agarose gel structure." *Journal of Molecular Biology*, 90(2), 269-272.
- Arunyanart, T., and Charoenrein, S. (2008). "Effect of sucrose on the freeze-thaw stability of rice starch gels: Correlation with microstructure and freezable water." *Carbohydrate Polymers*, 74(3), 514-518.

- Aymard, P., Martin, D.R., Plucknett, K., Foster, T.J., Clark, A.H., and Norton, I.T. (2001). "Influence of thermal history on the structural and mechanical properties of agarose gels." *Biopolymers*, 59, 131-144.
- Bae, H. K., Jeon, J. H., and Lee, H. (2004). "Influence of co-solvent on dye solubility in supercritical carbon dioxide." *Fluid Phase Equilibria*, 222-223, 119-125.
- Bart, J. C. J. (2006). "Microscopy and microanalysis of polymer/additive formulations." *Plastics additives: advanced industrial analysis*, IOS Press US, pp.521-532.
- Beckett, S. (2008). "The science of chocolate." Royal Society of Chemistry.
- Ben-Yoseph, E., and Hartel, R. W. (2006). "Computer simulation of sugar crystallization in confectionery products." *Innovative Food Science & Emerging Technologies*, 7(3), 225-232.
- Berna, A., Chafer, A., and Monton, J. B. (2001). "High-pressure solubility data of the system resveratrol (3)+ethanol (2)+CO₂ (1)." *The Journal of Supercritical Fluids*, 19(2), 133-139.
- Blake-Hedges, L. (1998). "Cleaner technologies substitutes assessment: professional fabricare processes." *Rep. No. EPA 744-B-98-001*, U.S. Environmental Protection Agency.
- Brantley, N. H., Bush, D., Kazarian, S. G., and Eckert, C. A. (1999). "Spectroscopic measurement of solute and cosolvent partitioning between supercritical CO₂ and polymers." *The Journal of Physical Chemistry B*, 103(45), 10007-10016.
- Brodsky, C. J., and Ko, E. I. (1996). "Effects of preparative and supercritical drying parameters on the physical properties of niobia aerogels." *Langmuir*, 12(25), 6164-6166.
- Brown, Z. K., Fryer, P. J., Norton, I. T., Bakalis, S., and Bridson, R. H. (2008). "Drying of foods using supercritical carbon dioxide - investigations with carrot." *Innovative Food Science & Emerging Technologies*, 9(3), 280-289.
- Brown, Z. K., Fryer, P. J., Norton, I. T., and Bridson, R. H. (2010). "Drying of agar gels using supercritical carbon dioxide." *The Journal of Supercritical Fluids*, 54, 89-95.
- Brunner, G. (2005). "Supercritical fluids: technology and application to food processing." *Journal of Food Engineering*, 67(1-2), 21-33.
- Bulone, D., and San Biagio, P.L. (1991). "Microgel regions in dilute agarose solutions: the notion of non-gelling concentration, and the role of spinodal demixing." *Chemical Physical Letters*, 179(4), 339-343.

Bulone, D., Emanuele, A., and San Biagio, P.L. (1999). "Effects of solvent perturbation on gelation driven by spinodal demixing." *Biophysical Chemistry*, 77, 1-8.

Bulone, D., Newman, J., and San Biagio, P.L. (1997). "Mesoscopic gels at low agarose concentration: perturbation effects of ethanol." *Biophysical Journal*, 72, 388-394.

Cabaço, M. I., Danten, Y., Tassaing, T., Longelin, S., and Besnard, M. (2005). "Raman spectroscopy of CO₂-acetone and CO₂-ethanol complexes." *Chemical Physics Letters*, 413(4-6), 258-262.

Carpenter, T. M. (1940). "Composition of some common foods with respect to the carbohydrate content." *The Journal of Nutrition*, 19(5), 415-422.

Carrington, A. K., Goff, H. D., and Stanley, D. W. (1999). "Structure and stability of the glassy state in rapidly and slowly cooled carbohydrate solutions." *Food Research International*, 29(2), 207-213.

Coviello, T., Alhaique, F., Parisi, C., Matricardi, P., Bocchinfuso, G., and Grassi, M. (2005). "A new polysaccharidic gel matrix for drug delivery: preparation and mechanical properties." *Journal of Controlled Release*, 102(3), 643-656.

Cunningham, S. E., McMinn, W. A. M., Magee, T. R. A., and Richardson, P. S. (2008). "Effect of processing conditions on the water absorption and texture kinetics of potato." *Journal of Food Engineering*, 84(2), 214-223.

Cygnarowicz, M. L., Maxwell, R. J., and Seider, W. D. (1990). "Equilibrium solubilities of [beta]-carotene in supercritical carbon dioxide." *Fluid Phase Equilibria*, 59(1), 57-71.

Davies, O. R., Lewis, A. L., Whitaker, M. J., Tai, H., Shakesheff, K. M., and Howdle, S. M. (2008). "Applications of supercritical CO₂ in the fabrication of polymer systems for drug delivery and tissue engineering." *Advanced Drug Delivery Reviews*, 60(3), 373-387.

del Valle, J. M., Jiménez, M., and de la Fuente, J. C. (2003). "Extraction kinetics of pre-pelletized Jalapeno peppers with supercritical CO₂." *The Journal of Supercritical Fluids*, 25(1), 33-44.

Department of Aquatic Products (1990). "Chapter 3: Properties, manufacture and application of seaweed polysaccharides - agar, carrageenan and algin". Retrieved August 14, 2009, from <http://www.fao.org/docrep/field/003/ab730e/ab730e03.htm>

Di Matteo, P., Donsi, G., and Ferrari, G. (2003). "The role of heat and mass transfer phenomena in atmospheric freeze-drying of foods in a fluidised bed." *Journal of Food Engineering*, 59(2-3), 267-275.

- Doymaz, I. (2004). "Convective air drying characteristics of thin layer carrots." *Journal of Food Engineering*, 61(3), 359-364.
- Ekart, M., Bennett, K., Ekart, S., Gurdial, G., Liotta, C., and Eckert, C. (1993). "Cosolvent interactions in supercritical fluid solutions." *AIChE Journal*, 39(2), 235-248.
- Estella, J., Echerverría, J. C., Laguna, M., and Garrido, J. J. (2007). "Effects of aging and drying conditions on the structural and textural properties of silica gels." *Microporous and Mesoporous Materials*, 102(1-3), 274-282.
- Femenia, A., Sanchez, E. S., Simal, S., and Rossello, C. (1998). "Effects of drying pretreatments on the cell wall composition of grape tissues." *Journal of Agricultural and Food Chemistry*, 46(1), 271-276.
- Fleming, O. S., Chan, K. L. A., and Kazarian, S. G. (2006). "High-pressure CO₂-enhanced polymer interdiffusion and dissolution studied with in situ ATR-FTIR spectroscopic imaging." *Polymer*, 47(13), 4649-4658.
- Foster, N. R., Singh, H., Yun, S. L. J., Tomasko, D. L., and Macnaughton, S. J. (2002). "Polar and nonpolar cosolvent effects on the solubility of cholesterol in supercritical fluids." *Industrial & Engineering Chemistry Research*, 32(11), 2849-2853.
- Freile-Peigrín, Y., Madera-Santana, T., Robledo, D., Veleza, L., Quintana, P., and Azamar, J. A. (2007). "Degradation of agar films in a humid tropical climate: thermal, mechanical, morphological and structural changes." *Polymer Degradation and Stability*, 92, 244-252.
- Fried, J. R., and Li, W. (1990). "High-pressure FTIR studies of gas-polymer interactions." *Journal of Applied Polymer Science*, 41(5-6), 1123-1131.
- Fuchigami, M., Miyazaki, K., and Hyakumoto, N. (1995). "Frozen carrots texture and pectic componenets as affected by low-temperature-blanching and quick freezing." *Journal of Food Science*, 60(1), 132-136.
- Fuchigami, M., and Teramoto, A. (2003). "Changes in temperature and structure of agar gel as affected by sucrose during high pressure freezing." *Journal of Food Science*, 68(2), 528-533.
- Fuchigami, M., Ogawa, N., and Teramoto, A. (2002). "Trehalose and hydrostatic pressure effects on the structure and sensory properties of frozen tofu (soybean curd)." *Innovative Food Science & Emerging Technologies*, 3(2), 139-147.
- Fuchigami, M., Teramoto, A., and Jibu, Y. (2006). "Texture and structure of pressure-shift-frozen agar gel with high visco-elasticity." *Food Hydrocolloids*, 20(2-3), 160-169.

Furer, V. L. (1990). "Carbamate-group conformation and IR band intensities." *Journal of Applied Spectroscopy*, 53(2), 860-863.

Gendron, R., Champagne, M. F., Delaviz, Y., and Polasky, M. E. (2006). "Foaming polystyrene with a mixture of CO₂ and ethanol." *Journal of Cellular Plastics*, 42(2), 127-138.

Georget, D. M. R., Ng, A., Smith, A. C., and Waldron, K. W. (1998). "The thermomechanical properties of carrot cell wall material." *Journal of the Science of Food and Agriculture*, 78, 73-80.

Greve, L. C., McArdle, R. N., Gohlke, J. R., and Labavitch, J. M. (1994). "Impact of heating on carrot firmness: changes in cell wall components." *Journal of Agricultural and Food Chemistry*, 42(12), 2900-2906.

Güçlü-Üstündag, O., and Temelli, F. (2004). "Correlating the solubility behavior of minor lipid components in supercritical carbon dioxide." *The Journal of Supercritical Fluids*, 31(3), 235-253.

Güçlü-Üstündag, O., and Temelli, F. (2005). "Solubility behaviour of ternary systems of lipids, cosolvents and supercritical carbon dioxide and processing aspects." *The Journal of Supercritical Fluids*, 36(1), 1-15.

Haarhaus, U., Swidersky, P., and Schneider, G. M. (1995). "High-pressure investigations on the solubility of dispersion dyestuffs in supercritical gases by VIS/NIR-spectroscopy. Part I - 1,4-Bis-(octadecylamino)-9,10-anthraquinone and disperse orange in CO₂ and N₂O Up to 180 MPa." *The Journal of Supercritical Fluids*, 8(2), 100-106.

Han, X., Cheng, L., Zhang, R., and Bi, J. (2009). "Extraction of safflower seed oil by supercritical CO₂." *Journal of Food Engineering*, 92(4), 370-376.

Higginbotham, C. P., Browner, R. F., Jenkins, J. D., and Rice, J. K. (2003). "Dependence of drying technique on surface area and pore size for polyethylene glycol/tetramethoxysilicate hybrid gels." *Material Letters*, 57, 3970-3975.

Hills, B. (1998). "MRI and food processing: mapping mass transport and phase behaviour." *Magnetic Resonance Imaging in Food Science*, John Wiley & Sons, pp.35-75.

Hirogaki, K., Tabata, I., Hisada, K., and Hori, T. (2005). "An investigation of the interaction of supercritical carbon dioxide with poly(ethylene terephthalate) and the effects of some additive modifiers on the interaction." *The Journal of Supercritical Fluids*, 36(2), 166-172.

Hubers, J. L., Striegel, A. C., Heindel, T. J., Gray, J. N., and Jensen, T. C. (2005). "X-ray computed tomography in large bubble columns." *Chemical Engineering Science*, 60(22), 6124-6133.

Hui, Y. H. (2005) *Handbook of food science, technology and engineering*. Taylor and Francis Ltd. (3rd ed.), pp.103

Isengard, H. D. (2001). "Water content, one of the most important properties of food." *Food Control*, 12(7), 395-400.

James, B. (2009). "Advances in "wet" electron microscopy techniques and their application to the study of food structure." *Trends in Food Science & Technology*, 20(3-4), 114-124.

Jay, J. M., Loessner, M. J., Golden, D. A. (2005). "Chapter 18: Protection of foods by drying" *Spoilage in vegetables: modern food microbiology* Springer (7th ed.) pp.445-447

Job, N., Théry, A., Pirard, R., Marien, J., Kocon, L., Rouzaud, J. N., Béguin, F., and Pirard, J. P. (2005). "Carbon aerogels, cryogels and xerogels: influence of the drying method on the textural properties of porous carbon materials." *Carbon*, 43(12), 2481-2494.

Kalab, M., Ian-Wojtas, P., and Miller, S. S. (1995). "Microscopy and other imaging techniques in food structure analysis." *Trends in Food Science & Technology*, 6(6), 177-186.

Kalichevsky-Dong, M., Ablett, S., Lillford, P.J., and Knorr, D. (2000), "Effects of pressure-shift freezing and conventional freezing on model food gels." *International Journal of Food Science and Technology*, 35, 163-172.

Kazarian, S. G., Vincent, M. F., Bright, F. V., Liotta, C. L., and Eckert, C. A. (1996). "Specific intermolecular interaction of carbon dioxide with polymers." *Journal of the American Chemical Society*, 118(7), 1729-1736.

Kazarian, S. G., Vincent, M. F., West, B. L., and Eckert, C. A. (1998). "Partitioning of solutes and cosolvents between supercritical CO₂ and polymer phases." *Journal of Supercritical Fluids, The*, 13(1-3), 107-112.

Ke, J., Jin, S., Han, B., Yan, H., and Shen, D. (1997). "Hydrogen bonding of some organic acid in supercritical CO₂ with polar cosolvents." *The Journal of Supercritical Fluids*, 11(1-2), 53-60.

Khalloufi, S., Almeida-Rivera, C., and Bongers, P. (2010). "Supercritical-CO₂ drying of foodstuffs in packed beds: Experimental validation of a mathematical model and sensitive analysis." *Journal of Food Engineering*, 96, 141-150.

Khalloufi, S., and Ratti, C. (2006). "Quality deterioration of freeze-dried foods as explained by their glass transition temperature and internal structure." *Journal of Food Science*, 68(3), 892-903.

Khraisheh, M. A. M., McMinn, W. A. M., and Magee, T. R. A. (2004). "Quality and structural changes in starchy foods during microwave and convective drying." *Food Research International*, 37(5), 497-503.

Kiliç, K., Onal-Ulusoy, B., Yildirim, M., and Hakki Boyaci, İ. (2007). "Scanner-based color measurement in L* a* b* format with artificial neural networks (ANN)." *European Food Research and Technology*, 226, 121-126.

King, J. W., and Williams, L. L. (2003). "Utilization of critical fluids in processing semiconductors and their related materials." *Current Opinion in Solid State and Materials Science*, 7(4-5), 413-424.

King, M. B., Mubarak, A., Kim, J. D., and Bott, T. R. (1992). "The mutual solubilities of water with supercritical and liquid carbon dioxides." *The Journal of Supercritical Fluids*, 5(4), 296-302.

Kiran, E., and Brennecke, J. F. (1993). "Current state of supercritical fluid science and technology." *Supercritical Fluid Engineering Science: Fundamentals and Applications*, American Chemical Society, Washington, D.C..

Knox, D. E. (2005). "Solubilities in supercritical fluids." *Pure Applied Chemistry*, 77(3), 513-530.

Kopcak, U., and Mohamed, R. S. (2005). "Caffeine solubility in supercritical carbon dioxide/co-solvent mixtures." *The Journal of Supercritical Fluids*, 34(2), 209-214.

Krokida, M. K., Karathanos, V. T., Maroulis, Z. B., and Marinos-Kouris, D. (2003). "Drying kinetics of some vegetables." *Journal of Food Engineering*, 59(4), 391-403.

Krokida, M. K., and Marinos-Kouris, D. (2003). "Rehydration kinetics of dehydrated products." *Journal of Food Engineering*, 57(1), 1-7.

Krokida, M. K., and Maroulis, Z. B. (1999). "Effect of drying on some quality properties of dehydrated products." *Drying Technology*, 17(3), 449-466.

Krokida, M. K., and Maroulis, Z. B. (1997). "Effect of drying method on shrinkage and porosity." *Drying Technology*, 15(10), 2441-2458.

Lahaye, M., and Rochas, C. (1991). "Chemical structure and physico-chemical properties of agar." *Hydrobiologia*, 221, 137-148.

Laintz, K. E., Hale, C. D., Stark, P., Rouquette, C. L., and Wilkinson, J. (1998). "A comparison of liquid and supercritical carbon dioxide as an extraction solvent for plating bath treatment." *Analytical Chemistry*, 70(2), 400-404.

Lalanne, P., Rey, S., Cansell, F., Tassaing, T., and Besnard, M. (2001). "Attempt to explain the changes in solvation of polystyrene in supercritical CO₂/ethanol mixtures using infrared and Raman spectroscopy." *The Journal of Supercritical Fluids*, 19(2), 199-207.

Lalanne, P., Tassaing, T., Danten, Y., Cansell, F., Tucker, S. C., and Besnard, M. (2004). "CO₂-ethanol interaction studied by vibrational spectroscopy in supercritical CO₂." *The Journal of Physical Chemistry A*, 108(14), 2617-2624.

Laudise, R. A., and Johnson, J. (1986). "Supercritical drying of gels." *Journal of Non-Crystalline Solids*, 79(1-2), 155-164.

Lee, F. A. (1945). "Vitamin retention in blanched carrots. Alcohol-insoluble solids as a reference base." *Industrial & Engineering Chemistry Analytical Edition*, 17(11), 719-720.

Lee, M. Y., Do, K. M., Ganapathy, H. S., Lo, Y. S., Kim, J. J., Choi, S. J., and Lim, K. T. (2007). "Surfactant-aided supercritical carbon dioxide drying for photoresists to prevent pattern collapse." *The Journal of Supercritical Fluids*, 42(1), 150-156.

Léonard, A., Blacher, S., Marchot, P., and Crine, M. (2001). "X-ray microtomography: a new tool to follow soft material shrinkage during convective drying." 2nd World Congress on Industrial Process Tomography, 110-117.

Levi, G., and Karel, M. (1995). "Volumetric shrinkage (collapse) in freeze-dried carbohydrates above their glass transition temperature." *Food Research International*, 28(2), 145-151.

Lewicki, P. P., and Porzecka-Pawlak, R. (2005). "Effect of osmotic dewatering on apple tissue structure." *Journal of Food Engineering*, 66(1), 43-50.

Lewicki, P. P., Vu Le, H., and Pomaranska-Lazuka, W. (2002). "Effect of pre-treatment on convective drying of tomatoes." *Journal of Food Engineering*, 54(2), 141-146.

Liang, M. T., and Wang, C. M. (2000). "Production of Engineering Plastics Foams by Supercritical CO₂." *Industrial & Engineering Chemistry Research*, 39(12), 4622-4626.

Lim, K. S., and Barigou, M. (2004). "X-ray micro-computed tomography of cellular food products." *Food Research International*, 37(10), 1001-1012.

Lin, T. M., Durance, D., and Scaman, C. H. (1998). "Characterization of vacuum microwave, air and freeze dried carrot slices." *Food Research International*, 31(2), 111-117.

- Litvin, S., Mannheim, C. H., and Miltz, J. (1998). "Dehydration of carrots by a combination of freeze drying, microwave heating and air or vacuum drying." *Journal of Food Engineering*, 36(1), 103-111.
- Loeker, F., Marr, P. C., and Howdle, S. M. (2003). "FTIR analysis of water in supercritical carbon dioxide microemulsions using monofunctional perfluoropolyether surfactants." *Colloids and Surfaces A: Physicochemical and Engineering Aspects*, 214(1-3), 143-150.
- Louka, N., and Allaf, K. (2004). "Expansion ratio and color improvement of dried vegetables texturized by a new process "Controlled Sudden Decompression to the vacuum": Application to potatoes, carrots and onions." *Journal of Food Engineering*, 65(2), 233-243.
- Louka, N., Juhel, F., and Allaf, K. (2004). "Quality studies on various types of partially dried vegetables texturized by Controlled Sudden Decompression: General patterns for the variation of the expansion ratio." *Journal of Food Engineering*, 65(2), 245-253.
- Maharaj, V., and Sankat, C. K. (1996). "Quality changes in dehydrated dasheen leaves: effects of blanching pre-treatments and drying conditions." *Food Research International*, 29(5-6), 563-568.
- Maltesen, M. J., and van de Weert, M. (2008) "Drying methods for protein pharmaceuticals." *Drug Discovery Today: Technologies*, 5(2-3) e81-88.
- Maltini, E., Torreggiani, D., Venir, E., and Bertolo, G. (2003). "Water activity and the preservation of plant foods." *Food Chemistry*, 82(1), 79-86.
- Manno, M., Emanuele, A., Martorana, V., Bulone, D., San Biagio, P.L., Palma-Vitorelli, M.B., and Palma, M.U. (1999), "Multiple interactions between molecular and supramolecular ordering." *Physical Review E*, 59(2), 2222-2230.
- Marabi, A., Thieme, U., Jacobson, M., and Saguy, I. S. (2006). "Influence of drying method and rehydration time on sensory evaluation of rehydrated carrot particulates." *Journal of Food Engineering*, 72(3), 211-217.
- Marabi, A., and Saguy, I. S. (2004). "Effect of porosity on rehydration of dry food particulates." *Journal of the Science of Food and Agriculture*, 84, 1105-1110.
- Mariam, I., Yul Cho, K., and Rizvi, S. S. H. (2008). "Thermal properties of starch-based biodegradable foams produced using supercritical fluid extrusion (SCFX)." *International Journal of Food Properties*, 11, 415-426.
- Mathlouthi, M., and Reiser, P. (1994). "Sucrose: properties and applications." Blackie Academic and Professional, London.

Mayor, L., and Sereno, A. M. (2004). "Modelling shrinkage during convective drying of food materials: a review." *Journal of Food Engineering*, 61(3), 373-386.

Meena, R., Prasad, K., and Siddhanta, A. K. (2006). "Studies on "sugar-reactivity" of agars extracted from some Indian agarophytes." *Food Hydrocolloids*, 20(8), 1206-1215.

Milburn, D. R., Adkins, B. D., Sparks, D. E., Srinivasan, R., and Davis, B. H. (1996). "Applications of supercritical drying in catalyst preparation." *Advanced Catalysts and Nanostructured Materials*, R. M. William, ed., Academic Press, San Diego, 117-142.

Mousavi, R., Miri, T., Cox, P. W., and Fryer, P. J. (2007). "Imaging food freezing using X-ray microtomography." *International Journal of Food Science & Technology*, 42(6), 714-727.

Mujumdar, A. S., and Devahastin, S. (2000). "Fundamental principles of drying." *Practical Guide to Industrial Drying*, S. Devahastin, ed., Exergex, Montreal.

Muthukumar, P., Gupta, R. B., Sung, H.-D., Shim, J.-J., and Bae, H.-K. (1999). "Dye solubility in supercritical carbon dioxide. Effect of hydrogen bonding with cosolvents." *Korean Journal of Chemical Engineering*, 16(1), 111-117.

Mwithiga, G., and Olwal, J. O. (2005). "The drying kinetics of kale (*Brassica oleracea*) in a convective hot air dryer." *Journal of Food Engineering*, 71(4), 373-378.

Naewbanij, M., and Thepent, V. (n.d.) "Batch and continuous drying". Retrieved August 14, 2009, from <http://www.fao.org/docrep/X5036E/x5036E0X.HTM#Batch%20and%20continuous%20drying>

Nagaya, K., Li, Y., Jin, Z., Fukumuro, M., Ando, Y., and Akaishi, A. (2006). "Low-temperature desiccant-based food drying system with airflow and temperature control." *Journal of Food Engineering*, 75(1), 71-77.

Nalawade, S. P., Picchioni, F., Marsman, J. H., Grijpma, D. W., Feijen, J., and Janssen, L. P. B. M. (2006a). "Intermolecular interactions between carbon dioxide and the carbonyl groups of polylactides and poly([epsilon]-caprolactone)." *Journal of Controlled Release*, 116(2), e38-e40.

Nalawade, S. P., Picchioni, F., Marsman, J. H., and Janssen, L. P. B. M. (2006b). "The FT-IR studies of the interactions of CO₂ and polymers having different chain groups." *The Journal of Supercritical Fluids*, 36(3), 236-244.

Namatsu, H., Yamazaki, K., and Kurihara, K. (1999). "Supercritical drying for nanostructure fabrication without pattern collapse." *Microelectronic Engineering*, 46(1-4), 129-132.

- Ng, A., Parr, A. J., Ingham, L. M., Rigby, N. M., and Waldron, K. W. (1998). "Cell wall chemistry of carrots (*Daucus carota* cv. Amstrong) during maturation and storage." *Journal of Agricultural and Food Chemistry*, 46(8), 2933-2939.
- Nijhuis, H. H., Topping, H. M., Muresan, S., Yuksel, D., Leguijt, C., and Kloek, W. (1998). "Approaches to improving the quality of dried fruit and vegetables." *Trends in Food Science & Technology*, 9(1), 13-20.
- Normand, V., Aymard, P., Lootens, D. L., Amici, E., Plucknett, K. P., and Frith, W. J. (2003). "Effect of sucrose on agarose gels mechanical behaviour." *Carbohydrate Polymers*, 54(1), 83-95.
- Norton, I. T., and Frith, W. J. (2001). "Microstructure design in mixed biopolymer composites." *Food Hydrocolloids*, 15(4-6), 543-553.
- Norton, I.T., Jarvis, D.A., and Foster, T.J. (1999), "A molecular model for the formation and properties." *International Journal of Biological Macromolecules*, 26, 255-261.
- Novak, Z., Kotnik, P., and Knez, Z. (2004). "Preparation of WO₃ aerogel catalysts using supercritical CO₂ drying." *Journal of Non-Crystalline Solids*, 350, 308-313.
- Nussinovitch, A., Corradini, M., Normand, M., and Peleg, M. (2000). "Effect of sucrose on the mechanical and acoustic properties of freeze-dried agar, K-carrageenan and gellan gels." *Journal of Texture Studies*, 31(2), 205-223.
- Nussinovitch, A., Velez-Silvestre, R., and Peleg, M. (1993). "Compressive characteristics of freeze-dried agar and alginate gel sponges." *Biotechnology Progress*, 9, 101-104.
- Nussinovitch, A., Velez-Silvestre, R., and Peleg, M. (1992). "Mechanical properties of hydrocolloid gels filled with internally produced carbon dioxide gas bubbles." *Biotechnology Progress*, 8(5), 424-428.
- Park, J. Y., Lim, J. S., Lee, Y. W., and Yoo, K. P. (2006). "Phase behavior of water-in-supercritical carbon dioxide microemulsion with sodium salt of bis(2,2,3,3,4,4,5,5-octafluoro-1-pentanol) sulfosuccinate." *Fluid Phase Equilibria*, 240(1), 101-108.
- Pasquali, I., Andanson, J. M., Kazarian, S. G., and Bettini, R. (2008). "Measurement of CO₂ sorption and PEG 1500 swelling by ATR-IR spectroscopy." *The Journal of Supercritical Fluids*, 45(3), 384-390.
- Peleg, M. (1996). "On modeling changes in food and biosolids at and around their glass transition temperature range." *Critical Reviews in Food Science and Nutrition*, 36(1-2), 49-69.

Perrut, M., and Reverchon, E. (2000). "Particle design - materials and natural products processing." International Society for the Advancement of Supercritical Fluids, Proceedings of the 7th meeting on supercritical fluids, 47-48.

Pongsawatmanit, R., Ikeda, S., and Miyawaki, O. (1999). "Effect of sucrose on physical properties of alginate dispersed aqueous systems." *Food Science and Technology Research*, 5(2), 183-187.

Portsmouth, R. L., and Gladden, L. F. (1991). "Determination of pore connectivity by mercury porosimetry." *Chemical Engineering Science*, 46(12), 3023-3036.

Rahman, M. S., Al-Amri, O. S., and Al-Bulushi, I. M. (2002). "Pores and physico-chemical characteristics of dried tuna produced by different methods of drying." *Journal of Food Engineering*, 53(4), 301-313.

Rangarajan, B., and Lira, C. T. (1991). "Production of aerogels." *The Journal of Supercritical Fluids*, 4(1), 1-6.

Rassis, D. K., Saguy, I. S., and Nussinovitch, A. (2002). "Collapse, shrinkage and structural changes in dried alginate gels containing fillers." *Food Hydrocolloids*, 16(2), 139-151.

Ratti, C. (2001). "Hot air and freeze-drying of high-value foods: a review." *Journal of Food Engineering*, 49(4), 311-319.

Rayner, C.M. (n.d.) "More about supercritical carbon dioxide". Retrieved August, 14, 2009, from <http://www.chem.leeds.ac.uk/People/CMR/criticalpics.html>

Rees, D. A., and Welsh, J. E. (1977). "Secondary and tertiary structure of polysaccharides in solutions and gels." *Angewandte Chemie International Edition in English*, 16, 214-224.

Reh, C., Bhat, S. N., and Berrut, S. (2004). "Determination of water content in powdered milk." *Food Chemistry*, 86(3), 457-464.

Reid, R. C., Prausnitz, J. M., and Poling, B. E. (1987). "The Properties of gases and liquids." McGraw-Hill, New York.

Reilly, J. T., Bokis, C. P., and Donohue, M. D. (1995). "An experimental investigation of lewis acid-base interactions of liquid carbon dioxide using fourier transform infrared (FT-IR) spectroscopy." *International Journal of Thermophysics*, 16(3), 599-610.

Renard, D., van de Velde, F., and Visschers, R. W. (2006). "The gap between food gel structure, texture and perception." *Food Hydrocolloids*, 20(4), 423-431.

Reverchon, E. (1997). "Supercritical fluid extraction and fractionation of essential oils and related products." *The Journal of Supercritical Fluids*, 10(1), 1-37.

Sabirzyanov, A. N., Il'in, A. P., Akjunov, A. R., and Gumerov, F. M. (2002). "Solubility of water in supercritical carbon dioxide." *High Temperature*, 40(2), 203-206.

Sabirzyanov, A. N., Shagiakhmetov, R. A., Gabitov, F. R., Tarzimanov, A. A., and Gumerov, F. M. (2003). "Water solubility of carbon dioxide under supercritical and subcritical conditions." *Theoretical Foundations of Chemical Engineering*, 37(1), 51-53.

Saguy, I. S., Marabi, A., and Wallach, R. (2005). "Liquid imbibition during rehydration of dry porous foods." *Innovative Food Science & Emerging Technologies*, 6(1), 37-43.

San Biagio, P.L., Bulone, D., Emanuele, A., Palma-Vittorelli, M.B. and Palma, M.U. (1996), "Spontaneous symmetry-breaking pathways: time resolved study of agarose gelation." *Food Hydrocolloids*, 10(1), 91-97.

San Biagio, P.L., Madonia, F., and Newman, J. (1986), "Sol-sol structural transition of aqueous agarose systems." *Biopolymers*, 25, 2255-2269.

San Biagio, P.L., Newman, J., Madonia, F., and Palma, M.U. (1989). "Co-solute control of the self-assembly of a biopolymeric supramolecular structure." *Chemical Physics Letters*, 154, 477-483.

Sanjuán, N., Hernando, I., Angeles Lluich, M., and Mulet, A. (2005). "Effect of low temperature blanching on texture, microstructure and rehydration capacity of carrots." *Journal of the Science of Food and Agriculture*, 85, 2071-2076.

Schaefer, D. W., Pekala, R., and Beaucage, G. (1995). "Origin of porosity in resorcinol-formaldehyde aerogels." *Journal of Non-Crystalline Solids*, 186, 159-167.

Segnini, S., Dejmek, P., and Öste, R. (1999). "Reproducible texture analysis of potato chips." *Journal of Food Science*, 64(2), 309-312.

Sereno, A. M., and Medeiros, G. L. (1990). "A simplified model for the prediction of drying rates for foods." *Journal of Food Engineering*, 12(1), 1-11.

Shieh, Y. T., and Liu, K. H. (2003). "The effect of carbonyl group on sorption of CO₂ in glassy polymers." *The Journal of Supercritical Fluids*, 25(3), 261-268.

Shimek, J. (n.d.). "Practical water management food systems". Retrieved August 14, 2009, from <http://trc.ucdavis.edu/srdungan/fst100a/disc5water/sld005.htm>

Shin, J. E., Cornillon, P., and Salim, L. (2002). "The effect of centrifugation on agar/sucrose gels." *Food Hydrocolloids*, 16(2), 89-94.

Sila, D. N., Smout, C., Elliot, F., Van Loey, A., and Hendrickx, M. (2006). "Non-enzymatic depolymerization of carrot pectin: toward a better understanding of carrot texture during thermal processing." *Journal of Food Science*, 71(1), E1-E9.

Simal, S., Garau, C., Femenia, A., and Rosselló, C. (2005). "Drying of red pepper (*Capsicum annuum*): water desorption and quality." *International Journal of Food Engineering*, 1(4), 1-12.

Sinesio, F., Moneta, E., Spataro, P., and Quaglia, G. B. (1995). "Determination of sensory quality of dehydrated vegetables with profiling." *Italian Journal of Food Science*, 1, 11-18.

Smith, R. L., and Malone, M. F. (1997). "Attainable regions for polymerization reaction systems." *Industrial & Engineering Chemistry Research*, 36(4), 1076-1084.

Sovova, H., Stateva, R. P., and Galushko, A. A. (2001). "Solubility of [beta]-carotene in supercritical CO₂ and the effect of entrainers." *The Journal of Supercritical Fluids*, 21(3), 195-203.

Srikiatden, J., and Roberts, J. S. (2006). "Measuring moisture diffusivity of potato and carrot (core and cortex) during convective hot air and isothermal drying." *Journal of Food Engineering*, 74(1), 143-152.

Stephen, A. M., Phillips, G. O., and Williams, P. A. (2006). "Agars." *Food polysaccharides and their applications (food science and technology)*, CRC Press, pp.217-239.

Sun, D.-W. (2008). "Advances in food dehydration." CRC Press.

Suzuki, H., Sawai, Y., and Takada, M. (2001). "The effect of apparent molecular weight and components of agar on gel formation." *Food Science and Technology Research*, 7(4), 280-284.

Takishima, S., Suzuki, Y., Konishi, Y., Ohmori, T., Sato, Y., and Masuoka, H. (1997). "Production of silica aerogels by supercritical CO₂ drying." The 4th International Symposium on Supercritical Fluids.

Tamon, H., Ishizaka, H., Mikami, M., and Okazaki, M. (1997). "Porous structure of organic and carbon aerogels synthesized by sol-gel polycondensation of resorcinol with formaldehyde." *Carbon*, 35(6), 791-796.

Tanaka, H., and Nakanishi, K. (1994). "Solubility in supercritical fluid mixtures with co-solvents: an integral equation approach." *Fluid Phase Equilibria*, 102(2), 107-120.

Tassaing, T., Oparin, Y., Danten, Y., and Besnard, M. (2004). "Water-carbon dioxide mixtures at high temperatures and pressures as studied by infrared and Raman spectroscopies." The 14th International Conference on the properties of Water and Steam.

Tedjo, W., Taiwo, K. A., Eshtiaghi, M. N., and Knorr, D. (2002). "Comparison of pretreatment methods on water and solid diffusion kinetics of osmotically dehydrated mangos." *Journal of Food Engineering*, 53(2), 133-142.

Temtem, M., Casimiro, T., and guiar-Ricardo, A. (2006). "Solvent power and depressurization rate effects in the formation of polysulfone membranes with CO₂-assisted phase inversion method." *Journal of Membrane Science*, 283(1-2), 244-252.

Thermo Nicolet (n.d.). "FT-IR vs. dispersive infrared: theory of infrared spectroscopy instrumentation." TN-00128. Retrieved August 14, 2009, from http://www.thermo.com/eThermo/CMA/PDFs/Product/productPDF_21615.pdf

Torringa, E., Esveld, E., Scheewe, I., van den Berg, R., and Bartels, P. (2001). "Osmotic dehydration as a pre-treatment before combined microwave-hot-air drying of mushrooms." *Journal of Food Engineering*, 49(2-3), 185-191.

Trejo Araya, X. I., Hendrickx, M., Verlinden, B. E., Buggenhout, S. V., Smale, N. J., Stewart, C., and Mawson, A. J. (2007). "Understanding texture changes of high pressure processed fresh carrots: a microstructural and biochemical approach." *Journal of Food Engineering*, 80, 873-884.

Tsivintzelis, I., Angelopoulou, A. G., and Panayiotou, C. (2007a). "Foaming of polymers with supercritical CO₂: An experimental and theoretical study." *Polymer*, 48(20), 5928-5939.

Tsivintzelis, I., Pavlidou, E., and Panayiotou, C. (2007b). "Biodegradable polymer foams prepared with supercritical CO₂-ethanol mixtures as blowing agents." *The Journal of Supercritical Fluids*, 42(2), 265-272.

Tuan, D. Q., and Ilangantileket, S. G. (1997). "Liquid CO₂ extraction of essential oil from Star anise fruits (*Illicium verum* H.)." *Journal of Food Engineering*, 31(1), 47-57.

van Vliet, T., van Aken, G. A., de Jongh, H. H. J., and Hamer, R. J. (2009). "Colloidal aspects of texture perception." *Advances in Colloid and Interface Science*, 150(1), 27-40.

Vega-Mercado, H., Marcela Gongora-Nieto, M., and Barbosa-Canovas, G. V. (2001). "Advances in dehydration of foods." *Journal of Food Engineering*, 49(4), 271-289.

Verlinden, D. E., de Barys, T., de Baerdemaeker, J., and Deltour, R. (2009). "Modelling the mechanical and histological properties of carrot tissue during cooking in relation to the texture and cell wall changes." *Journal of Texture Studies*, 27(1), 15-28.

von Behren, J., Chimowitz, E. H., Kumaran, V., Shapir, Y., and Fauchet, P. M. (1997) "Critical behaviour in confined fluids: application to supercritical drying of porous silicon." The 4th International Symposium on Supercritical Fluids.

Wang, J., and Xi, Y. S. (2005). "Drying characteristics and drying quality of carrot using a two-stage microwave process." *Journal of Food Engineering*, 68(4), 505-511.

Wang, J., Tian, Z., Xu, J., Xu, Y., Xu, Z., and Lin, L. (2003). "Preparation of Mn substituted La-hexaaluminate catalysts by using supercritical drying." *Catalysis Today*, 83(1-4), 213-222.

Wang, P., Emmerling, A., Tappert, W., Spormann, O., Fricke, J., and Haubold, H. G. (1991). "High-temperature and low-temperature supercritical drying of aerogels - structural investigations with SAXS." *Journal of Applied Crystallography*, 24(5), 777-780.

Wentao, Z., Jian, Y., Weiming, M., and Jiasong, H. (2007). "Cosolvent effect of water in supercritical carbon dioxide facilitating induced crystallization of polycarbonate." *Polymer engineering and science*, 47(9), 1338-1343.

Witrowa-Rajchert, D., and Lewicki, P. P. (2006). "Rehydration properties of dried plant tissues." *International Journal of Food Science and Technology*, 41(9), 1040-1046.

Yam, K. L., and Papadakis, S. E. (2004). "A simple digital imaging method for measuring and analyzing color of food surfaces." *Journal of Food Engineering*, 61(1), 137-142.

Xu, Z. M., Jiang, X. L., Liu, T., Hu, G. H., Zhao, L., Zhu, Z. N., and Yuan, W. K. (2007). "Foaming of polypropylene with supercritical carbon dioxide." *The Journal of Supercritical Fluids*, 41(2), 299-310.

Zhang, X., Pham, J. Q., Ryza, N., Green, P. F., and Johnston, K. P. (2004). "Chemical-mechanical photoresist drying in supercritical carbon dioxide with hydrocarbon surfactants." *The Journal of Vacuum Science and Technology*, 22(2), 818-825.